

Utah State University

DigitalCommons@USU

Reports

Utah Water Research Laboratory

January 1970

Developing a Hydro-quality Simulation Model

Neal P. Dixon

David W. Hendricks

A. Leon Huber

Jay M. Bagley

Follow this and additional works at: https://digitalcommons.usu.edu/water_rep



Part of the [Civil and Environmental Engineering Commons](#), and the [Water Resource Management Commons](#)

Recommended Citation

Dixon, Neal P.; Hendricks, David W.; Huber, A. Leon; and Bagley, Jay M., "Developing a Hydro-quality Simulation Model" (1970). *Reports*. Paper 511.

https://digitalcommons.usu.edu/water_rep/511

This Report is brought to you for free and open access by the Utah Water Research Laboratory at DigitalCommons@USU. It has been accepted for inclusion in Reports by an authorized administrator of DigitalCommons@USU. For more information, please contact digitalcommons@usu.edu.



DEVELOPING A HYDRO-QUALITY SIMULATION MODEL

by

**Neal P. Dixon
David W. Hendricks
A. Leon Huber
Jay M. Bagley**

**Utah Water Research Laboratory
College of Engineering
Utah State University
Logan, Utah 84321**

June 1970

PRWG67-1

\$2.50

4

•

•

•

PROJECT ORGANIZATION

The project reported herein was begun in February 1966 upon award of a demonstration grant by the Division of Water Supply and Pollution Control, U.S. Public Health Service. Subsequent renewal grants were made by the Federal Water Pollution Control Administration, the third and last being grant number WPD-17-03.

Individuals who have assisted in various phases of the project include:

Mr. Eugene Israelsen—who initiated field studies at the beginning of the project.

Dr. Harvey Millar—who assisted in establishing laboratory chemical analyses procedures and in training the laboratory chemical analyst.

Dr. Frederick Post—who trained laboratory personnel to perform bacteriological analyses, and who initiated the concept of massive data scanning to explore for possible correlations between water quality variables (developed as Appendix H of this report). Dr. Post's motivation was oriented toward explaining bacterial counts in the stream.

Mrs. Ling Chu—who performed most of the chemical and bacteriological analyses on weekly water samples.

Dr. Allen Kartchner—who had the responsibilities of setting up two continuous monitoring field stations and for procuring and analyzing data from same (in collaboration with another project).

Appreciation is expressed to the U.S. Geological Survey, Logan Office, under the supervision of Mr. Wallace Jibson, who under special contract with the project set up four additional gaging stations and made available all current streamflow records in the project area.

Author responsibilities

Jay M. Bagley—conceived the project, initiated the hydrology phases of the study, and was project director at the beginning of the project (until July 1966 when he became Director, Utah Water Research Laboratory).

David W. Hendricks—initiated the water quality phases of the study and was project director, subsequent to Dr. Bagley.

Leon Huber—developed the hydrologic submodel, and was responsible for developing data processing procedures, and for acquisition of hydrologic data.

Neal P. Dixon—developed the water quality submodels, and was responsible for water quality sampling and analyses (Mr. Dixon's doctoral dissertation was based upon his contributions to the project).

TABLE OF CONTENTS

Chapter I

INTRODUCTION	1
Background	1
Need for modeling	1
Objective	1
Scope	2

Chapter II

PLAN OF OPERATION	3
Conspectus	3
The prototype system	3
Resolution	4
Submodels	4
Simulation algorithm	4

Chapter III

THE HYDROLOGY SUBMODEL	9
Model structure	9
Stochastic aspects	13
Hydrology modeling of the study area	13
Hydrology submodel results	15
Hydraulic considerations	15

Chapter IV

SALINITY SUBMODEL	23
Input conductances	23
Stream conductance	25
In-transit conductance changes	26
Reservoir routing	26
Simulation algorithm	26

Chapter V

STREAM TEMPERATURE SIMULATION	29
The temperature problem	29
Monthly water temperature simulation	29
Adjustment of discrete sampling data	34
Reservoirs	34
Algorithm for simulation	35
Diurnal water temperature simulation	37

Chapter VI

DISSOLVED OXYGEN SIMULATION 45

 In-transit changes 45

 Suspended BOD 47

 Determination of rate constants 48

 Discrete BOD loads in the Little Bear River 49

 Combination of hydrologic inputs 51

 The annual cycle 51

 Inputs 52

 Reservoir effects 55

 Simulation algorithm 55

 Diurnal dissolved oxygen 58

 Diurnal patterns of hydrologic inputs 61

 Reservoirs 63

 In-transit changes and the diurnal effect 64

 Simulation algorithm 64

Chapter VII

EXPLORATION FOR A COLIFORM SUBMODEL 69

 Literature search 69

 Alternatives considered 70

Chapter VIII

SIMULATION RESULTS—LITTLE BEAR RIVER 73

 System delineation 73

 Establishing model coefficients 73

 Electrical conductance 73

 Monthly water temperature 74

 Monthly dissolved oxygen 74

 Diurnal water temperature 76

 Diurnal dissolved oxygen 77

 Verification of model constants and coefficients 77

 Electrical conductance 78

 Monthly water temperature 78

 Monthly dissolved oxygen 78

 Diurnal water temperature 79

 Diurnal dissolved oxygen 79

Chapter IX

SUMMARY AND CONCLUSIONS 83

LITERATURE CITED 85

APPENDIX A: DESCRIPTION OF THE PROTOTYPE SYSTEM	A-1
Location and geography	A-1
Geology	A-1
Climate and hydrology	A-1
Canal diversions	A-1
Reservoirs	A-1
Cultural development	A-6
Sources of pollution	A-9
APPENDIX B: DATA COLLECTION SYSTEM	B-1
Stream gaging	B-1
Weather observation	B-1
Weekly quality sampling	B-1
Continuous quality monitoring	B-7
Quality of data	B-7
APPENDIX C: WATER QUALITY DATA PROCESSING PROGRAMS—	
for discrete sample data	C-1
1. QULPRT, Specific instructions	C-1
2. SCAN, Specific instructions	C-1
3. PRTPLT, Specific instructions	C-3
APPENDIX D: FOURIER SERIES CURVE FITTING	D-1
APPENDIX E: OPERATION OF THE WATER QUALITY SIMULATION MODEL	E-1
The program	E-1
Computer requirements	E-1
Program options	E-2
Data requirements	E-2
System definition	E-2
Equilibrium temperature	E-2
Diurnal temperature and D.O. model parameters	E-2
Hydraulic relationships	E-2
Monthly water quality submodel parameters	E-2
Reservoir data	E-3
Atmospheric data	E-4
Monthly data	E-4
APPENDIX F: COMPARISON OF OBSERVED AND SIMULATED 1968	
WATER QUALITY PROFILES	F-1
APPENDIX G: HYDROLOGY MODEL COMPUTER PROGRAMS—(1) HYDRO,	
(2) BUDGET—INSTRUCTIONS FOR USE	G-1
APPENDIX H: STATISTICAL ANALYSIS OF LITTLE BEAR RIVER WATER QUALITY	
DATA	H-1
The broad spectrum search	H-1
Specific parameter models	H-4
Summary	H-4

LIST OF FIGURES

Figure	Page
1 One branch system schematic	5
2 Typical nonreservoir reach flow components	5
3 System control model simulation procedure	6
4 Hydrologic model schematic of a water resource system	10
5 Flow chart for hydro model	11
6 Two hydrologic subareas	14
7 Temperature comparisons—Utah State University Climatological Station and E. K. Israelsen Farm in Hyrum	15
8 Phreatophyte growth stage coefficient curves	17
9 Gaged and computed outflows for both hydrologic subareas	19
10 Specific electrical conductance vs. discharge for station S-27.0 on the Little Bear River	25
11 Simulation algorithm for electrical conductance submodel	28
12 Typical annual stream temperature variation at station S-12.8	30
13 Annual stream temperature variation at SEC-4.3 below Porcupine Reservoir with best fit four-term Fourier series curve	35
14 Simulation algorithm for monthly water temperature	36
15 Water temperature variations for the period 22-29 April 1968 with Fourier series model	38
16 Annual variations in diurnal temperature index model parameters	39
17 Diurnal temperature index models for each month of the year	41
18 Comparison of stream temperature index patterns on the Little Bear River at Wellsville and Paradise on 11-12 Oct. 1968	41
19 Graphical representation of diurnal temperature computations	42
20 Simulation algorithm for diurnal water temperature	44
21 Dissolved oxygen variations at station S-12.8 for 1966-67 with best fit Fourier series curve	47

22	BOD survey below trout farm	50
23	Sphaerotilis growth on rocks downstream from trout farm discharge	51
24	BOD variations at station S-12.8 for 1966-67 with best fit Fourier series curve	52
25	Annual BOD cycle, station S-12.8	54
26	Comparison of D.O. concentrations observed below Porcupine Reservoir in 1967 with saturation concentration	55
27	Generalized monthly D.O. flow chart	57
28	Dissolved oxygen variations for the period 22-29 April 1968 with Fourier series model	59
29	Annual variation in diurnal D.O. index model parameters	60
30	Diurnal D.O. index curves for each month of the year	62
31	Comparison of D.O. index patterns on the Little Bear River at Wellsville and Paradise on 11-12 October 1968	62
32	Flow and strength variations in domestic waste	63
33	Graphical representation of diurnal D.O. computation	65
34	Generalized flow chart for diurnal D.O. simulation	67
35	Space profile of log (coliform count) for 11 September 1968	70
36	Annual variation in log (coliform count) at station S-12.5 for 1966-67	70
37	Log (coliform count) vs. stream temperature (station S-12.8)	71
38	BOD deviation vs. log (coliform) deviation (station S-12.8)	72
39	Little Bear River system schematic	73
40	Electrical conductance correspondence graphs for stations SEC-4.3, S-24.6, S-21.3 and S-12.8 from the final model development run (1966-67 data)	75
41	Comparison of observed and simulated electrical conductance profiles for January and July, 1967	75
42	Water temperature correspondence graphs for stations SEC-4.3, S-24.6, S-21.3 and S-12.8 from the final model development run (1966-67 data)	75
43	Comparison of observed and simulated water temperature profiles for January and July, 1967	75
44	Dissolved oxygen correspondence graphs for stations SEC-4.3, S-24.6, S-21.3 and S-12.8 from the final model development run (1966-67 data)	76
45	Comparison of observed and simulated D.O. profiles for January and July, 1967	76
46	May 1967 diurnal water temperature index pattern for station S-12.8	77

47	May 1967 diurnal dissolved oxygen index pattern for station S-12.8	77
48	Electrical conductance correspondence graphs from the model verification run (1967-68 data)	78
49	Comparison of observed and simulated electrical conductance profiles for January and July 1968	78
50	Annual electrical conductance distribution of stations S-12.8 and SEC-1.4	79
51	Water temperature correspondence graphs from the model verification run (1967-68 data)	79
52	Comparison of observed and simulated water temperature profiles for January and July, 1968	80
53	Annual water temperature distribution at stations S-12.8 and SEC-0.4	80
54	Dissolved oxygen correspondence graphs from the model verification run (1967-68 data)	81
55	Comparison of observed and simulated D.O. profiles for January and July, 1968	81
56	Annual dissolved oxygen distribution at stations S-12.8 and SEC-0.4	82
57	May 1968 diurnal water temperature index pattern for station S-12.8	82
58	May 1968 diurnal dissolved oxygen index pattern for station S-12.8	82
A-1	Little Bear River study area	A-3
A-2	Representative east-west geologic section of Cache Valley and watershed	A-5
A-3	Average monthly atmospheric temperatures for stations near the Little Bear River basin	A-5
A-4	Average monthly precipitation for stations near the Little Bear River basin	A-6
A-5	Normal annual precipitation isohyets for the Little Bear River basin	A-7
A-6	Mean monthly flow at two points on the Little Bear River	A-9
A-7	Canal system for Little Bear River system	A-10
B-1	Location of U.S.G.S. stream gaging stations	B-3
B-2	Location of water quality sampling stations	B-5
B-3	Temperature correction for conductivity bridge	B-9
B-4	Conductivity bridge calibration curve for standard samples at 25°C	B-10
C-1	Analysis summary sheet for individual water sample—sample output from QULPRT	C-1
C-2	Nomograph used in QULPRT to obtain percent dissolved oxygen saturation	C-2

C-3	List of water quality data by station for a given date—sample output from SCAN	C-3
C-4	List of water quality data by date for a given station—sample output from SCAN	C-4
C-5	Graphical display of water quality data by station for a given date—sample output from PRTPLT	C-5
C-6	Graphical display of water quality data by date for a given station—sample output from PRTPLT	C-6
C-7	Program listing of QULPRT—and input data set-up for run	C-7
C-8	Deck set-up for QULPRT data input	C-10
C-9	Program listing of SCAN—and input data set-up for a run	C-11
C-10	Deck set-up for SCAN data input	C-13
C-11	Program listing of PRTPLT—and input data set-up of run	C-14
C-12	Deck set-up for PRTPLT data input	C-16
D-1	Graphical representation of a two-term Fourier series	D-1
E-1	WAQUAL computer program listing	E-5
E-2	Sample WAQUAL data deck	E-9
E-3	Sample WAQUAL output	E-10
F-1	Comparison of observed and simulated 1968 electrical conductance profiles	F-1
F-2	Comparison of observed and simulated 1968 stream temperature profiles	F-3
F-3	Comparison of observed and simulated 1968 dissolved oxygen profiles	F-5
G-1	Schematic diagram of hydrologic mass balance model	G-2
G-2	HYDRO-BUDGET computer program flow chart	G-3
G-3	Deck set-up for running HYDRO or BUDGET	G-18
G-4	Listing of program HYDRO with data input and program output	G-19
G-5	Listing of program BUDGET with data deck set-up	G-25
G-6	Sample output for BUDGET	G-32
H-1	Venn diagram for a four variable system with X_2 as the dependent variable	H-2

LIST OF TABLES

Table	Page
1 Water related land use acreage for the Paradise and Wellsville subareas of the Little Bear River basin	16
2 Flow values in cfs for use in the water quality submodels	20
3 Relationship of electrical conductance to rate of discharge on the Little Bear River system	24
4 Electrical conductance at groundwater sampling points	26
5 Representation of annual changes in mean daily water temperature	31
6 Prediction of stream temperatures from atmospheric temperatures	32
7 Annual temperature variations of groundwater	32
8 Summary of mean monthly temperature equations for hydrologic inputs	34
9 Heat exchange coefficients	34
10 Diurnal temperature index (DTI) model parameters	38
11 Representation of annual changes in diurnal water temperature index model parameters	40
12 Estimated monthly values of diurnal temperature index model parameters	40
13 Diurnal temperature input models	40
14 Fourier series modeling of annual fluctuations in dissolved oxygen concentration	53
15 Fourier series modeling of annual variations in BOD (5 day, 20°C)	54
16 Summary of input D.O. and BOD equations over the annual cycle	56
17 Diurnal dissolved oxygen index model parameters	59
18 Representation of annual changes in diurnal D.O. index model parameters	61
19 Estimated monthly values of diurnal D.O. index model parameters by Equation 54 using coefficients from Table 18	61
20 Little Bear River reach description	74
A-1 Characteristics of Little Bear River system, Cache Valley, Utah	A-2
A-2 Grazing use patterns on watershed area	A-11

A-3	Estimated livestock numbers in pastures immediately adjacent to streams	A-11
B-1	Surface water gaging stations	B-1
B-2	Weather observation stations	B-2
B-3	Little Bear River water quality sampling stations	B-2
B-4	Groundwater sampling stations	B-7
C-1	Input data cards for program QULPRT	C-9
C-2	Input data cards for program SCAN	C-13
C-3	Input data cards for program PRTPLT	C-15
E-1	WAQUAL subprograms	E-1
E-2	Summary of simulation model dimensions	E-2
E-3	WAQUAL simulation model data deck set up	E-11
G-1	Notation used in HYDRO and BUDGET computer programs	G-7
G-2	Preparation instructions for Group I input cards	G-10
G-3	Preparation instructions for Group II input cards	G-12
G-4	Preparation instructions for Group III input cards for data vectors	G-15
G-5	Iteration specification codes (ISENS) that may be selected for HYDRO	G-16
H-1	Example of correlation coefficient table (A) and corresponding table of coefficients of determination (B)	H-1
H-2	Correlation table for 25 variables, using data composite from three stations on the Little Bear River	H-3
H-3A	Composite data from the three stations, S-12.5, S-15.2, and S-27.5	H-5
H-3B	Data from station S-12.5, 63 observations	H-5
H-3C	Data from station S-15.2, 54 observations	H-6
H-3D	Data from station S-27.5, 30 observations	H-6
H-4	Summary of results of regression analysis for four quality parameters	H-7

NOTATIONS

Symbol	Definition
A	Fourier series phase angle shift (radians)
a	regression coefficient
A_f	cross-sectional area of flow (sq. ft.)
A_q	antecedent flow index $\left(\frac{30 \sum_{d=1}^{30} Q_d}{d} \right)$
b	regression exponent
\overline{BOD}	mean monthly biochemical oxygen demand (mg/l)
\overline{BOD}	mean annual biochemical oxygen demand (mg/l)
C	Fourier series coefficient
cf	pressure correction factor for dissolved oxygen saturation concentration
C_s	dissolved oxygen saturation concentration (mg/l)
D	dissolved oxygen deficit (mg/l)
d	number of days counted back from the "k th" day
DDO _i	diurnal dissolved oxygen index (DO_i / \overline{DO})
DGW	interflow addition to groundwater during one time increment
DO	dissolved oxygen concentration (mg/l)
\overline{DO}	mean daily and mean monthly dissolved oxygen concentration (mg/l)
\overline{DO}	mean annual dissolved oxygen concentration
DTI	diurnal temperature index (T_i / \overline{T}) (mg/l)
E	equilibrium water temperature (°C)
e	naperian log base
EC	electrical conductance within a reach (μ mhos/cm)
ECB	electrical conductance of branch inflow (μ mhos/cm)
ECE	electrical conductance of waste discharges (μ mhos/cm)
ECGI	electrical conductance of groundwater inflows (μ mhos/cm)
ECIN	electrical conductance of combined reservoir inflows (μ mhos/cm)
ECIR	electrical conductance of irrigation return flows (μ mhos/cm)
ECS	electrical conductance of diffuse natural surface inflows (μ mhos/cm)
ECST	electrical conductance of water stored in surface reservoirs (μ mhos/cm)
f	constant
f	monthly consumptive use factor
g	regression coefficient
H	mean stream depth (ft.)
H _m	mean stream depth (meters)
h	regression coefficient
i	hour of the day, subscript
j	flow input designation
k	consumptive use coefficient
k_g	interflow groundwater decay constant
k_s	snowmelt constant
k_{sm}	snowmelt constant
K	$K_1 + K_r + K_3$
k_e	heat exchange coefficient (ft./hr.)
K_r	the difference between the actual in-stream deoxygenation rate constant and the laboratory rate constant (base e, day ⁻¹)
K_1	laboratory deoxygenation rate constant (base e, day ⁻¹)
k_1	laboratory deoxygenation rate constant (base 10, day ⁻¹)
K_2	re-oxygenation rate constant (base e, day ⁻¹)

k_2	reoxygenation rate constant (base 10, day^{-1})
K_3	rate constant for BOD removal by sedimentation and/or adsorption (base e, day^{-1})
K_4	rate constant for the anaerobic fermentation of organic benthic deposits (base e, day^{-1})
L_a	ultimate first stage BOD in solution and suspension (mg/l)
L_d	areal BOD of the benthic zone (g/sq. meter)
m	month of the year subscript, beginning with October
N	number of coliform bacteria left in the stream after a given time interval
N_o	maximum coliform density
n	coefficient of nonuniformity or retardation
nc	number of inflow components for a particular reach
O_p	photosynthetically produced oxygen (mg/l)
P	atmospheric pressure (millimeters of mercury)
p	rate of addition of BOD to the stream water from the benthose (mg/l \cdot day)
Pf	photosynthetic oxygen productivity factor (used as a scaling constant)
pv	vapor pressure (millimeters of mercury)
Q	rate of stream flow (cfs)
Q_c	groundwater contribution to flow (cfs)
Q_i	interflow contribution to flow (cfs)
Q_s	surface contribution to flow (cfs)
QBR	tributary branch inflow (cfs)
QD	diversions (cfs)
QEF	municipal-industrial effluent discharges (cfs)
QCI	groundwater inflow (cfs)
QIR	irrigation return flow (cfs)
QS	natural diffuse surface inflow (cfs)
q_j	discharge rate of the "j th" component of flow (cfs)
r	regression coefficient
R^2	coefficient of determination (percent of total variance explained by the model)
R_h	horizontal surface radiation index
R_s	the local radiation index
S	salinity
SM	snowmelt
s	exponent
ΔT	difference between mean monthly and snow threshold temperature
\bar{T}	stream temperature ($^{\circ}\text{C}$)
$\bar{\bar{T}}$	mean daily and mean monthly stream temperature ($^{\circ}\text{C}$)
T	mean annual stream temperature ($^{\circ}\text{C}$)
T_a	atmospheric temperature ($^{\circ}\text{F}$)
T_s	snowmelt threshold temperature
t	time (hours or days)
u	monthly consumptive use of the crop in inches
V	velocity of flow (ft./sec.)
VIN	monthly volume of reservoir inflow (acre-feet)
VOU	monthly volume of reservoir outflow (acre-feet)
VST	volume of reservoir storage (acre-feet)
w	average surface width for a river reach (ft.)
x	number of days since October first
y	number of coliform bacteria removed during the time of flow below the point of maximum bacterial density
τ_j	temperature of the "j th" component of flow ($^{\circ}\text{C}$)
$\bar{\tau}_j$	mean daily and mean monthly temperature of the "j th" component of flow ($^{\circ}\text{C}$)

CHAPTER I

INTRODUCTION

Background

River basin planning traditionally has been oriented toward water *quantity* considerations. Planning concepts, however, have evolved gradually in scope and comprehensiveness from the single project level to integrated river basin planning in a systems context (though methods for systems planning have yet to be assimilated formally into planning). Nevertheless, the existing legal structure and institutional framework are designed to support the traditional *quantity* planning procedures.

Comprehensive water *quality* planning developed separately with distinct legislation and administrative entities. Attention to quality began to expand about 1948 with federal legislation. The trend has been given added impetus by state and further federal legislation since that date. A legislative paradox exists, however, in that western water law and traditions of beneficial use are not cognizant of some of the values implicit in recent water quality legislation.

The intensity of river basin development has now increased to such a level that quantity depletion and quality degradation seriously impair both the diversity of uses and the total amount of use. Thus the quality dimension has emerged as one of the paramount factors in water planning, concomitant with the traditional quantity dimension.

Need for modeling

A dichotomy now exists between quantity and quality in legislation, in institutions, in planning concepts and criteria, and in the respective professional disciplines. This dichotomy has been recognized in the Federal Water Quality Act of 1965, which authorizes planning grants to state water planning agencies who incorporate quality considerations in river basin planning. Also, since about 1965, reports in the literature and patterns of professional activities appear increasingly geared to quality-quantity duality. Incorporating the duality concept into practice is difficult, not only because of the traditions in legal and

administrative structures, but because it has not been articulated in terms of planning methodology.

Multiple water uses have to be assessed considering quantity-quality requirements and quality degradation for each use, the response of the stream to various quality inputs, and the behavior of the stream in its natural state. This implies the need for a comprehensive river basin model that can simulate the quality-quantity characteristics of the stream and adjacent uses. Such a model of the physical system, while it does not totally satisfy the need for an overall planning approach, does constitute a significant step in that direction. With such a model, planning alternatives can be assessed in terms of desired goals whether this be maximizing water diversions, maintenance of quality, evaluating water quality standards, suggesting alterations in the water rights structure, or examining economic response to imposed alternatives in quality-quantity behavior.

In this report, the development of a water quality-hydrology simulation model is demonstrated, which has at least partial capability for usefulness in the manner described above. The demonstration of methodology of the model development is felt to be more important than the model *per se*.

Objective

The goal in this study was to demonstrate the development of a river basin hydro-quality simulation model, utilizing known principles and knowledge where possible. The model was to simulate the water quality time profile for any given station, or the water quality distance profile along the main channel for a given time. The model should be responsive in time and the one-dimensional space of the stream channel to atmospheric and hydrologic conditions and to time varying waste discharges at various points in the system. Actual field data from a selected prototype river basin system was used to develop and verify the model. The tenor of the study was entirely pragmatic in all respects: the model development dealt with real data and the resulting model was expected to be problem oriented in its potential.

Scope

Although the model is developed for a specific prototype system, the Little Bear River in this case, the approach, the methods, and the conceptual framework can be transferable to other systems, hopefully with less effort than needed for the original study. The model is deterministic in nature. The stochastic nature of some inputs such as atmospheric temperature and basin inflows has not been simulated, though the model could accommodate this feature.

The quality parameters selected for simulation include specific electrical conductivity, dissolved oxygen, and temperature, BOD, and coliform count. Although not a complete definition of water quality, these parameters: (1) are reasonably representative of the range in *types* of water quality parameters, with respect to stream behavior and nature of the parameter; (2) are significant measures

of water quality, and (3) could be measured. Item (1) is particularly important because a *pattern of modeling* can be established which is reasonably representative of important water quality parameters. The modeling effort for the latter two parameters, BOD and coliform count, was not as exhaustive as for the first three, primarily because of time limitations and the less certain promise of success.

The development of equations for individual water quality parameters is not a primary goal of this study as long as reasonably adequate relationships are available. Therefore, when previously developed equations satisfactorily represented the behavior of a given parameter (as determined by their application to data gathered from the prototype system) they were incorporated into the overall river basin simulation model, as individual parameter submodels. When available relationships did not appear to fit the prototype data, or if no suitable submodel was found, a relationship was developed if this was feasible.

CHAPTER II

PLAN OF OPERATION

Conspectus

Very grossly, the development of the water quality simulation model consisted of defining the following elements.

1. The prototype system. The river basin system was defined with respect to all characteristics that might relate to the quality-quantity response in the main stream. The process included obtaining all relevant hydrologic data, delineating agricultural patterns, and defining waste inputs. In addition, a monitoring program was established to measure surface inflows and outflows, climatological data, and to sample water quality at important spatial node points at regular time intervals.

2. Parameter simulation. For each of the water quality parameters simulated, relationships from the literature were utilized insofar as possible. The first year data from the prototype system were used to determine the most suitable equations and to define coefficients.

3. Hydrology submodel. The system hydrology was developed as a model responsive to inputs of surface inflow and capable of yielding any flow quantities (groundwater or surface) required for simulation of the water quality parameters.

4. Simulation algorithm. Each of the submodels was programmed in Fortran IV for incorporation into an algorithm for simulating the time and space behavior of each parameter. This algorithm comprises the hydro-quality simulation model.

The prototype system

The Little Bear River basin at the southern extremity of Cache Valley in northern Utah was selected as the prototype from which data were obtained for model development and verification. This basin was chosen because: (1) its size and definition permitted the meeting of data requirements; (2) problems of nominal magnitude exist in the basin, and its cultural characteristics, hydrologic features, and values of concern were of sufficient

variety to be of interest without any one dominating the system; (3) it is reasonably close to Logan.

This basin, described in detail in Appendix A, is a typical intermountain valley, encompassing some 245 square miles. The topography ranges from rolling to rugged with elevations from 4500 feet to 9445 (Figure A-1). The portion of the basin referred to herein as the valley floor generally lies below the 5000 ft. contour, with the area above this elevation being designated as the watershed.

The climate of the region is temperate and semi-arid, with well defined seasons. Monthly averages of mean daily temperature range from 21°F in January to 73°F in July at the nearby Logan, USU weather station (Figure A-3). Normal annual precipitation at this station is 16.6 inches per year, occurring primarily as winter snowfall and spring rains (Figure A-4). Figure A-5 shows the orographic influence of the mountains on the areal distribution of precipitation. Normal annual runoff is on the order of 50,000 acre feet per year, with the bulk of the runoff taking place during the spring snow melt period (Figure A-6).

The project area is predominantly agricultural, containing about 13,000 acres that are farmed, of which 8,100 acres are irrigated. Hay, grain, pasture, and corn are the principal crops. Industries include a cheese plant, two meat packing plants, a rendering plant and a commercial fish farm. The streams, reservoirs, and mountain areas of the system sustain considerable recreational activity, consisting of trout fishing in the stream and the two reservoirs, and boating and water skiing at Hyrum Reservoir, Hyrum State Park. The watershed area and flood plain are heavily utilized for domestic livestock grazing. Tables A-1 and A-2 show estimated numbers and time distribution of grazing units on these areas.

Factors contributing to the organic, chemical, and thermal degradation of the water quality of this system include natural inputs, livestock grazing, return flows from agricultural irrigation, industry, municipal waste discharges, garbage dumps, and recreation. These inputs are both discrete and diffuse in nature.

The city of Wellsville discharges untreated domestic sewage from about one third of its 1500 population, combined with the liquid waste from the cheese factory located there, in a small stream that is tributary to the Little Bear River just below Wellsville. The discharge from the trout farm is the only other discrete input. The other two basin communities (Hyrum and Paradise) and their rural residents employ septic tanks and leach fields for waste disposal. Each of these towns maintains an open garbage dump on the bluffs along the river.

The data collection network established on or near the Little Bear River system is composed of eight stream-flow gaging stations, one reservoir stage observation point, five weather stations, 17 weekly water quality sampling stations and two continuous quality monitoring stations. The stream gaging network was designed to account for all surface flows into and out of the basin, plus changes in the main channel. The water quality monitoring system was set up to account for all discrete inputs in the main channel, and important changes in the channel such as reservoirs. These networks are described in detail in Appendix B. Locations and periods of record are shown in Figures B-1 and B-2 and Tables B-1 through B-4.

Resolution

Resolution has to do with the amount of detail in time or space which the model will provide. This must be consistent with needs and with funds of those applying the model. In this model, two levels of time resolution are used—the month and the hour. This was necessary to adequately describe dissolved oxygen and temperature, since they exhibit diurnal variations whose characteristics changed monthly. For electrical conductivity the month was an adequate time increment.

For the space resolution, the main channel and its immediate large tributaries was focused on with respect to water use. Thus the water quality submodels are oriented about the stream channel. The channel was divided into reaches with node points at the significant changes in the channel. This isolates reservoirs and marks discrete inputs into the main channel.

These resolutions in time and space were consistent with the pragmatic tenor of the study—fine enough to be useful but not so fine as to constitute an unwise expenditure of funds.

Submodels

A submodel is defined here as the set of equations and coordinating statements that simulate the behavior of a particular parameter in time and space. The parameters for which submodels were synthesized in this study are: (1) hydrology, (2) electrical conductivity, (3) temperature, and (4) dissolved oxygen. Attempts to develop BOD and coliform submodels were less successful.

Submodel equations were taken from the literature if they existed and were suitable. Considerations used in determining suitability included: (1) ease, feasibility, and cost of data procurement, (2) reliability in simulations using project data, and (3) mathematical complexity. When mathematical equations for phenomena behavior do not exist, such as in diurnal dissolved oxygen and temperature simulation, they were project-developed using project data. Pragmatism was the underlying philosophy, whether the equations ultimately used were project-developed or extracted from the literature and whether empirical or rational.

Equation coefficients and constants were established by regression analysis of first-year field data or by adjusting coefficients such that submodel output corresponded with field measurements. The latter approach was used almost exclusively in the hydrology submodel verification.

Sophistication in theory is justified herein only as (1) data requirements are realistic and obtainable, and (2) the results are commensurate with pragmatic objectives.

In each submodel, the solution consists of two basic parts: (1) the time variation in the respective quality parameters for the incoming flow components for each reach, and (2) the changes in the quality parameter along the reach. For each parameter, the alternative modeling approaches are reviewed, the modeling assumptions are outlined, the approach selected is justified in terms of field data from the Little Bear River, and the simulation algorithm is summarized. Thus, the phenomenological behavior of each component is described in terms of suitable mathematical descriptions and the logic for utilizing those mathematical descriptions in parameter simulation.

Simulation algorithm

The *system control model* is a set of statements designed to: (1) control the manner of operation of the individual submodels, (2) specify the inputs needed to operate the submodels, and (3) provide the necessary feedback between submodels. The Fortran IV program that accomplishes this is given the name WAQUAL. This program contains each of the five submodels.

The system control model embodies the river basin configuration shown in Figure 1, consisting of the main stem and any number of tributaries. The main stem and tributaries are divided into numbered reaches, ascending numerically in the upstream direction. Reservoirs may be included also.

Inputs to the typical nonreservoir reach, as sketched in Figure 2, are considered to be concentrated at the upstream end of the reach and may consist of any one or more of the following:

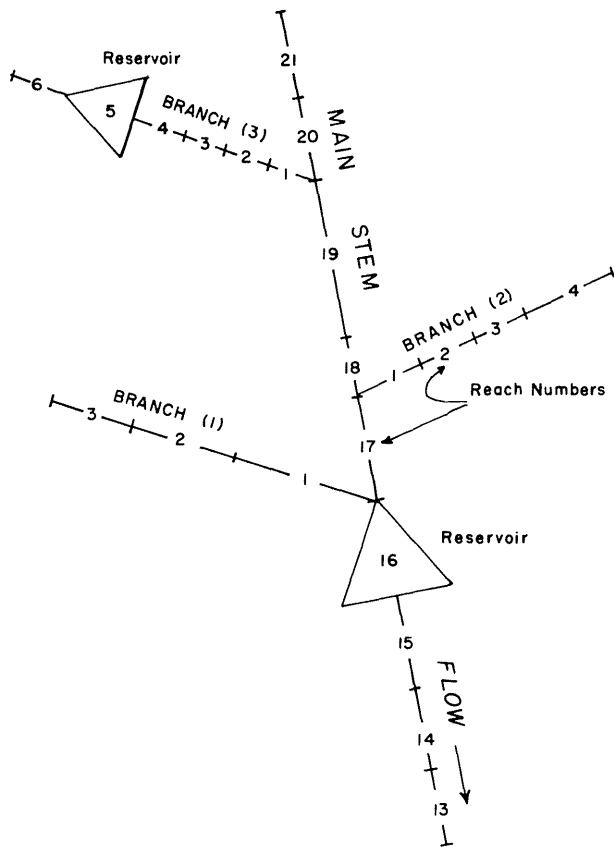


Figure 1. One branch system schematic.

- Q_{i+1} = stream inflow
- QS_i = natural diffuse surface inflow
- QGI_i = groundwater inflow
- QIR_i = surface irrigation return flow
- QBR_i = tributary branch inflow
- QEF_i = municipal-industrial effluent discharges
- i = reach designation

Outflows are assumed to be located at the downstream end of the reach. These outflows may consist of in-stream outflows (QS_i) or diversions (QD_i). All flows are monthly averages in cubic feet per second. In addition to the flows listed above, evaporation, direct precipitation, and change in storage must be considered in the hydrologic simulation of surface impoundments.

A generalized flow chart for the system control model is shown in Figure 3. The simulation begins at the upstream end of the main stem of the surface water system. Moving downstream, each reach is checked for tributary inflow. If a tributary discharges into this reach, control shifts to the upstream end of that tributary and proceeds with the simulation. As each reach is simulated, hydrologic data, describing all the various components of flow pertinent to that reach, are read into the computer. Next, the desired water quality subprograms are called. Subprograms that generate information required in the evaluation of other parameters are run first.

After all quality parameters are simulated for this reach, control passes to the next reach downstream and the process is repeated. When the last reach on a branch is completed, the main stem reach to which that branch is tributary is considered, with the outflow from the tributary branch becoming an inflow (QBR) to the new reach.

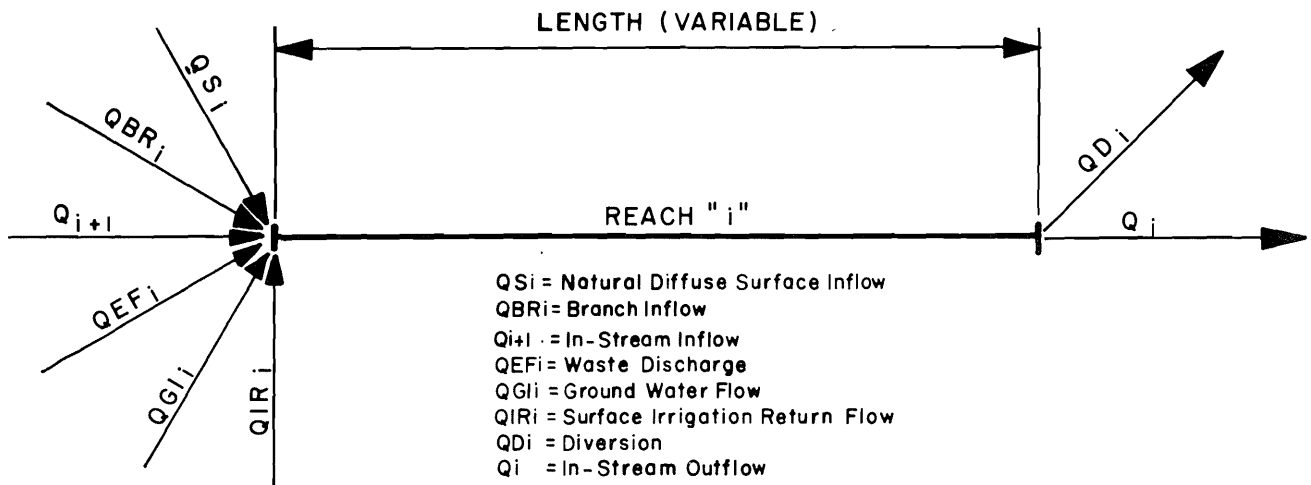


Figure 2. Typical nonreservoir reach flow components.

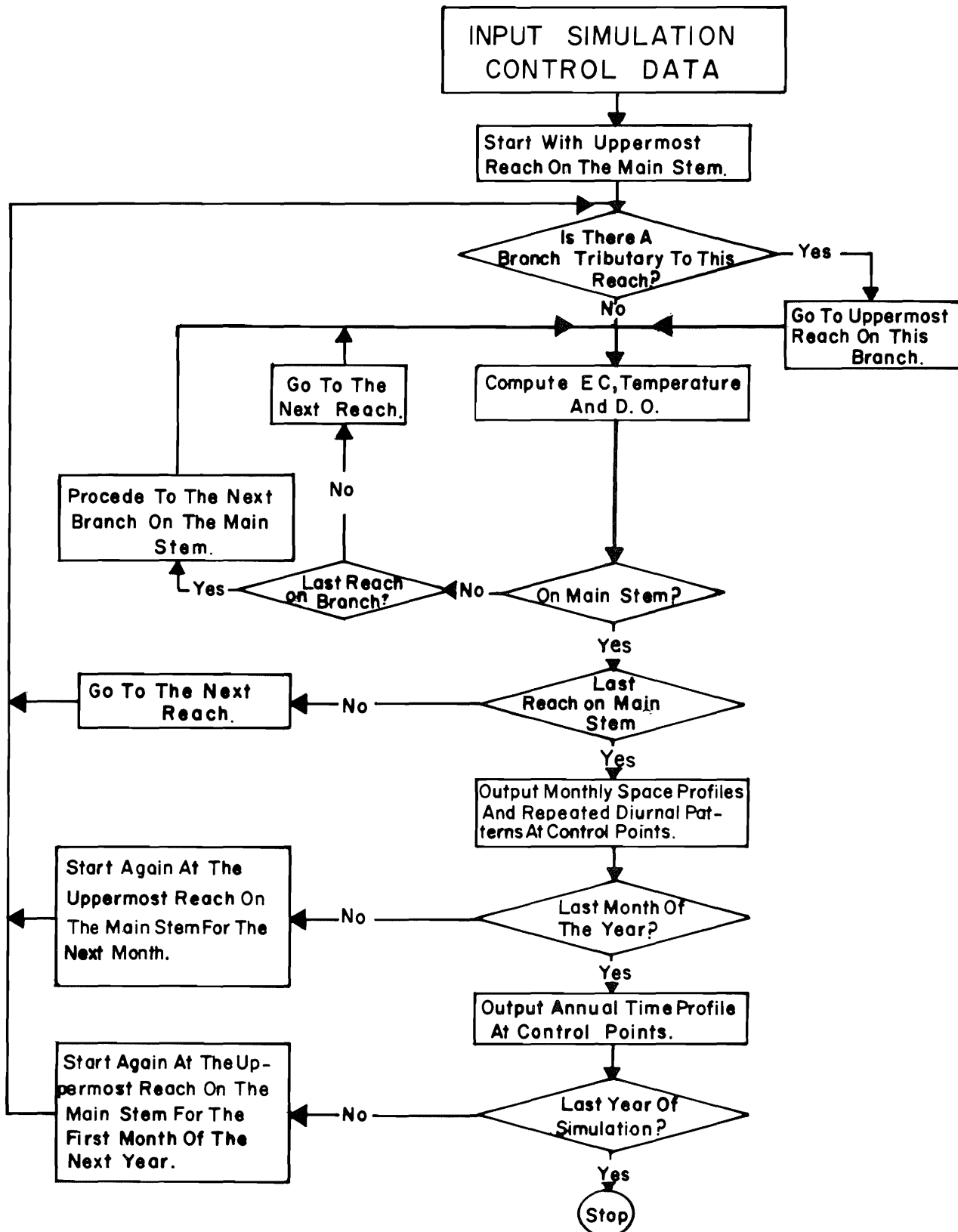


Figure 3. System control model simulation procedure.

After the last reach on the main stem has been simulated, monthly spatial profiles are printed out in tabular form as shown in Appendix E. These profiles list monthly average values for flow rate, conductivity, temperature, dissolved oxygen, BOD, and percent D.O. saturation at both ends of every reach, as well as the magnitude of these parameters in all hydrologic inputs to the reach. If diurnal representation of stream temperature and/or dissolved oxygen is requested, the predicted diurnal varia-

tions in temperature, dissolved oxygen, and percent D.O. saturation are printed out for each predesignated control point.

This procedure is followed until the entire period of simulation has been covered. In addition, annual time profiles of rate of flow, conductivity, temperature, D.O., percent D.O. saturation, and BOD are printed out for predesignated control points at the end of each year of simulation.

CHAPTER III

THE HYDROLOGY SUBMODEL

The hydrologic mass-balance submodel is a central component of the hydro-quality simulation model developed during the project. The hydrology submodel simulates the area through which the river flows and provides the quality submodels with the flow components that occur as tributary items along the channel. The criteria that had to be satisfied by the submodel were:

1. It had to simulate the hydrologic mass balance of a typical Utah river basin utilizing monthly climatological data, and to yield monthly streamflow data that could be input to the water quality submodels under concurrent development.
2. It had to identify and rapidly evaluate the hydrologic effect of alternative conditions that might or could be imposed upon the study area.

The equation of continuity,

$$\text{Output} = \text{Input} - \text{Changes in Storage} \quad \dots (1)$$

applied to the mass of water flowing within and through the geographic boundaries of the area provides the conceptual framework for the hydrology submodel. The size of the area to which this submodel may be satisfactorily applied is primarily limited by the degree of spatial resolution required to meet the overall objectives of a particular simulation effort.

For this study, system hydrologic inputs consist of precipitation (PREC), measured stream inflow in the main channel (RIF), measured surface imports (SIMP), and unmeasured surface and subsurface inflow (TIF). The cropland diversions (CD), reservoir storage (RES), municipal and industrial diversions (EMID) net consumptive municipal and industrial use (EMI), pumped water (PW), surface exports (EXPO), and air temperature (TEMP) are other variables supplied as input data to the model.

The system outputs consisted of reservoir evaporation (EVAP), cropland consumptive use (ACU), wetland consumptive use (AWLCU), surface exports (EXPO),

municipal and industrial consumptive use (EMI), surface outflow (SOF), and subsurface outflow (GWOF).

The hydrology submodel accounts for monthly changes in: reservoir storage (DRES), cropland soil moisture storage (ASMS), interflow groundwater storage (SGW), wetland soils moisture storage (AWLSM), and groundwater storage (DELGW).

The outflow values are obtained by routing and storing the input quantities through the four principal components of the system which are:

1. Surface water reservoirs
2. Cropland area
3. Interflow routing and groundwater storage
4. Wetland area

A schematic diagram of the hydrology submodel is shown in Figure 4 and a macro flow chart is included as Figure 5. A micro flow chart, computer program notation, data card preparation, user instructions, and problem solutions are given in Appendix G.

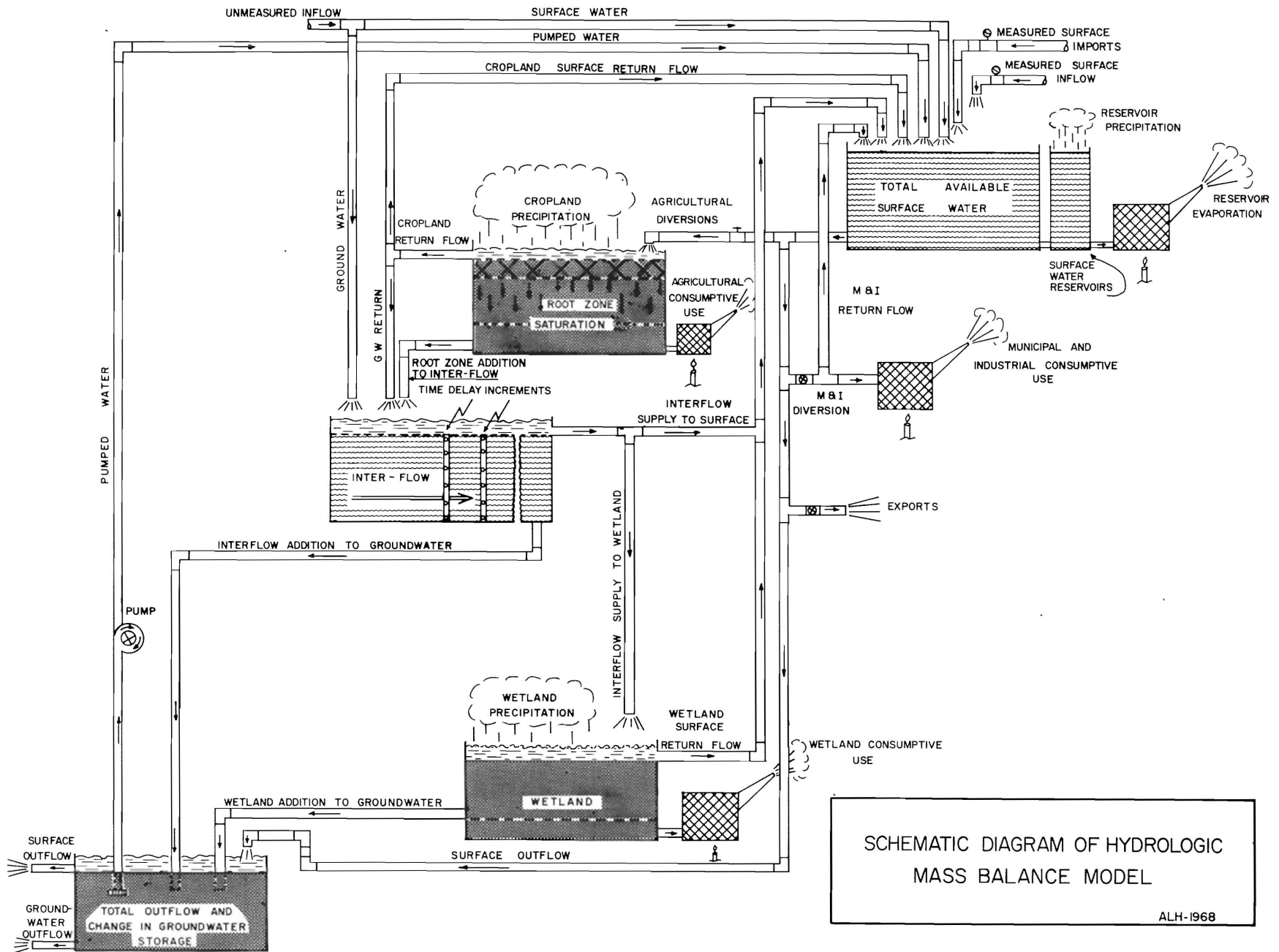
Model structure

In any simulation effort, each component of Equation 1 must be carefully selected and evaluated. The various components appearing in Figures 4 and 5 are described in the following paragraphs.

Precipitation

Precipitation is important to the surface reservoir, cropland, and wetland components of the submodel. Its allocation to rain or snow storage is achieved by comparing the mean monthly air temperature with a snow threshold temperature. Any precipitation occurring when the temperature is less than the threshold temperature is accumulated in snow storage and routed through a snow-melt equation of the form

$$SM = k_{sm} S(T_a - T_{sm}) \quad \dots (2)$$



SCHEMATIC DIAGRAM OF HYDROLOGIC
MASS BALANCE MODEL

ALH-1968

Figure 4. Hydrologic model schematic of a water resource system.

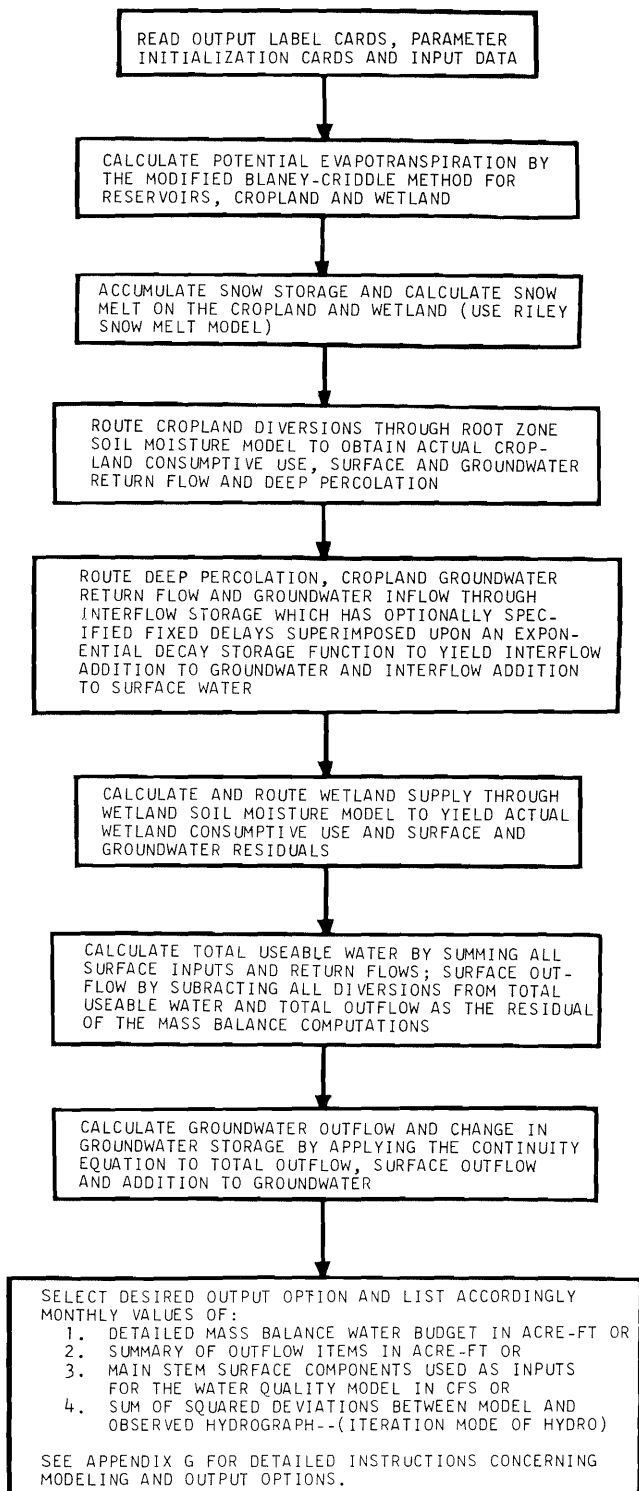


Figure 5. Flow chart for hydro model,

in which

- SM = snowmelt
- k_{sm} = a constant
- S = accumulated snow storage through the end of the month
- T_a = mean monthly air temperature in degrees F
- T_{sm} = snowmelt threshold temperature in degrees F

The rain and snowmelt are then routed through the cropland and wetland components of the system.

Consumptive use

The potential consumptive use by cropland and wetland and the potential evaporation from the reservoirs are obtained by using the method developed by Blaney and Criddle (1950) and modified by the U.S. Soil Conservation Service (1964). The basic Blaney-Criddle equation is:

$$u = kf \dots \dots \dots (3)$$

in which

- u = the monthly consumptive use of the crop in inches
- k = an empirically determined consumptive use crop coefficient
- f = a monthly consumptive use factor defined as the product of the mean monthly air temperature and the monthly proportion of daylight hours of the year (p)

The Soil Conservation Service modification consists of evaluating k as the product of two other coefficients k_t and k_c , where k_t is a climatic coefficient related to the mean monthly air temperature by the equation $k_t = 0.0173 T_a - 0.314$ and k_c is a coefficient reflecting the growth stage of the crop. Crop growth stage curves have been developed by the Soil Conservation Service (1964) for a variety of crops and phreatophytes.

Upon substituting the equivalent expressions for k and f, Equation 3 becomes:

$$u = k_c p (0.0173 T_a^2 - 0.314 T_a) \dots (4)$$

where all symbols are as defined previously.

The total potential consumptive use by the cropland and that by the wetland are obtained as the sum of the potential consumptive use by all crops and by all phreatophytes, respectively. These amounts are used as depletive factors in the routing and storage phases of the cropland and wetland components of the submodel. Potential water surface evaporation is treated similarly within the reservoir component of the system. The actual consumptive

use values may be less than the potential values if not enough water is routed into the soil moisture storage elements of the cropland and the wetland to satisfy the potential requirements. Any surplus water is used to fill the soil moisture storage to its capacity, after which the remaining surplus from the cropland component is routed through the interflow storage component of the model, and any surplus from the wetland soil moisture element is transferred to groundwater storage.

Interflow

Interflow groundwater storage includes water that is in transition between the surface and the groundwater basin and vice versa. The interflow component of the model causes a time delay and smoothing of the groundwater components of unmeasured inflow and cropland return flow and any surplus water or deep percolation from the cropland soil moisture storage. Two types of time delays are incorporated in the interflow equation. The first is a fixed time that is specified in monthly increments as a submodel parameter option. All water entering the interflow storage is held there until the specified time has elapsed unless the storage is at capacity, in which case the surplus is immediately routed to the surface supply. All water that has been in interflow storage for a time equal to or longer than the fixed delay is transferred to groundwater storage through the decay equation:

$$DGW_i = k_g [\bar{S}_{gw}] \dots \dots \dots (5)$$

in which:

- DGW_i = interflow addition to groundwater during time increment i
- k_g = interflow groundwater decay constant
- \bar{S}_{gw} = average amount of water that has been in interflow storage for a time equal to or greater than the fixed delay. This quantity is equal to one half of the sum of the quantity in storage at the beginning of the time increment and the storage at the end of the time increment or

$$\bar{S}_{gw} = 1/2 [TRI_i + (TRI_i + SGW_i - DGW_i)] \dots (6)$$

in which

- TRI_i = water in interflow storage longer than the fixed delay at the beginning of the time increment i
- SGW_i = water in interflow storage for a time equal to the fixed delay at the beginning of the time increment i

Upon substituting (6) for \bar{S}_{gw} in Equation 5 and solving for DGW Equation 5 becomes:

$$DGW_i = \frac{k_g}{2 + k_g} (2 TRI_i + SGW_i) \dots (7)$$

The values of the various quantities transferred from interflow storage must always be positive and a provision is available to transfer a minimum amount to groundwater storage during each time increment if the interflow storage meeting the time qualifications is large enough to satisfy it.

Groundwater. The groundwater basin is not modeled explicitly, but all items that go into or come from groundwater storage are accounted for, and the change in groundwater storage is identified. The groundwater outflow is usually treated as a submodel parameter and determined by iteratively operating the submodel until reasonable changes in groundwater storage are obtained. The submodel allows an estimate to be made of the proportion of the total annual residual that is groundwater outflow. If this option is used, the estimated annual groundwater outflow is proportionally distributed through the months of the year relative to the monthly groundwater additions.

M & I. Municipal and industrial flows were not simulated by a deterministic equation because of the great diversity of M & I users, each of which would require a separate equation. The hydrology submodel requires that the M & I diversions and net depletive use be entered as input data. The actual depletive or evapotranspirative use must be determined independently.

Other elements. The remaining elements of the submodel consist of measured or estimated values for the river surface inflow (RIF), the surface imports (SIMP), the surface exports (EXPO), the pumped water (PW), the gaged outflow (GFLO), the cropland or agricultural diversion (CD), and the unmeasured inflow (TIF). The values needed for the quality submodels are obtained by converting the required elements of the hydrology submodel from acre-feet per month to cubic feet per second. When W_i is the conversion coefficient for month i:

- Surface channel inflow (QI_i) = W_i RIF_i
- Unmeasured surface inflow (QS_i) = W_i STIF_i
- Groundwater to surface (QGI_i) = W_i (SINT_i + WLSFC_i)
- Total diversions (QD_i) = W_i (CD_i + EXPO_i + EMID_i)
- Cropland return flow (QIR_i) = W_i SRTF_i
- M & I effluent or return flow (QEF_i) = W_i EMIR_i
- Surface outflow (QO_i) = W_i SOF_i

These values are computed and obtained as optional output from the hydrologic submodel whenever specified.

Submodel parameters. Although each component and element of input data may, under specific circumstances, be treated as a submodel parameter, the para-

meters ordinarily consist of coefficients of routing functions, threshold values for selective routing, storage capacities and boundary conditions of the various submodel components. These parameters are explained in detail in the user instructions contained in Appendix G.

Stochastic aspects

The stochastic aspect of the hydrology submodel can be achieved by inputting historical data for a long period of years and then calculating the mean and standard deviation of every element in the resulting mass budgets. The entire output resulting from the historical data input is available for either calculating higher order moments to more fully characterize the distribution or ranking the data to obtain the empirical probability distributions.

The above method for obtaining stochastic information was selected because of major limitations in the other two methods that were considered. The first alternative method (inputting data, all having the same probability level of occurrence that had been derived from probability analyses) was rejected because of no satisfactory method for handling the interactions between the probability distributions of the various input elements such as precipitation, temperature, and streamflow.

The second alternative method evaluated used random process generating techniques to supply the input data to the model. This method was rejected because when these techniques were applied to Utah streams, they failed to synthesize realistic sequences of extreme events. Since these are the critical values about which information is needed, the validity of the method was questionable. A study which supports this conclusion is reported by Jeppson and Clyde (1969). Mandelbrot and Wallis (1968) have observed the same limitation and are working on techniques that may eventually improve the situation.

Two versions of the hydrology submodel were programmed (Appendix G). The same input data are used by both computer programs supplied in the same format. The first program (HYDRO) provides only one year of simulation but has the capability of iterating along many of the model parameters, which is helpful during the validation process. The other program (BUDGET) does not have the iteration capability but allows simulation of up to 30 years and provides a mean mass balance budget and standard deviation budget.

Hydrology modeling of the study area

The study area was divided into two subareas for hydrologic modeling purposes: one, called the Paradise subarea, ran from and including Porcupine Reservoir to the Paradise stream gage (10-1060) that is maintained by the U.S. Geological Survey; and the second, ran from the Paradise gage to the Wellsville stream gage (10-1076), and

is called the Wellsville subarea (Figure 6). These two subareas were selected because they both had gaged or observed streamflow data available for validating the submodel and because they were both close to the lower limit of resolution of the hydrology submodel and the available hydrologic data.

Hydrologic data collection and compilation

The input data necessary to operate the hydrologic submodel consists of streamflow, diversions, temperature and precipitation, soil water holding capacity, reservoir storage, well and spring flow, and land use data. Sources for these data included the U.S. Geological Survey, U.S. Weather Bureau, Utah State Engineer, U.S. Bureau of Reclamation, and the U.S. Soil Conservation Service.

Surface flow

Streamflow gages maintained by the U.S. Geological Survey provided input data for both subareas. For the Paradise subarea these were the gage above Porcupine Reservoir (10-1049) and the gage on the South Fork below Davenport Creek (10-1047). Gaging station 10-1060 provided input data for the Wellsville subarea as well as providing outflow values for validating the Paradise submodel. USGS gaging station 10-1076 provided the outflow data for validating the Wellsville submodel.

The Paradise subarea had one surface water export, the Hyrum Canal, carrying water to the Wellsville subarea. Flow data for the Hyrum Canal were obtained from the Little Bear River Water Commissioner's Annual Reports to the Utah State Engineer. Surface diversions to the cropland area were also obtained from the Little Bear River Water Commissioner's Annual Reports to the Utah State Engineer, as were the surface water storage data for Porcupine and Hyrum Reservoirs. The Wellsville subarea had two surface exports, the Wellsville East Field Canal near Hyrum and the Wellsville Mendon lower canal at Wellsville. Data for these were obtained from the USGS gages 10-1072 and 10-1074 respectively.

Precipitation

Precipitation data used for the hydrologic submodel were obtained from records of the U.S. Weather Bureau gage located at Utah State University. The isohyetal map of Utah prepared by the U.S. Weather Bureau and published in the "Hydrologic Atlas of Utah" (Jeppson et al., 1968) showed that the Logan USU gage would adequately represent the precipitation on the study area.

Temperature

The temperature values used in the consumptive use component of the hydrologic submodel were obtained from the records of the U.S. Weather Bureau station (Logan USU) that is located at Utah State University.

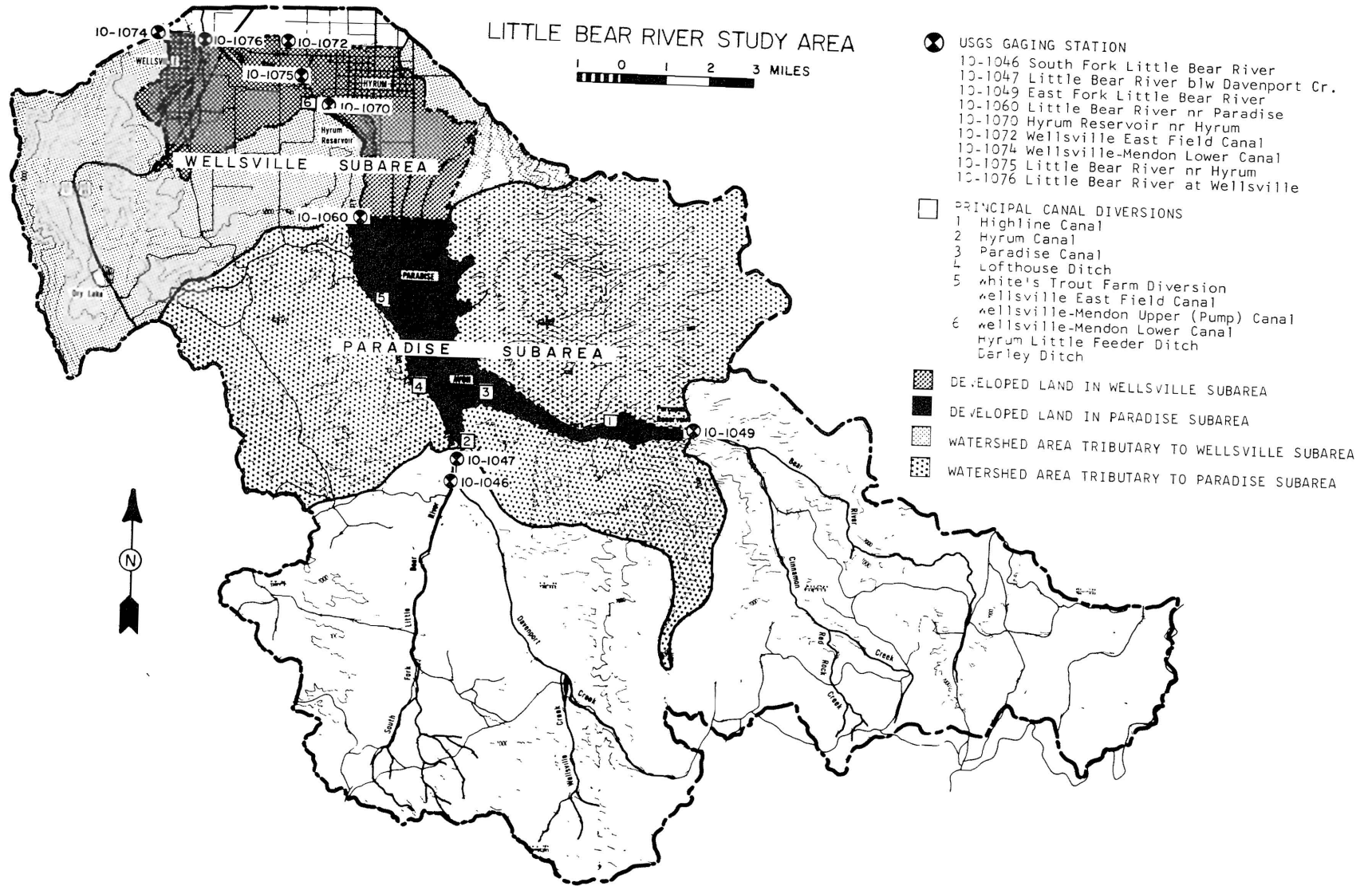


Figure 6. Two hydrologic subareas.

These data were used because a comparison of the mean monthly maximum and minimum temperatures at Logan USU and at the E. K. Israelsen farm near Paradise (Figure 7) indicated that the USU data were sufficiently representative of the model area to be used without adjustment.

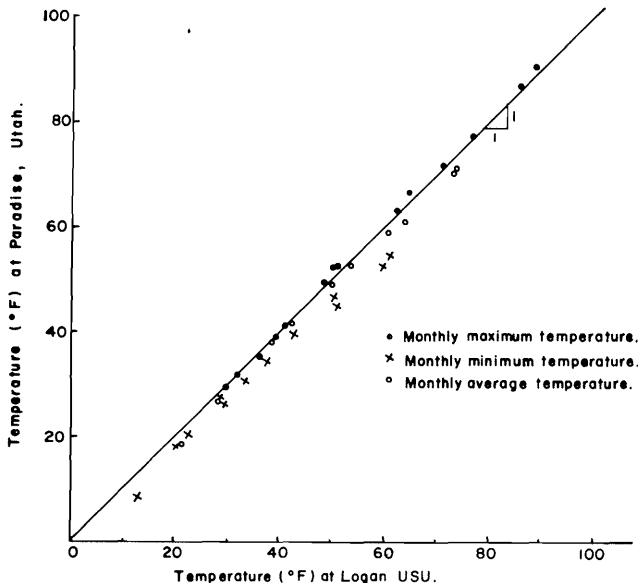


Figure 7. Temperature comparisons—Utah State University Climatological Station and E. K. Israelsen Farm in Hyrum.

Land use

There are eight crop categories; data for determining acreages were obtained from the report "Water Related Land Use in the Bear River Drainage Area" by Haws (1969). Data on the five classes of phreatophyte uses in the wetlands and the surface water evaporating from the two reservoirs (Table 1) were also obtained from Haws (1969).

The growth stage coefficient curves for the crops, phreatophytes and water surface were modifications of those developed by the Soil Conservation Service (1964) for California. The information contained in Technical Publication No. 8 of the Utah State Engineer (1962) was utilized in effecting the modifications. The growth stage coefficient curves developed for use in the submodel are given in Figure 8.

Unmeasured or tributary inflow

The first values used for the unmeasured or tributary inflow were those obtained from the mean annual iso-runoff map in the "Hydrologic Atlas of Utah"

(Jeppson et al., 1969). The map shows runoff distributed through the months and proportioned by the year at the same level as the sum of the two virgin gaged inflows to the Paradise subarea. Model validation could not be achieved with these data. The values that were finally used were obtained by treating unmeasured inflow as a model parameter until validation was achieved. The resultant values were then extended to obtain monthly proportionality coefficients for relating unmeasured inflow to measured inflow. The measured inflow to the Paradise subarea was used as the basis for estimating the unmeasured inflow in both subareas because it represented virgin flow conditions.

Municipal and industrial use

Apart from agricultural uses which were explicitly modeled by the cropland component of the submodel, the only significant M & I diversion in the Paradise subarea consisted of a trout farm. Input data for this element of the model were derived from actual measurements of the diversion and return flows where these occurred within the system. The Wellsville subarea had one effluent point (the Wellsville stream) which was also measured and thus provided the input data for the M & I component of that subarea.

Hydrology submodel results

After collecting the records from various sources, the data were prepared for input to the computer. As the validation process proceeded, some of the basic data were found to be in error and thus had to be changed. However, the process by which the errors were discovered aided materially in understanding the systems.

The general procedure followed in validating the hydrology submodel was to first achieve a balance in the annual figures and then work on the monthly distribution. By iteratively operating the submodel, validation was achieved (Figure 7). Figure 9 gives a comparison between the gaged and computed outflow for both subareas for the water years 1967 and 1968. A summary of the flow values generated for the water quality submodels is given in Table 2. A complete listing of the input data, water budgets, consumptive use calculations, and water quality hydrologic data is included in Appendix G.

Hydraulic considerations

In-transit changes in water quality often depend directly upon the mechanics of flow in the stream. The reaeration coefficient of the dissolved oxygen model is dependent upon velocity and depth of flow; the rate of temperature change depends upon, among other things, the surface area of the stream; and time of travel through a reach is determined by the velocity of flow. Because of these dependencies, depth and velocity of flow and surface width must be defined.

Table 1. Water related land use acreage for the Paradise and Wellsville subareas of the Little Bear River basin.^a

CROPLAND					
Crop	Mnemonic	Paradise Acres	Subarea Percent	Wellsville Acres	Subarea Percent
Alfalfa	ALFALF	1094	29.7	2657	28.4
Pasture	PASTRE	692	18.8	1824	19.5
Hay	HAY	169	4.6	215	2.3
Grain	GRAIN	932	25.3	2311	24.7
Corn	CORN	122	3.3	253	2.7
Sugar Beets	BEETS	52	1.4	94	1.0
Truck Crops	TRUCK	85	2.3	150	1.6
Idle Land	UR-IDL	538	14.6	1852	19.8
Cropland Total		3683	100.0	9355	100.0
WETLAND					
Phreatophyte	Mnemonic	Paradise Acres	Subarea Percent	Wellsville Acres	Subarea Percent
Very Dense—very high water use	VRDNPH	155	9.1	216	13.5
Dense—high water use	DNSPHY	818	48.1	354	22.1
Medium—water use	MEDPHY	498	29.3	350	21.9
Light—water use	LTPHRY	229	13.5	374	23.4
Very light water use	VLTPHY	0	0.0	306	19.1
Wetland Total		1700	100.0	1600	100.0
Surface Water in Reservoir Storage (WATER) (acres)		193		372	
Total Area in Acres		5576		11,327	

^aData obtained from maps and tabulations given in *Water Related Land Use in the Bear River Drainage Area* by Haws (1969).

Figure 8A.

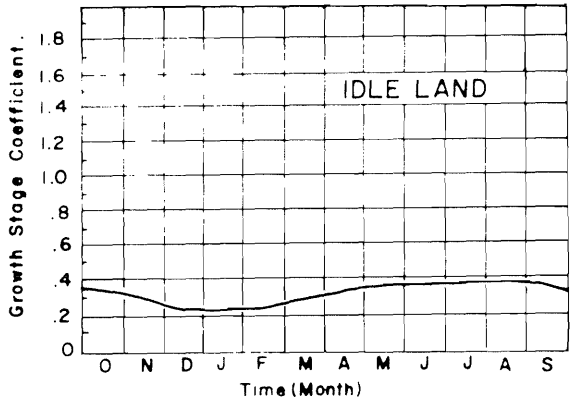
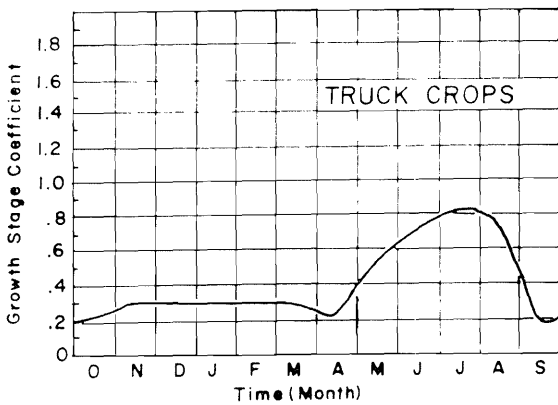
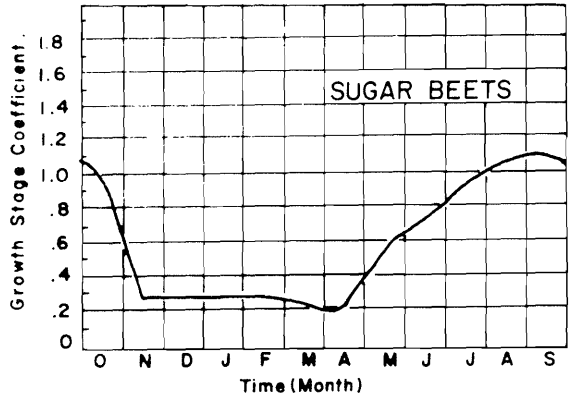
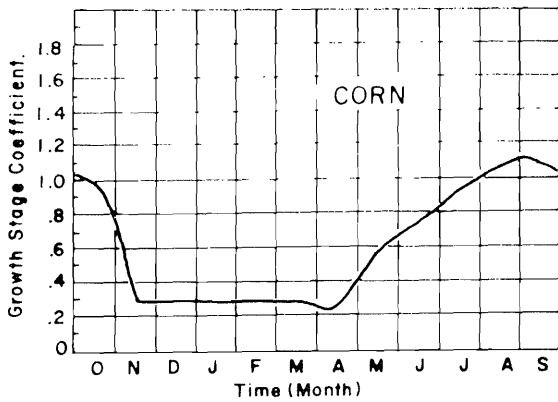
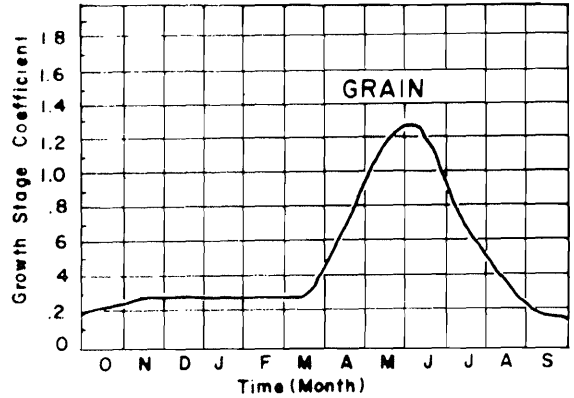
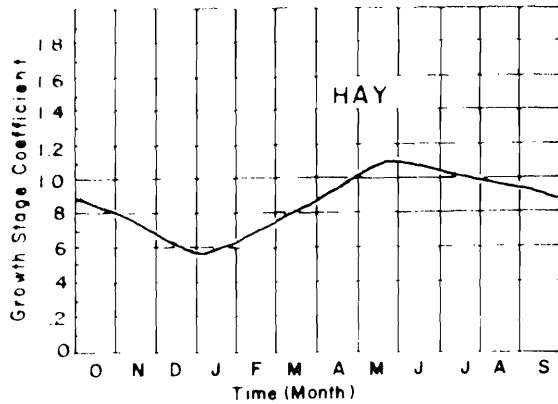
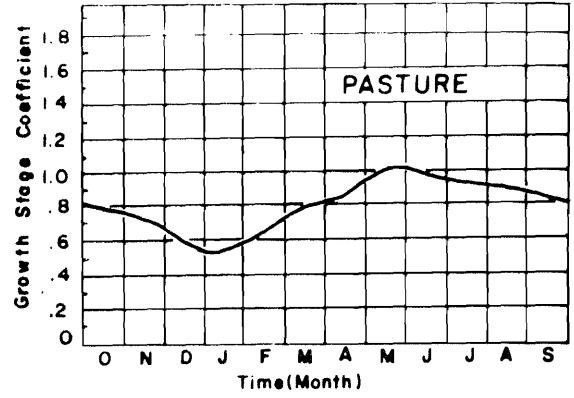
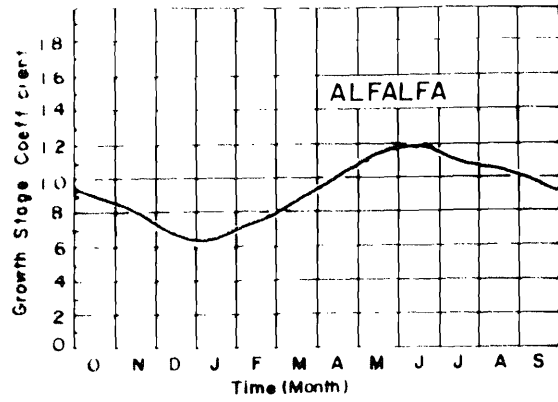


Figure 8. Phreatophyte growth stage coefficient curves.

Figure 8B.

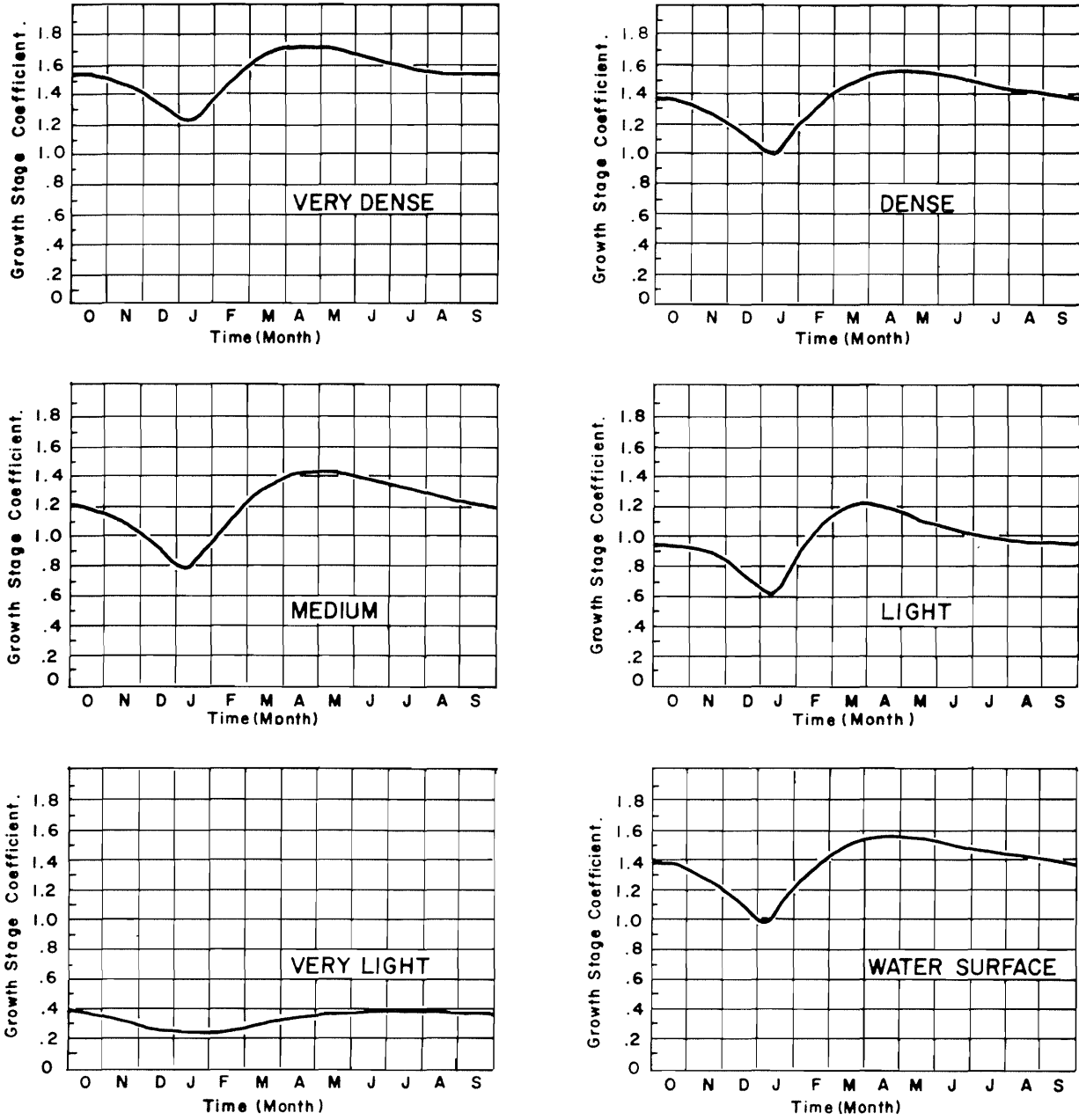


Figure 8. Continued.

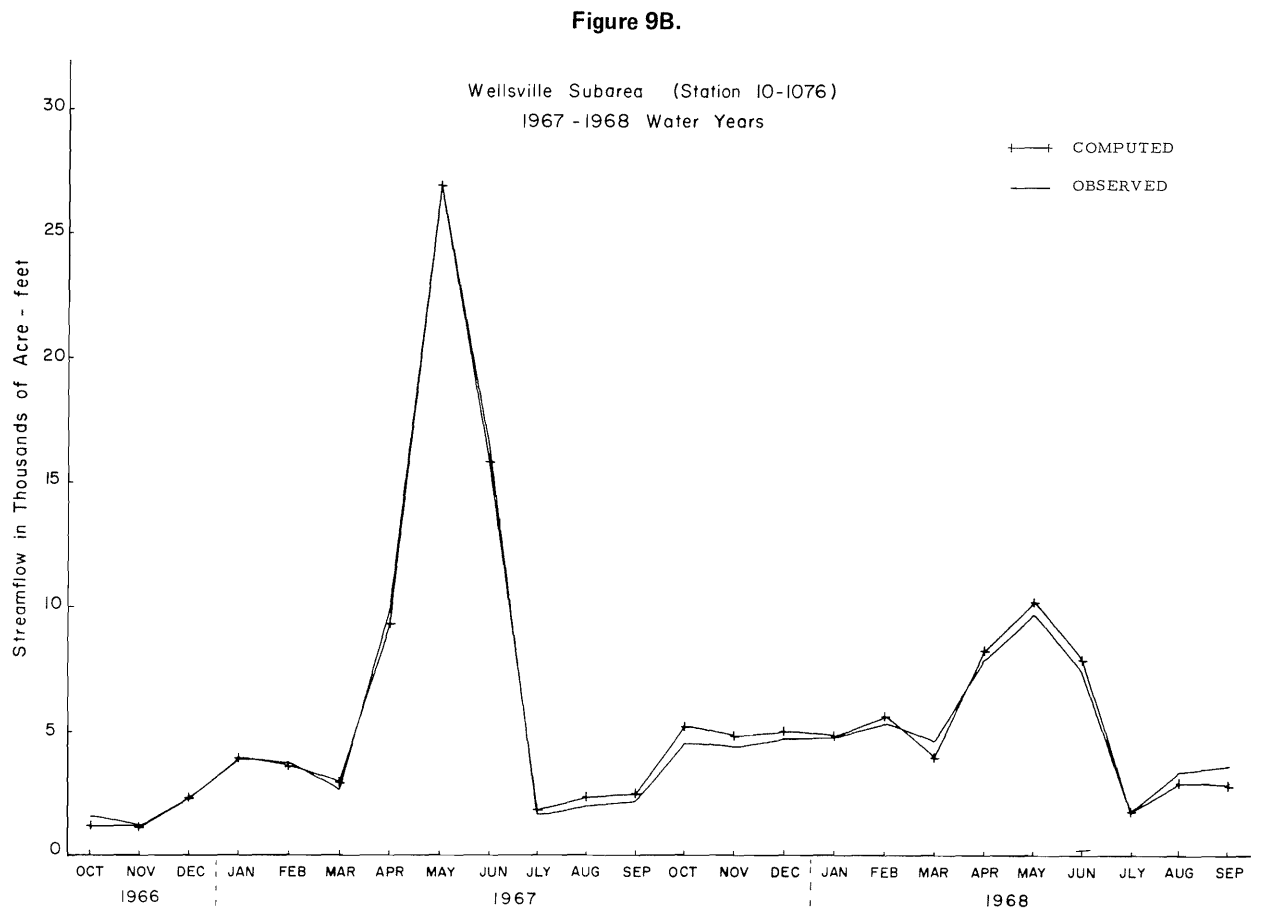
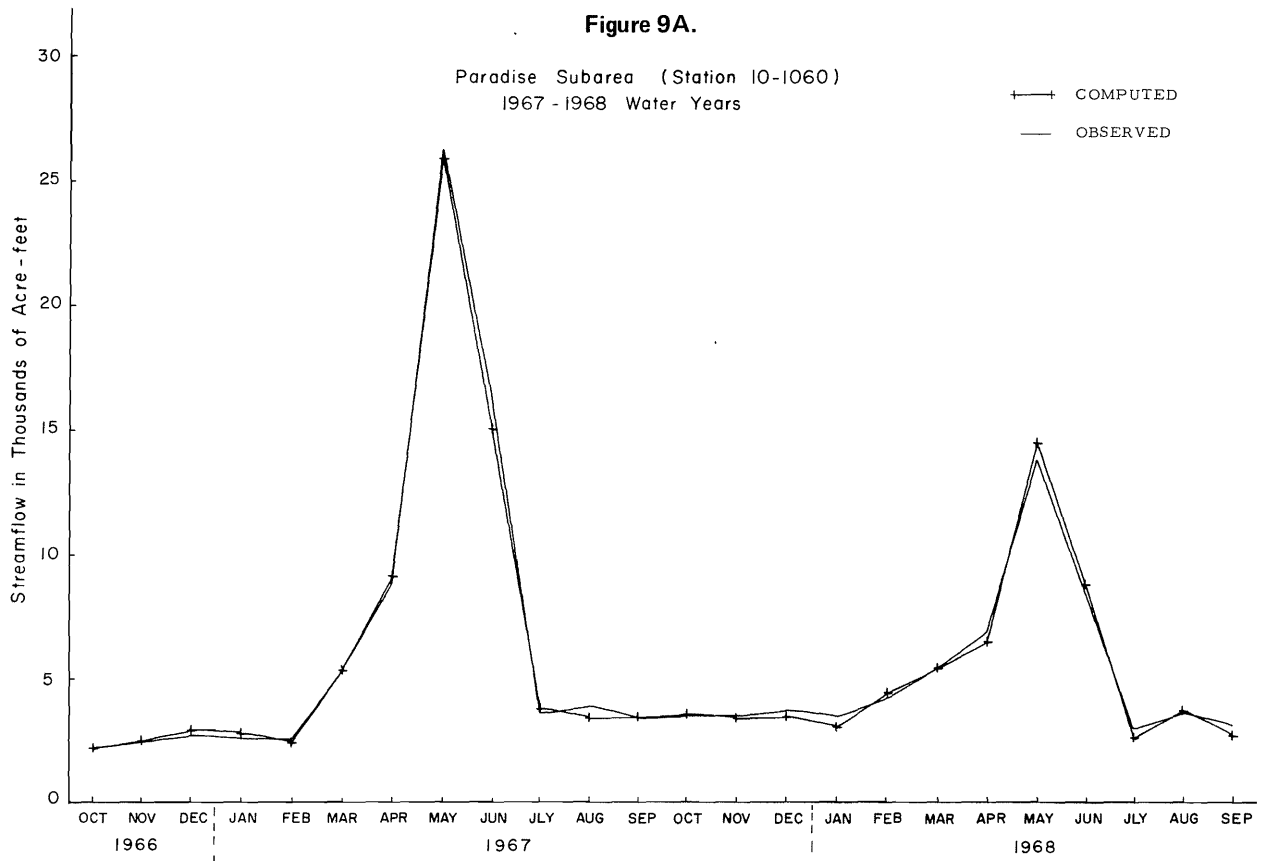


Figure 9. Gaged and computed outflows for both hydrologic subareas.

Table 2. Flow values in cfs for use in the water quality submodels.

Flow Symbol	Oct.	Nov.	Dec.	Jan.	Feb.	Mar.	Apr.	May	Jun.	Jul.	Aug.	Sep.	Annual
1967 Data for Paradise Subarea													
QI	28.51	29.17	31.29	31.44	32.61	78.06	172.76	421.71	246.37	85.87	50.38	40.74	104.46
QS	3.16	4.92	5.96	5.39	5.73	12.69	21.16	30.35	67.37	19.19	15.38	27.19	18.18
QGI	9.13	11.20	14.07	12.83	11.03	13.81	29.98	15.76	28.87	33.18	30.13	17.26	18.97
QD	29.88	25.01	25.00	25.00	24.99	25.00	30.00	30.01	128.88	165.09	143.30	105.71	63.37
QIR	.00	.00	.00	.00	.00	.00	.00	.00	5.32	8.58	4.59	4.10	1.89
QEF	29.99	30.01	29.99	29.99	30.00	29.99	35.01	35.00	35.01	35.00	35.00	35.01	32.51
QO	36.01	42.01	47.64	45.54	43.45	87.04	153.97	421.75	253.35	61.82	55.69	58.37	109.23
1968 Data for Paradise Subarea													
QI	38.28	35.63	33.57	32.40	47.16	72.05	144.53	271.60	168.73	59.36	45.77	37.39	82.34
QS	4.24	6.01	6.39	5.56	8.29	11.71	17.70	19.55	46.14	13.27	13.97	24.97	14.77
QGI	17.88	16.25	16.51	10.52	30.06	29.26	7.53	5.25	38.57	37.20	48.91	29.82	23.94
QD	25.00	25.01	25.00	25.00	24.99	25.00	30.00	66.01	159.01	170.99	127.00	110.01	67.96
QIR	.00	.00	.00	.00	.00	.00	.00	.74	7.37	10.33	4.34	4.75	2.30
QEF	29.99	30.01	29.99	29.99	30.00	29.99	35.01	35.00	35.01	35.00	35.00	35.01	32.51
QO	58.27	57.37	56.58	50.04	80.32	88.61	109.31	235.84	148.34	43.10	60.92	46.08	86.24
1967 Data for Wellsville Subarea													
QI	36.59	41.68	44.24	41.80	45.56	87.01	149.91	427.73	274.60	58.55	63.59	57.31	111.03
QS	.76	.39	1.26	2.53	.35	.35	5.57	7.53	30.30	5.50	2.19	15.64	6.00
QGI	12.02	10.73	10.27	11.61	7.81	14.89	4.43	2.60	16.17	15.22	32.83	27.44	13.88
QD	10.51	.00	.00	.00	.00	.00	.00	9.50	112.29	177.17	128.94	85.39	43.95
QIR	.00	.00	.00	.00	.00	.00	.00	.00	3.32	4.93	3.51	3.29	1.26
QEF	10.00	10.00	10.99	10.99	11.00	10.99	16.00	12.00	14.00	12.00	12.00	12.00	11.83
QO	19.60	19.42	37.61	63.88	64.67	47.71	157.12	438.24	266.69	30.36	38.59	42.07	102.26
1968 Data for Wellsville Subarea													
QI	57.41	58.82	60.99	56.60	76.53	89.12	116.46	224.92	142.51	48.79	59.04	52.94	87.03
QS	1.02	.48	1.35	2.61	.50	.33	4.66	4.85	20.75	3.81	1.99	14.36	4.70
QGI	25.00	17.28	12.46	12.56	17.51	16.01	11.98	12.75	17.21	12.30	19.34	19.58	16.15
QD	9.76	5.04	4.88	4.88	5.40	4.88	5.04	75.35	124.53	150.92	80.98	62.00	44.74
QIR	.00	.00	.00	.00	.00	.00	.00	.00	3.50	4.24	2.20	2.45	1.04
QEF	10.00	10.00	10.00	10.99	11.00	14.00	10.00	10.00	10.00	10.00	10.00	10.00	10.50
QO	84.63	81.20	81.53	78.36	101.19	64.44	139.37	166.27	132.71	29.45	47.86	47.76	87.65

Velocity of flow has been determined for several reaches at different stages of flow by fluorescent dye techniques. Velocities associated with normal flow conditions generally averaged between 1.0 and 1.5 feet per second over reaches of 0.2 to 1.0 miles in length. The highest velocities were observed during high spring runoff, with the maximum being 5 feet per second.

The mean cross sectional area of flow for the reach was calculated from measured discharge and mean velocity. A relationship of the form

$$A_f = a Q^b \dots \dots \dots (8)$$

was assumed, where A_f is the cross sectional area of flow in square feet obtained by the relationship

$$A_f = \sum_{i=1}^n d_i \cdot \Delta X_i$$

in which

$$d_i = \text{mean depth at a given vertical section}$$

$$\Delta X_i = \text{width of section}$$

and Q is rate of discharge in cubic feet per second. The a and b were essentially 2.0 and 0.7 at all reaches investigated.

Average stream width was also measured or estimated from high water marks. Mean stream depth was then calculated and regressed against rate of discharge, assuming an exponential equation:

$$d = a' Q^{b'} \dots \dots \dots (10)$$

Again, the a and b were practically the same for all reaches. Here the approximate values were taken as 0.2 and 0.6 respectively.

CHAPTER IV

SALINITY SUBMODEL

Dissolved mineral concentration (salinity) is an important measure of water quality, particularly for irrigated agriculture and, in some cases, for municipal and industrial water supplies. Specific electrical conductance (hereafter referred to as EC) is used as the salinity indicator because: (1) it is easily and accurately determined; (2) it is a better index of total ionic activity of dissolved salts than is a total dissolved solids (TDS) rating; and (3) the TDS test, as outlined in Standard Methods (American Public Health Association, 1965) may, in certain cases, result in significant diminution of dissolved mineral weight by volatilization of carbon dioxide (U.S. Salinity Laboratory Staff, 1954).

Electrical conductance was simulated by first developing relationships between EC and flow for each hydrologic input and then combining these inflows at the upstream end of the reach to yield a weighted average conductivity value for that reach. No "in-transit" equation is required, as conductance is a conservative water quality parameter.

Input conductances

As shown in Figure 2, the inflow to any reach (i) is composed of one or more of six inflow components: outflow from the reach immediately upstream on the same branch ($Q_{i+1,j}$); outflow from river branches which are tributary to the reach being studied ($QBR_{i,j}$); other natural surface inflow to the reach ($QS_{i,j}$); surface irrigation return flow ($QIR_{i,j}$); groundwater inflow ($QGI_{i,j}$); and municipal and industrial releases ($QEF_{i,j}$). The conductance of each of these hydrologic inputs must be determined to permit evaluation of the conductance of the combined flow.

Reach inflow

The conductance of the outflow from the upstream reach is taken as that resulting from the simulation of the upstream reach.

Branch inflow

Here again, the conductance is taken as that previously found for the tributary branch.

Surface inflow

Analysis of project data indicates that the conductance of natural diffuse surface waters is closely related to rate of flow. Coefficients of correlation range from .69 to .90 (Figures H-4, H-5, and H-6). These orders of magnitudes were supported in the review of published literature on the subject. Although the literature in this area is somewhat sparse, researchers have long recognized the relationship between salinity and rate of flow. In fact, Lentz and Sawyer (1944) attempted to estimate flow rates from salinity data for streams in the Madison Lakes area.

In what is generally regarded as the pioneering work in this field, Durum (1953) established that chloride concentrations in the Saline River, Kansas, were inversely related to flow. He found that the total salt load (salinity times flow rate) was nearly constant, though it did tend to be slightly higher during periods of high flow.

Extending on the work of Durum and using data from the Arkansas and Red Rivers, Ward (1958) proposed an exponential relationship of the form

$$S = a \cdot Q^b \dots \dots \dots (11)$$

in which

- S = salt concentration
- Q = rate of flow
- a and b = constants

Ledbetter and Gloyna (1964) extended the simple exponential model advanced by Ward by allowing "b" to vary with rate of flow, according to the relationship

$$b = p \cdot Q^s \dots \dots \dots (12)$$

in which

- b = exponent for Equation 11
- Q = rate of flow
- p and s = constants

As an alternate to this relationship, especially applicable with reference to rivers of the arid southwest, they suggest that "b" be related to current rate of flow and antecedent flow conditions by the equation

$$v_k = f + g \cdot \log(Aq_k) + h \cdot Q_k^s \quad \dots (13)$$

in which

- b_k = exponent for Equation 10

$$Aq_k = \text{antecedent flow index} \left(\frac{30}{\sum_{d=1}^d} \right) \frac{Q_d}{d}$$

- d = the number of days, counted back from the "k th" day
- Q = rate of flow
- f, g, h and s = constants

Ledbetter and Gloyna, Hart, King, and Tchobanglaus (1964) state that they have adequately represented changes in the salinity of the Russian River of northern California by breaking the total flow of the river into its component parts:

$$S = a_1 \cdot q_g^{b_1} + a_2 \cdot q_i^{b_2} + a_3 \cdot q_s^{b_3} \quad \dots (14)$$

in which

- S = salt concentration
- q_g = the groundwater component of flow
- q_i = the interflow component of flow
- q_s = the surface contribution to flow
- a_j and b_j = constants

Gunnerson (1967) in a study of Columbia River data found that variation from the exponential prediction equation of Ward (Equation 11) tended to follow a seasonal elliptical donut pattern; with winter and spring values generally plotting above the prediction line and summer and autumn points below. Each sampling point examined had a unique variation pattern.

In addition to the models outlined above, a simple semi-log relationship of the form

$$S = a + b \cdot \log Q \quad \dots (15)$$

in which

- S = salinity

Q = flow rate
a and b = constants
was fitted to the data.

The more complex relationships (Equations 12, 13, and 14) failed to demonstrate any significant improvement over the simple exponential and semi-log relationships in fitting data available from the current project. Ward's exponential formulation (Equation 11) fit the data slightly better than did Equation 15, the semi-log form. The values of the constants "a" and "b," as determined by least squares fitting of Equation 11 are given in Table 3, along with the coefficients of determination for several of the sampling points in the Little Bear River system. The constants a and b may vary considerably within the stream system, as illustrated in Table 3; data upon which Table 3 is based are from the period June 1966 to December 1967.

Table 3. Relationship of electrical conductance to rate of discharge on the Little Bear River system. (EC = a Q^b)

Station	a (constant)	b (constant)	R ^{2b} (%)
S-12.5	1000	-.16	66.
S-15.2	505	-.06	47.
S-27.0	815	-.34	92.
S-27.5	781	-.31	84.
SD-0.0	568	-.17	69.
SEC-6.2 ^a	363	-.002	00.

^aData were taken only during periods of relatively low flow due to access problems during the spring high water period.

^bPercent of total squared variation in the dependent variable explained by the model.

Figure 10 is a log-log plot of conductance vs. flow rate for data obtained from station S-27.0, for the period June 1966 to June 1967. Equation 11 is plotted also with constants determined by least squares regression analysis of data.

Irrigation return flow

On the average, about one-third to two-thirds of the water diverted for agricultural irrigation is used consumptively. The remainder finds its way back to the resource pool as deep percolation to groundwater, overflow from the distribution system, or surface runoff from irrigated fields (McGauhey, 1968).

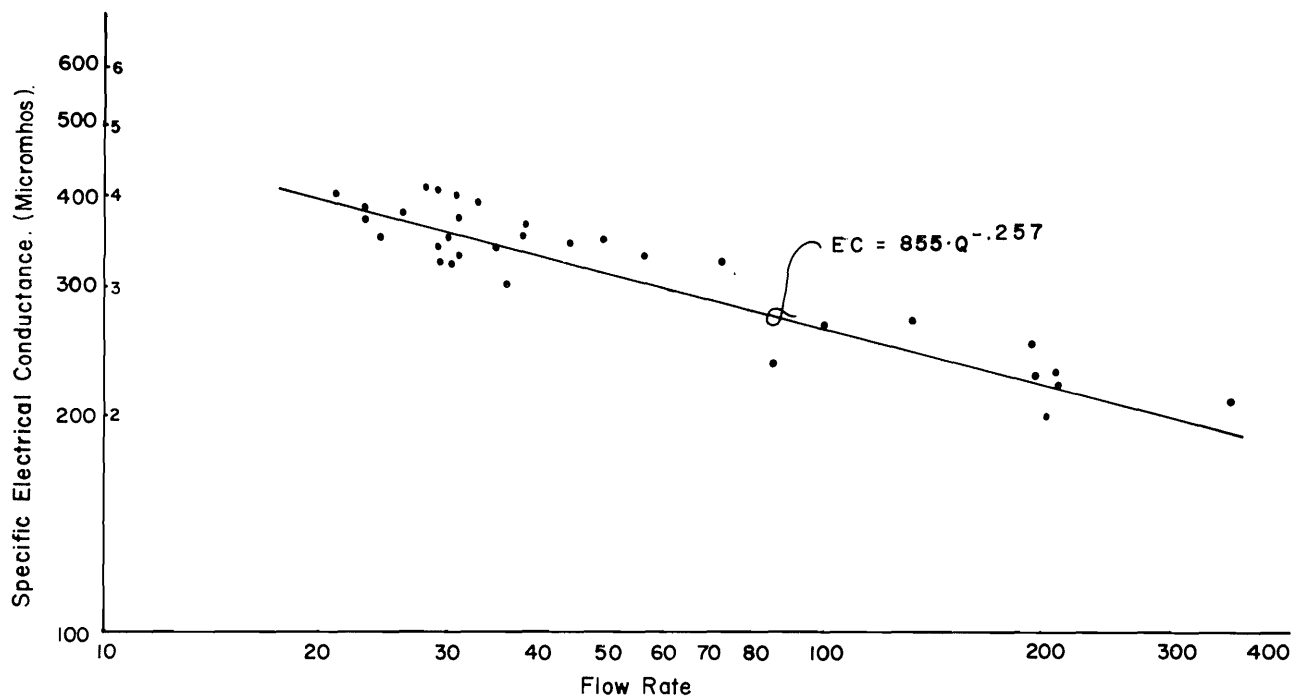


Figure 10. Specific electrical conductance vs. discharge for station S-27.0 on the Little Bear River.

Eldridge (1963) states that "return flows from irrigation projects contain at least three, and often as high as ten times the concentration of mineral salts as that of the initial irrigation water." The Utah State University Foundation (1969) suggests that a more realistic range of salinity multipliers might be two to seven. Undoubtedly, the highest concentrations occur in the percolating segment of the return, as this will carry with it a portion of the soil solution in which the salinity has been increased by transpiration, as well as any salts leached from the soil profile.

For purposes in this study, the deep percolating portion of the return flow is assumed to be included in groundwater; thus the salinity multipliers have automatically been restricted to the low end of the range mentioned above. A multiplier of approximately two has been assumed. This value is lower than mentioned in the literature, but seems to be more consistent with project data. This is supported particularly by comparing data from groundwater sampling point U-2510, as shown in Table 4, with conductance values of irrigation waters which are on the order of 300 to 400 μ mhos/cm.

Groundwater inflow

Four groundwater sampling points have been established along the Little Bear River system. These sampling

points include one natural spring, an improved spring, an artesian well, and a field drain.

Although the data for individual sampling points showed considerable scatter, no significant variation occurred with time of year. Considerable differences were observed between sampling points (Table 4). On the basis of this information, constant electrical conductance levels have been assigned to groundwater inflow to a given reach. The value assigned varies from reach to reach, in conformance to the tendencies disclosed in Table 4.

Municipal and industrial releases

The characteristics of municipal and industrial wastes are highly variable. Industrial wastes, however are highly specific to the type of industry from which they derive. The most logical approach to the simulation problem is to require data inputs to define the quantity and quality characteristics of each effluent being discharged into the stream system.

Stream conductance

Equation 16 calculates the conductance for reach *i* by the weighted average of all flow inputs for that reach. Stated algebraically:

Table 4. Electrical conductance at groundwater sampling points.

Sampling point	Number of Samples	Location	Description	Ave. ($\mu\text{mhos/cm}$)	Range ($\mu\text{mhos/cm}$)
U-2311	12	north of Wellsville	artesian well	576	340-715
U-2510	11	east of Wellsville	field drain	732	650-900
U-2907	11	south of Hyrum	improved spring	652	515-790
U-3198	10	west of Avon	natural spring	409	310-520

$$\begin{aligned}
 EC_i = & (EC_{i+1} \cdot Q_{i+1} + E C B R_i \cdot Q B R_i \\
 & + E C S_i \cdot Q S_i + E C I R_i \cdot Q I R_i \\
 & + E C G I_i \cdot Q G I_i + E C E F_i \cdot Q E F_i) / (Q_i \\
 & + Q D_i) \dots \dots \dots (16)
 \end{aligned}$$

in which

- Q_{i+1} , $Q B R_i$, $Q S_i$, $Q I R_i$, $Q G I_i$, $Q E F_i$, Q_i , and $Q D_i$ are all as previously defined and
- EC_i = electrical conductance of reach "i" outflow
- EC_{i+1} = electrical conductance of outflow from the adjacent upstream reach on the same branch
- $E C B R_i$ = electrical conductance of outflow from a branch tributary to reach "i"
- $E C S_i$ = electrical conductance of surface inflow
- $E C I R_i$ = electrical conductance of irrigation returns
- $E C G I_i$ = electrical conductance of groundwater inflow
- $E C E F_i$ = electrical conductance of municipal and industrial discharges

In-transit conductance changes

Because salinity (and thus electrical conductance) is a conservative parameter of water quality, (ignoring possible precipitation reactions), no changes in level result from the passage of time or distance covered. The conductance at the lower end of a reach is taken to be the same as that at the upper end, after mixing inflow components.

Reservoir routing

Reservoir inflows are combined with waters of different levels of conductivity carried over in storage from

previous time periods. Complete mixing of these inflows with reservoir contents has been assumed, even though stratification and/or short circuiting may tend to prevent it. This simplification was invoked because of the lack of detailed data on the variation of density and conductivity within the impoundment. Employing the principle of mass balance, the conductivity of storage carried over into the next time period may be shown to be

$$ECST_{k+1} = \frac{2(VST_k \cdot ECST_k + VIN_k \cdot ECIN_k) - VOUT_k \cdot ECST_k}{VOUT_k + 2 \cdot VST_{k+1}} \dots \dots \dots (17)$$

in which

- $ECST$ = the electro-conductivity of water stored in the reservoir at the beginning of time period k
- VST = the volume of water stored in the reservoir at the beginning of time period k
- VIN = the volume of inflow to the reservoir during time period k
- $ECIN$ = the electro-conductivity of this inflow as determined by Equation 16
- $VOUT_k$ = the volume of reservoir discharge during time period k

There are two assumptions implicit in Equation 17. First, the contents of the reservoir will be completely mixed so that the salt concentration in reservoir discharges will be the same as the average concentration of dissolved solids in the reservoir. This assumption may not be valid for time periods of short duration or for deep, thermally stratified bodies of water. Second, precipitation of calcium carbonate is not significant.

Simulation algorithm

The various elements of the electrical conductance submodel are integrated by a simulation algorithm which comprises the submodel.

Briefly, the simulation algorithm for monthly stream conductivity, for a given reach, consists of the following procedure, which is outlined also in Figure 11.

1. Obtain hydrologic input flows for each reach for each monthly time period of interest using hydrologic submodel.

2. Establish, by regression analysis using field data, the constants a and b for Equation 15, for appropriate hydrologic flow inputs.

3. Define salinity by card input for flows not amenable to Equation 15 application.

4. If reach is a reservoir, use Equation 17, which

mixes over two time periods.

5. Apply Equation 16 to all reach inputs to obtain reach salinity.

6. Go to next reach and repeat procedure beginning with step 1.

7. Go to next time period beginning with step 1.

The procedure for computer simulation of the above algorithm is described in Appendix E, where it is incorporated into the WAQUAL main program as the subprogram ELCON. Steps 3, 4, 5 are done by ELCON; steps 1, 6, and 7 by the system control model, and step 2 is done by the user, preparatory to simulation.

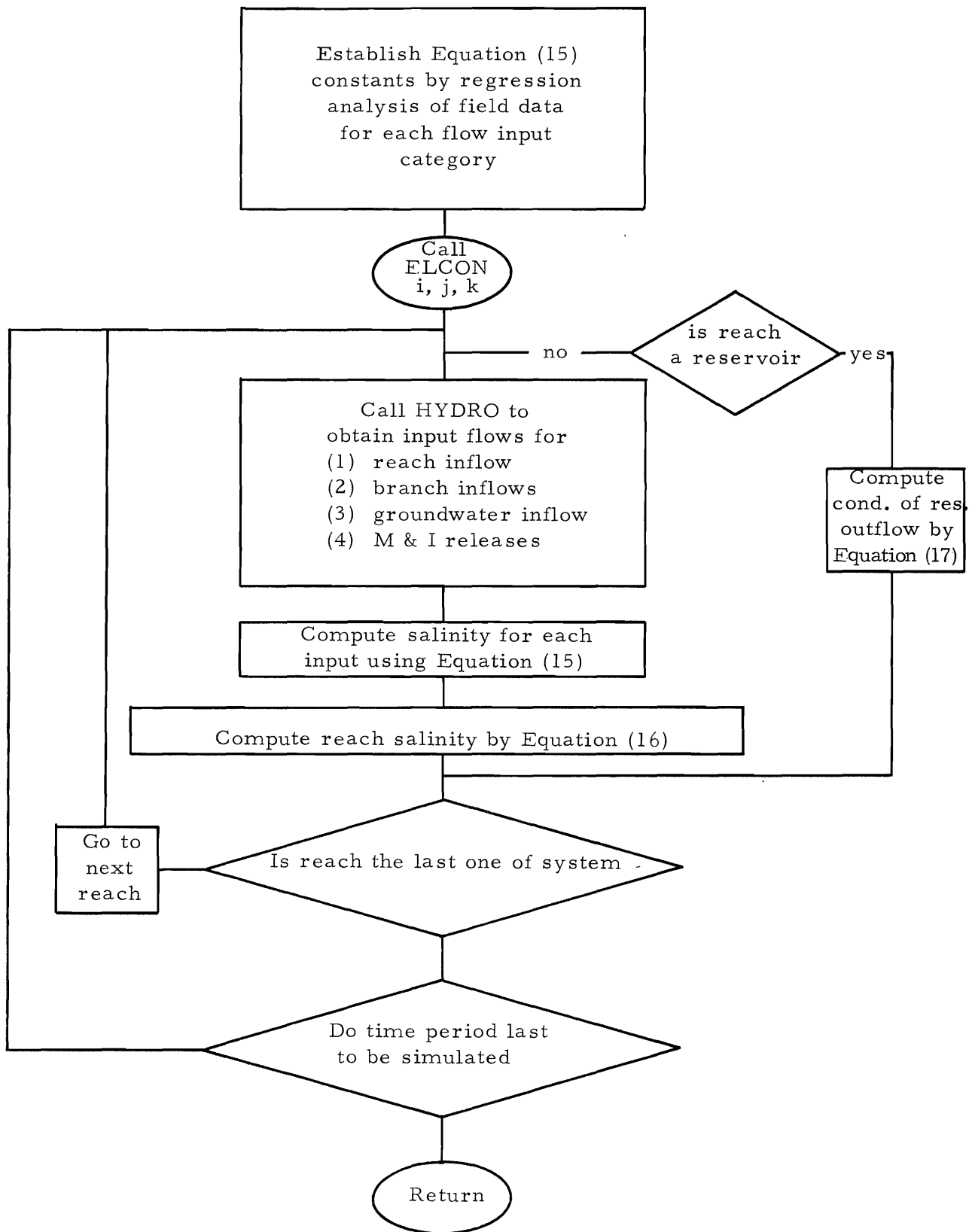


Figure 11. Simulation algorithm for electrical conductance submodel.

CHAPTER V

STREAM TEMPERATURE SIMULATION

The temperature problem

The factor of stream temperature has evolved only recently to a perspective commensurate with its environmental effects. This is partially because the current and projected magnitudes of the temperature problem are such that it cannot be ignored. In 1964 the cooling water intake by industries amounted to 50,065 billion gallons (FWPCA, 1968). The U.S. Senate Select Committee on National Water Resources in 1960 projected cooling withdrawals of 576 billion gallons per day by 2000.

Thermal pollution, as it is now called, exerts a profound influence upon the receiving water body. First, the direct and indirect effects on the biotic communities may in some instances be quite severe. The ecology of the water body may be changed entirely. Decreased oxygen solubility, increased oxygen demand, increased growth of some algae species, and increased toxicity to some substances are some of the peripheral synergistic effects. The mutual effects upon other cooling water users, and the change in palatability of the water for municipal use are among a few of the many additional considerations.

A natural stream will exhibit temperature behavior characteristics in both time and space, and these can have a significant bearing upon its reaction to thermal discharges. These characteristics include: (1) a diurnal temperature variation in the stream, (2) an annual cycle of mean daily stream temperatures, and (3) an in-transit decay of any point imposed temperature differentials. These characteristics are, of course, because the stream water body is virtually never at temperature equilibrium with its surroundings; thus the problem is one of heat transfer. Therefore, all of the factors relevant to heat transfer are pertinent to the problem of temperature behavior of a stream. These factors include: (a) size of stream, (b) turbulence characteristics of the stream, (c) solar insolation, (d) atmospheric turbulence, (e) temperature differential between the atmosphere and stream water body, and (f) mass inputs of new water. Inclusion of these factors is necessary to a rational comprehensive modeling treatment.

This comprehensive approach would not necessarily fit the philosophy of the project objective, however, which was to find a way to simulate the three effects listed above in the most pragmatic manner possible. The law of heat transfer is the basis for the empirical approach also, but applied in an empirical manner. In essence atmospheric temperatures (obtained from weather station records) are matched against corresponding stream temperatures and the stream temperature response is thus "calibrated." Obviously this method is gross as all of the many independent variables of heat transfer are absorbed and integrated in a single coefficient. Nevertheless it works and is empirically feasible—which is the principal objective.

The simulation procedure was divided into two basic phases: (1) computer simulation of mean monthly water temperature by a program called WATEMP, and (2) computer simulation of diurnal water temperature for each month, by a program called DITEMP. Each of these basic algorithms considers: (1) the time variations in temperature of all hydrologic mass inputs—discrete and diffuse, (2) in-transit changes within a reach, and (3) the effect of reservoirs.

Monthly water temperature simulation

The monthly temperature simulation model (WATEMP) accomplishes three tasks. First, it can simulate the mean monthly stream temperature through the annual cycle. Second, it can simulate the stream in-transit response to any imposed heat load. And third, it can call up the diurnal submodel, DITEMP (by means of WAQUAL). This section describes the equations used and how they operate to accomplish these tasks.

Temperature simulation of reach inputs

Each hydrologic input to a river reach has a unique pattern of temperature variation with time. Alternative methods of representing these variations for each input are outlined below. After each input temperature is simulated the weighted average of inputs equates with the temperature at the upstream end of the reach (Equation 16 applies).

River inflow. The simulation procedure begins at the upper extremity of each branch, and proceeds in a downstream direction. Results from the simulation of the adjacent upstream reach are always available as an input for the simulation of the next reach downstream. For the first reach analyzed on a branch, the stream inflow is assumed to be zero and all natural surface inflows are lumped together in the "surface inflow" category (QS). The method of approximating the temperature of this component is discussed below.

Branch inflow. Branches tributary to a reach are simulated before the reach is analyzed. The temperature of inflow from tributary branches is therefore available for incorporation into the analysis.

Surface inflow. The temperature of inflowing diffuse surface waters follows a sinusoidal pattern through the annual cycle. Superimposed upon this annual variation, there is a diurnal cycle, discussed in detail in the section following. Figure 12 illustrates the sinusoidal variation of water temperature through the year. Measured water temperatures have been adjusted to mean

daily values to remove the influence of diurnal fluctuations.

Ward (1963) fitted a sine curve of the form

$$\bar{T} = \bar{\bar{T}} + C \cdot \sin \left(\frac{2\pi}{365} \cdot x + A \right) \dots (18)$$

to temperature data from unheated natural streams by least squares procedures in which

- \bar{T} = mean daily stream temperature
- $\bar{\bar{T}}$ = mean annual stream temperature
- x = day of the year after October 1

The terms C and A are, respectively, a constant and a phase shift angle determined by least squares analysis. Ward found this model to fit temperature data well with little between-years variation in model constant and phase shift. Jaske (1968) employed the same method of characterizing annual water temperature variations in his study of the temperature characteristics of the Columbia River.

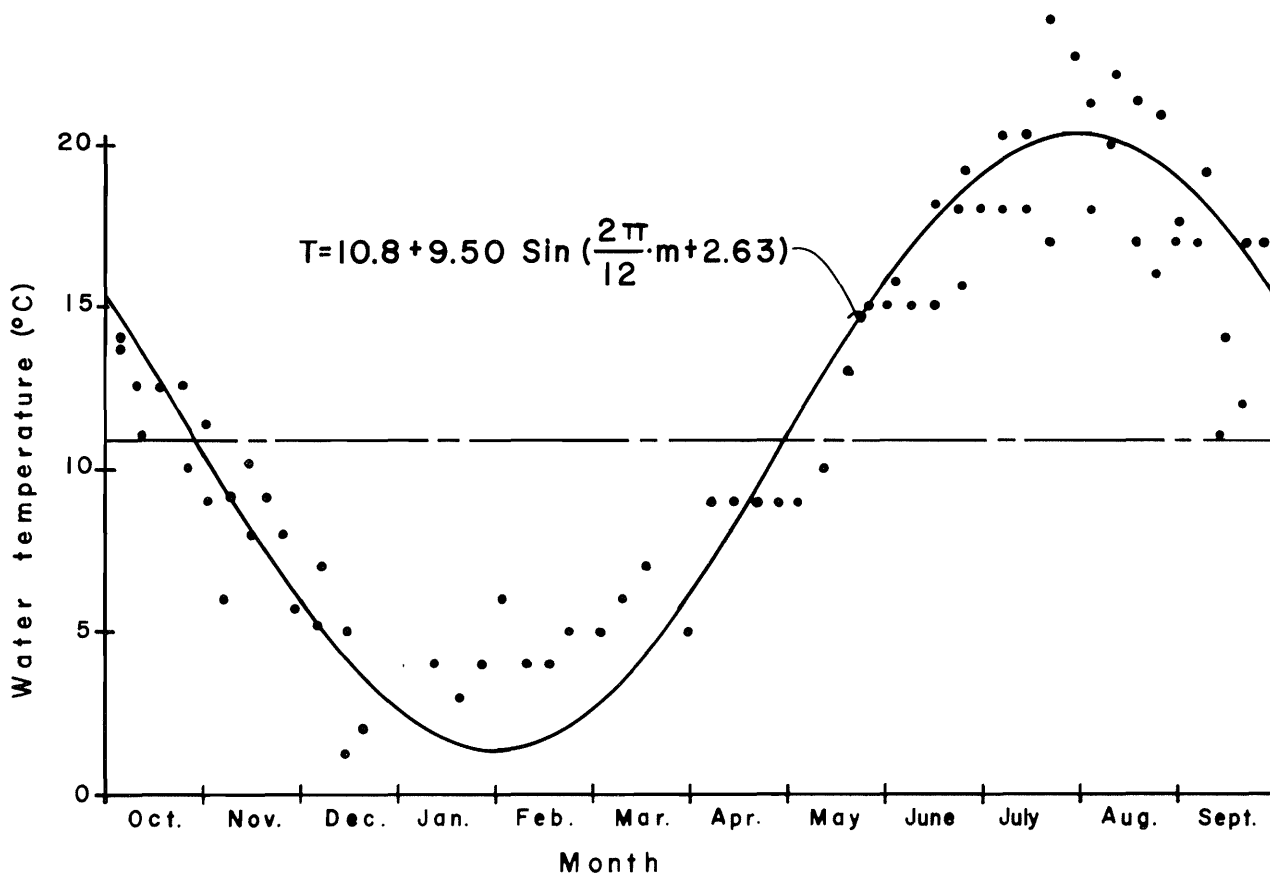


Figure 12. Typical annual stream temperature variation at station S-12.8.

Table 5 shows the results of applying Equation 18 to temperature data from the Little Bear River. The fit of Equation 18 to the data, as measured by the coefficient of determination (R^2), is consistently high at all but one of the twelve sampling points. The station for which the poor fit was obtained is the one designated SEC-4.3, located immediately downstream from the Porcupine Reservoir outlet works. Expanding Equation 18 into two and three-term Fourier series did improve the fit at this station (but not at the other stations).

Utilization of the procedure outlined above requires a record of stream temperatures at the point in question. Observations should be taken at least weekly over a period of one or more years. As noted in Table 5, data from the Little Bear River system indicate that the constant C and the phase shift angle A do not differ greatly from one station to another in the system, if the waters being compared are of the same basic make-up, i.e., have about the same proportions of groundwater at the two points, etc. It should be possible then, if judgment and discretion are exercised, to transfer these two coefficients from one station to another within a small hydrologic system.

A major disadvantage of the Equation 18 approach is that it ties water temperature directly to time of year, rather than to atmospheric temperature. This hinders the assessment of the effect of stochastic variations in monthly atmospheric temperature upon stream temperature. In addition, at least one complete cycle of stream temperature data is required to adequately determine the sine curve parameters.

Another approach in the modeling of surface inflow temperatures, is to correlate stream temperature and

atmospheric temperature. Where the modeling increment is one month, the monthly average of atmospheric temperature can be used to estimate mean monthly stream temperatures. Intervals shorter than one month, however, would require that antecedent atmospheric temperatures be considered.

Monthly averages of stream temperatures, adjusted to mean daily values, have been regressed against mean monthly atmospheric temperatures from the Logan USU Weather Bureau station located about ten miles north of the project area. A linear equation of the form

$$\bar{T} = a + b \cdot \bar{T}_a + \epsilon \dots \dots (19)$$

is assumed in which

- \bar{T} = mean monthly water temperature ($^{\circ}\text{C}$)
- \bar{T}_a = mean monthly atmospheric temperature ($^{\circ}\text{F}$)
- ϵ = deviation of observed water temperature from predicted values
- a and b = regression constants

Equation 19 is a desirable alternate because it more clearly portrays the cause-effect relationship responsible for changes in stream temperature. It should also be possible to satisfactorily define the coefficients for this equation with something less than a full annual cycle of data as long as the temperature measurements cover a period including both high and low stream and atmospheric temperatures. The results of applying Equation 19 to data from 14 water quality sampling stations are tabulated in Table 6.

Table 5. Representation of annual changes in mean daily water temperature.

$$\bar{T} = \bar{\bar{T}} + C \cdot \text{Sin} \left(\frac{2\pi}{365} \cdot x + A \right)$$

Station	$\bar{\bar{T}}$ ($^{\circ}\text{C}$)	C (constant)	A (radians)	R^2 (%)	Comments
S-12.7	10.7	7.135	2.675	88.	
S-12.8	10.8	9.505	2.630	90.	
S-15.2	10.5	9.102	2.573	92.	
S-16.8	10.2	14.477	2.515	88.	reservoir surface
S-21.3	8.7	7.209	2.659	90.	
S-24.6	8.7	7.466	2.663	87.	
S-27.5	9.4	6.565	2.670	85.	
SD-0.0	7.8	8.652	2.674	85.	
SEC-4.3	8.3	11.208	2.068	71.	reservoir outflow
SEC-6.2	7.1	7.288	2.604	85.	
SW-0.1	11.2	5.278	2.684	83.	largely spring fed
STF-0.0	8.8	6.977	2.653	86.	trout farm discharge

Table 6. Prediction of stream temperature from atmospheric temperatures. ($T = a + b T_a$)

Station	a (constant)	b (constant)	R ² (%)	Notes
S-12.7	- 4.09°C	.310	97.	
S-12.8	- 7.53	.387	93.	
S-15.2	- 6.90	.373	93.	
S-16.8	-10.22	.475	88.	reservoir surface
S-21.3	- 6.01	.312	95.	
S-24.6	- 5.92	.310	94.	
S-27.0	- 5.90	.308	93.	
S-27.5	- 2.24	.252	93.	
SD-0.0	- 8.77	.356	95.	
SEC-0.4	- 5.08	.295	90.	
SEC-4.3	- 1.75	.211	57.	reservoir discharge
SEC-6.2	- 5.10	.270	71.	
SW-0.1	0.63	.221	87.	largely spring fed
STF-0.0	- 5.54	.304	94.	

Again, a degree of consistency was noted in the relationships between air and water temperatures at all stations except those at which the stream is affected by reservoirs or proportionately large groundwater contributions. The coefficients of determination (R²) are uniformly high, except at two stations on the East Fork of the Little Bear River (SEC-4.3 and SEC-6.2). At station SEC-4.3 the flow is composed almost entirely of waters released from Porcupine Reservoir. These releases do not correlate well with atmospheric temperature. No explanation has been found for the relatively poor fit at SEC-6.2 which is upstream from Porcupine Reservoir.

Comparing the R² values in Tables 5 and 6, Equation 19 would appear to be a slightly better fit than Equation 18. Equation 19 also has the advantage of being based upon mean monthly air temperature and therefore Equation 19 was used.

Irrigation return flow. Surface return flows from irrigation are also assumed to be linearly related to atmospheric temperature as described by Equation 19. Because temperatures of these flows were not measured, it has been necessary to assume values for the model constants.

Eldridge (1963) suggests that the contributions of irrigation return flows to the thermal behavior of a stream are of minor importance. In considering surface return flows, it was assumed that such flows are warmer than natural surface inflows. Equation 19 was adopted to simulate the temperature behavior of return flows. Because temperatures of these flows were not measured, it has been necessary to assume values for the Equation 19 constants.

Groundwater inflow. Table 7 gives the results of fitting groundwater temperatures at four groundwater

Table 7. Annual temperature variations of groundwater.

$$\left[\bar{T} = \bar{\bar{T}} + C \cdot \sin \left(\frac{2\pi}{365} x + A \right) \right]$$

Sampling point	$\bar{\bar{T}}$ (°C)	C (Constant)	A (radians)	R ² (%)	Description
U-2311	10.5	1.519°C	2.367	58.	artesian well
U-2510	10.5	2.706	1.892	91.	field drain
U-2907	11.4	1.419	2.230	55.	improved spring
U-3198	10.8	1.993	2.239	87.	natural spring

sampling points in the project area to Equation 18. Although the determination coefficients for the artesian well and the improved spring are not good, the seasonal variation in temperature at these points is significant. At these two locations, the small proportion of the total variation explained by the seasonal model is probably due to the relatively great depths at which the flows originate. Because no distinction has been made in the simulation program as to the depth from which groundwater originates, the prediction model used is a composite of those obtained from the four sampling points.

Municipal and industrial releases. The thermal qualities of municipal and industrial waste waters discharged to the stream must be provided as a data input for each simulation run of the model.

In-transit temperature changes

The temperature of a moving body of water is subject to many influences along its course. Solar radiation and atmospheric convection tend to increase the temperature during daylight hours, while evaporation and other phenomena tend to decrease it. Until recently, relatively little work has been published concerning this important process in natural streams.

The American Society of Civil Engineers Committee on Thermal Pollution (1967) has assembled an extensive bibliography on thermal pollution. Publications listed in this bibliography, and other published material on this topic, fall generally into three classifications: (1) the occurrence of thermal pollution; (2) the effects of thermal pollution upon the aquatic environment; and (3) temperature prediction in natural and thermally polluted bodies of water. The latter class is notable for the relatively small number of contributions.

Most of the early work on temperature prediction techniques was done on cooling ponds and reservoirs. The first of these studies was by Ruggles (1912). Subsequent investigations were performed by Lima (1936), Thorne (1951), Langhaar (1953), and others.

The initial work on stream temperature prediction was published by LeBosquet (1946). He assumed an exponential decay of warm water toward the prevailing air temperature. His derived relationship was of the form

$$\bar{T}_2 = \bar{T}_1 \cdot e^{\left(- \frac{.0235 \cdot k_e \cdot w}{Q} \cdot H \right)} \quad \dots (20)$$

in which

- $\Delta \bar{T}_1$ = "excess" temperature of water over air at the initial point "1" (°F)
- $\Delta \bar{T}_2$ = "excess" temperature of water over air a distance "D" miles downstream from the initial point "2" (°F)
- k_e = heat loss coefficient (BTU/sq. ft./hr./°F of "excess" temperature)
- w = average stream width (ft.)
- Q = average discharge (cfs)
- H = mean stream depth (ft.)

LeBosquet found values of the heat loss coefficient ranging from 6 to 18 BTU/sq. ft./hr./°F (0.2 to 0.6 ft./hr.).

This technique has been criticized on two counts. First, values of the heat loss coefficient must either be guessed or calculated from measurements after the thermal pollution has occurred. It would seem that this difficulty could be partially mitigated by experimental analysis. The second question concerns the assumption that in the absence of thermal pollution, air and water temperatures would tend to be equal. Although air temperature is an important factor in determining the temperature of a body of water, other variables, such as evaporation, back radiation, etc., tend to lower the "equilibrium" temperature of the stream below atmospheric temperature.

Gameson, Hall, and Preddy (1957) used essentially the same approach as that advocated by LeBosquet to analyze the thermal characteristics of the Thames estuary. They avoided the second criticism of LeBosquet's model by using temperature excess above some "equilibrium" water temperature instead of the excess of water temperature over air temperature. From estimated rates of heat addition by urban and industrial developments along the estuary, they estimated the coefficient of heat loss at 4.0 centimeters (0.13 feet) per hour. For the River Lea, Gameson, Gibbs, and Barret (1959) found heat loss coefficients, averaged over four days for four different reaches, to range from 1.66 to 3.83 cm/hr. (.054 to .126 ft./hr.). The overall average for the river was 2.6 cm/hr. (.085 ft./hr.).

Recent work has been directed to the heat-budget analysis approach. Among those contributing to the literature on this topic are: Velz and Gannon (1960), the Johns

Hopkins Advanced Seminar (1961), Edinger and Geyer (1965), Edinger, Brady, and Graves (1968), and others. The heat-budget method requires data on solar radiation and wind velocities which are not generally available. No data of this nature were taken during this project so the heat-budget approach was eliminated from consideration for purposes of this work.

Duttweiler (1963) has developed a procedure, wherein the exponential decay theory is employed with "equilibrium" temperatures and heat exchange coefficients being estimated from heat-budget considerations. This is a rather rigorous approach which would seem to possess certain merit as a modeling technique. However, for application to the data available from the current project it was of limited usefulness because of the lack of more detailed climatological data such as windspeed and radiation.

The simulation procedure finally adapted for this work satisfied the pragmatic criteria of reliability and data availability. This procedure involved the LaBosquet Equation 20, for predicting decay of temperature excess, in conjunction with Equation 19 for assessing stream equilibrium temperature. Equation 19, which gives mean monthly stream temperature, was felt to be as reasonable estimate of equilibrium temperature as feasible.

In mathematical form, the complete model for a nonreservoir reach is

$$\bar{T}_2 = \left(\frac{\sum_{j=1}^{nc} q_j \cdot \bar{\tau}_j}{Q} - E_1 \right) \cdot e^{-\phi} + E_2 \quad \dots \dots \dots (21)$$

in which

- $\frac{q_j}{\tau_j}$ = rate of flow for input j
- $\frac{q_j}{\tau_j}$ = mean monthly temperature of input j
- Q = $\sum_{j=1}^{nc} q_j$
- nc = number of hydrologic inputs to the reach
- \bar{T}_2 = mean monthly stream temperature at the downstream end of the reach
- E = "equilibrium" temperature
- ϕ = $\frac{.0235 \cdot k_e \cdot w}{Q} \cdot D$

In Equation 21, the subscript 1 indicates the upstream end of the reach, while 2 denotes the downstream end. All flows and temperatures are monthly averages for the month of simulation. Mean monthly input temperatures, $\bar{\tau}_j$, are estimated according to the equations shown in Table 8.

Table 8. Summary of mean monthly temperature equations for hydrologic inputs.

Input	Model
River inflow	output from previous simulation
Branch inflow	output from previous simulation
Surface inflow	$\bar{T}_s = a + b \cdot T_a$
Irrigation return flow	$\bar{T}_i = a + b \cdot T_a$
Groundwater inflow	$\bar{T}_g = \bar{T}_g + C \cdot \sin\left(\frac{2\pi}{12} \cdot m + A\right)$
M & I releases	card input

Heat exchange constants for streams of this system were approximated from the river reach downstream from Porcupine Reservoir. During the summer irrigation season, releases from the reservoir originate in the cold hypolimnetic zone, resulting in significant temperature deficits at the reservoir outlet. The rate at which these deficits approach zero, as these cold waters are warmed toward the "equilibrium" temperature in the reach below the reservoir, was employed in the evaluation of the heat exchange constant, k_e .

On seven different days during the summer of 1968, temperature observations were made at the outlet from Porcupine Reservoir and at Avon, 3.9 miles downstream. Temperature deficits (ΔT_1 and ΔT_2) were taken as the difference between temperatures observed at the points in question and those measured at nearby sampling points not affected by reservoir releases, respectively. These deficits were then inserted into Equation 20, the exponential decay expression, which was solved for k_e . Values obtained are compared with those reported by other researchers in Table 9. A heat exchange constant of 0.20 has been assumed in the development of the present model. Provision is made to allow this "constant" to vary with rate of discharge, according to a hypothetical relationship of the form

Table 9. Heat exchange coefficients.

Researcher	Min. (ft./hr.)	Max. (ft./hr.)	Water body
LeBosquet (1946)	0.2	0.6	
Gameson et al. (1957)		0.13	Thames estuary
Gameson et al. (1959)	0.054	0.13	River Lea
Duttweiler (1963)	0.047	0.15	Winter's Run
Edinger et al. (1968)		0.12	Cooling pond
Current research	0.09	0.40	Little Bear River

$$k_e = a \cdot Q^b \dots \dots \dots (22)$$

Because of the dearth of data here and the lack of a significant source of thermal pollution on which to test a prediction equation, a constant level for the exchange coefficient is all that is justified.

Adjustment of discrete sampling data

As depicted in Figure 19, temperatures during the 8:00 a.m. to 5:00 p.m. working day, when samples were gathered, vary over a large part of the amplitude of the diurnal fluctuation. Because temperatures were not measured at the same time at each sampling point, a more or less random appearing error was introduced into the data. Had a rigid time schedule been followed, so that each site was always visited at the same hour, the diurnal effect would have imparted a systematic downward bias for those points sampled early in the day, while those sampled later in the day would have been biased upward.

To isolate the diurnal component of variation, the model of diurnal fluctuations (called DITEMP and discussed in the following section) was utilized. By employing the diurnal model to adjust all discrete temperature data to mean daily values, it was possible to achieve considerable improvement in the fit of the inflow temperature prediction relationships over that resulting from the use of unadjusted data. Consequently, all stream temperatures, obtained by discrete measurement, have been adjusted to mean daily stream temperature.

Reservoirs

The primary effect of impoundments on downstream temperatures is that of cooling during summer irrigation months if, as is true in the case of Porcupine Reservoir, releases are discharged from the hypolimnion directly into the stream channel below the dam. Temperature data from station SEC-4.3, below Porcupine Dam, are shown in Figure 13. These data have not been adjusted for diurnal effects because the deep waters of the hypolimnion are not subjected to diurnally varying factors. As a result, temperatures in this zone are constant through the diurnal cycle.

These data fit nicely into a theory presented by Churchill (1965) in which he considers the reservoir as being thermally stratified during summer months. He assumes the outlet works to draw only from a relatively thin layer at the depth of the discharge, so that during the irrigation season coldest waters are released first. Released water temperatures gradually increase as the reservoir level recedes and the warm upper layers fall to the level of the discharge opening. Although temperature data available for the station below Porcupine Reservoir indicate that this procedure would apply, it has not been employed because its application requires a complete thermal map-

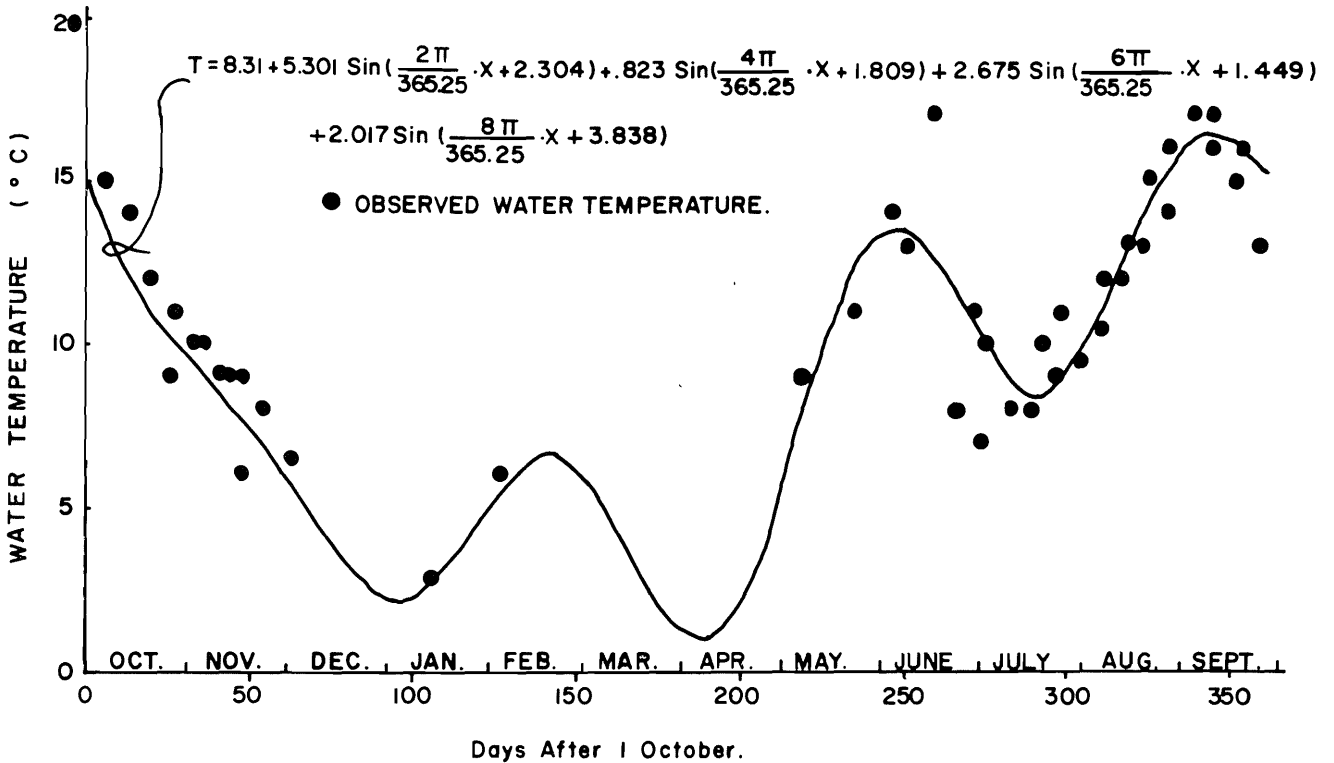


Figure 13. Annual stream temperature variation at SEC-4.3 below Porcupine Reservoir with best fit four-term Fourier series curve.

ping of the reservoir each spring to define the temperature-depth profile throughout the reservoir at the beginning of the irrigation season. Such a survey was beyond the scope and economic resources of this project.

The procedure finally adopted is that of obtaining a temperature record for reservoir releases covering at least one full year and fitting a four term Fourier series model

$$\bar{T} = \bar{T} + \sum_{j=1}^4 C_j \sin\left(\frac{2\pi}{365} j \cdot x + A_j\right) \quad (23)$$

to the data, as outlined in Appendix D. The best fit Fourier series prediction is shown in Figure 13, superimposed on the observed temperature of released waters. The lack of data during winter and spring months, caused by difficult access during this period, allowed the Fourier series best-fit curve to drop again in early spring. This would not be expected in actual field observation. Had data been available for this time of year, the curve would have been forced to follow the data, rather than being free to take the path of least resistance.

The curve-fitting approach means, of course, that unless more than one year's data are available, data from

that year must be accepted as representative of all years of data. This may be a serious limitation if the operating procedures for the reservoir are subject to significant change from year to year.

Algorithm for simulation

Figure 14 outlines the simulation algorithm for monthly stream temperature and this algorithm also is summarized below.

1. Obtain monthly flow values for all inputs from hydrologic model.
2. Establish constants a and b in Equation 19 for each inflow by regression analysis of data.
3. Compute temperature of each input to reach for month in question using Equation 19—where applicable; otherwise define flow input temperature by punched cards; use Equation 18 for shallow groundwater inputs.
4. Compute stream temperature, consisting of combined inflows, using Equation 16.
5. If reach is a reservoir apply Equation 23 to obtain temperature of outflow and simulate next reach beginning with step 1 again.
6. For non-reservoir reaches, if a "temperature excess" (difference between mean monthly water temperature and mean monthly equilibrium water temperature)

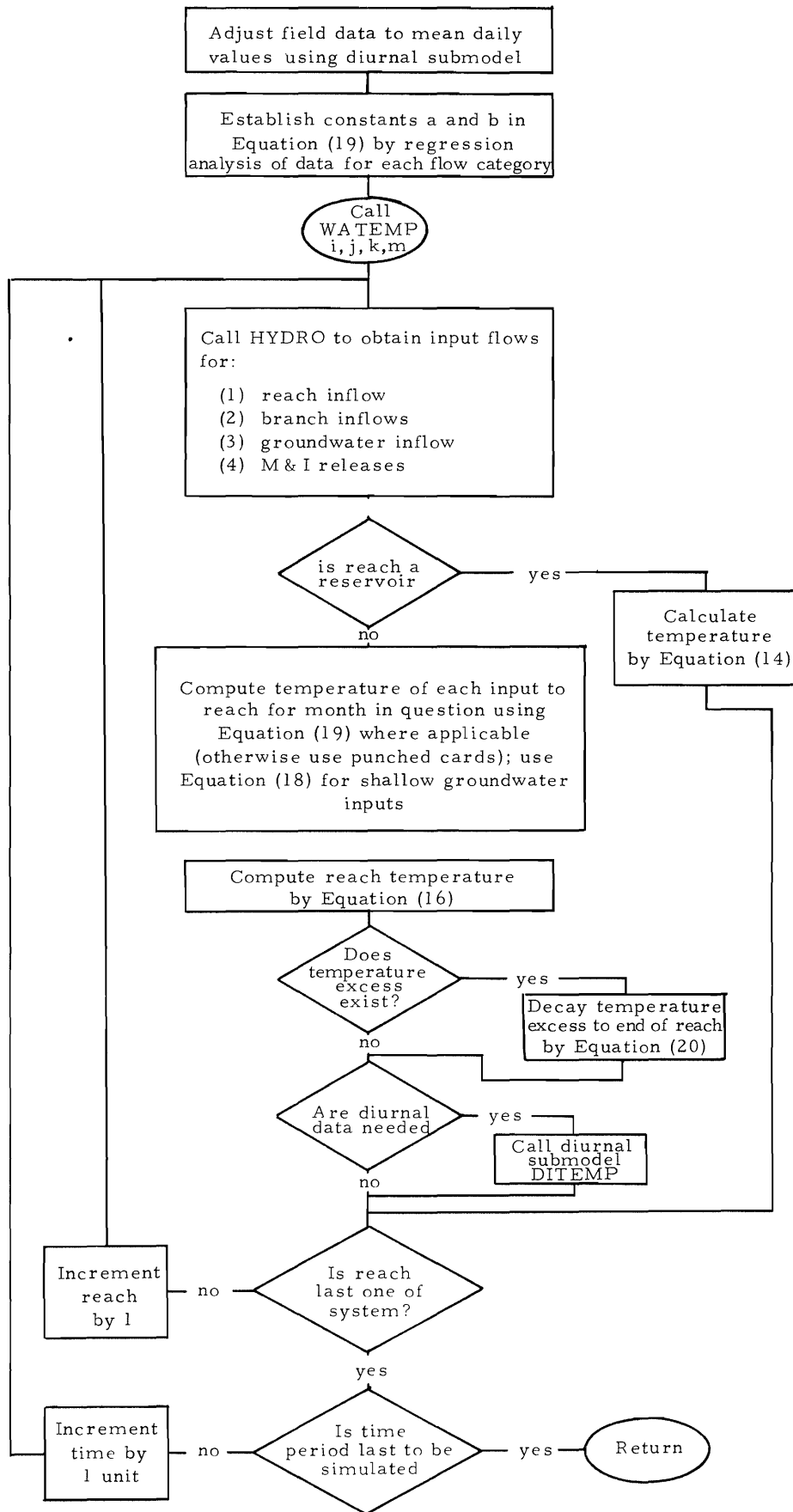


Figure 14. Simulation algorithm for monthly water temperature.

exists at beginning of reach, apply Equation 20 to decay the excess temperature to the end of the reach.

7. Call diurnal submodel if desired.
8. Go to next reach and return to step 1.
9. If last reach is simulated, increment time by one month and return to step 1.

Steps 1, 7, 8, and 9 are done by WAQUAL; step 2 is done by the investigator in data preparation; steps 3, 4, 5, and 6 are done by WATEMP.

Diurnal water temperature simulation

Two continuous modeling stations were established at S-12.5 and S-20.5, respectively, to ascertain diurnal fluctuations and any stochastic effects for temperature, dissolved oxygen, pH, and conductivity. Analysis of thermographs from the continuous monitoring station at S-12.5 (which has about 18 months record) disclosed significant amplitudes in the 24 hour cycles in stream temperature. Since the diurnal temperature effect may well overshadow an annual variation or effects due to point discharges, any comprehensive model should include the diurnal effect for temperature. Thus a simulation procedure for assessing the temperature variation for the 24 hour cycle has been developed.

Researchers reporting diurnal variations in surface water temperature include Macan (1954), who has observed daily patterns of variation in water temperature of small streams in Britain. Duttweiler (1963) used diurnal variations in water temperature of a small stream in Maryland to estimate values of the heat exchange constant for that stream. Thomann (1967), on the other hand, found no significant 24 hour cycles in data from the Potomac estuary. This literature contains little information on the characterization of diurnal water temperature variations.

Establishing diurnal temperature equations

Thermographs were obtained at station S-12.5 in continuous blocks of from three to seven days in length. Twenty of these blocks of temperature data were recorded intermittently over an 18-month period. The diurnal data for each of these data blocks were then fitted to Equation 24, a two term Fourier series.

$$T_i = \bar{T} + \sum_{j=1}^2 C_j \cdot \sin\left(\frac{2\pi j}{24} \cdot i + A_j\right) + \epsilon_i \quad \dots \dots \dots (24)$$

In Equation 24

T_i = observed stream temperature at the "i th" hour (°C)

- \bar{T} = mean daily stream temperature (°C)
- i = hour of the day (measured continuously through the day, beginning with 0100 at 1:00 a.m. and ending with 2400 at midnight)
- ϵ_i = deviation of the observed temperature for the "i th" hour from the model prediction for that hour
- C_j and A_j = coefficient and phase shift for the "j th" term of the Fourier series, as determined by least squares analysis

Figure 15 shows hourly stream temperatures from a typical seven day continuous thermograph, with the best-fit Fourier series curve superimposed. During this particular period, the range of maximum stream temperatures was relatively high, as illustrated by the broad band of observation points about the curve. In spite of these relatively large deviations, Table 10 shows the coefficient of determination for this set of data to be 74 percent, meaning that Equation 24 explains 74 percent of the total variation in stream temperature during this period.

Dividing Equation 24 through by the mean daily temperature yields a predictive equation for the ratio of hourly to mean daily stream temperature

$$DTI_i = 1.0 + \sum_{j=1}^2 C_j \cdot \sin\left(\frac{2\pi j}{24} \cdot i + A_j\right) + \epsilon_i \quad \dots \dots \dots (25)$$

where now C_j and ϵ_i have been coded by division by \bar{T} , and $DTI_i = T_i / \bar{T}$. With patterns of diurnal temperature variation given in terms of this diurnal temperature index (DTI), the stream temperature at any hour of the day may be estimated by multiplying the mean daily temperature by the DTI for the hour in question.

Table 10 lists constants, C_1 and C_2 , and phase angles, A_1 and A_2 , for each of the two Fourier series terms and coefficient of determination, and average stream temperature over the period and corresponding average mean daily atmospheric temperature. It is interesting to note the apparent annual cyclic tendency in each of the Fourier series model parameters. This tendency is more obvious in Figure 16, where each model parameter is plotted as a function of time of year. These cyclic patterns probably result from seasonal variations in the number of daylight hours per day and intensity of solar radiation.

The Fourier series has again been employed in the characterization of the annual cyclic variations for each of the Equation 25 coefficients. Mean daily atmospheric temperature has also been incorporated to yield another Fourier series having the form

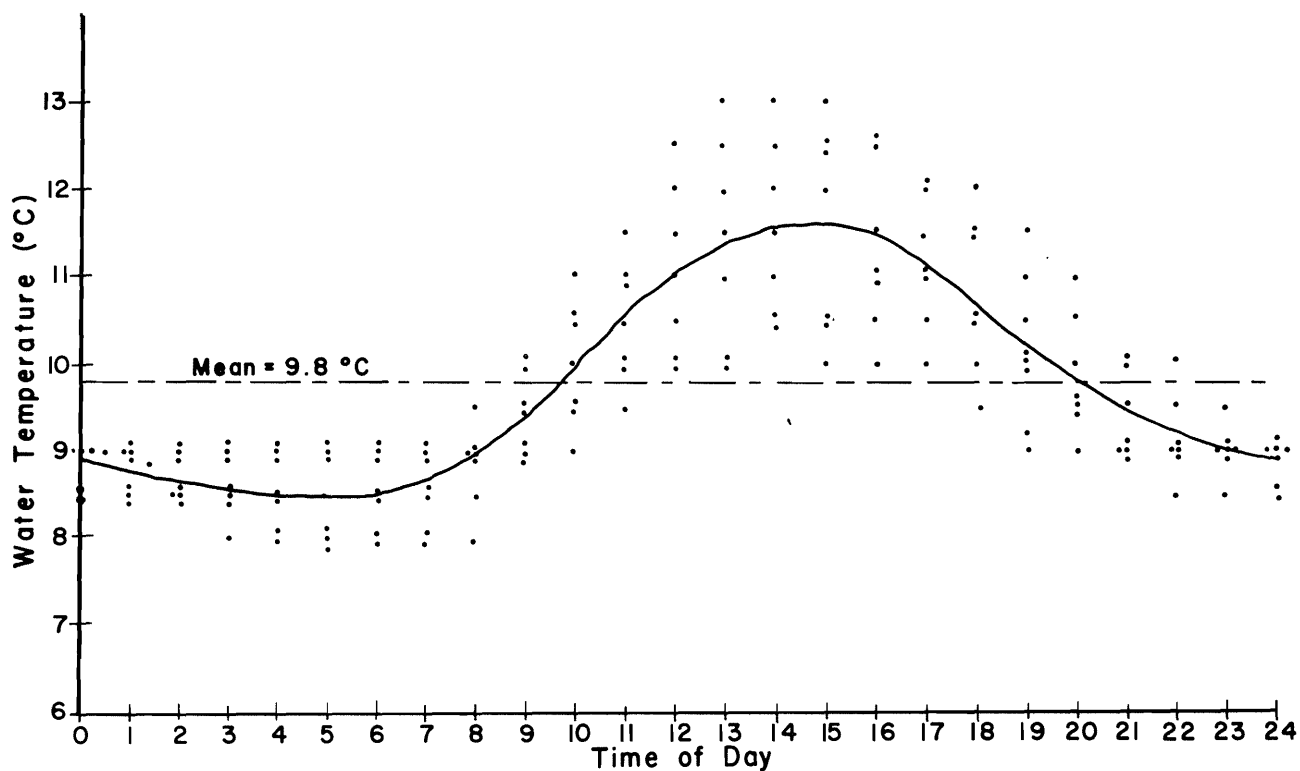


Figure 15. Water temperature variations for the period 22-29 April 1968 with Fourier series model.

Table 10. Diurnal temperature index (DTI) model parameters.

$$\left[DTI_i = 1.0 + \sum_{j=1}^2 C_j \cdot \sin\left(\frac{2\pi j}{24} \cdot i + A_j\right) \right]$$

Date	No. of days	C ₁	A ₁	C ₂	A ₂	R ²	T _w	\bar{T}_a	Notes
1127-120167	4	.169	3.654	.0760	.350	.45	6.4	26.8	
222-22968	6	.449	3.938	.2230	.294	.83	3.3	35.2	
229-30668	6	.514	3.908	.2234	.373	.91	4.3	39.2	
318-32568	7	.319	3.681	.0974	.267	.82	7.6	36.8	
325-32868	3	.328	3.669	.0761	-.054	.83	7.5	42.8	
404-40668	2	.093	3.910	.0351	.575	.68	7.0	40.5	Rain
417-42268	5	.101	4.047	.0185	1.047	.85	9.2	35.2	
422-42968	7	.150	3.946	.0179	1.140	.74	9.8	42.8	
517-52468	7	.094	3.624	.0182	-.428	.65	13.3	52.6	
524-53168	7	.119	3.556	.0202	-.316	.55	14.0	55.7	
531-60468	4	.142	3.164	.0247	-1.212	.76	15.4	59.3	
606-61268	6	.107	3.413	.0254	-.133	.41	7.1	56.8	Rain
624-62768	3	.182	3.222	.0292	-.520	.97	14.8	63.7	
701-70868	7	.244	3.292	.0479	-.501	.93	14.2	68.2	
1004-100668	2	.206	3.249	.0443	-.491	.97	12.4	53.7	
1009-101368	4	.145	3.277	.0429	-.631	.56	11.7	54.5	
1023-102968	7	.222	3.339	.0836	-.552	.85	8.6	47.7	
1030-110568	7	.136	3.458	.0348	-.343	.62	7.5	42.4	
1106-111068	5	.183	3.682	.0667	-.016	.71	6.6	38.5	
1203-121068	7	.516	3.533	.1838	-.093	.75	2.4	29.3	

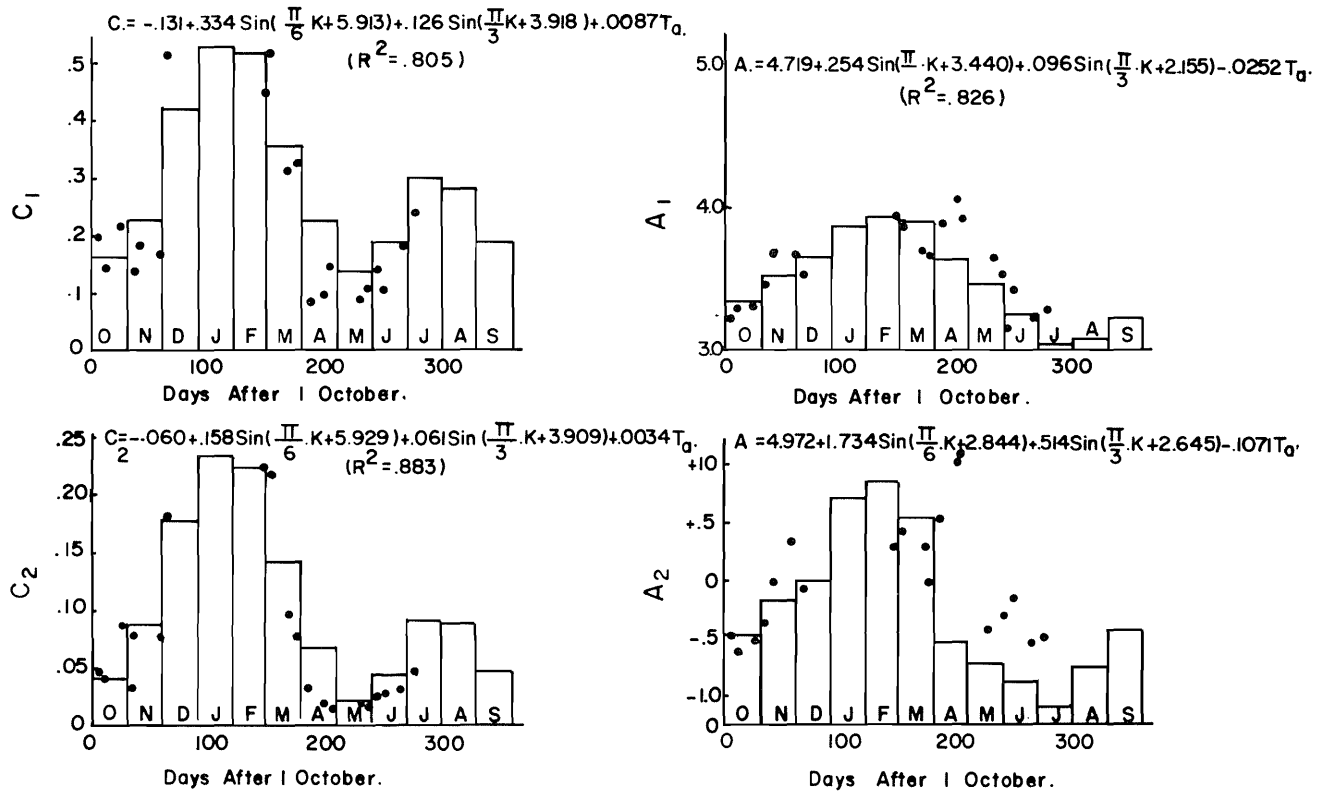


Figure 16. Annual variations in diurnal temperature index model parameters.

$$Y = c_0 + \sum_{j=1}^2 c_j \cdot \sin\left(\frac{2\pi j}{365} \cdot x + a_j\right) + r \cdot \bar{T}_a + \epsilon \dots \dots \dots (26)$$

in which

- Y = diurnal index equation coefficient, A₁, A₂, C₁ or C₂ for a given month
- x = days since 1 October
- \bar{T}_a = mean daily atmospheric temperature for a given month (°F)
- ε = deviation of predicted model parameter value for a given date from the value calculated from diurnal variations observed on that date

c₀, c_j, a_j and r = constants and phase shift as determined by least squares analysis for the respective Y

Monthly values of the DTI model parameters (A₁, A₂, C₁ and C₂), as estimated by Equation 26 are shown in Figure 16 as bars and are listed also in Table 12. The dearth of data points in Figure 16 for the months of

January, August, and September was caused by malfunctions in the continuous monitoring instrumentation for those months.

Table 11 lists the coefficients c₀, a₁, a₂, c₁ and c₂ belonging to Equation 26. These coefficients were obtained by regression analysis of each coefficient represented by Y in Equation 26.

Figure 17 shows graphically Equation 25 for each month of the year. The seasonal pattern exhibited in the monthly diurnal index sine curves is allowed by the monthly assessment of Equation 25 coefficients, which is done by Equation 26. To convert from index display to real temperature it is necessary only to multiply each ordinate by \bar{T}_a , the mean monthly stream temperature.

Diurnal stream temperature simulation

The diurnal distribution of temperature and flow in all hydrologic input streams must be defined before hourly variations in stream temperature may be approximated. All natural surface inflows to the system are assumed to exhibit the same hourly distribution of temperature indexes. Figure 18 shows substantial similarity in patterns of variation at stations S-12.5 and S-20.5

Table 11. Representation of annual changes in diurnal water temperature index model parameters for Equation 26.

Parameter	c_0 (constant)	c_1 (constant)	a_1 (radians)	c_2 (constant)	a_2 (radians)	r (constant)	R^2 (%)
$Y = C_1$	-.131	.334	5.913	.126	3.918	.009	80.
$Y = A_1$	4.719	.254	3.440	.096	2.155	-.025	83.
$Y = C_2$	-.060	.158	5.929	.061	3.908	.003	88.
$Y = A_2$	4.972	1.734	2.844	.514	2.645	-.107	79.

Table 12. Estimated monthly values of diurnal temperature index model parameters for Equation 25, calculated by Equation 26 using Table 11 coefficients.

Month	C_1 (constant)	A_1 (radians)	C_2 (constant)	A_2 (radians)
October	.160	3.333	.039	-.476
November	.230	3.531	.083	-.161
December	.420	3.647	.179	.000
January	.530	3.860	.235	.703
February	.513	3.934	.223	.839
March	.357	3.896	.140	.547
April	.227	3.618	.067	-.536
May	.139	3.463	.020	-.731
June	.191	3.257	.042	-.875
July	.300	3.037	.088	-1.156
August	.281	3.077	.082	-.747
September	.191	3.216	.046	-.419

on October 11-12, 1968. While the agreement is not exact, the approximation is satisfactory for the purposes of this study. Hourly temperatures, τ , of natural surface inflows are estimated by multiplying the mean monthly temperature, $\bar{\tau}$, for these inflows, taken from the monthly simulation, by the diurnal temperature index. Table 13 summarizes the methods employed in simulating hourly time variations in the temperature of the hydrologic inputs to the reach. Diurnal fluctuations in expected "equilibrium" stream temperature are also assumed to be characterized by this same temperature index distribution; mean monthly water temperature, \bar{T} , from Equation 19 is the basis for applying the DTI for the input in question.

It is shown in Table 13 that groundwater flows are assumed free from diurnal influences. Also shown in Table 13 is the card input characterization of municipal-industrial discharges.

Table 13. Diurnal temperature input models.

Input	Model
River inflow	previous simulation of upstream reach
Branch inflow	previous simulation of upstream reach
Surface inflow	$\tau_s = \bar{\tau}_s \cdot DTI$
Irrigation return flow	$\tau_i = \bar{\tau}_i \cdot DTI$
Groundwater inflow	$\tau_g = \bar{\tau}_g$
M & I releases	card input

Reservoir releases may or may not exhibit diurnal variations, depending upon the depth from which they are drawn. Waters spilled from the upper several feet of reservoir storage would be expected to show diurnal patterns of variation in response to the influence of daily cycles in

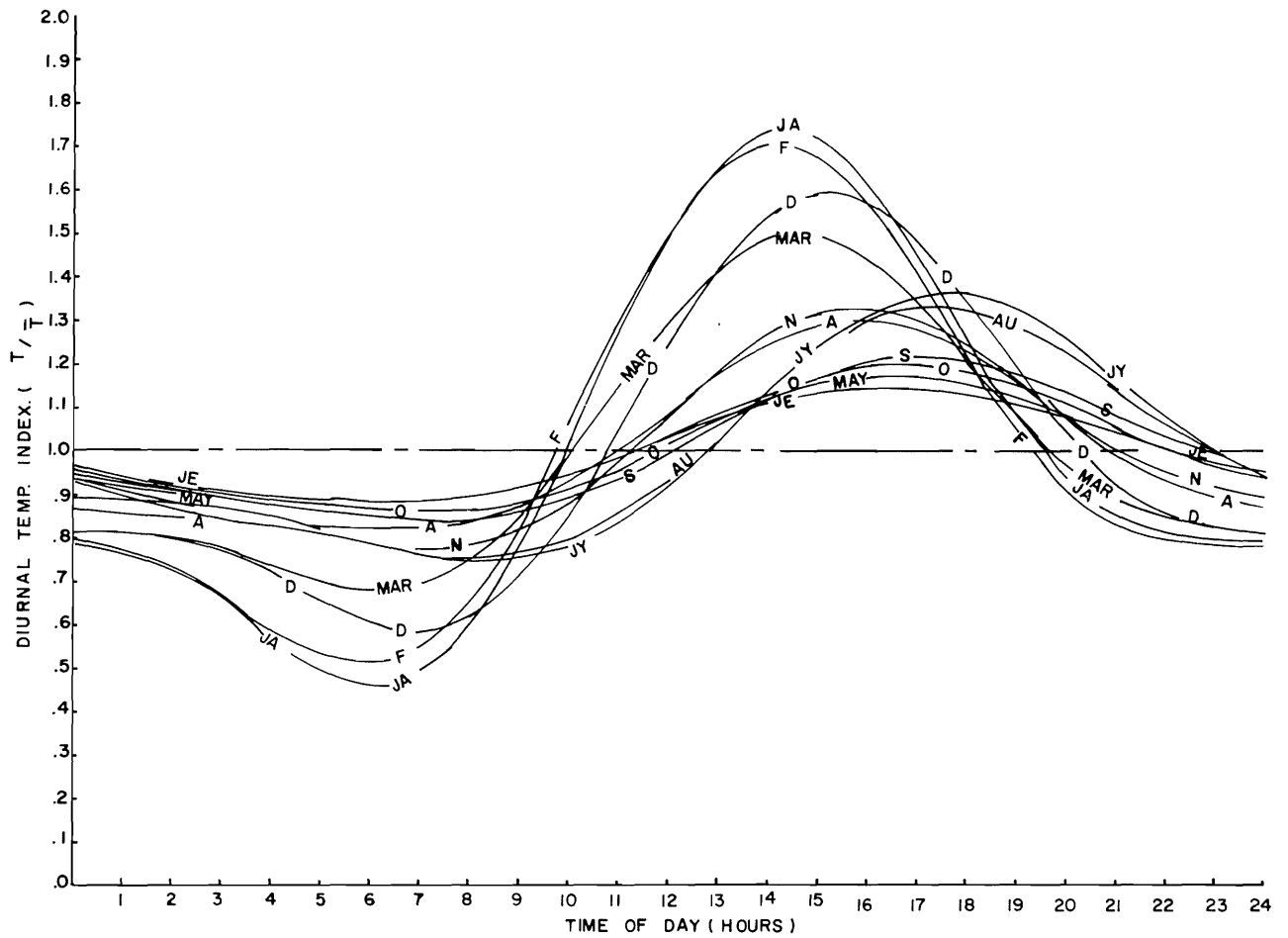


Figure 17. Diurnal temperature index models for each month of the year.

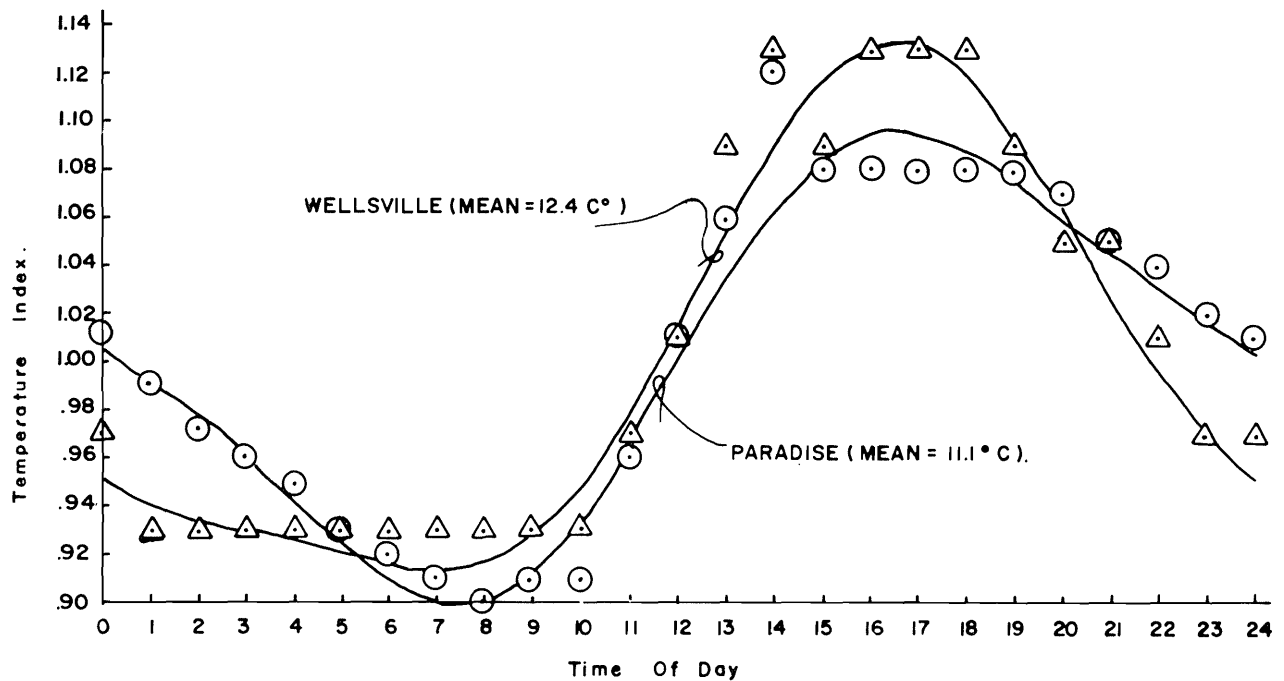


Figure 18. Comparison of stream temperature index patterns on the Little Bear River at Wellsville and Paradise on 11-12 Oct. 1968.

atmospheric conditions. Waters originating in the hypolimnion, on the other hand, are shielded from the effect of atmospheric conditions so that diurnal fluctuations are not observed.

Each of the inputs described above are "mixed" on an hour by hour basis in accordance with Equation 16 (again used with temperatures); this gives the hourly stream temperature distribution at the upstream end of the reach.

A graphical example of the combination of a natural stream inflow and a municipal waste discharge is presented in parts (a), (b) and (c) of Figure 19. Diurnal temperature distributions for the two components of flow (QS and QEF) are depicted in (a) and (b) respectively. The distribution of rate of waste discharge is also shown

in part (b). Ordinates to the hourly temperature distribution for the combined flow, shown in part (c), are calculated for each hour by the mixing formula (Equation 16), with hourly temperatures for each of the components being substituted for conductivity.

In-transit and diurnal changes

Diurnal changes in water temperature within a river reach are determined in the same manner as in the monthly temperature simulation, except that any "temperature excess" due to heat inputs into the stream must be routed through the reach except that in routing the temperature excess through the reach time of travel must be considered. The simulation is performed hour-by-hour over the full 24 hour cycle. The procedure is illustrated with conditions and results shown in Figure 19. Figure 19a is the diurnal temperature pattern of the "natural" stream. Figure 19b is the diurnal patterns of temperature and flow for a hypothetical municipal input. Figure 19c shows the temperature variation of the combined flow in the top boundary, calculated by Equation 16 for each hour. The bottom boundary is the "equilibrium temperature," which was obtained by multiplying the hourly diurnal temperature index, DTI_i, by the mean monthly temperature obtained from Equation 19. The difference between these boundaries is the "temperature excess," at the upstream end of the reach. Figure 19d is the temperature pattern at the downstream end of the reach, which is assumed two hours in travel time from the upstream end. This result is obtained by decaying the excess in Figure 19c by Equation 27. Repeating this procedure for each hour of the day gives the hourly distribution of temperatures at the downstream end of the reach.

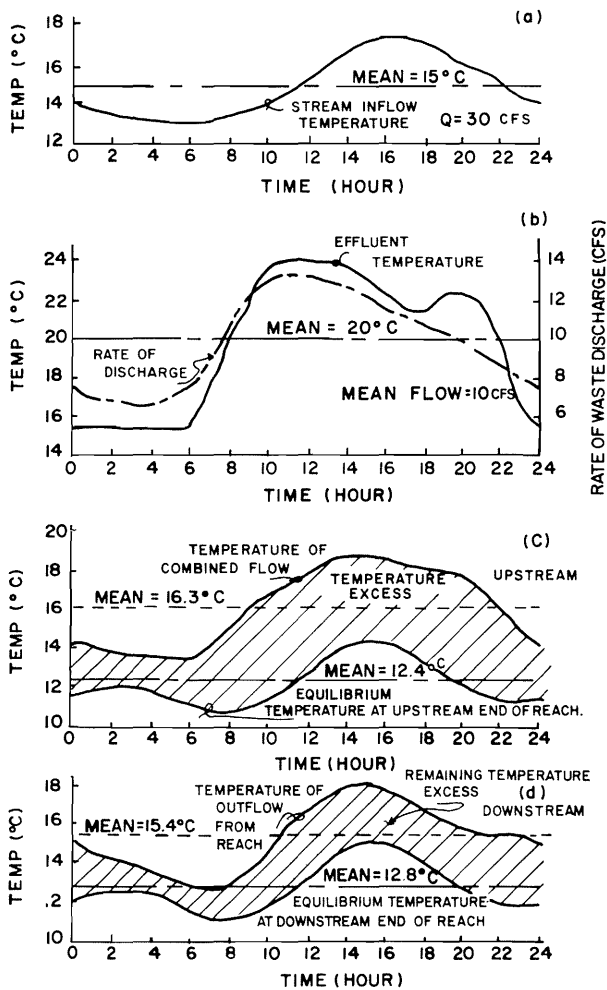


Figure 19. Graphical representation of diurnal temperature computations.

$$T_2(t_2) = \frac{\sum_{j=1}^{nc} [q_j(t_i) \cdot \tau_j(t_1)]}{Q} \cdot e^{-\Phi} + E_2(t_2) \quad (27)$$

in which

- $T_i(t)$ = time distribution of stream temperature at point i , evaluated at time t
- $E_i(t)$ = time distribution of "equilibrium" temperature at point i , and time t ; [$E_i(t) = E_i \cdot DTI_i(t)$]
- $q_j(t)$ = rate of flow of input j at time t
- $\tau_j(t)$ = temperature of input j at time t

$$Q = \sum_{j=1}^n q_j(t)$$

- nc = number of hydrologic inputs to the reach
- $$\phi = \frac{.0235 \cdot k \cdot W}{Q} \cdot D$$
- t₁ = time of inflow at upstream end of reach
- t₂ = time of outflow at downstream end of reach

In this formulation the subscript 1 designates the upstream end of the reach, while 2 indicates the downstream end. Allowing t₁ to vary in increments of one hour through 24 results in the definition of the diurnal temperature distribution at the downstream end of the reach at one hour intervals. The difference between t₁ and t₂ is the travel time through the reach.

Algorithm for simulation

Figure 20 conceptually outlines the simulation algorithm for monthly stream temperature, and is summarized below.

1. Obtain monthly flow values for all inputs from hydrologic model.
2. Feed in mean daily atmospheric temperature for each month.
3. Obtain mean monthly temperature for month in question using monthly model WATEMP.

4. Obtain Fourier coefficients a₁, a₂, c₁, c₂ for Equation 26 by regression analysis.
5. Compute monthly values of Fourier coefficients C₁, C₂, A₁, A₂, for Equation 25.
6. Compute diurnal temperature index, DTI_i, for each hour of day (for the given month) by Equation 25.
7. Compute hourly temperatures by multiplying DTI_i by mean daily water temperature for month in question.
8. For each hour compute temperature of all inputs and obtain mixed stream temperature as per Equation 16.
9. For each hour decay any temperature excess at beginning of reach to the downstream end of reach—as per Equation 27; using proper values of equilibrium temperature for the hour in question.
10. Return to step 1 and repeat procedure for following reach.
11. If entire stream is simulated go to step 1 and repeat, incrementing time by one month.

Steps 4 and 5 are the data preparation steps; steps 1, 2, 3, 10, 11 are done by WAQUAL; steps 6, 7, 8, and 9 are done by DITEMP.

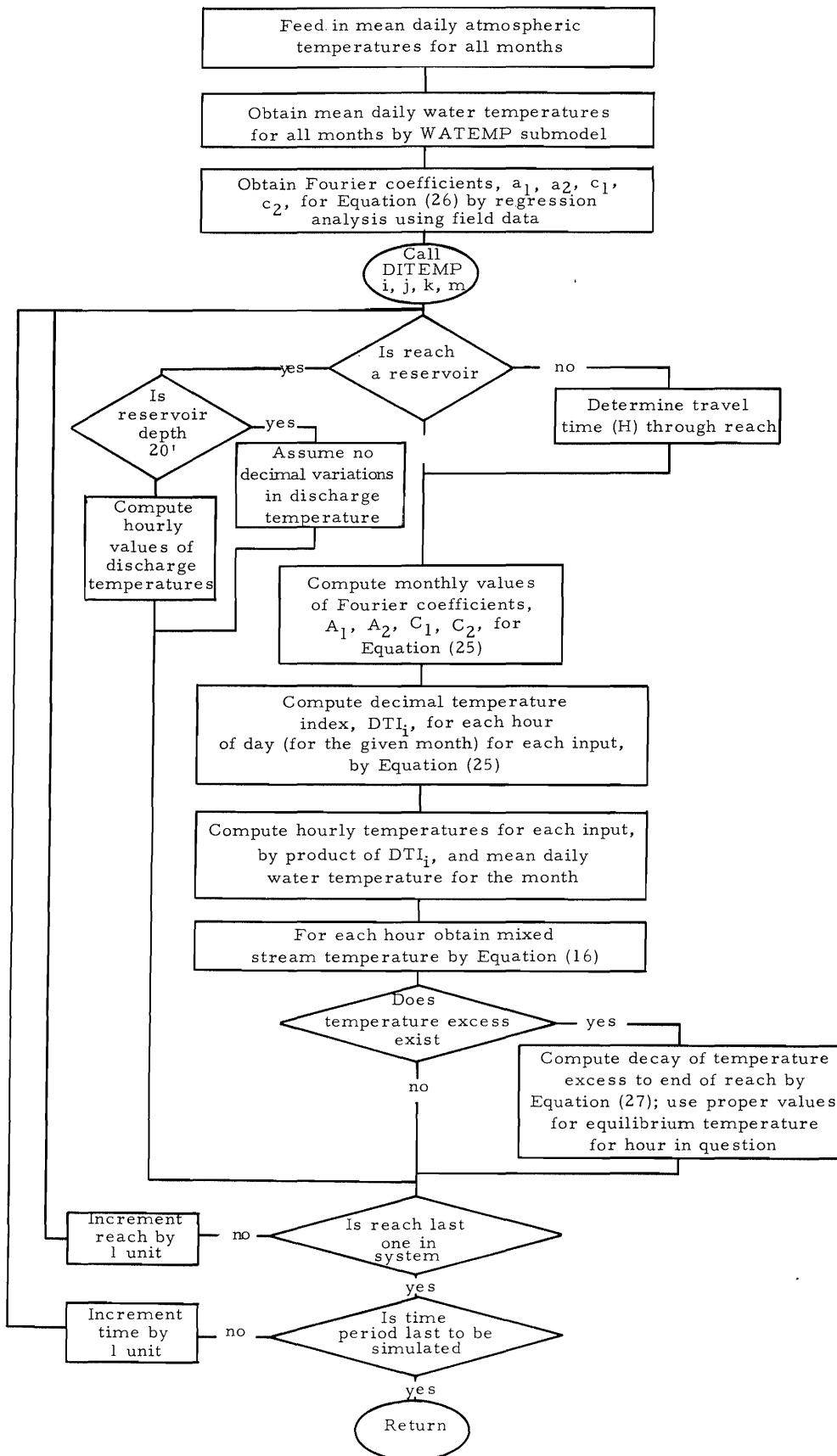


Figure 20. Simulation algorithm for diurnal water temperature.

CHAPTER VI

DISSOLVED OXYGEN SIMULATION

Dissolved oxygen concentration (D.O.) is probably the one characteristic of the water resource pool most frequently cited as an indication of its quality. Whether at saturation, excess, or deficient, the level of D.O. tells considerably about the biotic state of a water body. Low D.O. levels are associated with esthetically undesirable conditions and carry an implication of possible health hazard. Maintenance of a desirable freshwater fishery is perhaps the most important reason for concern about D.O. conditions. In addition, nuisance conditions may prevail should the D.O. levels reach an extreme in either direction of saturation. Thus it is important to understand the temporal D.O. behavior of a stream and also its spatial and temporal response to any imposed waste conditions.

The submodels developed herein consider the temporal changes in D.O. at two levels of time resolution—the month and the hour, for simulation of annual and diurnal cycles, respectively. In addition, the effects of waste inputs are assessed with respect to distance. Again the approach is quite pragmatic; this consists of finding a suitable mathematical relationship which can simulate the D.O. behavior of the stream, and then determining the proper coefficient values by regression analysis of a set of arguments consisting of field data.

In-transit changes

The term “in-transit change” is used with reference to the effects of the processes associated with movement within the stream. In its simplest form the “in-transit change” is simulated by the familiar Streeter-Phelps equation consisting of dissipation by decomposition and respiration reactions and mass transfer of oxygen by turbulent diffusion through the surface. Both are first order kinetic reactions. As originally proposed by Streeter and Phelps (1925), the equation for stream deoxygenation is:

$$\frac{dL_s}{dt} = -K_1 \cdot L_s = -\frac{dD}{dt} \quad \dots (28)$$

in which L_s is the ultimate biochemical oxygen demand (BOD), t is time and K_1 is the first-order rate constant.

The process of stream reoxygenation is first order with respect to oxygen deficit:

$$\frac{dDO}{dt} = K_2 \cdot (C_s - DO) = K_2 \cdot D = -\frac{dD}{dt} \quad \dots (29)$$

Here D.O. is the concentration of dissolved oxygen, C_s is the oxygen saturation concentration, $D = (C_s - C)$ is the D.O. deficit and K_2 is the unimolecular reaeration rate constant.

After combining the deoxygenation and reoxygenation process and integrating, the equation takes the form:

$$D_b = \frac{K_1 \cdot L_{sa}}{K_2 - K_1} \cdot e^{-K_1 \cdot t} - e^{-K_2 \cdot t} + D_a \cdot e^{-K_2 \cdot t} \quad \dots \dots \dots (30)$$

in which the subscripts “a” and “b” designate initial and subsequent concentrations, respectively, after an elapsed time, t .

Although this original formulation is a gross simplification of the complex interrelated processes involved, it has been of great importance in the development of the theory, as it stands today. In fact, most of the models currently found in the literature are based upon the unimolecular rate theory with modifications added, to account for the influence of other processes, such as scour, sedimentation, oxygen demand by benthic deposits, photosynthesis, etc.

The Streeter-Phelps oxygen sag equation (Equation 30) is the classical representation of in-transit dissolved oxygen level changes for a polluted stream. This simple formulation considers only the surface reaeration and bacterial deoxygenation processes. Many other processes may enter into the oxygen balance of a stream. Dobbins (1964) lists several of these processes as:

1. Sedimentation or adsorption of BOD.
2. Resuspension of settled organic deposits by scour action on benthic deposits or upward diffusion of partly decomposed organic matter from the stream benthos.
3. BOD increase by local runoff.
4. Oxygen demand by the aerobic zone of the benthic layer.
5. Oxygen removal by the stripping action of gases rising from the anaerobic decomposition of the benthic layer.
6. Photosynthetic oxygen production by plankton and periphyton.
7. Oxygen removal by respiration of plankton and periphyton.
8. Longitudinal dispersion.

Several researchers have proposed modifications to the Streeter-Phelps equation to integrate into it one or more of the above processes (Thomas, 1948; Li, 1962; Dobbins, 1964; Camp, 1965; and O'Connor, 1967). The work of Hansen and Frankel (1965) brings together, in a rather concise form and in a consistent set of nomenclature, most of the basic concepts presented by their predecessors. In addition, they propose a cyclic expression to represent diurnal variations in photosynthetic production and respiratory uptake of oxygen by photosynthetic organisms. Their equation in integrated form is:

$$D_b = D_a \cdot e^{-K_2 \cdot t} + \frac{(K_1 + K_r) \cdot (1 + K_3/K)}{(K_2 - K)} \cdot \left(L_{s_a} - \frac{p}{K} \right) \cdot \left(e^{-K_1 \cdot t} - e^{-K_2 \cdot t} \right) + \frac{K_4}{K_2 - K_4} \cdot \left(\frac{L_{d_o}}{H} + \frac{p}{K_4} \right) \cdot \left(e^{-K_4 \cdot t} - e^{-K_2 \cdot t} \right) - \alpha (K_2 \cos \beta + \omega \sin \beta) e^{-K_2 \cdot t} + \alpha [K_2 \cos(\omega t + \beta) + \omega \sin(\omega t + \beta)] \dots \dots \dots (31)$$

in which
 D_a = oxygen deficit of a volume of water as it enters the reach (mg/l)
 D_b = oxygen deficit of the same volume as it leaves the reach (mg/l)

- L_{s_a} = ultimate first stage BOD in solution and suspension as the flow enters the reach (mg/l)
- L_{d_o} = initial areal BOD of the benthic zone (g/sq * meter)
- K_1 = laboratory rate of deoxygenation (base e, day⁻¹)
- K_2 = reoxygenation rate constant (base e, day⁻¹)
- K_3 = rate constant for BOD removal by sedimentation and/or adsorption (base e, day⁻¹)
- K_4 = rate constant for the anaerobic fermentation of benthic deposits (base e, day⁻¹)
- K_r = the difference between the actual in-stream deoxygenation constant and laboratory rate constant (base e, day⁻¹)
- K = $K_1 + K_r + K_3$
- p = rate of addition of BOD to the stream water from the benthic layer (mg/l * day)
- t = travel time through the reach (days)
- H = stream depth (meters)
- α = $a/(\omega^2 + K_2^2)$ (mg/l * day)
- a = maximum rate of production (consumption) of oxygen by photosynthesis (respiration) (mg/l * day)
- ω = $2\pi/24$
- β = $2\pi/24 \cdot lt$
- lt = lag time at which respiration of aquatic organisms in the stream below the tributary is a maximum

Assuming no net increase in D.O. due to the activity of photosynthetic organisms over the typical 24 hour cycle, the monthly average of changes in D.O. within a reach may be represented by the first three terms of Equation 31, which is restated as Equation 32:

$$D_b = D_a \cdot e^{-K_2 \cdot t} + \frac{(K_1 + K_r) \cdot (1 + K_3/K)}{(K_2 - K)} \cdot \left(L_{s_a} - \frac{p}{K} \right) \cdot \left(e^{-K_1 \cdot t} - e^{-K_2 \cdot t} \right) + \frac{K_4}{K_2 - K_4} \cdot \left(\frac{L_{d_o}}{H} + \frac{p}{K_4} \right) \cdot \left(e^{-K_4 \cdot t} - e^{-K_2 \cdot t} \right) \dots \dots (32)$$

Equation 32 was programmed as a part of the dissolved oxygen submodel used in this work.

The assumption of no net effect due to photosynthetic organisms may require further justification. During daylight hours, photosynthetic oxygen production exceeds the respiratory requirements of the aquatic community as indicated in Figure 21. These same photosynthetic organisms become users of oxygen during periods of darkness. The net effect of the photosynthetic organisms over a 24 hour cycle is the difference between the amount of oxygen produced during the day (the cross hatched area under the curve) and the amount consumed at night (the cross hatched and stippled area above the curve).

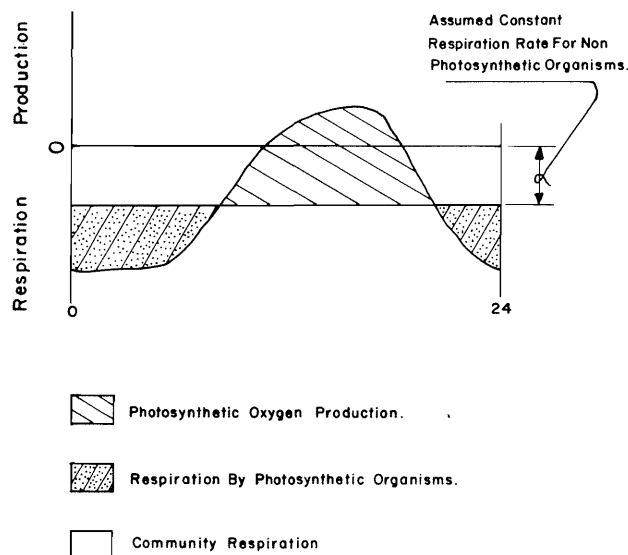


Figure 21. Dissolved oxygen variations at station S-12.8 for 1966-67 with best fit Fourier series curve.

Studies have been conducted to assess the productivity of certain streams. Hoskin (1960) reports photosynthetic oxygen production rates of 87.7 pounds per acre of stream surface per day and community respiration rates of 192 pounds per acre per day in streams of North Carolina. Edwards and Owens (1962) found oxygen production in an English chalk stream to vary from 28.6 to 158 pounds per acre per day while community respiration ranged between 59.9 and 139 pounds per acre per day. It should be emphasized that the above respiration figures relate to the combined respiration of photosynthetic and nonphotosynthetic organisms, represented in Figure 21 as the area bounded by the assumed respiration rate for non-photosynthetic organisms and the zero abscissa, plus the stippled area.

O'Connell and Thomas (1965), in their study of the Truckee River below Reno, Nevada, found oxygen production to average about 72.5 pounds per acre per day, while respiration of photosynthetic organisms proceeded at the rate of 65.4 pounds per acre per day. While the figures of O'Connell and Thomas indicate a possible net production of oxygen by photosynthesis, some of the oxygen produced undoubtedly escapes to the atmosphere.

Suspended BOD

Changes in dissolved and suspended BOD within a reach have been represented as

$$L_{s_b} = \left(L_{s_a} - \frac{p}{k} \right) \cdot e^{-K \cdot t} + \frac{p}{K} \quad \dots (33)$$

by Hansen and Frankel (1965) where L_{s_b} is the BOD of the flow as it leaves the reach being studied and other variables are as defined above.

For the case where scour is taking place ($K_3 = 0$), but not sedimentation ($p \neq 0$), the change in BOD of the benthic deposit within the reach was represented by Hansen and Frankel as

$$L_{d_t} = L_{d_0} \cdot e^{-K_4 \cdot t} - \left(1 - e^{-K_4 \cdot t} \right) \cdot \frac{H_m \cdot p}{K} \quad \dots (p \neq 0, K_3 = 0) \quad \dots (34)$$

in which L_{d_0} is the initial areal BOD of the benthic deposit and L_{d_t} in the areal BOD of the deposit after time "t." This equation may be applied directly to the simulation of month to month changes in the benthal BOD of a stream simply by letting $t = 30$ days.

In the case of sedimentation ($K_3 \neq 0$ and $p = 0$), Hansen and Frankel assume that the rate of deposition is exactly balanced by the rate of anaerobic fermentation so that there is no net buildup of organic material in the benthic region. This assumption seems unduly restrictive for modeling over an extended period. To fill the need for a model to simulate possible increases in benthic BOD during certain periods of the year, the following has been developed.

It is obvious that BOD removed from suspension by sedimentation and/or adsorption must appear as increased

benthic BOD. Assuming that this removal rate is adequately represented by a first order kinetics model of the form

$$\frac{dL_s}{dt} = K_3 \cdot L_s$$

integration yields

$$L_{s_b} = L_{s_a} \cdot e^{-K_3 \cdot t} \quad \dots \dots \dots (35)$$

The change in L_s , due to sedimentation and adsorption, as the flow passes through the reach a-b is

$$\Delta L_s = L_{s_a} - L_{s_b} = L_{s_a} \cdot \left(1 - e^{-K_3 \cdot t}\right) \quad \dots \dots \dots (36)$$

where L_s is measured in mg/l or gm/meter³. On an areal basis this means that the amount of BOD deposited is (assuming uniform deposition over the benthic region of the reach):

$$\Delta L_d = Hm \cdot \Delta L_s = Hm \cdot L_{s_a} \cdot \left(1 - e^{-K_3 \cdot t}\right) \quad \dots \dots \dots (37)$$

in gm/meter².

Using monthly averages, the amount deposited in this reach per month is

$$\Delta L_d = Hm \cdot L_{s_a} \cdot \left(1 - e^{-30 \cdot K_3}\right) \quad \dots (38)$$

in which H is the monthly average of the mean stream depth (in meters), and L_{s_a} is the monthly average of suspended and dissolved BOD in the flow entering the reach.

Assuming areal BOD of the benthos at the beginning of the month to be L_{d_o} and that during the month one half of the amount of BOD deposited is subjected to anaerobic decomposition for a period of 30 days, the equivalent initial areal BOD (L_{d_o}) may be written

$$L_{d_{30}} = L_{d_o} + 1/2 Hm \cdot L_{s_a} \cdot \left(1 - e^{-30K_3}\right) \quad \dots \dots \dots (39)$$

Substituting into the integrated first order reaction equation for anaerobic fermentation for $p = 0$:

$$L_{d_t} = L_{d_o} e^{-K_4 \cdot t} \quad \dots \dots \dots (40)$$

gives

$$L_{d_{30}} = \left[L_{d_o} + 1/2 Hm \cdot L_{s_a} \cdot \left(1 - e^{-30K_3}\right) \right] \cdot e^{-30K_4} \quad \dots \dots \dots (41)$$

This expression predicts L_d at the beginning of the following month when $p = 0$ and $K_3 \neq 0$. Equation 34 applies where $p \neq 0$ but $K_3 = 0$. If both K_3 and p are zero this means that only anaerobic fermentation is affecting the amount of organic material in the benthic deposit. Both Equations 34 and 41 reflect this situation.

Determination of rate constants

The in-transit dissolved oxygen equation of Hansen and Frankel contains many rate constants and other parameters. Estimation procedures for a few of these are found in the literature. Those for which estimation procedures are available include oxygen saturation concentration (C_s), stream reaeration rate constant (K_2), ultimate dissolved and suspended BOD (L_s) and laboratory deoxygenation rate constant (K_1). The relationships employed herein for the estimation of these parameters are discussed below.

Oxygen saturation. The ASCE Committee on Sanitary Engineering Research (1960) has established the relationship between oxygen saturation concentration, C_s , and water temperatures, T (in degrees Centigrade), for fresh water exposed to standard atmospheric at mean sea level as

$$C_s = 14.652 - .41022 T + .0079910 T^2 - .000077774 T^3 \quad \dots \dots \dots (42)$$

Saturation concentrations calculated from this expression differ slightly from those published in Standard Methods for the Examination of Water and Wastewater (American Public Health Association, 1965).

Saturation concentrations obtained from Equation 42 are for sea level (760 millimeters of mercury) and may be adjusted for other atmospheric pressures by multiplying by the following pressure correction factor (cf):

$$cf = \frac{P - pv}{760 - pv} \dots (43)$$

in which P is the observed atmospheric pressure in millimeters of mercury and pv is the vapor pressure of water at the prevailing water temperature. Figure E-2, Appendix E, is a nomograph showing such relationships.

Reoxygenation rate constant. The reoxygenation rate constant has been demonstrated to be closely related to the flow characteristics of the stream. Owens, Edwards, and Gibbs (1964) have integrated data collected by themselves and others, covering a wide range in flow conditions, in the derivation of the expression

$$k_2(20) = 9.41 \cdot V^{.67} \cdot H^{-1.85} \dots (44)$$

in which $k_2(20)$ is the reoxygenation rate constant (base 10) for a natural stream at 20°C, V is the mean velocity of flow (ft./sec.) and H is the mean flow depth (ft.). The relationship between the rate constant and water temperature has been characterized as

$$k_2(T) = k_2(20) \cdot 1.0241^{(T-20)} \dots (45)$$

by Elmore and West (1961). This expression was later used by Churchill et al. (1962) in their exhaustive study of the reaeration of natural streams. In Equation 45 T is water temperature (°C) and $k_2(T)$ is the rate constant at temperature T (base 10, day⁻¹). Because the reaeration rate constant is a characteristic of the channel reach and not of inflowing waters, it was not necessary to define this variable for each inflow.

Deoxygenation rate constant. The deoxygenation rate constant is affected by water temperature, as depicted by the expression

$$k_1(T) = k_1(20) \cdot \theta^{(T-20)} \dots (46)$$

where $k_1(20)$ is the rate constant for 20°C and $k_1(T)$ is that for the temperature under which the actual oxygen consuming reaction takes place. Fair, Geyer, and Okun (1968) report values of θ ranging from 1.15 at 5°C to 0.97 at 35°C. This variation has been approximated in this study as follows:

$$\left. \begin{aligned} \theta &= 1.065 - .0012 \cdot (T-5) \text{ for } T < 20^\circ\text{C} \\ \theta &= 1.047 \text{ for } T > 20^\circ\text{C} \end{aligned} \right\} \dots (47)$$

The rate of oxygen demand is governed by the rate of aerobic decomposition of organic materials dissolved or suspended in the water, which is influenced by the density and type of microbial population, concentration and composition of the waste, water temperature, etc. Deoxygenation rate constants found in the literature vary widely. Hansen and Frankel (1965) used values of $K_1 + K_r$ (deoxygenation rate in the stream) of from 0.30 to 0.42 (day⁻¹). Fair, Geyer, and Okun (1968) and McGahey (1968) cite a value of 0.23 as the "nominal" value for K_1 (base e) for waters receiving settled domestic waste water. Kothandaraman (1968) cites data from the Ohio River in which K_1 varies from 0.31 to 0.05 (day⁻¹). These are equivalent to base 10 constants (k_1) of 0.134 and 0.022 respectively.

Several procedures for estimating the ultimate BOD and the rate constant have been presented in the literature (Thomas, 1937; Moore, Thomas and Snow, 1950; and Sheehy, 1960). Attempts to apply these methods to the low level BOD's of this system were largely unsuccessful because the BOD's were below the range for which the techniques were established. In a short reach immediately below the trout farm discharge, BOD levels were found to be high enough to allow the application of these procedures.

Samples from several points on the river downstream from the trout farm exhibited laboratory rate constants, k_1 (base 10), ranging from 0.15 to 0.08 day⁻¹. Figure 22 shows the results of these tests. Similar values were obtained below the Wellsville sewer outfall, though here again low BOD levels rendered the computational procedure approximate at best. Values for the deoxygenation rate constant (base 10) in surface inflows were assumed to be 0.15 (day⁻¹) for this work.

Discrete BOD loads in the Little Bear River

To assess the effect of a municipal or industrial waste on the oxygen resource of a river system, the initial dissolved oxygen concentration, BOD level, and deoxygenation rate constant of the waste stream need to be defined. Data from the two concentrated waste sources on the Little Bear River show a small annual variation in oxygen concentration. Concentrations ranged from 6.8 to 11.5 mg/l at the Wellsville discharge and from 3.7 to 10.6 mg/l at the trout farm.

Though BOD levels in the two effluents are not high, as municipal and industrial wastes go, they are sig-

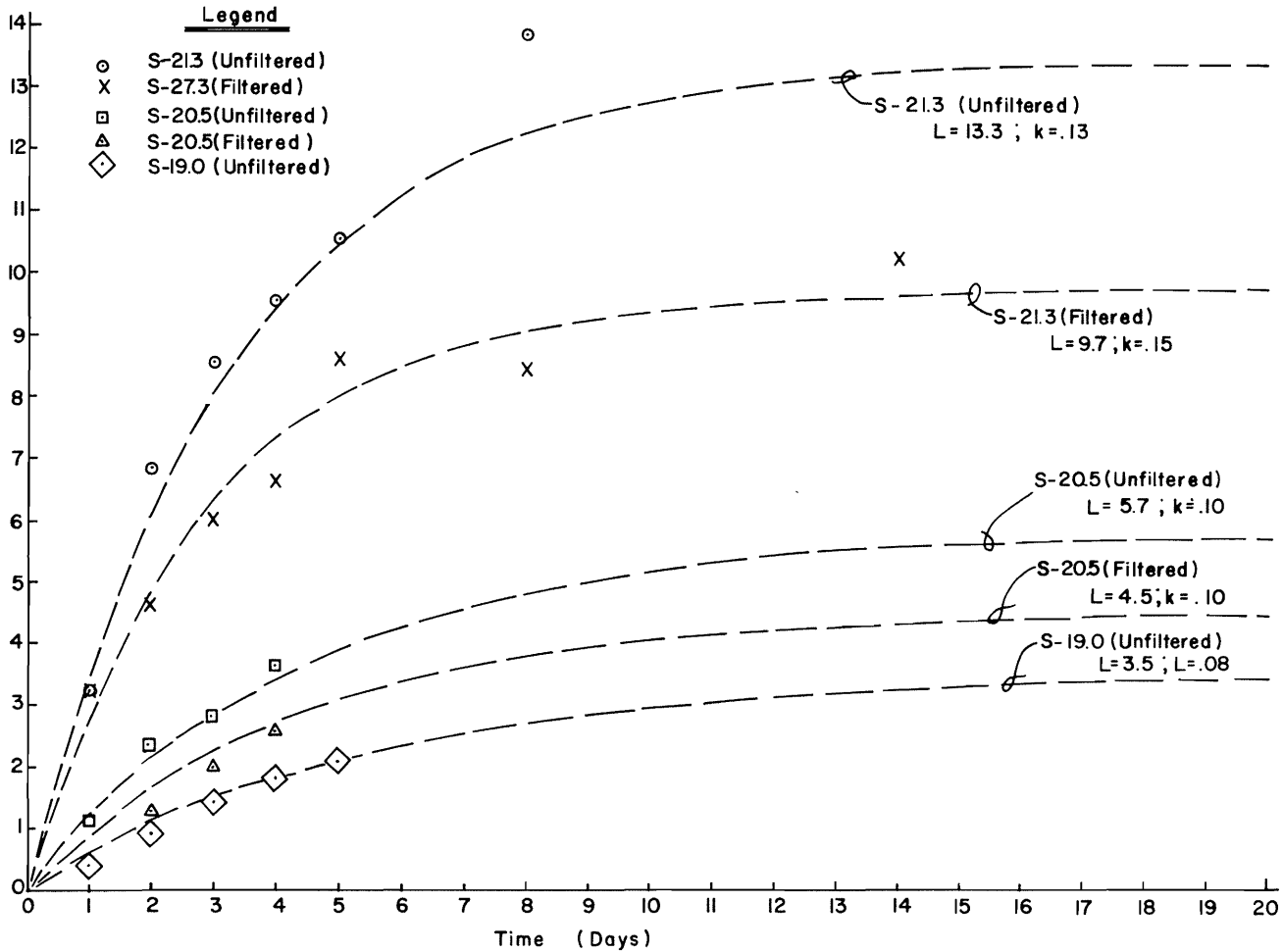


Figure 22. BOD survey below trout farm.

nificantly higher than those of the receiving stream. No meaningful cyclic tendencies were discovered in the BOD data from either effluent. Both discharges exhibit large, apparently random, deviations in BOD, the trout farm waste being erratic in this respect. BOD levels vary from 1.5 to 25.5 mg/l at the trout farm and from .4 to 9.0 at the Wellsville stream.

A BOD survey conducted on 29 August 1968, in the reach between the trout farm and Hyrum Reservoir, revealed a rather surprising rate of recovery from the load applied in the trout farm effluent. Three sampling points were studied, one immediately downstream from the point of discharge, a second 0.8 mile downstream and the third 2.3 miles downstream, just above Hyrum Reservoir. Travel time from the point of discharge (S-21.3) to the second sampling point (S-20.5) was estimated at 30 minutes while that from the second to third points was about one hour.

In this short time, the ultimate BOD of the unfiltered samples, as determined by the method of moments (Moore, Thomas, and Snow, 1950) dropped from 13.3 to 5.7 mg/l. The rate constant also decreased from 0.13 to 0.10 during this time, as mentioned previously and indicated in Figure 22. It is hypothesized that this rapid rate of recovery is brought about by the heavy Sphaerotilis growth found attached to the stony bottom (Figure 23). The density of this growth decreases rapidly in the downstream direction until it is hardly noticeable at the sampling point near Hyrum Reservoir. The results of this study are shown graphically in Figure 22. Analyses of filtered samples were conducted to determine whether or not the rapid change in BOD could be explained in terms of removal of suspended matter within the reach. BOD levels for filtered samples were found to be lower than those of unfiltered samples, but did not approach the low level observed at the downstream point. The luxurious growth on the gravel stream bed appears to act as a fixed bed



Figure 23. Sphaerotilis growth on rocks downstream from trout farm discharge.

reactor, quickly removing a large proportion of the organic matter carried into the stream by the trout farm discharge.

Combination of hydrologic inputs

Dissolved oxygen and BOD concentrations at the upstream end of the reach are calculated by the Equation 16 mixing formula. The deoxygenation rate constant of the combined flows is assumed to be the weighted average of the rate constants for all components of inflow, where the weighting factor is the total BOD contributed by each input:

$$K_1 = \frac{\sum_{j=1}^{nc} K_{1j} \cdot q_j \cdot \overline{BOD}_j}{\sum_{j=1}^{nc} q_j \cdot \overline{BOD}_j} \dots (48)$$

in which

- K_1 = deoxygenation rate constant of the combined inflow (base 10)
- n = number of hydrologic inputs to the reach
- K_{ij} = deoxygenation rate constant for the "j th" hydrologic input (base 10)
- q_j = rate of flow for the "j th" hydrologic input
- BOD_j = mean monthly BOD of the "j th" hydrologic input

The annual cycle

Mean daily dissolved oxygen exhibits an annual cycle. Figure 24 illustrates the pattern, which is sinusoidal. Simulation of this pattern is of value for its own sake to give the time distribution in dissolved oxygen at a given station; however, the value derived is also the initial D.O. input for the in-transit simulation. The annual D.O. simulation is the composite of the simulation of many individual inputs, described subsequently.

The simulation computer program for this phase is called MIDOX, implying monthly dissolved oxygen. This program, which is a part of the system program

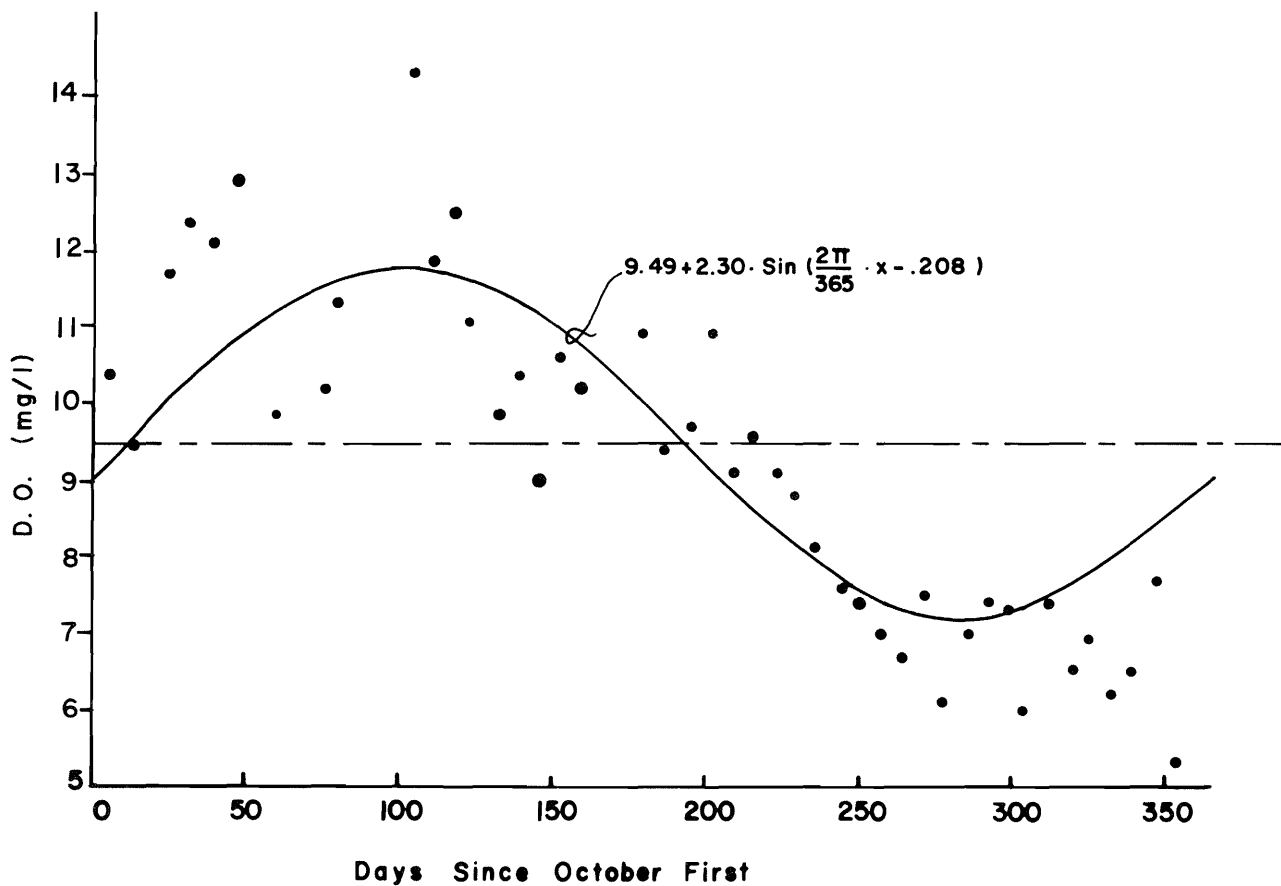


Figure 24. BOD variations at stations S-12.8 for 1966-67 with best fit Fourier series curve.

WAQUAL, also absorbs the "in-transit" and "diurnal" components; in aggregate then, MDISOX is the dissolved oxygen submodel.

Inputs

Adjustment of discrete sampling data. D.O. data from the weekly sampling program were adjusted for the effect of diurnal variation and varying sampling time by dividing by the diurnal D.O. index (DDOI) for the time at which the grab sample was taken. The DDOI is the ratio of observed D.O. concentration at the time of observation to mean daily concentration, as determined from continuous monitoring data. This adjustment considerably improved the fit of the annual cycle D.O. model over that attained using the raw D.O. data. Thus for all data discussed, which is to be representative of a single sample, it will be understood that the value reported is an adjusted mean daily value.

River inflow. The simulation procedure begins at the upper extremity of each branch, proceeding downstream. Results from the simulation of the adjacent up-

stream reach are employed as input for the simulation of the next reach downstream. For the first reach analyzed on a branch, the stream inflow is assumed to be zero and all natural surface inflows are lumped together in the "surface inflow" category (QS). The method of approximating D.O., BOD, and deoxygenation rate constant for this component is discussed below.

Branch inflow. Branches tributary to a reach are simulated before the analysis of that reach is attempted. The D.O., BOD, and deoxygenation rate constant of inflow from tributary branches are therefore available for incorporation into the analysis.

Surface inflow. Field data from analysis of weekly samples showed significant annual cycles for mean daily dissolved oxygen, with high values during winter months, which decreased to minimums in the summer and early fall. Figure 24 illustrates the trend using representative field data. The data were adjusted to mean daily values by dividing observed concentrations by the diurnal dissolved oxygen index (discussed later) for the time of sampling. A simple sine-curve linearizing equation:

$$\overline{DO} = \overline{\overline{DO}} + C \cdot \sin\left(\frac{2\pi}{365} \cdot x + A\right) + \epsilon \quad (49)$$

was fitted to the adjusted data by least squares analysis, where D.O. is mean daily dissolved oxygen concentration (mg/l) on the "x th" day of the year, $\overline{\overline{DO}}$ is the mean annual D.O. concentration, x is the number of days since October 1, C and A are parameters determined by least squares regression procedures, and ϵ is the deviation of the oxygen concentration observed on the "x th" day of the year from the model prediction for that date. Fourier series containing more terms were tried, but without any significant improvement in fit. The model has been programmed, however, to allow a two term Fourier series should it be needed.

Table 14 lists the results of this Fourier series curve fitting at 12 sampling points on the system. The degree of fit, as measured by R^2 , is not high, but statistical analyses indicate that Equation 31 does explain a significant portion of the total annual variation in D.O. at all stations. Figure 24 illustrates the relatively large residual deviations from the model. These variations appear to be random in nature, possibly resulting from random sampling errors and variations in oxygen concentrations caused by randomness in such controlling variables as water temperature and cloud cover.

Equation 49 has been adopted for the prediction of mean monthly D.O. concentrations in natural surface inflows despite the typically low R^2 because it does represent a significant cyclic annual variation at all points sampled.

In some cases, discernible annual cycles were also observed in the weekly BOD data (Figure 25). Therefore, a sine-curve equation, similar to that applied in the case of

dissolved oxygen concentrations, was fitted to weekly BOD data from 12 sampling points in the Little Bear River drainage:

$$\overline{BOD} = \overline{\overline{BOD}} + C \cdot \sin\left(\frac{2\pi}{365} \cdot x + A\right) + \epsilon \quad (50)$$

As shown in Table 15, the degree of fit varied considerably from one location to another. Statistical significance could be claimed for eight of the twelve sets of data.

Though the degree of correlation between time of year and BOD concentration was not high, a significant portion of the total variation at a majority of the sampling points was explained by Equation 50. Because a better procedure for predicting BOD concentrations in surface inflows was not forthcoming, Equation 50 has been incorporated into the simulation to approximate annual cycles for the BOD of natural surface inflows.

Irrigation return flow. Dissolved oxygen concentrations in surface irrigation return flows are assumed relatively constant over the three or four month irrigation season, though provision is made in the modeling program to allow variation with time.

The BOD of return flow is also considered constant. Because waters applied to agricultural lands have more opportunity to pick up organic matter from animal and vegetal matter in and on the soil, the level of oxygen demand in return flows is assumed to be somewhat above that found in natural surface inflows. The deoxygenation rate constant for irrigation return flows is assumed to be the same as that for natural surface inflows.

Groundwater inflow. Dissolved oxygen concentrations in groundwater inflows were not sampled during

Table 14. Fourier series simulation of annual fluctuations in dissolved oxygen concentration.

$$\left[\overline{DO} = \overline{\overline{DO}} + C \cdot \sin\left(\frac{2\pi}{365} \cdot x + A\right) \right]$$

Station	$\overline{\overline{DO}}$ (mg/l)	C (constant)	A (radians)	R^2 (%)	Comments
S-12.7	8.55	1.517	-.407	56.	below sewer outfall
S-12.8	9.49	2.303	-.208	66.	
S-15.2	9.97	1.808	-.573	36.	
S-16.8	8.77	1.863	-.897	74.	reservoir surface
S-21.3	7.23	1.591	-.660	61.	below trout farm
S-24.6	8.95	1.321	-.148	60.	
S-27.5	8.61	1.032	-.247	52.	
SD-0.0	8.82	1.896	-.401	62.	
SEC-4.3	8.59	.998	-1.243	27.	below reservoir
SEC-6.2	8.48	1.163	-.394	62.	
STF-0.0	6.35	1.520	-.773	31.	trout farm effluent
SW-0.1	8.08	1.126	-.425	62.	sewer outfall

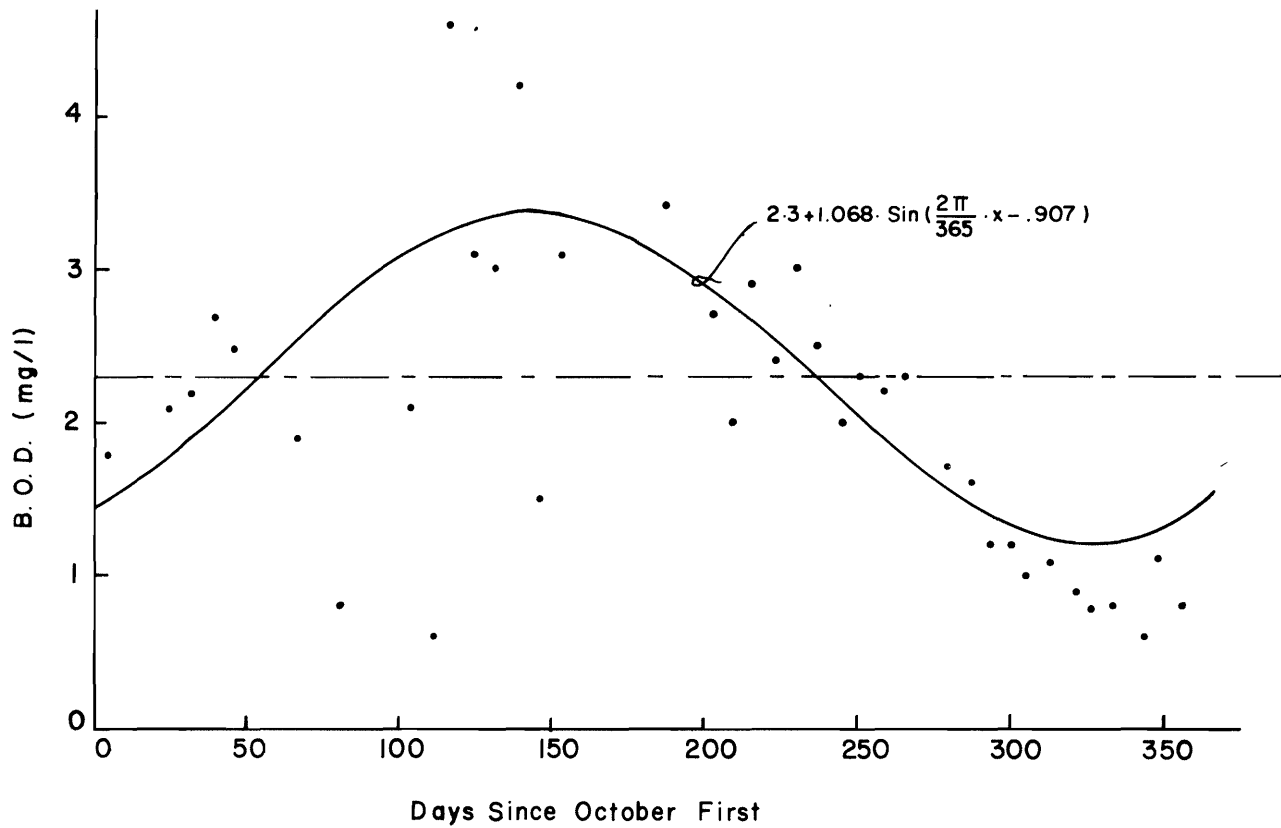


Figure 25. Annual BOD cycle, station S-12.8.

Table 15. Fourier series modeling of annual variations in BOD (5 day, 20°C).

$$\left[\overline{\text{BOD}} = \overline{\text{BOD}} + C \cdot \sin\left(\frac{2\pi}{365} \cdot x + A\right) \right]$$

Station	BOD (mg/l)	C (constant)	A (radians)	R ² (%)	Comments
S-12.7	2.5	.956	-1.048	30. ^a	below sewer outfall
S-12.8	2.3	1.068	-.907	32. ^a	
S-15.2	2.6	1.022	-.937	23. ^a	
S-16.8	2.9	1.617	-.171	21. ^a	reservoir surface
S-21.3	6.8	1.772	-1.553	16.	below trout farm
S-24.6	1.7	.485	-.690	13.	
S-27.5	1.7	.897	-1.154	43. ^a	
SD-0.0	1.9	1.002	-.813	50. ^a	
SEC-4.3	1.6	.898	-1.272	62. ^a	below reservoir
SEC-6.2	1.8	1.022	-.930	30. ^a	
STF-0.0	8.9	3.301	3.820	17.	trout farm effluent
SW-0.1	3.8	.986	4.353	12.	sewer outfall

^a Statistically significant at the $\alpha = .05$ level.

this project. A sinusoidal pattern of annual variation, similar to that found in natural surface inflows, was assumed for groundwater inflows.

Biochemical oxygen demand of groundwater was not measured, but is assumed to be zero. This assumption is based upon the ability of the biologically active soil mantle to stabilize dissolved organics as the water passes through enroute to the groundwater aquifer. Suspended organics are removed by the screening action of soil particles. For modeling purposes, the BOD of groundwater inflows is taken as zero.

Municipal and industrial releases. Annual variations in municipal and industrial releases are simulated by card input based upon historical records where possible.

Summary. Table 16 summarizes the simulation for each hydrologic input. The stream is considered reach by reach along the main stem and immediate tributaries; all or part of these inputs may be significant for any given reach. The mean daily dissolved oxygen value, D.O., for that reach is calculated by the weighted average of all inputs.

Reservoir effects

Of the two reservoirs on the Little Bear River, only Porcupine Reservoir was sampled to assess the effect of the impoundment on the oxygen resource of the stream. Dissolved oxygen concentrations at the sampling point immediately below Porcupine Reservoir were consistently at or near the level of saturation as indicated in Figure 26. This is reasonable for this situation, even though releases from this reservoir are from the hypolimnion, because of the intense turbulence in the discharge stilling basin.

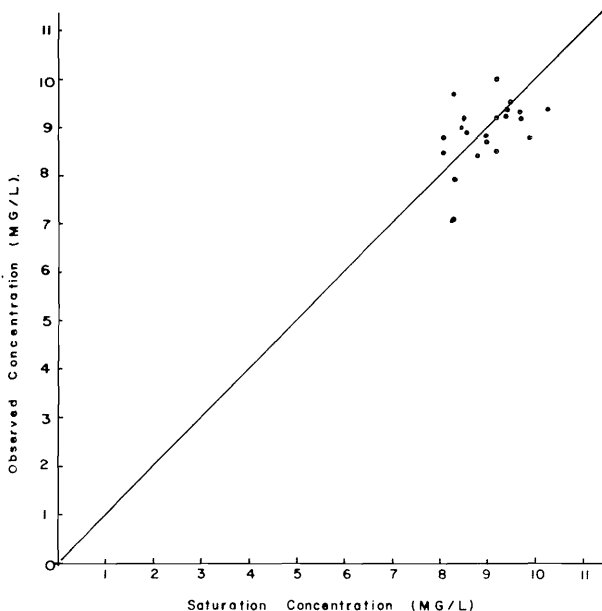


Figure 26. Comparison of D.O. concentrations observed below Porcupine Reservoir in 1967 with saturation concentration.

Therefore a simulation run was made with the D.O. in the reservoir discharge set equal to the saturation concentration. This assumption resulted in significant deviations of simulated concentrations from measured values, both at the reservoir discharge and at points downstream.

Time series analysis of weekly D.O. data from Porcupine Reservoir discharge disclosed a small, but statistically significant correlation between time of year, and D.O. concentration, represented by the equation

$$\overline{DO}_r = \overline{DO}_r + C_r \cdot \sin \left(\frac{2\pi}{365} \cdot x + \frac{A}{y} \right) + \epsilon \quad (51)$$

This time series equation improved the correspondence between simulated and measured D.O. concentrations at reservoir discharges and at points downstream. Therefore, Equation 51 was used to simulate D.O. concentrations in reservoir releases, rather than to assume saturation.

Because of the high degree of randomness in the BOD data, it was difficult to determine precisely what hydrologic or hydraulic parameters relate best to the BOD load in released water. Again, some degree of time dependence was observed. A simple sine-curve representation of monthly variations in BOD at reservoir releases was incorporated into the simulation model.

To summarize: monthly variations in D.O. and BOD of reservoir releases were both assumed to follow a sinusoidal pattern through the annual cycle. The annual mean, coefficient, C, and phase shift, A, were determined by the least squares fitting of Equation 51 to observed D.O. and BOD data for the reservoir release.

Simulation algorithm

Figure 27 outlines the simulation algorithm for mean monthly dissolved oxygen. This algorithm is summarized below.

1. Obtain monthly flow values for all inputs listed in Table 16 from the hydrologic model.
2. Establish mean annual D.O., and Fourier constants, A and C, for Equation 49 by regression analysis of field data; do likewise for Equation 50.
3. Compute D.O. and BOD of each input to reach for month in question by Equations 49 and 50, respectively; use card input where these equations are not applicable.
4. Compute stream D.O., consisting of combined inflows, by Equation 16.
5. If each is a reservoir, calculate output D.O. by Equation 15, skipping steps 6, 7, 8, 9, 10, 11, 12, 13.
6. Compute weighted deoxygenation rate constant, k_1 , by Equation 48, and correct for temperature by Equations 46 and 47.
7. Estimate the reoxygenation rate constant, k_2 , using Equation 44 and adjust for temperature by Equation 45.

8. Calculate saturation concentration for reach using output of temperature simulation as argument for Equation 42; also adjust for altitude pressure by Equation 43; alternately, Figure E-2 may be used.

9. Calculate oxygen deficit at the upstream end of the reach ($D_a = C_{s_a} - DO_a$) and apply the sag equation (Equation 32).

10. Subtract the remaining deficit from the saturation concentration at the downstream end of the reach to estimate the dissolved oxygen concentration at the outflow from the reach.

11. Determine residual BOD in reach outflow (Equation 36).

12. Compute areal BOD of the benthos at the end of the month (Equation 34 or 41).

13. Call diurnal submodel if desired.

14. Go to next reach and return to step 1.

15. If last reach is simulated, increment time by one month and return to step 1.

Step 2 is input preparation; steps 1, 13, 14, and 15 are done by WAQUAL; steps 3-12 are done by DDISOX.

Table 16. Summary of input D.O. and BOD equations over the annual cycle.^a

Input	Parameter	Model
River inflow	D.O.	result from previous simulation
	BOD	
	K_1	
Branch inflow	D.O.	result from previous simulation
	BOD	
	K_1	
Surface inflow	D.O.	$\overline{DO_s} = \overline{DO_s} + C \cdot \sin\left(\frac{2\pi}{12} \cdot m + A\right)$
	BOD	$\overline{BOD} = \overline{BOD} + C \cdot \sin\left(\frac{2\pi}{12} \cdot m + A\right)$
	K_1	card input
Irrigation return flow	D.O.	$\overline{DO_i} = \overline{DO_i} + C \cdot \sin\left(\frac{2\pi}{12} \cdot m + A\right)$
	BOD	card input
	K_1	
Groundwater inflow	D.O.	$DO_g = \overline{DO_g} + C \cdot \sin\left(\frac{2\pi}{12} \cdot m + A\right)$
	BOD	card input
	K_1	
Municipal and industrial release	D.O.	card input
	BOD	
	K_1	

^aSubmodel constants (\overline{DO} and \overline{BOD}), coefficients (C) and phase shifts (A) are determined by analysis of field data and provided to the simulation program by punched card input.

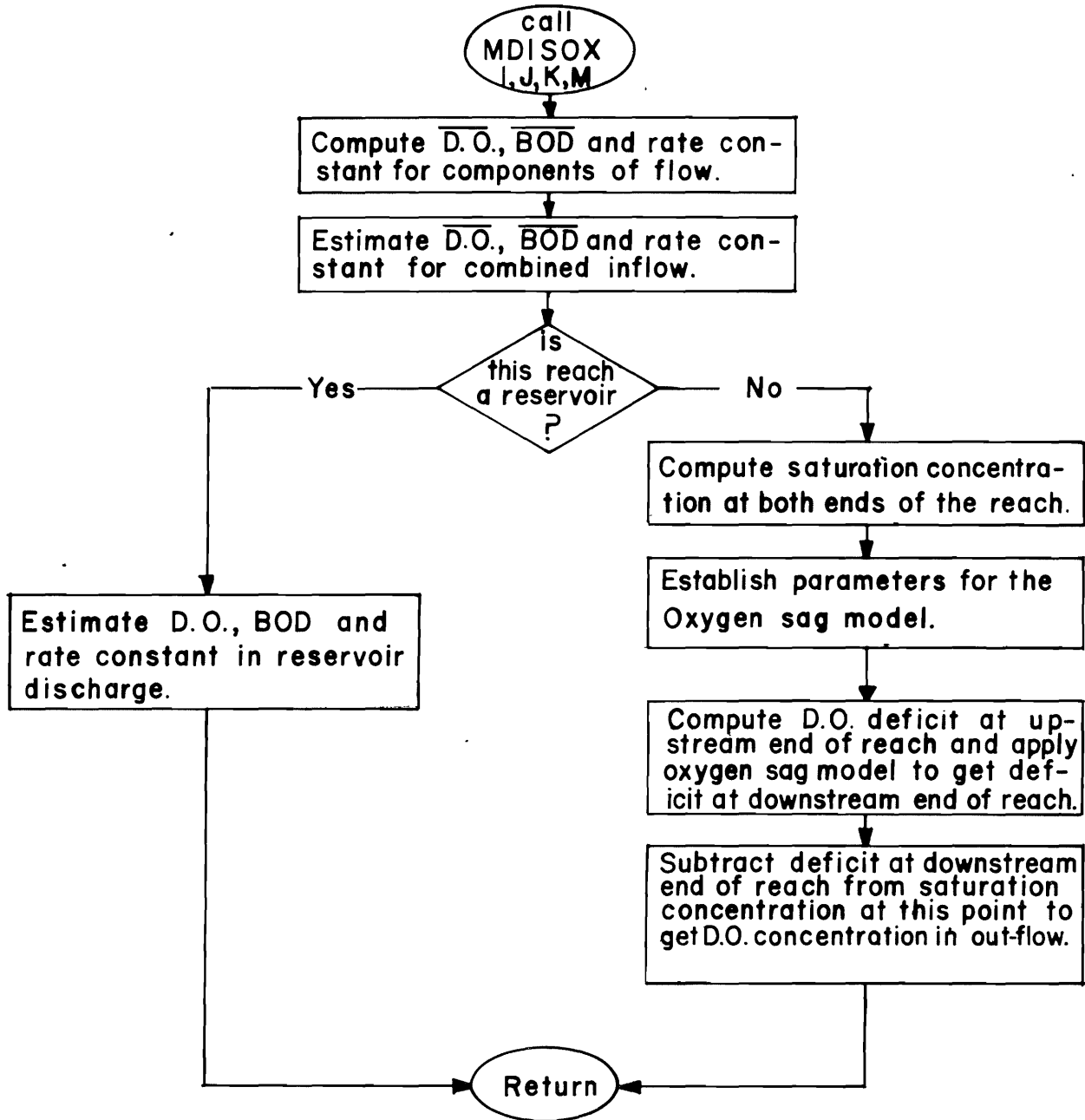


Figure 27. Generalized monthly D.O. flow chart.

Diurnal dissolved oxygen

Several observers have reported diurnal variations in dissolved oxygen concentrations in natural streams. Hoak and Bramer (1961) found relatively minor diurnal cycles in D.O. in several Pennsylvania streams. Gunnerson and Bailey (1963), however, report significant daily variation in D.O. along the Sacramento River from Redding to the delta. O'Connell and Thomas (1965), in reporting their studies of the Truckee River in Nevada, indicate relatively large diurnal fluctuations in D.O. These fluctuations were attributed to the activity of photosynthetic organisms attached to the stream bottom.

Frankel (1965), in discussing the cyclic pattern of deviations from mean daily dissolved oxygen, proposes a photosynthetic factor for each reach. This factor is a function of the time of day, and is defined in terms of the ratio of hourly D.O. to mean daily D.O. Thomann (1967), in his study of the Potomac estuary, found significant diurnal fluctuations in D.O. only above the zone of tidal influence.

Many comments found in the literature emphasize the importance of considering these diurnal variations, but surprisingly little has been published concerning their characterization. As with temperature, a single measurement is not representative of the stream. To assess the dissolved oxygen quality of a stream, it is imperative that the diurnal effect be characterized. It is the purpose of this section to ascertain the mathematical description of the diurnal dissolved oxygen fluctuations. As with temperature, the monthly effect on the diurnal variation is also defined. This is done using continuous monitoring field data from station S-12.5, located below Wellsville on the Little Bear River. A sample of these data is shown in Figure 28.

Modeling diurnal dissolved oxygen variations

Nineteen blocks of continuously monitored dissolved oxygen data, varying from 3 to 7 days in length and covering an 18-month period, have been fitted, as described in Appendix D, with a two term Fourier series of the form

$$DO_i = \overline{DO} + \sum_{j=1}^2 C_j \cdot \sin\left(\frac{2\pi j}{24} \cdot i + A_j\right) + \epsilon_i \dots \dots \dots (52)$$

in which

- $\frac{DO_i}{\overline{DO}}$ = D.O. concentration (mg/l)
- \overline{DO} = average mean daily oxygen concentration (mg/l) for the time period covered by the block of continuous data being fitted

- C_j = coefficient of the "j th" term
- A_j = phase shift for the "j th" term
- ϵ_i = deviation from the model
- i = hour of the day

The two-term model provides essentially the same fit as did three- and four-term series. This fit was considerably better than that obtained from the one-term model. Figure 28 depicts a typical set of hourly D.O. observations over a 7-day period, with the best-fit two-term Fourier series model superimposed.

Two interesting characteristics of this typical diurnal pattern should be noted. First, notice the time period during which D.O. concentrations are typically higher than average. For this particular set of data it runs from 8:00 a.m. through 6:00 p.m. (the hours during which water quality samples are usually taken). This factor results in an upward bias of most "grab sample" stream D.O. data. Another characteristic is the long flat region in the curve, extending from about 9:00 p.m. through 5:00 a.m. During this 8-hour period, the D.O. concentration is 2 mg/l lower than a sample taken at 1:00 p.m. would have indicated. The importance of considering diurnal D.O. variations is obvious.

Dividing Equation 52 through by mean daily D.O. yields a defined term, called the diurnal dissolved oxygen index (DDOI):

$$DDOI_i = 1.0 + \sum_{j=1}^2 C_j \cdot \sin\left(\frac{2\pi j}{24} \cdot i + A_j\right) + \epsilon_i \dots \dots \dots (53)$$

in which

- $DDOI_i$ = $\frac{DO_i}{\overline{DO}}$, diurnal dissolved oxygen index
- C_j = coded coefficient of the "j th" term
- A_j = phase angle of the "j th" term
- ϵ_i = coded error term
- i = hour of the day

In Equation 53, the coefficient, C_j , and error term, ϵ_i , are now coded by division by mean daily D.O. The resulting coefficients and phase shifts are shown in Table 17, along with the coefficient of determination (R^2), average D.O. and average atmospheric temperature for the period covered by each block of continuous data. Annual cyclic tendencies may be detected in the tabulated model parameters. The cyclic variations become more evident when the DDOI model parameters (C_1 , C_2 , A_1 and A_2) of Equation 53 are plotted versus time of year as shown in Figure 29.

Equation 54 augments Equation 53 by representing the annual cycles in the A_j and C_j parameters:

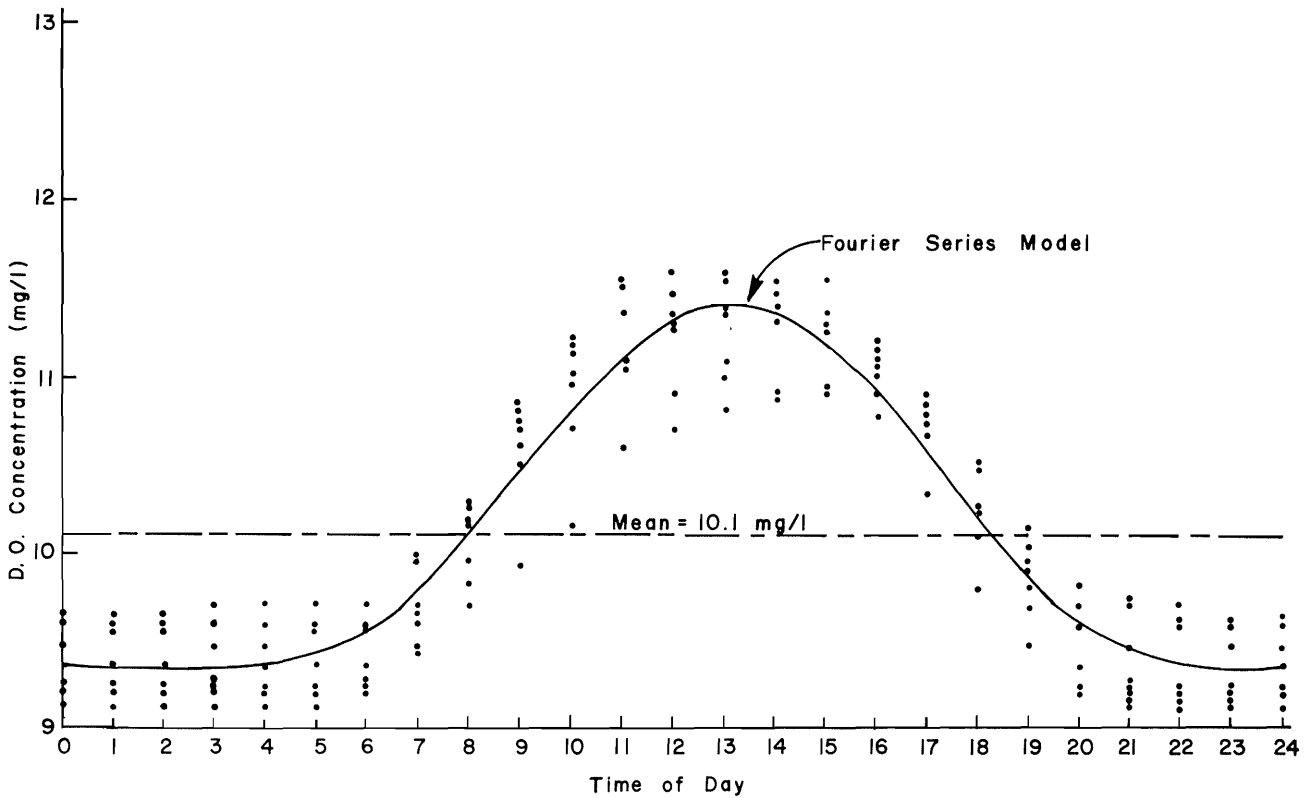


Figure 28. Dissolved oxygen variations for the period 22-29 April 1968 with Fourier series model.

Table 17. Diurnal dissolved oxygen index model parameters.

$$\left[\text{DDOI}_i = 1.0 + \sum_{j=1}^2 C_j \cdot \sin \left(\frac{2\pi j}{24} \cdot i + A_j \right) \right]$$

Date	No. of days	C ₁ (constant)	A ₁ (radians)	C ₂ (constant)	A ₂ (radians)	R ² (%)	DO	T _a	Notes
1127-120167	4	.0767	4.405	.0400	.844	74.	10.0	26.8	
222-22968	6	.0304	4.777	.0144	1.287	67.	11.3	35.2	
229-30668	6	.0284	4.829	.0117	1.205	53.	11.0	39.2	
318-32568	7	.0596	4.865	.0220	1.032	66.	9.9	36.8	
325-32868	3	.0666	4.868	.0295	1.013	87.	9.5	42.8	
404-40668	2	.0196	4.483	.0047	.723	73.	10.0	40.5	Rain
417-42268	5	.0752	4.518	.0220	1.211	80.	9.9	35.2	
422-42968	7	.0999	4.422	.0271	.956	91.	10.1	42.8	
517-52468	7	.1197	4.307	.0302	.734	61.	7.9	52.6	
524-53168	7	.1542	4.169	.0364	.612	67.	8.5	55.7	
531-60468	4	.2060	4.194	.0564	.275	83.	7.3	59.3	
606-61268	6	.0450	4.104	.0082	-.114	60.	9.3	56.8	Rain
624-62768	3	.2005	4.457	.0481	.450	94.	7.6	63.7	
1004-100668	2	.0921	4.468	.0503	.251	55.	9.2	53.7	
1009-101368	4	.1053	4.315	.0560	.350	91.	8.6	54.5	
1023-102968	7	.0736	4.448	.0429	.675	89.	9.3	47.7	
1030-110568	7	.0690	4.374	.0396	.521	74.	9.6	42.4	
1106-111068	5	.0995	4.455	.0567	.814	89.	10.2	38.5	
1203-121068	7	.1008	4.399	.0588	.787	94.	12.1	29.3	

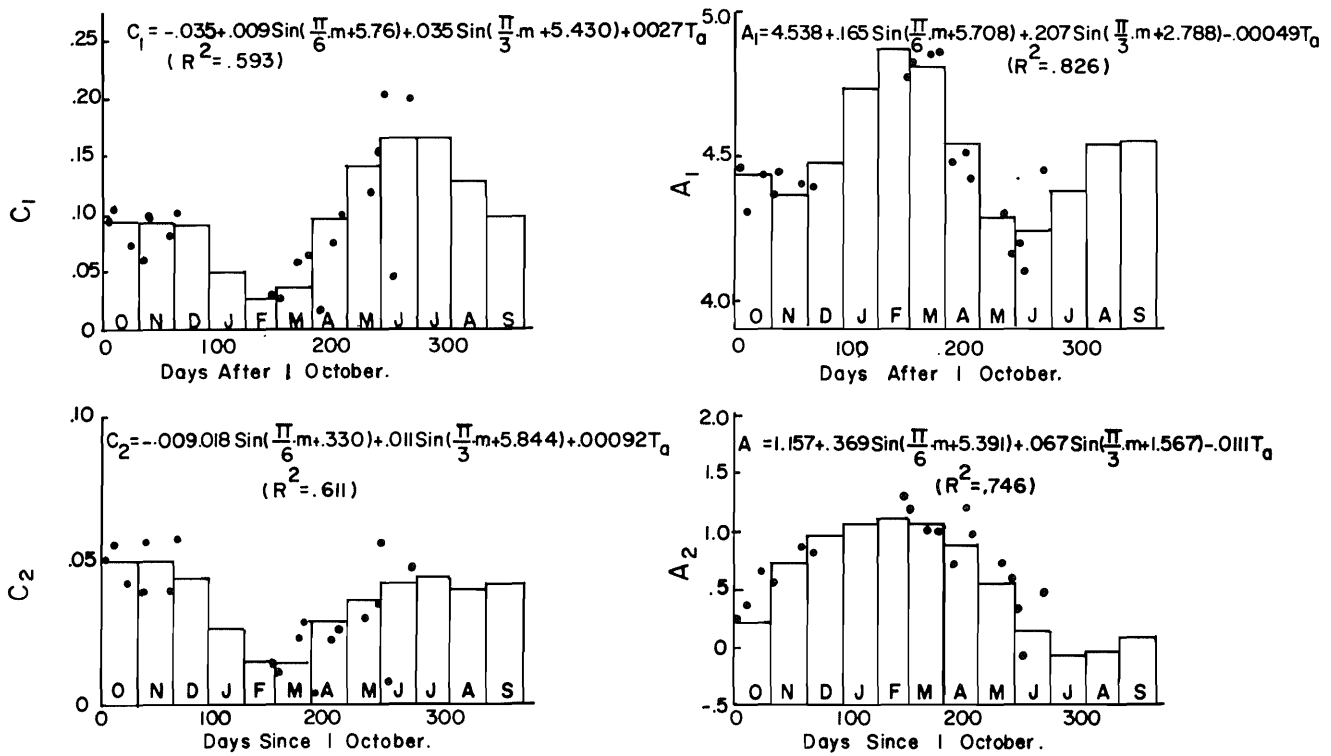


Figure 29. Annual variation in diurnal D.O. index model parameters.

$$Y = c_o + \sum_{j=1}^2 c_j \cdot \sin\left(\frac{2\pi j}{365} \cdot x + a_j\right) + \bar{T}_a + \epsilon \dots \dots \dots (54)$$

- in which
- Y = diurnal D.O. index model parameter (A₁, A₂, C₁ or C₂)
 - x = days since 1 October
 - \bar{T}_a = mean daily atmospheric temperature (°F)
 - ε = deviation of predicted diurnal D.O. model parameter from that calculated from diurnal D.O. variations observed
 - c_o, c_j, and a_j = constant, coefficient and phase shift, respectively as determined from least squares analyses of diurnal data blocks

Equations 53 and 54 comprise the augmented Fourier series simulation equations for diurnal dissolved oxygen. Table 18 shows the constant, c_o, coefficient, c_j, and phase shift, a_j, for an annual cycle; these values were determined by least squares analysis of the data blocks indicated in Table 17 for A₁, A₂, C₁, and C₂ respectively. From this analysis of Table 17 data blocks, the annual cycle in C_o, C_j, and A_j is assigned monthly values which

are shown in Table 19; the Table 19 values were calculated by Equation 54 using coefficients from Table 18. Figure 29 shows a comparison of the application of these assigned monthly values, indicated by the bar lengths, to values from the data block analyses shown in Table 17, and indicated as plotted points in Figure 29.

Graphical representation of the diurnal dissolved oxygen index (DDOI), Equation 53, for each month of the year is shown in Figure 30. These curves display the patterns of D.O. variation to be expected for each month of the year. Seasonal differences in the relative magnitudes of daily D.O. swings are also shown. A phase shift of about two hours in time appears between the curves, representing winter and early spring months and those for summer months. Considerable deviation from this "typical" pattern should be expected during periods of extensive cloud cover.

Hourly estimates of dissolved oxygen concentration may be made by multiplying the hourly ordinates to the DDOI curve by mean daily D.O. In the simulation procedure, the mean daily D.O. concentration is taken as the same as the mean monthly value provided by the monthly D.O. simulation model.

Table 18. Representation of annual changes in diurnal D.O. index model parameters.

$$\left[Y = c_0 + \sum_{j=1}^2 c_j \cdot \sin \left(\frac{2\pi}{365} \cdot x + a_j \right) + \bar{T}_a \right]$$

Parameter	c_0 (constant)	c_1 (constant)	a_1 (radians)	c_2 (constant)	a_2 (radians)	r (radians)	R^2 (%)
$Y = C_1$	-.035	.009	5.746	.035	5.430	.0027	59.
$Y = A_1$	4.538	.165	5.708	.201	2.788	-.0005	83.
$Y = C_2$	-.009	.018	.330	.011	5.844	.0009	61.
$Y = A_2$	1.157	.369	5.394	.067	1.567	-.0111	75.

Table 19. Estimated monthly values of diurnal D.O. index model parameters by Equation 54 using coefficients from Table 18.

Month	C_1 (constant)	A_1 (radians)	C_2 (constant)	A_2 (radians)
October	.0900	4.428	.0496	.428
November	.0877	4.366	.0503	.717
December	.0827	4.479	.0443	.931
January	.0491	4.717	.0272	1.132
February	.0276	4.873	.0159	1.206
March	.0366	4.796	.0154	1.142
April	.0932	4.529	.0292	.867
May	.1388	4.287	.0373	.566
June	.1667	4.241	.0416	.235
July	.1666	4.379	.0436	-.017
August	.1280	4.530	.0403	-.010
September	.0948	4.539	.0420	.177

Diurnal patterns of hydrologic inputs

Diurnal patterns of D.O. variation for each of the various hydrologic inputs to a given stream reach must be known in order to simulate hourly changes in dissolved oxygen concentration for that reach. The diurnal index concept analysis is the basis for doing this.

Surface inflow. The diurnal dissolved oxygen index simulation of the Wellsville continuous monitoring station is assumed to represent the hourly variation in D.O. in all natural surface inflows to the system. Figure 31 compares the index patterns for the Wellsville and Paradise continuous monitoring stations; though the correspondence is not one to one, it does indicate at least a reasonable similarity and indicates the order of magnitude of possible deviations. Spot checks on the Little Bear River system have also confirmed this degree of confidence.

Hourly D.O. concentrations in surface inflows are approximated by multiplying the index value for each hour of the day by the mean monthly D.O. concentration for the input stream. Mean monthly D.O. is taken as previously calculated by the monthly D.O. model. BOD and deoxygenation rate constants are assumed to be constant over the "typical" 24 hour period. These variables are evaluated in the monthly D.O. model.

Irrigation return flow. The lack of data on surface irrigation return flows prevents any authoritative assertion as to the pattern of diurnal D.O. variation to be expected in this input. The extent of photosynthetic activity in the return flow stream would depend on the nature of the channel and upon stream turbidity. Both of these factors are expected to be highly variable. For example, return flows from well stabilized hay and pasture land would be expected to be relatively low in turbidity, while those from more extensively cultivated croplands (row crops

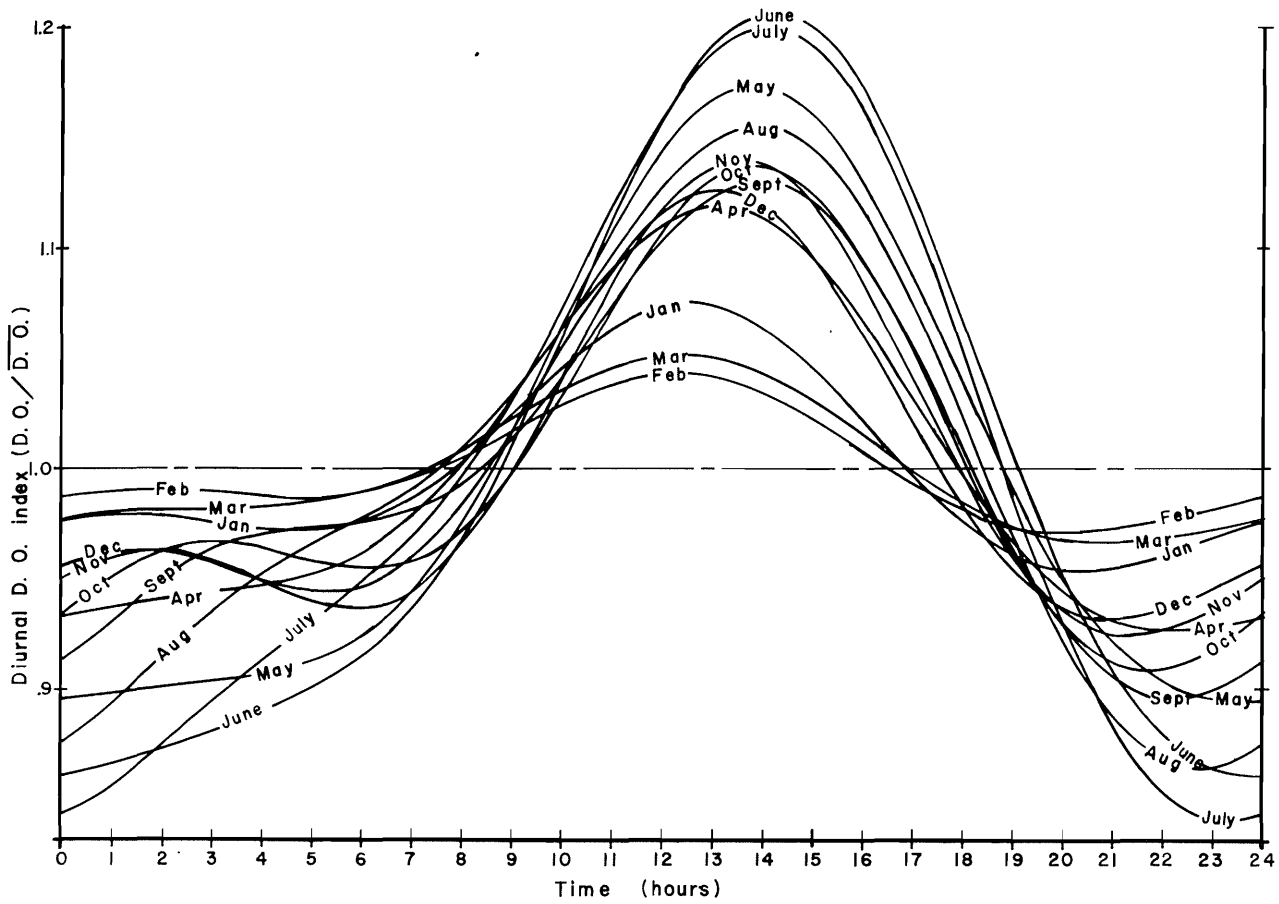


Figure 30. Diurnal D.O. index curves for each month of the year.

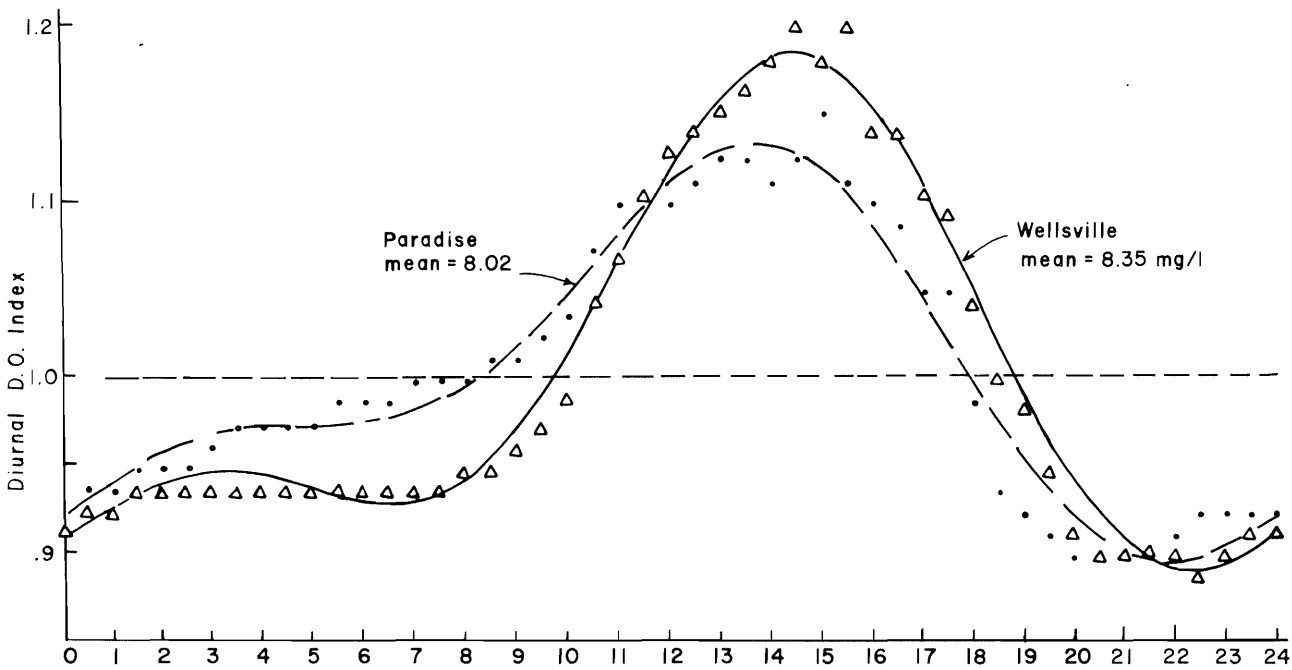


Figure 31. Comparison of D.O. index patterns on the Little Bear River at Wellsville and Paradise on 11-12 October 1968.

and grains) would carry heavier silt loads with resulting high turbidity levels. These high levels of turbidity hinder the passage of light into the water, thus effectively limiting photosynthetic activity. In many instances, however, irrigation return flows pass through quiescent pools and sloughs enroute to the river, so that ample opportunity is afforded for sedimentation and subsequent reestablishment of the photosynthetic process. Despite these uncertainties, hourly variations in irrigation return flow dissolved oxygen are assumed to follow the diurnal D.O. index pattern.

Groundwater inflow. Inputs originating from subsurface flows are assumed to exhibit no daily fluctuations in dissolved oxygen content. The BOD of groundwater inflows is taken to be zero.

Municipal-industrial releases. Dissolved oxygen concentrations in municipal or industrial discharge streams may vary diurnally, depending upon the scheduling of process work, type of treatment provided, organic and hydraulic loading of treatment facilities, and whether or not there is an opportunity for photosynthetic activity in the waste treatment or discharge systems. Fair, Geyer, and Okun (1968) suggest the patterns depicted in Figure 32 as

typical of flow and organic load variation for domestic waste water streams. Treatment of the waste may result in modifications of these distributions. The quantity and strength of industrial wastes also may vary considerably on an hourly basis.

The specific pattern is unique to the situation; thus hourly variations of quantity, BOD and D.O. must be provided as input to the simulation program for each waste stream entering the system.

Combination of inputs. Dissolved oxygen concentrations, BOD and deoxygenation rate constant are determined for the hour-by-hour combination of inflow components to obtain a weighted average for the stream, which can be accomplished again by the use of Equation 16.

Reservoirs

Dissolved oxygen concentrations in reservoir releases are assumed to be constant and equal to the mean monthly value determined from the monthly D.O. model.

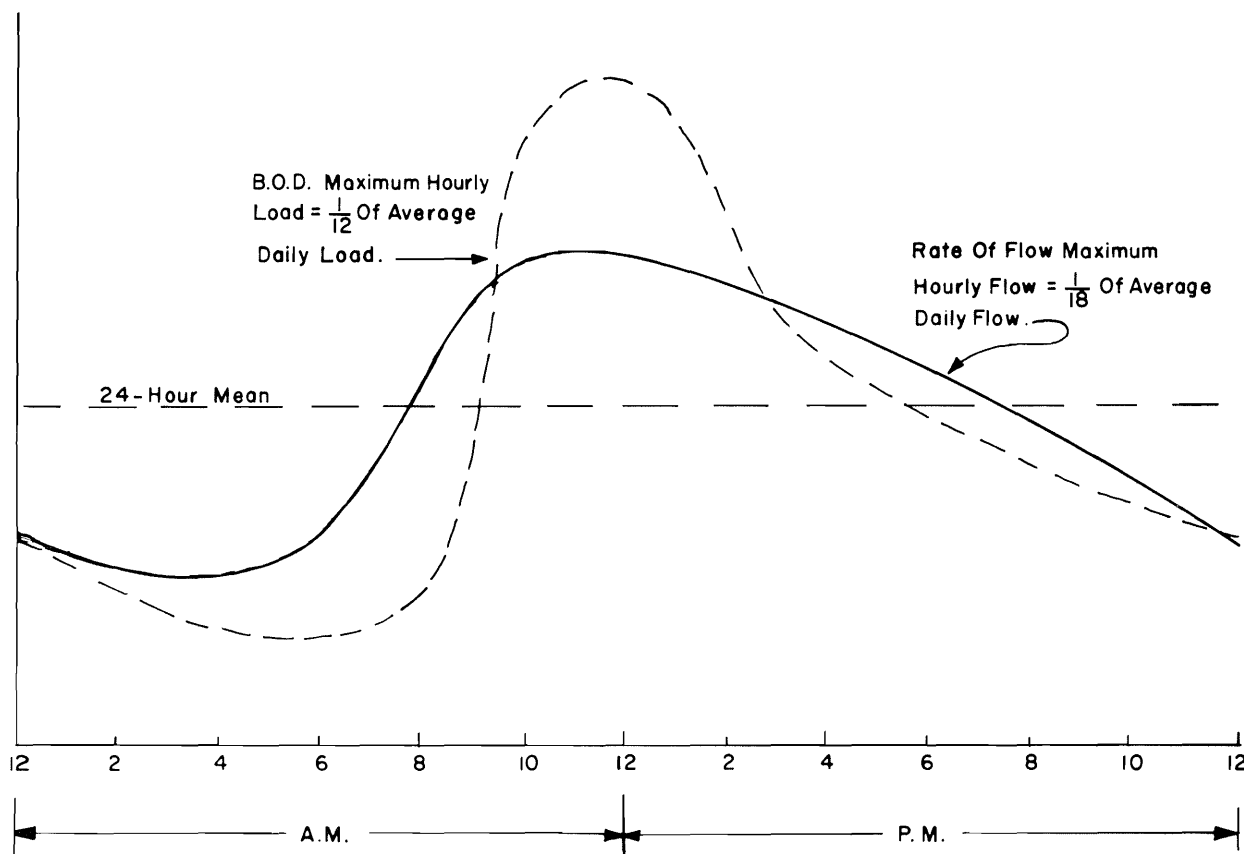


Figure 32. Flow and strength variations in domestic waste.

In-transit changes and the diurnal effect

The effect of a discrete waste input on the stream is assessed by the dissolved oxygen sag Equation 32, as discussed previously. For a realistic assessment, however, the photosynthesis-respiration effects must also be considered. This is done herein by superposing one result upon the other as shown in Figure 33, in terms of a hypothetical example problem. The corresponding steps are outlined as follows. The diurnal dissolved oxygen behavior at two ends of a stream reach is simulated for a waste input at the upper end.

1. At upstream end of reach, determine and input hourly stream values of D.O., BOD, and k_1 , as shown in Figure 33a.
2. Obtain hourly distribution of D.O. and BOD for the waste input, as shown in Figure 33b.
3. Calculate weighted average of D.O. and BOD for streamflow mixed with waste for each hour to obtain the two lower curves shown in Figure 33c. From the diurnal temperature distribution, calculate the diurnal distribution in saturation concentrations, which is the top curve of Figure 33c. The deficit distribution is the amplitude of the cross hatched area.
4. Obtain the travel time through the reach, tt . Calculate D.O. deficit, D_b , at downstream end of reach for each hour of day (incremented by travel time, tt) by Equation 32, using hourly values of D_a from Figure 33c as successive arguments.
5. Obtain the saturation distribution for the downstream end of the reach; this is the top curve in Figure 33d. Subtract from this the calculated deficits, D_b , to get the D.O. distribution devoid of the effects of photosynthesis and respiration.

6. The photosynthesis-respiration activity in a reach is represented by the equation:

$$O_p = Pf \cdot (DDOI - 1.0) \dots (55)$$

in which

- O_p = oxygen produced by photosynthetic organisms (negative for respiration)
DDOI = diurnal dissolved oxygen distribution
Pf = productivity factor

The "productivity factor," as used in this simulation, is a scaling factor, applied to the diurnal dissolved oxygen index distribution to represent the activity of photosynthetic organisms within the reach being simulated.

Application of Equation 55 results in the lower sine curve of Figure 33d.

7. Adding the result of step 6 to the result of step 5 results in the *net* dissolved oxygen distribution curve, also shown in Figure 33d.

Simulation algorithm

Figure 34 outlines the steps necessary to simulate representative diurnal variations in dissolved oxygen for any given month or months specified. This algorithm works for the main stem or any branch of the main stem. The effect of BOD loadings is simulated by an hour by hour application of the oxygen sag equation to obtain the D.O. effect at the downstream end of the reach. After the reaches in the main stem and branches are simulated, time is incremented by one month and the simulation is repeated.

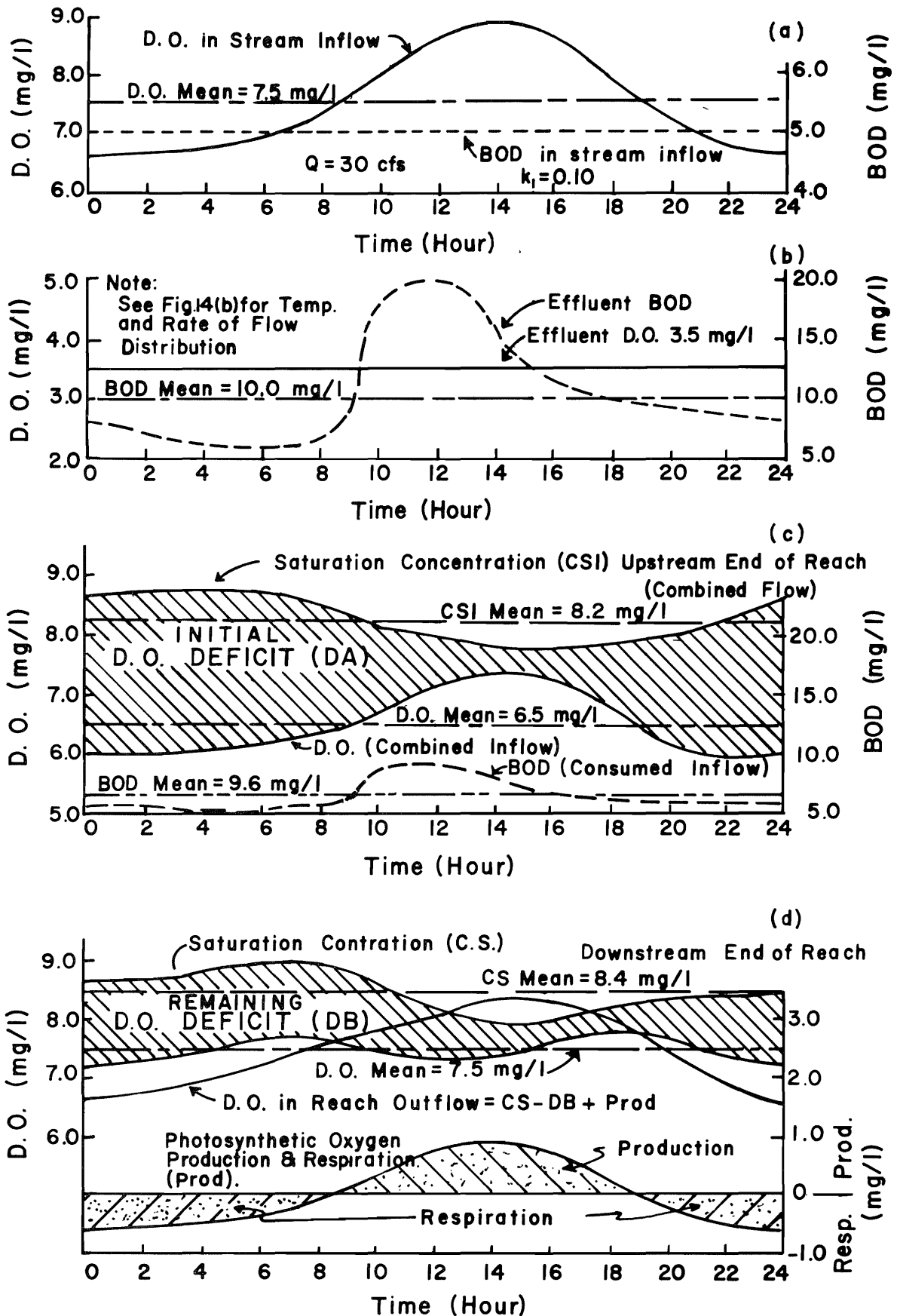


Figure 33. Graphical representation of diurnal D.O. computation.

1

2

3

4

5

6

7

CHAPTER VII

EXPLORATION FOR A COLIFORM SUBMODEL

The concentration of coliform organisms is often cited as a parameter of water quality. Though coliform organisms themselves are not pathogenic, their presence in a water supply is generally taken as presumptive evidence of possible contamination by pathogenic bacteria, as some coliform organisms and pathogenic bacteria originate in the intestines of warm blooded animals and exhibit approximately the same die-away characteristics in the aquatic environment. Some coliform bacteria, however, originate in the soil and are carried into the stream by surface runoff and shallow interflow. Virus organisms do not exhibit the same die-away characteristics as coliform bacteria. For these reasons, many authorities argue against the use of the coliform organism as an indicator of pathogenic organisms. However, because coliform count is the parameter in most prevalent use at the present time, and because it is so frequently cited in water quality literature as an index to the bacterial quality of water supplies, coliform count has been studied for possible incorporation into the water quality simulation model.

Literature search

Relatively few works related to the modeling of coliform organisms in natural streams are discussed in the literature. Kunkle and Meiman (1968) have studied the behavior of coliform, fecal coliform, and fecal streptococci in a small high mountain stream flowing through an irrigated meadow pasture. At one of their points of observation, they found analytical technique to be the most significant source of variation in coliform numbers, while at the other location, analytical technique was second only to time-of-day as a source of variation. They made no attempt at establishing a mathematical representation of coliform behavior in the stream.

Frankel (1965), in his study of water quality evaluation, discusses the problem of modeling coliform die-away, finally using Equation 56, as presented by Fair and Geyer (1954). This formulation, also contained in Fair, Geyer, and Okun (1968) is

$$(N_o - y)/N_o = N/N_o = (1 + n \cdot \kappa \cdot t)^{-1/n} \quad (56)$$

in which

- N_o = original number of bacteria in the stream
- y = number of bacteria removed during time of flow (t) below the point of maximum bacterial density
- N = number of bacteria left in the stream after time of travel (t)
- t = time in days
- κ = initial rate of die-away for a specific bacterial population in the environment of the receiving stream
- n = associated coefficient of nonuniformity or retardation

In this die-away equation, both κ and n are functions of the bacterial population being studied and the environment of the receiving stream into which this population is introduced. These important model parameters must be quantified analytically from samples taken from the stream at points downstream from the point of maximum coliform number. To adequately define the die-away curve, it is necessary to sample over a relatively long flow time, which is the case of the Little Bear River. Its high velocity of flow means that the length of stream sampled should be relatively great.

Because of the location of sources of concentrated bacterial pollution, it was impossible to adequately sample the stream below the points of discharge. The first source of large numbers of coliform is the trout farm which is located about 2.8 miles upstream from Hyrum Reservoir. This distance represents a travel time of approximately 1 to 1.5 hours, depending on the rate of discharge; considerably less than the 10-12 hours suggested by Fair, Geyer, and Okun (1968) as that required to reach maximum coliform density below a sewer outfall.

The second source of concentrated bacterial pollution is the stream into which untreated waste from the town of Wellsville is released. This discharge is located only a few hundred yards upstream from the lower limit of the project study area, with another reservoir pool not far downstream. The inability to establish κ and n for Equation 56 have frustrated attempts to simulate bacterial die-away by this approach. This representation of bacter-

ial die-away appears to be the best that is currently available in the literature.

Figure 35 shows the profile of the logarithm of coliform count, as observed along the length of the main stem of the Little Bear River on 11 September 1968. This profile should not be taken as typical of the pattern of spatial variation; however, as large, apparently random, deviations occur at each individual station. Figure 36 for station 12.5 is a typical annual distribution of the logarithm of the coliform count, showing the stochastic deviation from the mean.

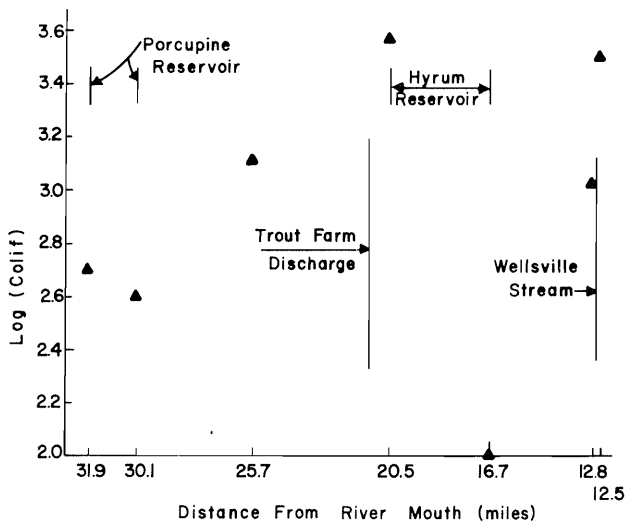


Figure 35. Space profile of log (coliform count) for 11 September 1968.

The density of coliform organisms in a given bacterial sample was assessed by the membrane filter technique. Multiple dilutions of a single replicate sample were processed simultaneously. Bacterial samples were limited to about 10 per weekly sampling period, because of time limitations in the laboratory. This restriction resulted in a rotating schedule for the 16 sampling stations.

Alternatives considered

Post (1968) indicated that the logarithm of coliform density in waste stabilization ponds had been found to be

closely related to water temperature. On the strength of this suggestion, an attempt was made to relate the logarithm of coliform density to stream temperature at several locations along the stream. Figure 37 is typical of the results obtained.

In searching for some means to explain the large amount of variation remaining after regressing with water temperature, it was suggested that possibly the random nature of bacterial loading could be the source of at least part of the residual variance. This hypothesis was tested by comparing the residual of the log coliform variation with that of BOD after the influence of temperature had been removed from both. This test was based upon the assumption that both coliform and BOD originate at the same source, i.e. the intestines of warm blooded animals. Figure 38 depicts the result obtained at station S-12.8, which is typical of the stations studied. There is no apparent positive correlation between log of coliform density and BOD. In fact, this particular set of data displays what might be taken as a slight tendency toward negative correlation (larger positive log coliform deviations being associated with negative BOD deviations). These observations tend to eliminate random loading as the major source of residual variation in either coliform or BOD if the assumption of common sources for the two pollutants is valid.

No coliform model, that could be adequately defined from available project data, was discovered in the literature. Analysis of project data failed to produce an equation capable of representing a significant portion of the total variation in coliform count. A random probability model based upon the statistics of available data would suffice as well as any.

Further research in this area would be helpful. Probably the most fruitful approach would be the quantification of relationships governing the die-away rate constant (κ) and coefficient of nonuniformity (n) of Equation 56. Fair, Geyer, and Okun (1968) have suggested that these model parameters are influenced by the bacterial population and the characteristics of the stream into which the bacteria have been injected. In any future investigation involving the coliform count, the data of Kunkel and Meiman (1968) would suggest that replicate laboratory tests be conducted for each dilution to facilitate the assessment of the variance component attributable to analytical technique.

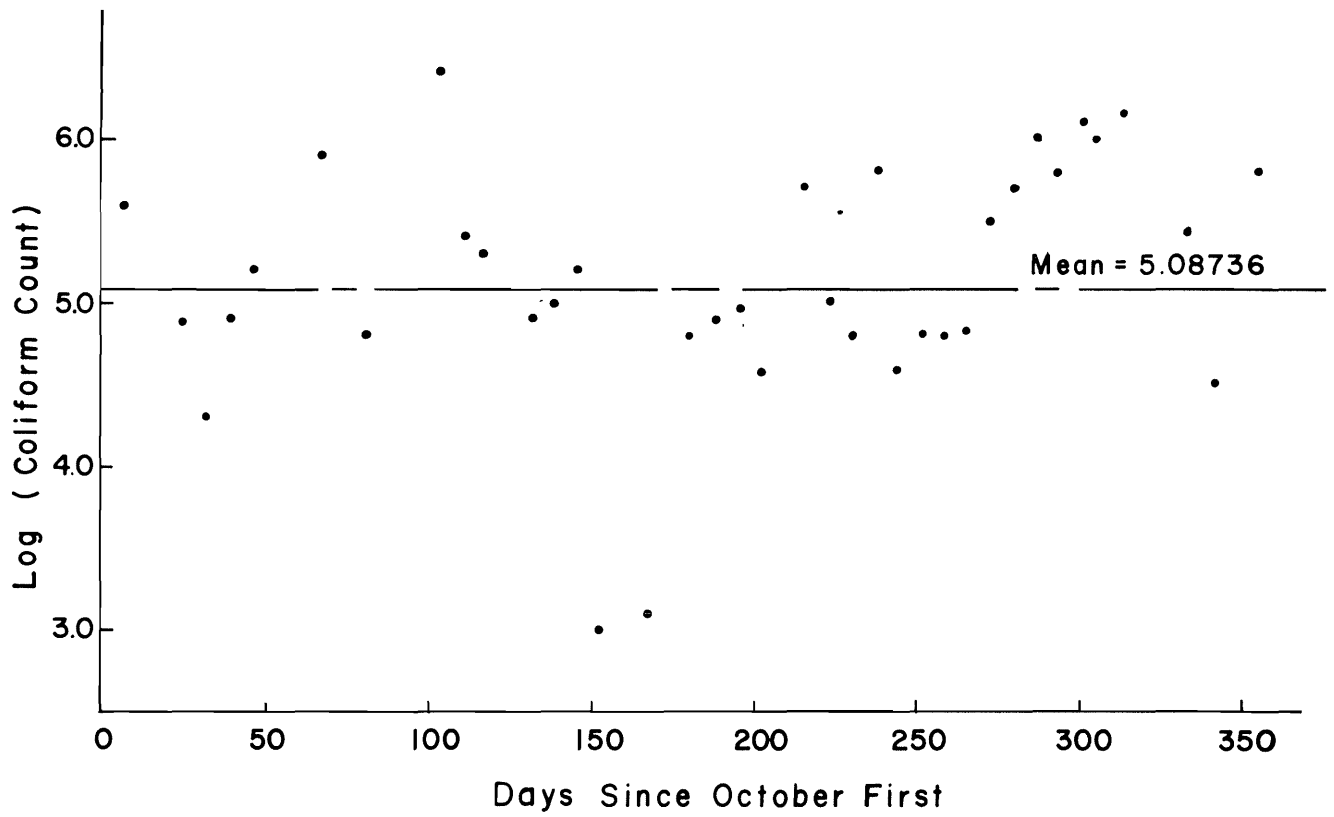


Figure 36. Annual variation in log (coliform count) at station S-12.5 for 1966-67.

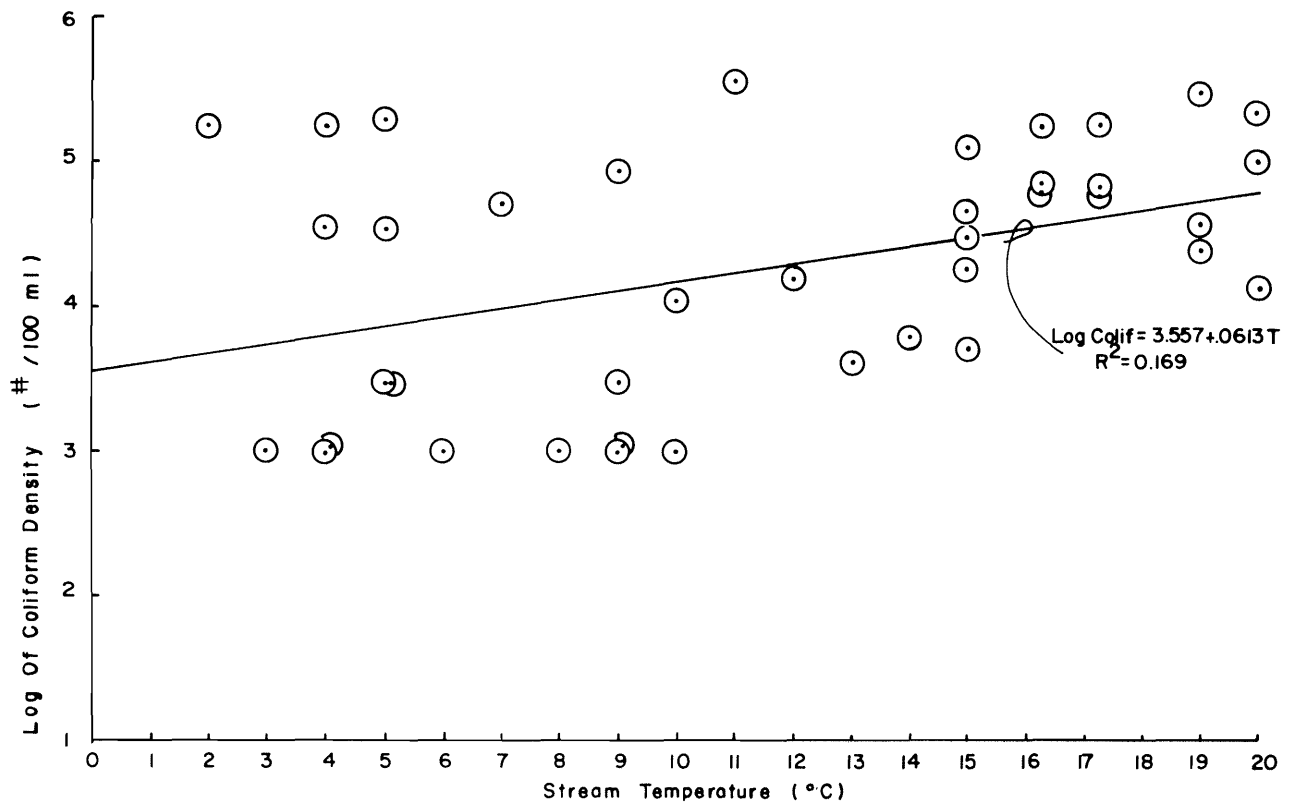


Figure 37. Log (coliform count) vs. stream temperature (station S-12.8).

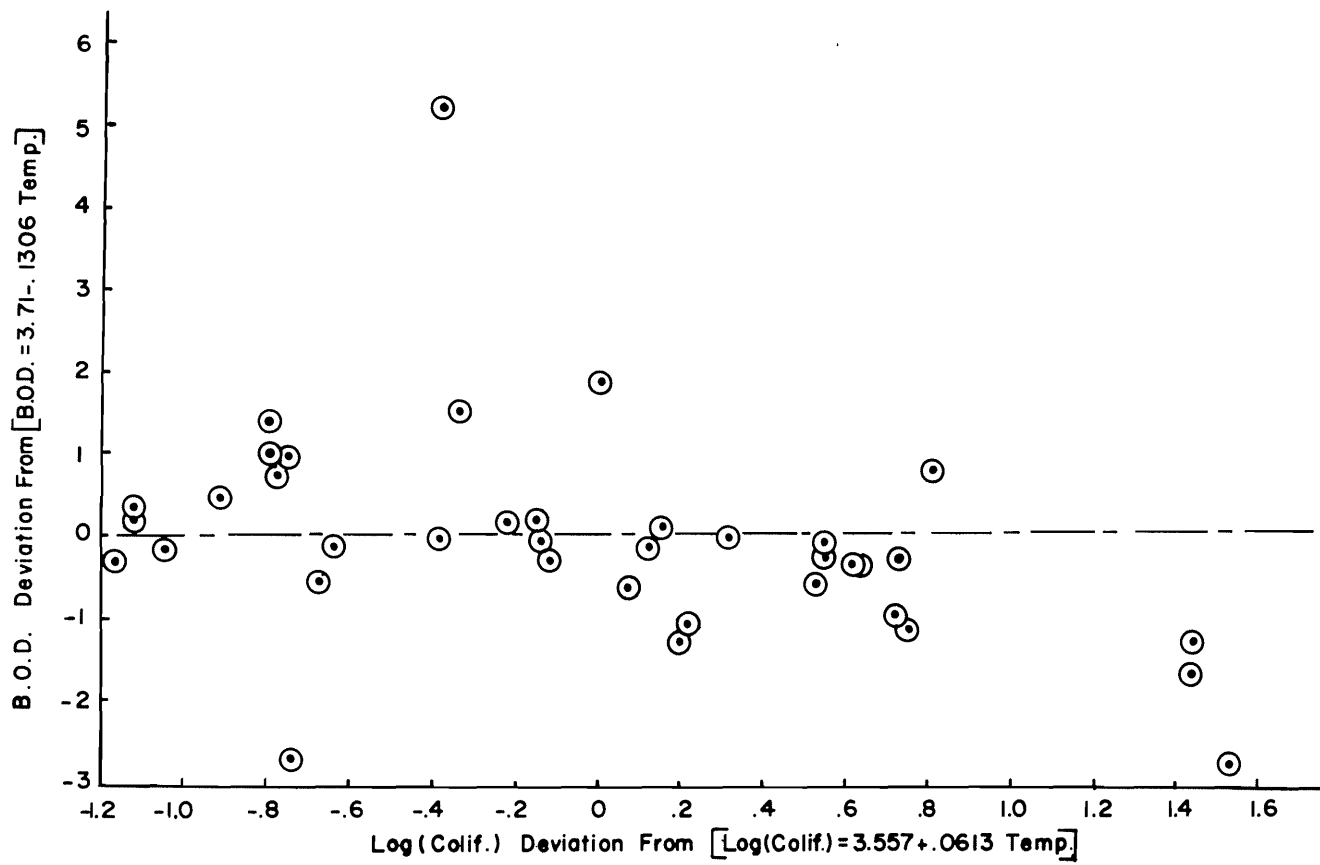


Figure 38. BOD deviation vs. log (coliform) deviation (station S-12.8).

CHAPTER VIII

SIMULATION RESULTS—LITTLE BEAR RIVER

Establishing a simulation model can be summarized as two steps: (1) establishment of model constants and coefficients, and (2) verification of the resulting model. This was done using 1966-1967 and 1967-68 data for the first and second steps respectively. The following is a discussion of results. The submodels and procedures outlined in the previous chapter were used to derive all results presented herein.

System delineation

The Little Bear River system, shown in Figure 59, is represented schematically in Figure 39. This sketch shows the breakdown of the stream system into major tributary

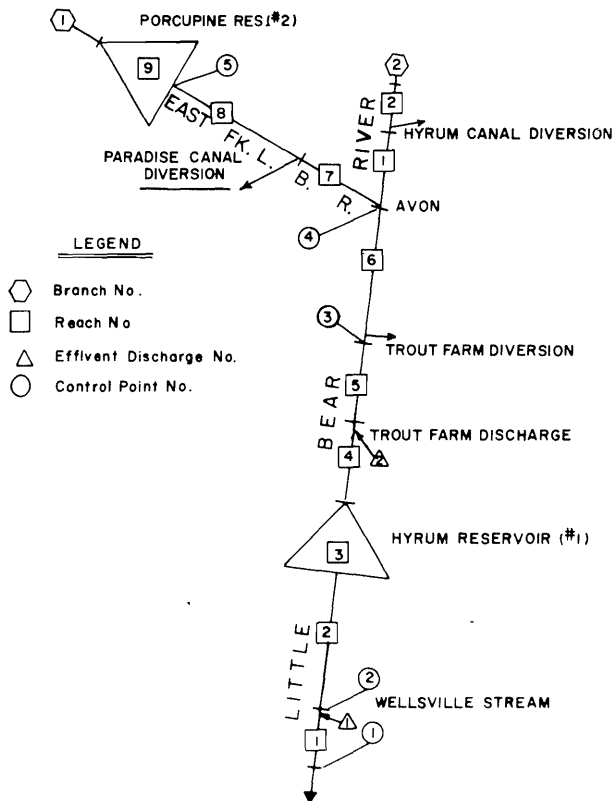


Figure 39. Little Bear River system schematic.

branches and reaches, as well as locations of reservoirs, waste discharge points, and control points. Node points between reaches fall at hydrologically significant break points in the system. Reach eight on the main stem, for instance, extends from Porcupine Reservoir discharge on the upstream end to the Paradise Canal diversion at the downstream end of the reach. Locations and designations of system node points are tabulated in Table 20.

Establishing model coefficients

Submodel coefficients have been determined, where possible, by least squares analysis of 1966-67 data using equations selected and described in the previous chapter. Where data required for evaluation of constants and coefficients were not available, estimated values were used in the simulation. These estimates were revised, where necessary, to achieve correspondence between simulated water quality and monthly averages of observed data. Procedures followed and results obtained are outlined below for each submodel.

Electrical conductance

Electrical conductance was found to be quite sensitive to changes in the ratios of groundwater to surface water inflows. After the first simulation run, the groundwater coefficients in the hydrologic submodel were altered to change the proportions of these unmeasured inflows. Estimates of irrigation return flow conductivity were also revised downward to achieve better correspondence between observed and simulated conductivities. Correspondence graphs from the last 1966-67 run are shown in Figure 40 for four typical observation stations along the Little bBear River main stem.

Sample simulation profiles are shown in Figure 41 for the months of January and July, 1968. A full year of profiles is shown in Appendix F. Average values of field data, for corresponding months, are also shown for comparison. The gradual build-up in electrical conductance in the downstream direction is characteristic of the field data. Drops at stations 30.1 and 16.7 are due to carryover of low-conductance spring runoff in Porcupine and Hyrum Reservoirs, respectively.

Table 20. Little Bear River reach description.

Branch No.	Reach No.	From	To	Location ^a	Length (mi.)
1	1	Wellsville	telemetry site	1.125	0.3
1	2	Hyrum dam	Wellsville	1.128	3.9
1	3	—Hyrum Reservoir		1.167	1.8
1	4	trout farm discharge	Hyrum res.	1.185	2.8
1	5	trout farm diversion	trout farm discharge	1.213	1.1
1	6	South Fork	trout farm diversion	1.224	3.2
1	7	Paradise canal diversion	South Fork	1.257	1.3
1	8	Porcupine dam	Paradise canal diversion	1.270	3.1
1	9	—Porcupine Reservoir—		1.301	1.8
2	1	Hyrum canal diversion	Avon	2.000	1.0
2	2	Davenport Creek	Hyrum canal diversion	2.010	0.3

^aThe location designation is "b.xxx" where b is the branch number and xxx is the distance from the mouth of the branch, in tenths of a mile (2.010 = one mile above the mouth of branch two).

Monthly water temperature

After the initial adjustment of hydrologic inputs, using conductance data as a guide, no further changes were made in the system hydrology. The simulation sub-model for water temperature was adjusted by changing the "equilibrium" water temperature model coefficients and the heat exchange coefficient.

Typical correspondence graphs from the final model development run are shown in Figure 42. The maximum deviation from stream temperatures, measured at eight observation points along the stream is about 4°C at station S-12.8. Departures of this magnitude occur during May and June; simulated temperatures being high in May and low in June at this particular location. These larger deviations at the lower sampling points are probably attri-

butable to the approximate nature of the simulation of release water temperatures at Hyrum Reservoir.

Comparisons of simulated and observed stream temperature profiles for the months of January and July are depicted in Figure 43. It is interesting to note that in January the influence of groundwater inputs on stream temperature is positive, while in July it is negative. Sharp temperature drops through the thermally stratified reservoirs are prominent in the July profile.

Monthly dissolved oxygen

For the low BOD levels observed in the Little Bear River, the D.O. simulation was more sensitive to changes in D.O. inputs than to changes in oxygen sag model parameters. Had BOD levels been higher, it is quite likely that

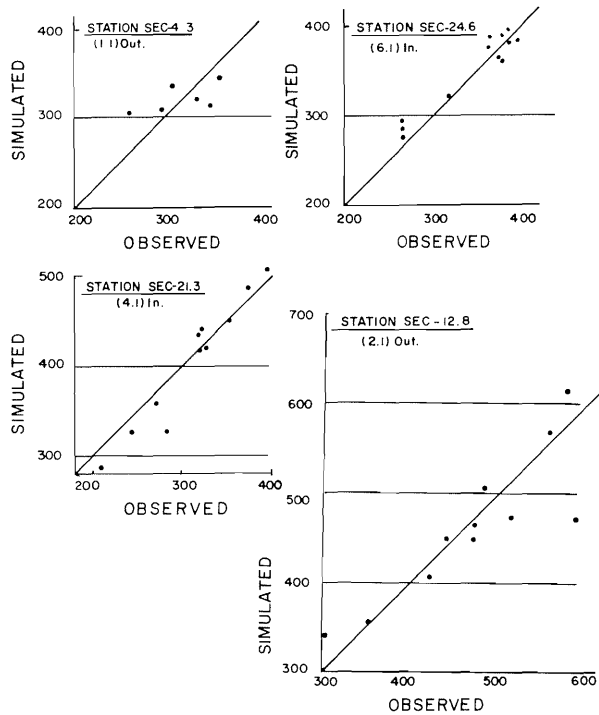


Figure 40. Electrical conductance correspondence graphs for stations SEC-4.3, S-24.6, S-21.3 and S-12.8 from the final model development run (1966-67 data).

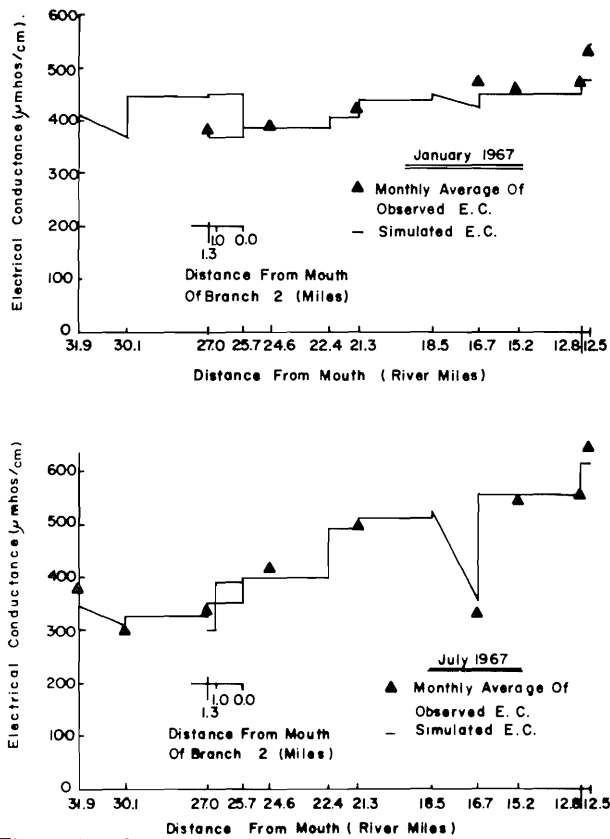


Figure 41. Comparison of observed and simulated electrical conductance profiles for January and July, 1967.

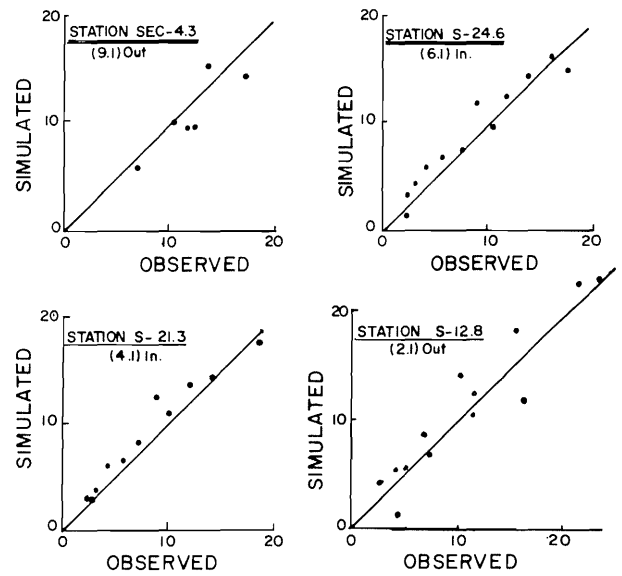


Figure 42. Water temperature correspondence graphs for stations SEC-4.3, S-24.6, S-21.3 and S-12.8 from the final model development run (1966-67 data).

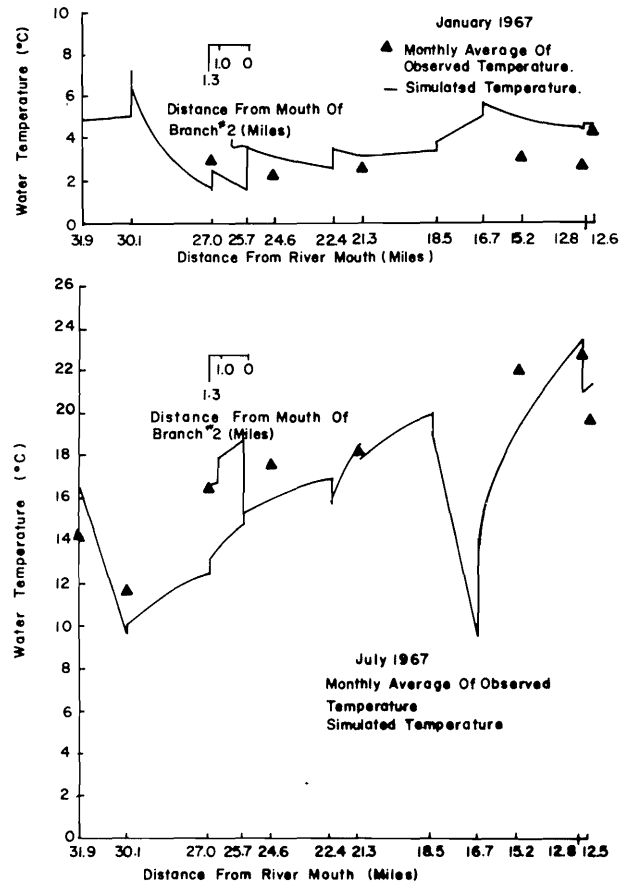


Figure 43. Comparison of observed and simulated water temperature profiles for January and July, 1967.

adjustment of the oxygen sag model parameters would have significantly improved the model results.

Dissolved oxygen correspondence graphs are shown in Figure 44 for 1966-67 data. With the exception of

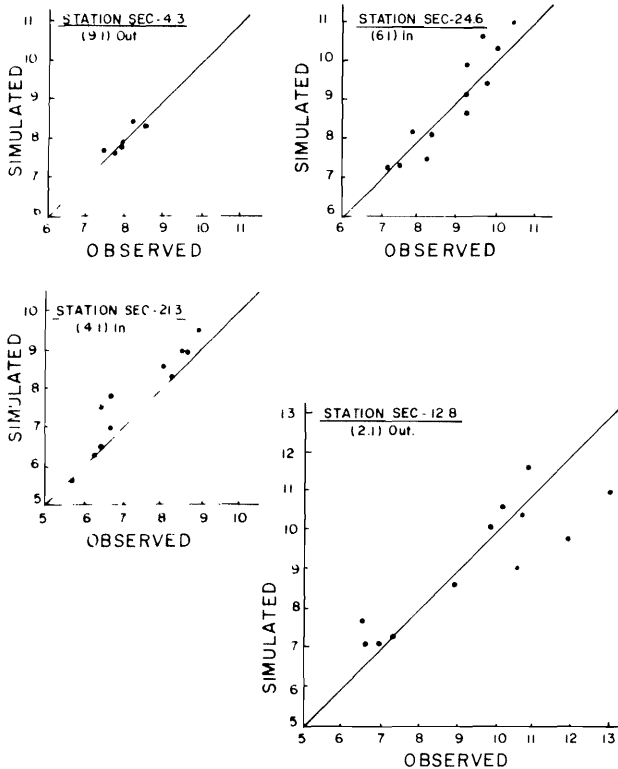


Figure 44. Dissolved oxygen correspondence graphs for stations SEC-4.3, S-24.6, S-21.3 and S-12.8 from the final model development run (1966-67 data).

station S-12.8, simulated D.O. concentrations were generally within 1 mg/l of observed concentrations. Departures on the order of 2 mg/l may be noted at S-12.8. These greater deviations occurred during the months of October, November, and January. Observed data show a high degree of supersaturation during these three months. As will be shown later (Figure 54) these heavy supersaturations were not observed in 1967-68 data. The departures at station S-12.8 in 1966-67 are unexplained at this point.

The simulated D.O. profiles for January and July exhibit discontinuities at node points between branches (Figure 45). These discontinuities result from the assumption that oxygen deficient groundwater inflows are concentrated at the upstream end of the reach. Combining this concentrated low D.O. inflow with the other inflows at the upstream end of the reach results in a noticeable

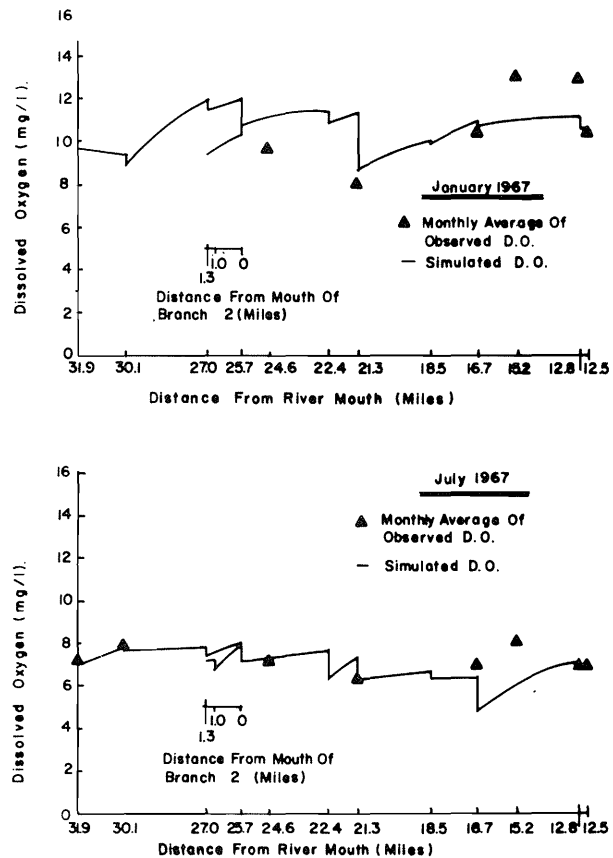


Figure 45. Comparison of observed and simulated D.O. profiles for January and July, 1967.

depression of the D.O. profile at this point. This is particularly true where groundwater inflow makes up a significant portion of the total input to the reach, as it does in many reaches of this system during periods of low streamflow. The downward step in D.O. at station 21.3 results from the release of large quantities of oxygen deficient waters from the ponds and channels of the commercial fish farm. The relatively large deviations at station 15.2 are apparently caused by a small quiescent pool immediately upstream from the field observation point. During low flow periods, velocity is low through this pool and photosynthetic organisms abound.

A full year of simulated D.O. profiles for 1967-68 years are shown in Appendix F. These profiles are based upon coefficients established using 1966-67 data.

Diurnal water temperature

It has been assumed that the hourly distribution of the ratio of observed temperature to mean daily temperature should be approximately the same at any point in the stream system as was recorded at Wellsville. In the case of the Little Bear River, where there are no concentrated

sources of thermal pollution, this assumption is justifiable. Some departure from this relationship should be expected, however, especially immediately downstream from surface impoundments.

The variation pattern for the simulated diurnal temperature index, at control points not immediately downstream from reservoirs, was adjusted to conform to the pattern calculated from continuous monitoring data at S 12.5. The simulated diurnal temperature index was found to be quite sensitive to the heat exchange coefficient and the magnitude of "equilibrium" temperature variations. Trial and error adjustment of these factors was the principal means of adjusting the simulated temperature index distribution. In Figure 46 the simulated and measured diurnal temperature index patterns for station S-12.8 are shown for the month of May 1967.

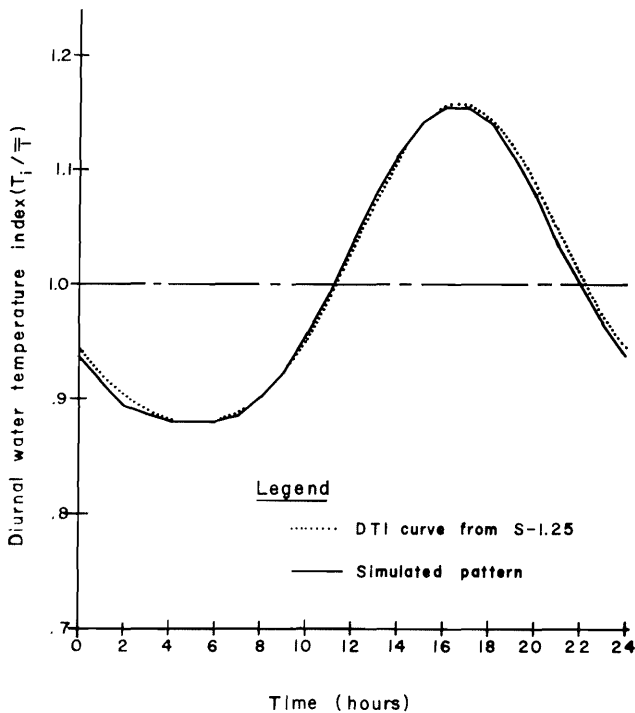


Figure 46. May 1967 diurnal water temperature index pattern for station S-12.8.

Diurnal dissolved oxygen

As with diurnal modeling of water temperature, the basis for adjusting the simulated dissolved oxygen index distribution was the assumption that this distribution should approximate that calculated from continuous data from the Wellsville monitoring station. Differing environmental conditions, such as prevailing direction of flow, bank vegetation and topographic relief, result in spatial variations in light intensity patterns through the day.

These influences may be expected to impart deviations from the relationship assumed.

The simulated D.O. distributions were found to be sensitive to changes in the diurnal temperature distribution, primarily because of the dependent relationship between oxygen saturation concentration and water temperature. After attaining a satisfactory distribution of water temperature, D.O. distributions were adjusted by altering the "productivity coefficient" on a month-by-month basis for each reach. This "productivity coefficient" is the scaling factor in Equation 55, enabling the diurnal dissolved oxygen index curve to be used to simulate photosynthetic activity within a stream reach.

The diurnal D.O. index pattern for station S-12.8 is shown for the month of May 1967, in Figure 47, along with the index curve derived from continuously monitored D.O. data. A consistent tendency toward somewhat later peaks in the simulated diurnal D.O. distribution pattern was observed.

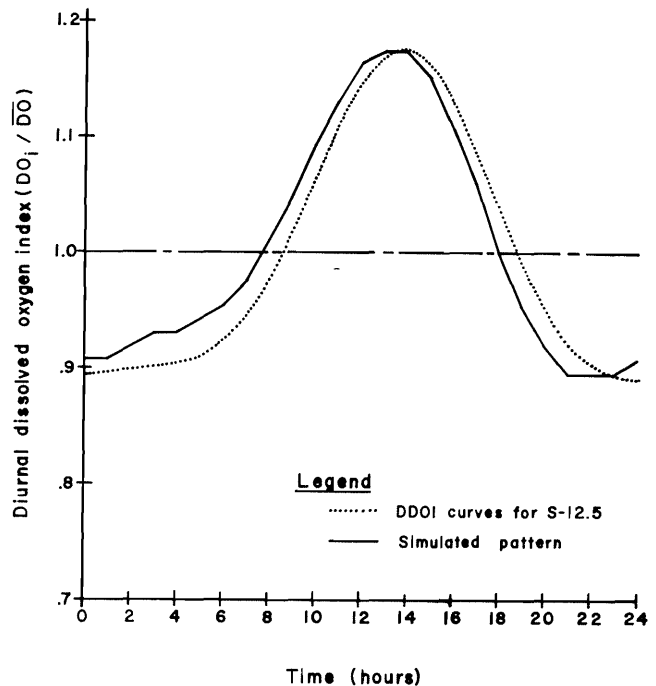


Figure 47. May 1967 diurnal dissolved oxygen index pattern for station S-12.8.

Verification of model constants and coefficients

For verification, the completed water quality model was applied to hydrologic data taken during the 1967-68 water year and compared to 1967-68 water quality data. The results from each submodel will be discussed briefly.

Electrical conductance

Hydrologic coefficients and inputs for the hydrologic simulation submodel were adjusted using 1966-67 data. No further changes were made in the hydrologic submodel. The correspondence graphs for six stations (Figure 48) show roughly the same degree of scatter for the 1967-68 run as were observed in Figure 40 from the last 1966-67 run. The inadvertent omission of temperature compensation on a conductivity meter for the period June 1966 through February 1968, undoubtedly contributes somewhat to the deviations for exact correspondence observed in Figure 48.

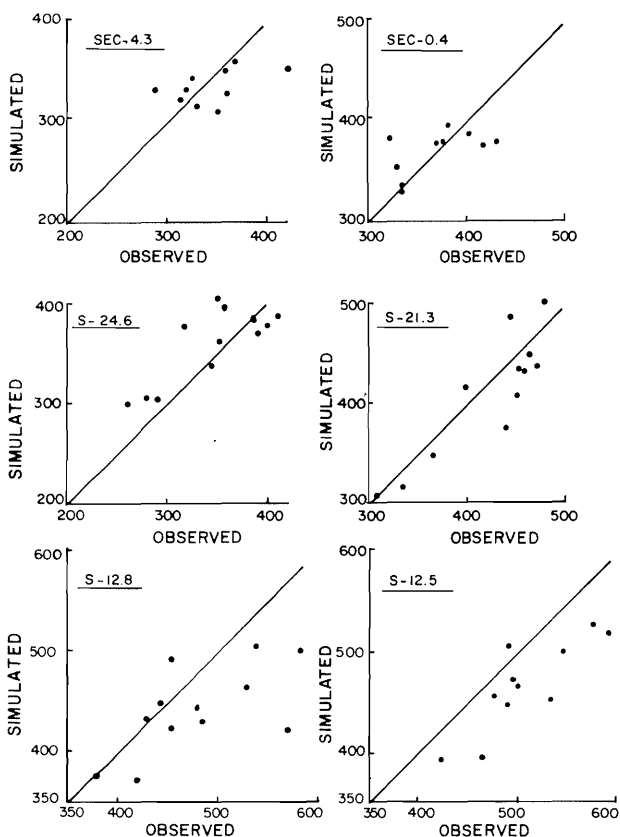


Figure 48. Electrical conductance correspondence graphs from the model verification run (1967-68 data).

Conductivity profiles for the months of January and July, 1968, are shown in Figure 49 as samples of the profiles resulting from the model verification run. A complete set of plotted conductivity profiles is included in Figure F-1 of Appendix F. Comparison of simulated and observed annual distributions of mean monthly conductivity is featured in Figure 50 for quality sampling stations S-12.8 and SEC-0.4. The good correspondence between

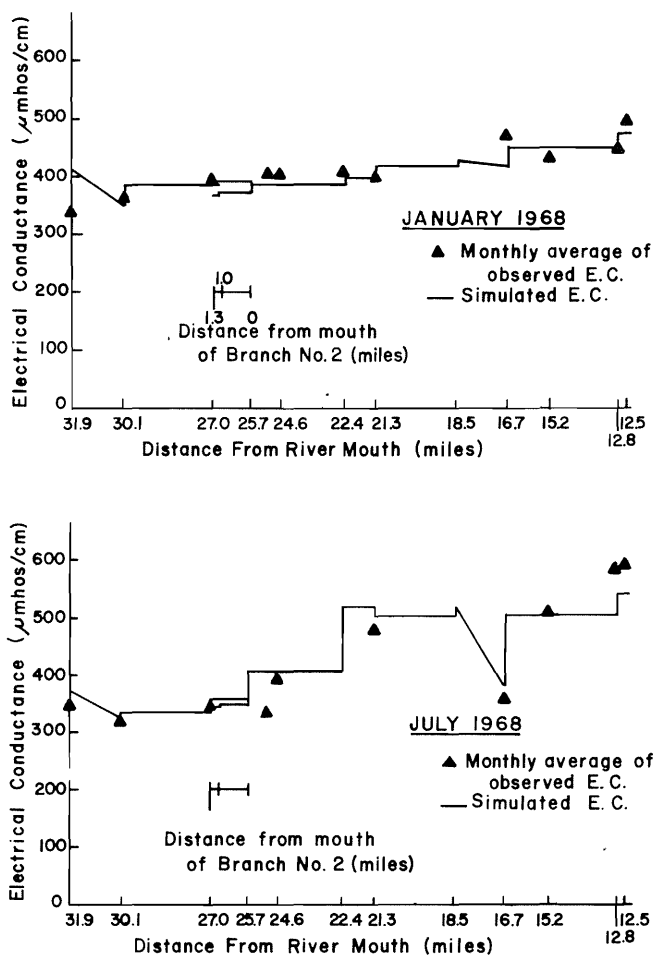


Figure 49. Comparison of observed and simulated electrical conductance profiles for January and July 1968.

observed and simulated electrical conductance values is readily apparent in all of these figures.

Monthly water temperature

The simulated 1967-68 stream temperatures correspond well with observed temperatures as Figure 51 shows. This correspondence is similar to that depicted in Figure 42 for the last 1966-67 run. Sample stream temperature profiles for the months of January and July, 1968, are illustrated in Figure 52. Figure F-2, Appendix F, provides a complete set of plotted stream temperature profiles for each month of the simulation year. Observed and simulated annual distributions of mean monthly stream temperature are compared in Figure 53.

Monthly dissolved oxygen

Relatively good correspondence was found between observed and simulated dissolved oxygen concentrations as shown in Figure 54. This agreement, however, should

Groundwater quality sampling points were established at four locations in the valley floor area, as shown in Figure B-2. These sampling sites are described in Table B-4. Groundwater samples were taken at monthly intervals.

In setting up the water quality monitoring network it was necessary to consider such factors as accessibility and winter conditions in addition to the obvious requirement of sampling to indicate sources of pollution and stream reaction to this and external factors. Those stations for which winter access was limited were sampled as conditions permitted. Station SEC 6.2 above Porcupine Reservoir was sampled irregularly during winter months due to the road being snowbound.

Continuous quality monitoring

Continuous water quality monitoring stations were installed at stations S-12.5 below Wellsville and S-20.5 near Paradise in cooperation with a water quality telemetry project at Utah Water Research Laboratory (Woffinden and Kartchner, 1968). The initial intent was to provide continuous strip chart recording at both sites, but excessive power consumption of the system installed at the Paradise site prevented its continuous operation from battery power supply. Specific electrical conductance, pH, dissolved oxygen concentration, and water temperature were monitored with commercially obtained battery powered electronic sensing systems. For a detailed description of the electronic systems employed, refer to the work of Woffinden and Kartchner (1968).

Because of instrument malfunction and problems relating to the adaptation of instruments for telemetry transmission, extended periods have occurred during which no valid continuous monitoring records were obtained. Reliable recordings were made, in blocks of from three to seven days in length, over a period extending from November 1967 through January 1969 at the Wellsville station. Periods of missing data occurred during the winter of 1967-68 and the summer of 1968. The Paradise continuous monitoring station was set up in April 1968, but reliable readings were obtained only during relatively short periods. Despite the difficulties sufficient data were available to allow comparisons between stations and to establish a pattern over the annual cycle using data from the Wellsville station.

Quality of data

Stream gaging was done by the USGS using rating curves and stage recorders. They felt the data provided were reliable and good and within normal tolerances.

Weekly sampling data from water quality sampling were provided by both field and laboratory analyses. Field tests were pH (by colorimetric kit), dissolved oxygen (Winkler-- fixed in the field), carbon dioxide (phenothalein titration), and alkalinity (methylene orange titration); and temperature. Figure C-1, Appendix C, shows all tests conducted and summarizes all data taken for each sample. Test results reported with and (F) indicate field measurement. Laboratory tests for chemical species were

Table B-4. Groundwater sampling stations.

Station No.	Coordinates (Meters)	Description of Sampling Point	Period of Sampling
U-2311	235110	Artesian well discharging to stock watering trough about 75 yd. east of the first road east of Wellsville lower road bridge at about 200 yd. north of Highway.	101767 - 121868
U-2510	258108	Manhole for subsurface field drain about 100 yd. north of the railroad track and 100 yd. east of the Wellsville East Field Canal directly east of Greens Corner.	101767 - 121868
U-2907	294068	Spring House overflow on north side of spring house located just north of E. K. Israelsen's home on west side of highway about 1.5 miles south of Hyrum, Utah.	101767 - 121868
U-3198	312985	Seeping spring area inside curve in Forsberg Road northwest of Avon about 0.2 miles east of Little Bear River.	101767 - 121868

conducted in accordance with *Standard Methods* 1965 edition. There is no reason to suspect the quality of these data, with the exception of the specific electrical conductivity test results. The values reported for the period June 1966 to January 1968 were not corrected for temperature deviations from 25°C at the time of measurement. The room in which this measurement was taken would deviate about $\pm 2^\circ\text{C}$ from this temperature, though it was probably close to 25°C most of the time. After January 1968

all subsequent EC values are reported as EC at 25°C. The temperature calibration for the instrument used is shown in Figure B-3. Figure B-4 shows the instrument calibration against a standard sample at 25°C.

Total count and coliform counts were done by the membrane filter method. Samples were collected using a sterile bottle, which was handled in accordance with usual sterile technique.

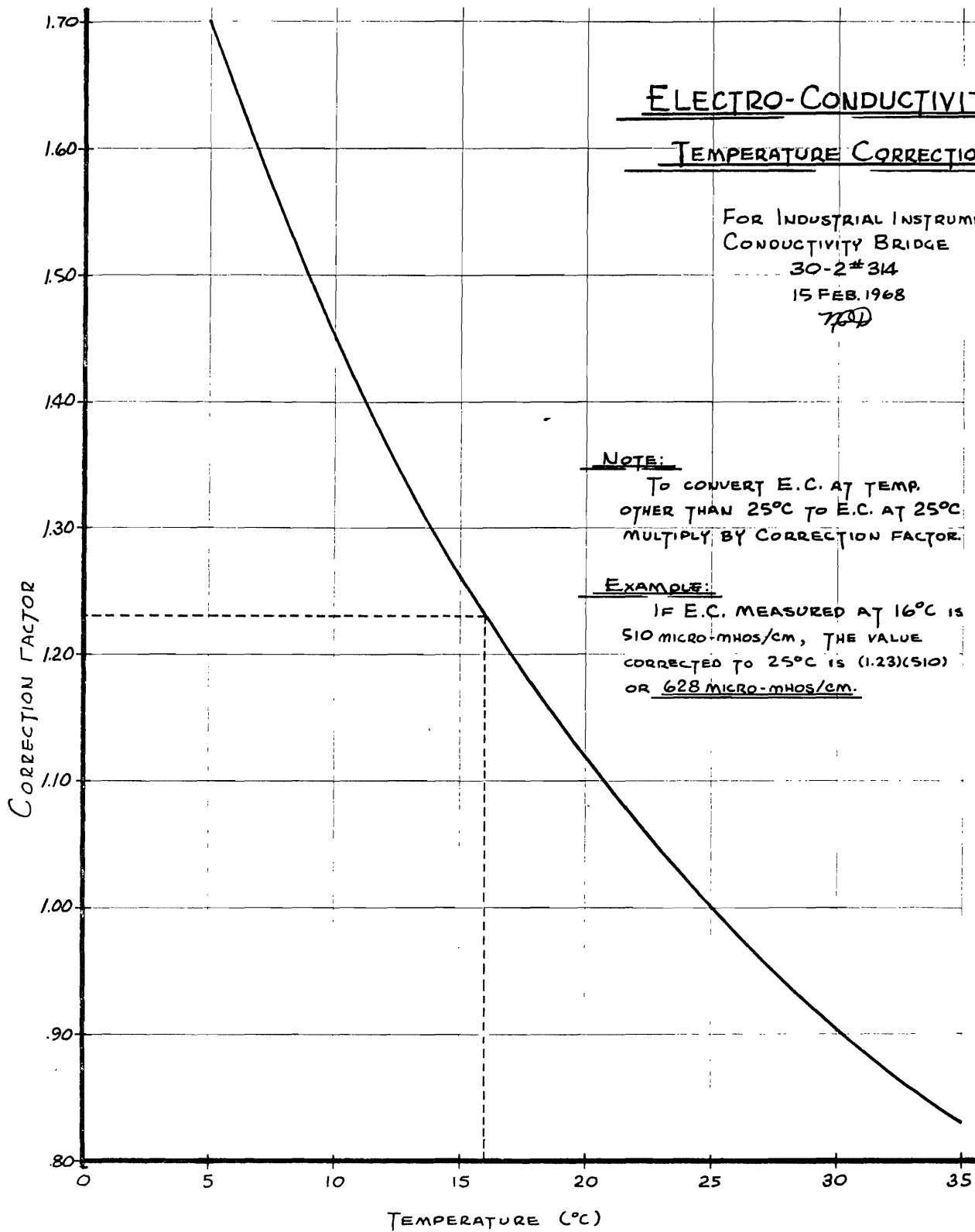
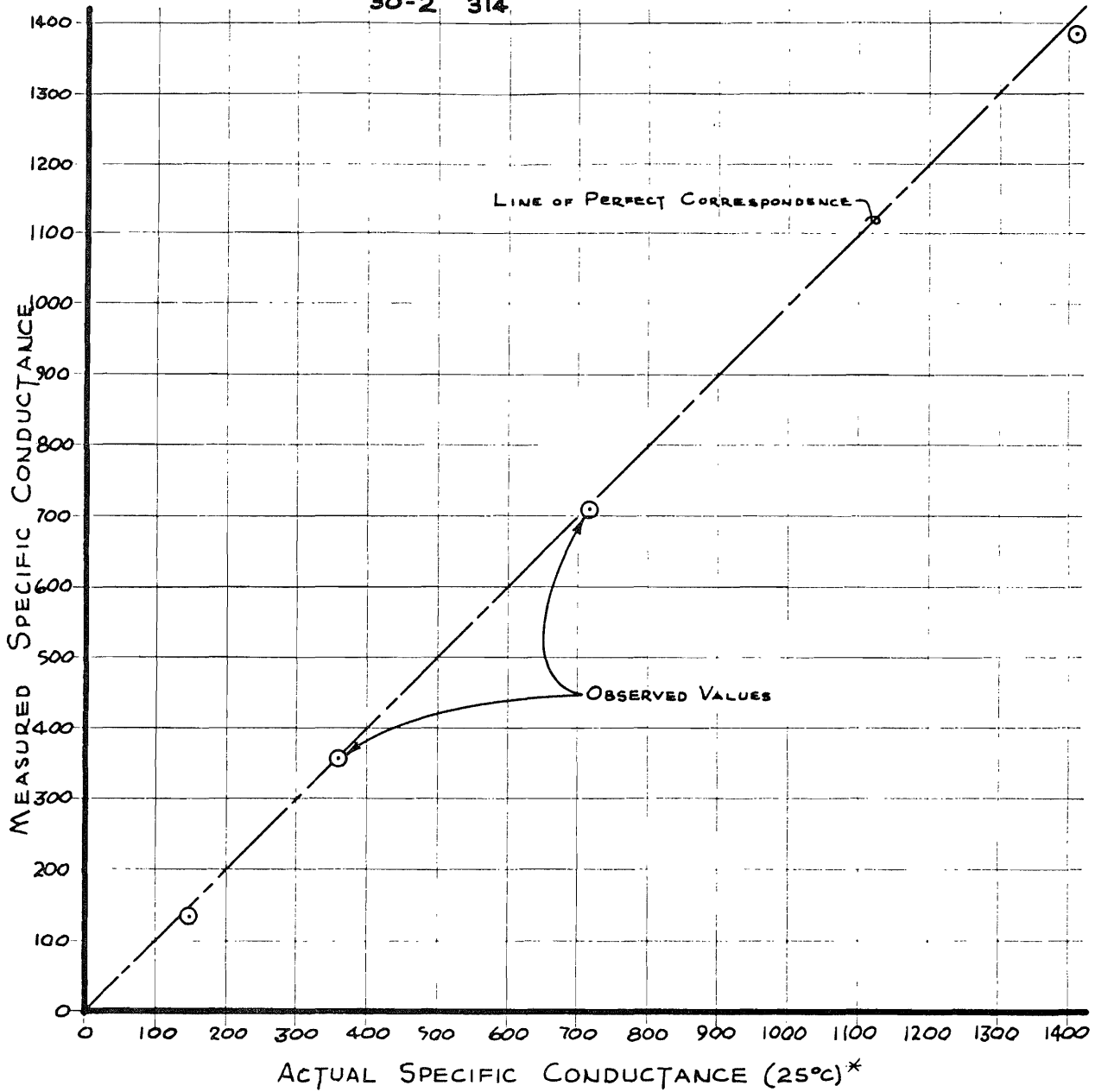


Figure B-3. Temperature correction for conductivity bridge.

CALIBRATION CURVE

FOR
INDUSTRIAL INSTRUMENTS
CONDUCTIVITY BRIDGE
30-2 #314



SOLUTION CONC.	ACTUAL S.C.	OBS. S.C.	Δ	% Δ
0.01 M	1413	1385	-28	-1.98
.005	718	710	-8	-1.12
.0025	360	358	-2	-0.56
.0010	147	136	-11	-7.50

15 FEB. 1968

Handwritten initials

* REF. STANDARD METHODS (12TH ED.)

Figure B-4. Conductivity bridge calibration curve for standard samples at 25°C.

APPENDIX C

WATER QUALITY DATA PROCESSING PROGRAMS

For Discrete Sample Data

Three basic utility programs were written to process weekly sampling data from 10 to 15 stations on the Little Bear River. These programs were:

- (1) QULPRT—which: (a) produces an analysis summary sheet, Figure C-1, for an individual water sample; (b) calculates me/L for each anion and cation, sums total anions and total cations, and (c) calculates percent dissolved oxygen as function of temperature and elevation, as outlined in Figure C-2.
- (2) SCAN—produces a list of all water quality data arranged consecutively by: (a) station for a given date, Figure C-3, and (b) chronologically by date for each station, Figure C-4.
- (3) PRTPLT—produces a graphical display of desired sample data points by: (a) station for a given date, Figure C-5, or (b) chronologically by date for each station, Figure C-6. (Both plots may be produced from the same data if the data are rearranged as specified and separate runs are made.)

The first program, QULPRT, was useful in producing an orderly summary of a given sample; also several computations were done, and the output provided a means for verification of card punching. The second and third programs provided a means for visually scanning the water quality data for the Little Bear River in both time and space; this type of output was important in looking for any cyclic trends with time or in correlations between variables. Instructions for using each of these programs¹ are outlined in the following sections.

1. QULPRT

Figure C-7 is a program listing of QULPRT as programmed in Fortran V, and run on the Univac 1108. Following the program listing is a listing of input cards used by the program. The details of the input cards are described in the following section. Figure C-1 is a sample of program output.

Specific instructions

Program QULPRT requires three groups of data input cards to follow the Fortran source deck. Table C-1

¹ Each of these programs could be improved or modified should a user so desire. For example the four weather and water quality comment cards used in QULPRT could be omitted by categorizing and number coding comments. Also the PRTPLT program has been substantially modified (by Professor Post) to add greater generality and usefulness to the program.

specifies the exact sequence and format for each card. Figure C-8 shows the deck arrangement for each of the three groups, along with the complete deck set-up for running the program.

Group I consists of a single control card, containing the single variable, NSTATS, which is the number of stations for which sample data are punched. Group II contains NSTATS cards, each containing the mnemonic station identification designation, the UMT station coordinates, and the description of the station (i.e. S1276259093 Little Bear River at Salt Lake Meridian). Group III consists of NSTATS number of lots having six data cards (described above) for each lot; each lot of six represents one station.

2. SCAN

Figure C-9 is a program listing of SCAN as programmed in Fortran V and run on the Univac 1108. Following the program listing is a listing of input cards used by the program. Figures C-3 and C-4 are the two options of program output; either or both options may be specified.

Specific instructions

Program SCAN requires four groups of data input cards to follow the Fortran source deck. Table C-2 specifies the exact sequence and format for each card. Figure

S152 259093 LITTLE BEAR RIVER AT SALT LAKE MERIDIAN											
STATION	S152	DATE	071367	TIME	1020	DAY OF YEAR	194				
APPEARANCE	CLLAR	COLLECTION POINT	ADJACENT TO BRIDGE	WEATHER CONDITIONS	CLLAR	COMMENTS					
CATIONS	MG/L	ME/L	ANIONS	MG/L	ME/L						
CA	50.40	2.51	CL	11.50	.32						
CU	MISSING DATA		CO3	.00	.00						
FE	MISSING DATA		HCO3	355.02	5.82						
MG	38.80	3.19	NO3	1.90	.03						
K	3.10	.08	PO4	.00	.00						
NA	12.20	.53	SO4	13.30	.28						
TOTAL CATIONS	6.32	ME/L	TOTAL ANIONS	6.45	ME/L						
GASES ¹	LO	9.6	MG/L	120.6	PCT SAT	NH3	.6	MG/L	CO2	5.0	MG/L
ORGANIC MATTER			ORGANISMS								
HOD	1.80	MG/L	TOTAL COUNT	650000./100ML							
COLOR	5. COBALT UNITS		COLIFORMS	100000./100ML							
COL	MISSING DATA		PLANKTERS	MISSING DATA							
CHLOROPHYLL	MISSING DATA										
OTHER PARAMETERS											
PH(P)	7.7		TEMPERATURE(F)	18.0 DEG. CENTIGRADE							
TURBIDITY	.25.		TDS	331.0 MG/L							
CONDUCTIVITY	528. UMHOS		SI02	15.8 MG/L							
TOTAL HARDNESS AS CaCO3	285.00 MG/L										

Figure C-1. Analysis summary sheet for individual water sample—sample output from QULPRT.

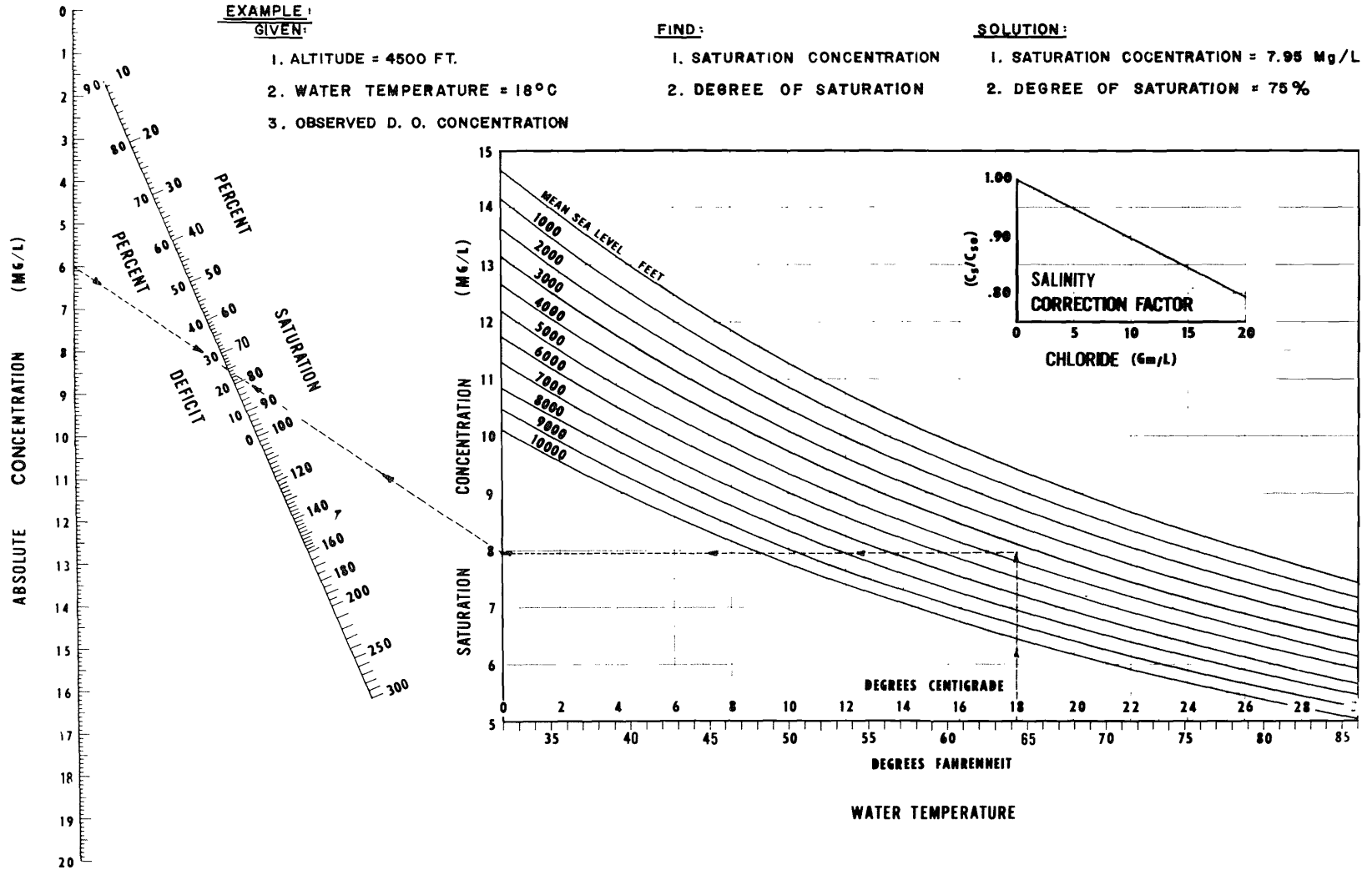


Figure C-2. Nomograph used in QULPRT to obtain percent dissolved oxygen saturation.

C-10 shows the deck arrangement for each of the four groups, along with the program source deck and run control cards.

Group I consists of a single control card containing three variables, NSTATS, N WEEKS, and IOUT, which are described in Table C-2, Group II contains the station designation and descriptions, one for each station from which a sample was obtained, with a total of NSTATS cards in this group. Group III consists of N WEEKS/8 cards containing the data and corresponding day of the year, arranged in the sequential order in which output is desired. Group IV consists of subgroup A and subgroup B. Subgroup A contains two cards of chemical and bacteriological data for each date for the designated station (Group III cards 5 and 6 from QULPRT); these cards are arranged consecutively in order of date for a given station. Subgroup B consists of two trailer cards which are control cards for indicating that all data cards containing water quality for a given station have been read. The subgroup B trailer cards for the last station are punched differently in the last column to indicate all data have been read.

3. PRTPLT

Figure C-11 is a program listing of PRTPLT as programmed in Fortran V and run on the Univac 1108. Following the program listing is a listing of input cards used by the program. The details of the input cards are described in the following section. Program PRTPLT outputs a plot of data contained in a 54 by 120 size matrix on a 9 x 12 inch rectangular area, as shown by Figures C-5 and C-6 (reduced in size).

Two Y axis transformation options are available: one allows plotting up to 10 Y variables against a common X variable; another obtains a log transformation of any Y variable. Separate runs are required for Figures C-5 and

C-6 respectively, each requiring different control card specifications and arrangement of data cards.

Specific instructions

Program PRTPLT requires two groups of data input cards to follow the Fortran source deck. Table C-3 specifies the exact sequence and format for each card. Figure C-12 shows the deck arrangement for each of the two groups, along with the deck set-up for running the program.

Group I consists of six control cards which must precede the data to be plotted. These control cards are made out in form (a) or form (b), which specifies whether the Figure C-5 type plot or the Figure C-6 type of plot will be produced; data cards must be arranged commensurately as outlined in Table C-3 and in Figure C-12.

Group II consists of three subgroups, A, B, and C. For the first station subgroups A and B are absent (actually Group I control cards replaces subgroups A and B for the first station). Subgroup A consists of a single dummy data card, which must have a zero or nine punch in column 80. If the column 80 punch is 0, then subgroup B consists of control card I-1 (but made out for the data in the subgroup C following); if this punch is 9, then subgroup C consists of control cards I-1 to I-6 (but made out for the specific manner in which the data in the subgroup C following is to be plotted). Subgroup C contains the water quality data cards (they can be cards III-5 and III-6 from Table C-1). Only ten variables may be plotted on any one plot and the selection is done by means of the format statement (see Table C-3, card I-2). The data cards are arranged in two alternate ways depending upon whether the Figure C-5 or Figure C-6 types of plots are desired; Table C-3 and Figure C-12 outline the manner of data arrangement.

DATA FOR THE WEEK 071367 DAY OF YEAR 194																		
STATION	DATE	TIME	CATIONS (MG/L)								ANIONS (MG/L)				OTHER PARAMETERS			
			CA	CU	FE	K	NA	CL	HCO3	CO3	NO3	PO4	SO4	PHF	PHL	HARD	Q	
S127	071367	1000	64.4	*****	*****	38.8	5.0	19.5	13.5	395.9	.0	4.7	.6	15.6	7.9	8.3	320.0	27.0
S128	071367	1010	23.6	*****	*****	60.0	5.0	19.6	5.3	396.5	.0	1.3	.1	14.0	7.9	8.3	305.0	*****
S152	071367	1020	50.4	*****	*****	36.8	3.1	12.2	11.5	355.0	.0	1.9	.0	13.3	7.7	8.3	285.0	3.3
S169	071367	1040	18.0	*****	*****	36.4	1.2	5.9	9.3	209.8	7.2	.6	.0	9.0	8.4	8.4	195.0	*****
S213	071367	1155	42.6	*****	*****	43.0	2.5	17.2	13.3	333.1	.0	3.7	.1	14.8	7.8	8.1	283.0	*****
S246	071367	1220	33.8	*****	*****	40.3	1.8	7.6	9.5	301.3	2.4	1.7	.0	8.0	9.1	8.3	250.0	*****
S270	071367	1330	*****	*****	*****	*****	*****	*****	7.0	*****	*****	*****	*****	8.4	***	*****	56.0	*****
S275	071367	1250	30.2	*****	*****	27.8	.6	7.2	9.8	212.3	6.0	.7	.0	6.5	8.4	8.5	190.0	19.0
SEC43	071367	1350	34.8	*****	*****	19.0	.6	4.1	6.5	201.3	3.6	1.0	.0	6.7	8.1	8.4	165.0	*****
SEC62	071367	1415	17.4	*****	*****	43.0	1.2	4.7	6.0	258.5	3.6	.0	.0	7.5	8.2	8.4	220.0	29.0
SD00	071367	1305	43.2	*****	*****	23.6	.6	4.1	5.8	230.5	4.8	.1	.0	5.7	9.4	8.5	205.0	37.0
S1F00	071367	1200	55.8	*****	*****	33.0	1.8	9.6	13.5	333.1	.0	4.0	.2	16.1	7.8	8.2	275.0	*****
SW01	071367	0945	53.0	*****	*****	45.6	5.0	21.2	17.8	384.3	.0	6.2	.7	20.6	7.8	8.1	320.0	*****
SLR00	071367	0850	41.0	*****	*****	21.8	.6	2.4	3.5	220.8	3.6	.3	.0	5.4	8.0	8.4	192.0	*****

STATION	DATE	TIME	GASES (MG/L)				OTHER PARAMETERS (MG/L)				ORGANIC MATTER (MG/L)			ORGANISMS	
			DO	PCT SAT	NH3	CO2	TURB	CNDN	TDS	TSMP	SI07	BOD	COLOR	TOTCNT	COLIFM
S127	071367	1000	7.3	86.3	.0	5.0	- 25.	64.5	425.0	15.0	19.1	1.7	- 5.	1900000.	1060000.
S128	071367	1010	7.5	94.2	.7	3.0	- 25.	55.0	381.0	14.0	15.8	1.6	- 5.	1400000.	450000.
S152	071367	1020	9.6	120.6	.6	5.0	- 25.	52.8	331.0	18.0	15.8	1.8	- 5.	5500000.	1000000.
S169	071367	1040	7.6	103.0	.1	.0	- 25.	30.0	211.0	22.0	8.6	1.1	- 5.	900000.	2000.
S213	071367	1155	6.9	83.3	.3	4.0	- 25.	51.5	330.0	16.0	9.1	5.9	- 5.	6000000.	6000000.
S246	071367	1220	8.2	103.0	.6	3.0	- 25.	43.5	274.0	18.0	10.7	.8	- 5.	*****	*****
S270	071367	1330	*****	*****	*****	*****	*****	33.0	*****	18.0	*****	*****	*****	*****	*****
S275	071367	1250	9.5	119.3	.5	.0	- 25.	30.0	200.0	18.0	7.8	1.0	- 5.	120000.	20000.
SEC43	071367	1350	9.7	117.1	.7	7.0	- 25.	292.	187.0	16.0	7.2	.3	- 5.	*****	*****
SEC62	071367	1415	8.9	111.8	.0	.0	- 25.	37.0	227.0	18.0	5.0	1.5	- 5.	*****	*****
SD00	071367	1305	8.0	98.5	.1	.0	- 25.	339.	209.0	17.0	5.2	.5	- 5.	240000.	67000.
S1F00	071367	1200	6.9	86.7	.3	6.0	- 25.	51.9	321.0	18.0	12.7	4.5	- 5.	1830000.	7000000.
SW01	071367	0945	7.3	86.5	.1	5.0	- 25.	61.8	449.0	14.0	21.4	4.1	- 5.	6000000.	1900000.
SLR00	071367	0850	9.2	97.4	.0	4.0	- 25.	30.0	179.0	10.0	4.0	.7	- 5.	30000.	16008.

Figure C-3. List of water quality data by station for a given date—sample output from SCAN.

STATION S152 259093 LITTLE BEAR RIVER AT SALT LAKE MERIDIAN

STATION	DATE	TIME	CA	CU	CATIONS (MG/L)					ANIONS (MG/L)					OTHER PARAMETERS				
					FE	MG	K	NA	CL	HCO3	CO3	NO3	PO4	SO4	PHF	PHL	HARD	Q	
S152	011267	1430	112.0	.0	.0	23.2	2.2	8.3	12.0	430.7	21.6	1.3	.2	11.9	8.0	8.0	8.0	280.0	40.0
S152	011967	1145	72.0	.0	.0	22.3	2.2	9.6	12.5	275.7	8.4	.5	.1	10.6	9.2	8.3	270.0	40.0	
S152	012667	1155	60.0	.0	.0	26.8	2.2	9.6	12.5	277.1	12.0	.1	.0	11.3	8.2	8.3	260.0	51.0	
S152	020267	1600	54.4	.0	.0	25.3	1.8	9.0	13.0	257.4	13.2	.6	.0	15.3	9.4	8.4	240.0	53.0	
S152	070967	1025	56.2	.0	.0	21.8	1.5	5.9	11.3	246.4	10.8	.4	.0	11.3	9.2	8.3	230.0	44.0	
S152	021667	1000	57.8	.0	.0	23.2	1.5	9.0	12.0	245.2	14.4	.7	.0	12.2	8.2	8.1	240.0	46.0	
S152	022367	1110	51.6	.0	.0	25.8	1.5	8.3	12.0	241.6	14.4	1.0	.0	14.0	9.2	8.4	235.0	44.0	
S152	030267	1130	70.4	.0	.0	15.5	1.8	8.3	12.0	247.7	10.8	.4	.1	13.1	8.5	8.4	240.0	53.0	
S152	030967	1010	38.6	.0	.0	32.0	1.5	8.3	12.3	245.3	7.2	.4	.0	10.8	8.2	8.4	228.0	48.0	
S152	031667	1345	50.2	.0	.0	27.8	1.8	9.0	12.6	251.3	9.6	.2	.0	10.6	8.2	8.2	240.0	30.0	
S152	032967	1520	55.4	.0	.0	30.8	1.8	9.6	14.9	294.0	3.6	2.5	.2	7.3	8.0	8.2	265.0	3.3	
S152	040667	1715	48.0	.0	.0	26.8	2.8	13.6	12.3	244.0	4.8	.5	.1	8.5	8.0	8.3	230.0	92.0	
S152	041367	1800	51.4	.0	.0	22.8	1.5	10.2	12.0	258.6	1.2	.7	.1	9.6	7.8	8.3	222.0	99.0	
S152	042067	1640	24.4	.0	.0	38.8	1.8	10.8	12.5	252.5	.0	.4	.2	11.6	8.0	8.2	220.0	195.0	
S152	042767	1725	51.4	.0	.0	19.8	1.5	9.6	12.3	246.4	.0	.8	.2	10.0	8.0	8.2	210.0	163.0	
S152	050367	1730	68.8	.0	.0	8.3	1.5	10.2	12.8	241.6	3.6	.8	.1	9.8	8.2	8.3	200.0	185.0	
S152	051167	1810	27.4	****	****	32.0	1.2	7.8	11.0	240.3	1.2	.7	.1	9.0	8.6	8.4	200.0	440.0	
S152	051867	1725	23.8	****	****	33.0	1.2	7.8	10.5	228.1	1.2	.5	.1	8.3	9.0	8.4	195.0	390.0	
S152	052567	1705	4.4	****	****	16.0	.9	5.3	8.5	200.1	1.2	1.9	.1	9.0	8.0	8.4	177.0	654.0	
S152	060167	1125	18.2	****	****	27.8	1.2	5.9	6.8	201.3	.0	.8	.0	8.5	9.4	8.4	160.0	212.0	
S152	060867	1150	31.8	****	****	20.8	1.2	5.9	7.0	187.9	6.0	.5	.0	6.4	8.4	8.5	165.0	218.0	
S152	061567	1200	2.0	****	****	40.3	.9	5.9	7.0	201.3	.0	.4	.1	7.5	8.1	8.2	170.0	418.0	
S152	062267	1520	12.1	****	****	34.0	.9	5.3	7.5	207.4	2.4	.9	.0	8.5	8.1	8.4	170.0	256.0	
S152	062967	0955	26.2	****	****	37.6	2.5	9.6	10.3	270.8	.0	2.3	.1	9.8	7.9	8.2	220.0	185.0	
S152	070667	0955	39.8	****	****	40.3	3.1	10.8	11.0	320.4	.0	2.1	.1	9.0	7.7	8.2	255.0	3.6	
S152	071367	1020	50.4	****	****	38.8	3.1	12.2	11.5	355.0	.0	1.9	.0	13.3	7.7	8.3	285.0	3.3	
S152	072067	1955	65.8	****	****	33.3	7.5	10.9	12.3	359.4	.0	1.3	.0	15.1	7.5	8.0	300.0	55.0	
S152	072767	1010	71.4	****	****	32.0	5.0	17.7	6.5	395.3	.0	2.6	.0	13.1	7.4	7.9	310.0	3.4	
S152	080367	1000	62.4	****	****	38.8	3.1	11.5	12.5	389.2	.0	1.9	.0	15.3	7.8	7.8	315.0	1.3	
S152	080967	1510	69.2	****	****	23.6	3.1	5.7	12.2	322.1	.0	.5	.0	12.2	7.6	8.1	270.0	1.4	
S152	081767	0955	70.2	****	****	27.8	3.8	6.3	12.5	355.0	.0	1.0	.1	12.8	7.6	8.0	290.0	.9	
S152	082367	0930	39.7	****	****	46.4	3.1	9.6	12.5	341.6	.0	1.0	.5	10.8	7.6	8.1	290.0	3.2	
S152	082967	0930	61.2	****	****	23.6	2.5	13.5	18.0	313.5	.0	1.5	.3	11.9	8.4	8.2	250.0	9.9	
S152	090667	0950	63.4	****	****	32.0	3.1	10.7	3.5	389.2	.0	1.0	.1	12.8	7.6	8.2	290.0	3.8	
S152	091367	0935	58.4	****	****	31.4	3.1	9.6	12.0	341.6	.0	.6	.1	10.3	***	7.5	275.0	5.0	
S152	092067	1000	59.7	****	****	33.0	3.1	9.6	13.0	341.6	.0	.5	.1	9.0	7.6	8.0	285.0	3.2	
S152	100467	1005	55.8	****	****	33.5	3.1	9.0	13.5	330.6	3.6	.6	.0	11.9	7.7	8.3	280.0	3.8	
S152	101067	1200	55.4	****	****	32.0	2.2	7.0	11.5	312.7	.0	1.3	.2	11.0	7.8	8.2	270.0	10.0	
S152	101767	1000	3.8	****	****	57.3	2.2	7.4	14.5	287.9	1.2	1.1	.2	12.8	9.6	8.5	245.0	73.0	
S152	102467	1015	50.2	****	****	27.8	2.2	8.3	12.0	281.8	3.6	.8	.0	11.9	9.2	8.5	240.0	71.0	
S152	103167	1020	27.3	****	****	44.2	2.2	7.8	11.5	292.3	2.4	.6	.5	9.3	8.7	8.4	250.0	57.0	
S152	110867	1100	52.2	****	****	27.8	2.2	9.1	12.5	264.7	5.6	1.0	.1	9.3	8.2	8.4	245.0	56.0	
S152	111467	1100	23.0	****	****	45.6	2.2	7.3	13.3	272.1	9.6	.8	.1	8.3	8.1	8.4	245.0	55.0	
S152	112067	1110	15.5	****	****	51.4	1.8	4.1	16.0	290.4	.0	1.2	.1	9.8	8.4	8.4	250.0	56.0	
S152	112867	1025	48.4	****	****	31.4	1.8	7.6	16.0	281.8	3.6	1.2	.1	8.8	7.9	8.4	250.0	54.0	
S152	120567	1040	11.5	****	****	51.4	2.2	9.3	12.5	268.4	3.6	2.0	.1	10.0	***	9.4	240.0	58.0	
S152	121367	1045	26.4	****	****	42.4	2.2	7.8	10.5	268.4	9.6	1.5	.1	7.5	***	8.4	240.0	56.0	

STATION S152 259093 LITTLE BEAR RIVER AT SALT LAKE MERIDIAN

STATION	DATE	TIME	GASES (MG/L)			OTHER PARAMETERS (MG/L)					ORGANIC MATTER (MG/L)			ORGANISMS		
			DO	PCT SAT	NH3	CO2	TURB	COND	TDS	TEMP	STO2	POD	COLOR	TCTCNT /100ML	COLIFM /100ML	
S152	011267	1430	14.7	134.0	.1	.0	25.0	433.0	275.0	4.0	8.2	2.9	-	5.0	26000	31000
S152	011967	1145	14.1	125.0	.0	.0	25.0	452.0	287.0	3.0	14.0	1.7	0	5.0	30000	43000
S152	012667	1155	12.8	119.8	.4	.0	25.0	475.0	200.0	5.0	17.5	3.2	0	5.0	30000	1000
S152	020267	1600	10.0	92.6	.0	.0	25.0	406.0	763.0	5.0	11.3	4.0	0	5.0	*****	*****
S152	020967	1025	13.0	125.7	.2	.0	25.0	412.0	234.0	4.0	11.5	4.5	0	5.0	30000	106000
S152	021667	1000	11.6	105.7	.0	.0	25.0	395.0	760.0	4.0	11.0	4.0	0	5.0	36000	1000
S152	022367	1110	10.3	96.4	.0	.0	25.0	430.0	284.0	5.0	10.4	1.9	-	5.0	4000	1000
S152	030267	1130	12.9	123.3	.0	.0	25.0	394.0	257.0	6.0	10.4	3.7	-	5.0	36000	16000
S152	030967	1010	10.6	101.4	.0	.0	25.0	377.0	764.0	6.0	10.6	***	0	5.0	*****	*****
S152	031667	1345	9.6	92.2	.2	.0	25.0	395.0	289.0	6.0	12.1	4.2	-	5.0	2000	3000
S152	032967	1520	10.8	101.1	.0	.0	25.0	429.0	317.0	5.0	20.7	4.0	-	5.0	*****	*****
S152	040667	1715	10.7	104.0	.5	.0	25.0	432.0	248.0	8.0	12.1	3.1	-	5.0	32000	18000
S152	041367	1800	10.5	102.0	.0	.0	25.0	420.0	259.0	8.0	12.0	***	-	5.0	70000	5000
S152	042067	1640	11.2	113.1	.0	5.0	25.0	362.0	230.0	6.0	10.5	5.8	-	5.0	100000	4000
S152	042767	1725	9.7	100.4	.0	2.0	25.0	390.0	219.0	9.0	13.2	2.4	-	5.0	123000	1000
S152	050367	1730	10.0	105.9	.0	.0	25.0	354.0	263.0	10.0	12.1	2.4	-	5.0	*****	*****
S152	051167	1810	10.2	105.5	.6	.0	26.0	352.0	219.0	9.0	11.3	2.2	-	5.0	42000	1600
S152	051867	1725	10.0	110.8	.0	.0	25.0	363.0	227.0	12.0	10.6	2.6	-	5.0	30000	1000
S152	052567	1705	9.5	110.3	.0	.0	25.0	310.0	189.0	14.0	10.2	2.3	-	5.0	430000	1000
S152	060167	1125	9.1	105.3	.1	.0	25.0	281.0	216.0	14.0	9.1	2.7	-	5.0	70000	4000
S152	060867	1150	9.4	113.5	.5	.0	***	298.0	190.0	15.0	8.2	2.8	-	5.0	90000	12000
S152	061567	1200	8.6	99.6	.6	.0	***	302.0	173.0	14.0	8.4	2.2	-	5.0	70000	12000
S152	062267	1520	8.0	96.6	.5	.0	***	315.0	178.0	16.0	9.6	2.5	-	5.0	*****	*****
S152	062967	0950	9.4	118.1	.4	5.0	***	430.0	255.0	19.0	10.5	.2	-	5.0	210000	54000
S152	070667	0955	7.3	88.1	.1	3.0	***	478.0	286.0	16.0	14.9	1.8	-	5.0	80000	136000
S152	071367	1020	9.6	120.6	.6	5.0	25.0	528.0	331.0	13.0	15.4	1.8	-	5.0	65000	10000
S152	072067	1050	9.3	114.5	.1	9.0	25.0	582.0	351.0	17.0	14.5	1.0	-	5.0	240000	18000
S152	072767	1010	8.2	101.0	.1	9.0	25.0	587.0	376.0	17.0	15.4	1.5</				

MULTIPLE PLOT DATA FOR STATION S152, YEAR 1967, TIME ONE INCH = 30.0 DAYS, NORS = 47

VARIABLE PLOT CHAP ORIGIN UNITS/INCH NO MISSING	COND C 100 C	TDS S 100 C	PH(F) P 1 3	FLOW Q 80 Q
011267 12	439.	275.	P.0	40.0
011967 19	467.	287.	P.2	40.7
012667 26	475.	280.	P.2	51.0
020267 32	409.	283.	P.4	53.0
020967 40	412.	254.	P.2	44.0
021667 47	395.	260.	P.2	46.0
022367 54	430.	294.	P.2	44.0
030267 61	334.	257.	P.6	53.0
030967 68	377.	264.	P.2	48.0
031667 75	375.	280.	P.2	30.0
032367 82	499.	212.	P.0	3.3
040667 96	439.	243.	P.0	32.0
041367 103	420.	254.	P.2	99.0
042067 110	362.	236.	P.0	135.0
042767 117	390.	218.	P.0	153.0
050367 123	359.	263.	P.2	195.0
051167 131	352.	213.	P.6	440.0
051867 138	363.	227.	P.0	330.0
052567 145	310.	159.	P.0	654.0
060167 152	241.	210.	P.4	212.0
060867 159	289.	190.	P.4	216.0
061567 166	302.	173.	P.1	418.0
062267 173	315.	179.	P.1	256.0
062967 180	438.	255.	P.9	195.0
070667 187	479.	286.	P.7	3.5
071367 194	522.	331.	P.7	3.3
072067 201	582.	351.	P.5	5.0
072767 208	563.	376.	P.4	3.4
080367 212	537.	264.	P.9	1.3
080967 221	513.	315.	P.8	1.4
081767 229	515.	335.	P.6	.9
082367 234	470.	335.	P.6	3.2
082967 241	450.	340.	P.4	9.9
090667 249	535.	327.	P.6	3.8
091367 256	419.	270.	****	5.0
092067 263	429.	230.	P.6	3.2
100467 277	490.	321.	P.7	3.0
101167 283	467.	285.	P.9	10.0
101767 290	440.	271.	P.6	73.0
102467 297	395.	230.	P.2	71.0
110167 305	440.	273.	P.7	57.0
110867 312	450.	252.	P.2	56.0
111467 319	450.	262.	P.1	55.0
112067 324	450.	253.	P.4	56.0
112867 332	400.	259.	P.2	54.0
120567 339	400.	273.	****	58.0
121367 347	442.	257.	****	56.0

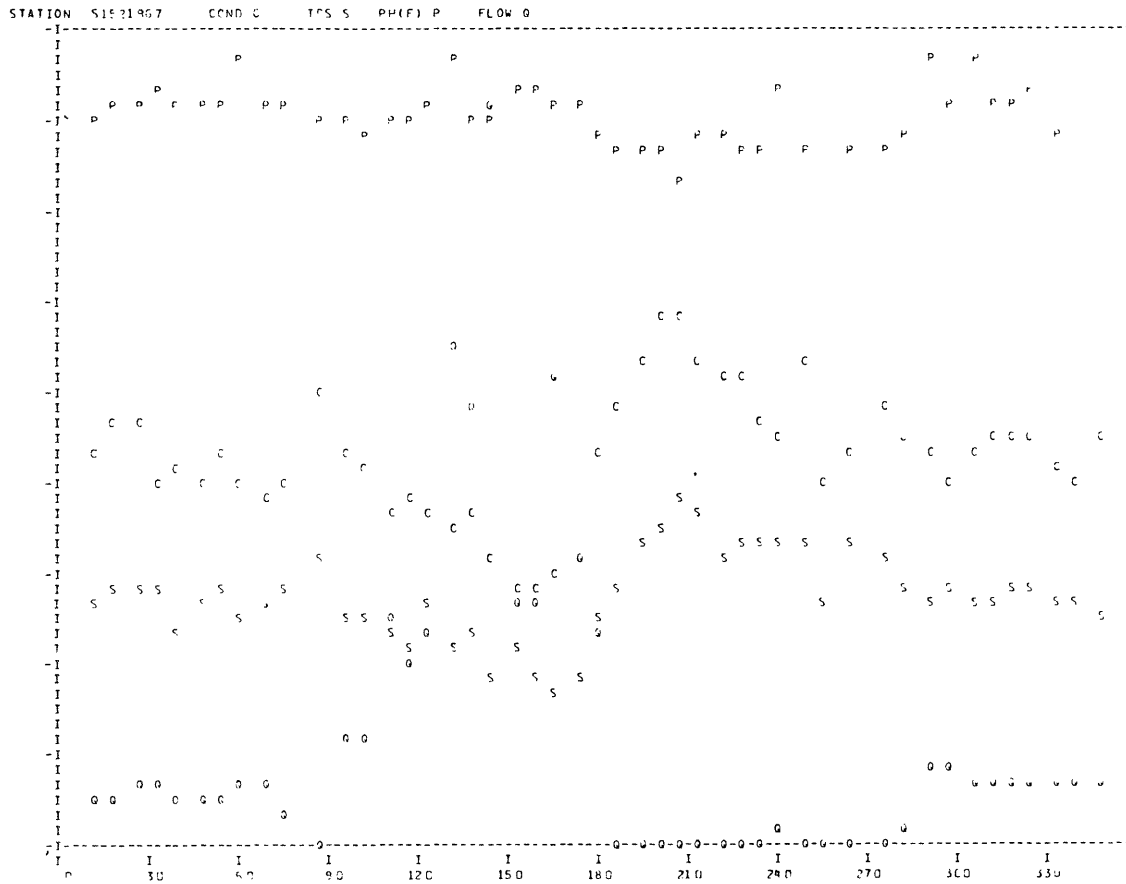


Figure C-6. Graphical display of water quality data by date for a given station—sample output from PRTPLT.

```

*1 FOR QULPRT,QULPRT
C C QUALITY DATA PRINTOUT AND VERIFICATION
DIMENSION APPEAR(15),COLL(15),WCOND(15),CMNTS(15)
REAL K,MG,NA,N03,NH3,MG1,K1,NA1,N031
INTEGER NAME(18,31),KTR(31),LL(31),ST1
HEAD(5,99)NSTATS,BK
99 FORMAT(I5,A6)
N=NSTATS+1
DO 2 J=1,18
2 NAME(J,N)=BK
Z=1.
Z1=1.
Z2=1.
Z3=1.
DO 300 I=1,NSTATS
300 READ(5,100) (NAME(J,I), J=1,18)
100 FORMAT(A6, 2X, A6, 16A4)
1 READ(5,101)ST1, DATE,TIME,APPEAR, L
101 FORMAT(A6, 2X, A6,2X,I4, 14A4,A3,I1)
IF(L.NE.1) GO TO 80
READ(5,102) COLL,L
102 FORMAT(20X,14A4,A3,I1)
IF(L.NE.2)GO TO 60
READ(5,102) WCOND,L
IF(L.NE.3) GO TO 80
READ(5,102) CMNTS, L
IF(L.NE.4) GO TO 80
READ(5,103)JULDAY,CA,CU,FE,MG,K,NA,CL,B,A,N03,P04,S04,PHF,0,L
103 FORMAT(13X13,4X13F4.1,F6.1,1X11)
IF(L.NE.5) GO TO 80
READ(5,104)DO,NH3,C02,PHB,TURBL,TURB,COND,TDS,T,HARD,SI02,POD,
1COLORL,COLOR,COTCNT,COLIFM,PLANKT,L
104 FORMAT(16X4F4.1,A1,F3.0,F4.0,2F4.1,F4.0,2F4.1,A1,F3.0,3F5.0,I1)
IF(L.NE.6)GO TO 80
DO 5 I=1,NSTATS
IF(NAME(I,I).EQ.ST1)GO TO 10
5 CONTINUE
I=NSTATS+1
NAME(I,I)=ST1
10 WRITE(6,200) (NAME(J,I),J=1,18)
200 FORMAT(1H1, A6, 2X, A6, 2X, 16A4)
WRITE(6,201) ST1, DATE,TIME, JULDAY
201 FORMAT(9H STATION, A6,5X$HDATE ,A6,5X$HTIME,I5,5X$1HDAY OF YEAR,I4)
WRITE(6,202) APPEAR
202 FORMAT(11H APPEARANCE, 9X,14A4,A3)
WRITE(6,203) COLL
203 FORMAT(17H COLLECTION POINT, 3X, 14A4,A3)
WRITE(6,204)WCOND
204 FORMAT(19H WEATHER CONDITIONS, 1X, 14A4, A3)
WRITE(6,205)CMNTS
205 FORMAT(9H COMMENTS, 11X, 14A4, A3)
WRITE(6,206)
206 FORMAT(8HOCATIONS5X4HMG/L5X4HME/L10X6HANIONS5X4HMG/L5X4HME/L)
DO 15 I=1,31
15 KTR(I)=1
SC=0
SA=0
Z=SIGN(Z,CA)
IF(Z.LT.0.)GO TO 20
CA1=CA*.04990
SC=SC+CA1
KTR(1)=0
20 Z=SIGN(Z,CU)
IF(Z.LT.0.)GO TO 21
CU1=CU*.03148
SC=SC+CU1
KTR(2)=0
21 Z=SIGN(Z,FE)
IF(Z.LT.0.)GO TO 22
FE1=FE*.05372
SC=SC+FE1
KTR(3)=0
22 Z=SIGN(Z,MG)
IF(Z.LT.0.)GO TO 23
MG1=MG*.08226
SC=SC+MG1
KTR(4)=0
23 Z=SIGN(Z,K)
IF(Z.LT.0.)GO TO 24
K1=K*.02557
SC=SC+K1
KTR(5)=0
24 Z=SIGN(Z,NA)
IF(Z.LT.0.)GO TO 25
NA1=NA*.04350
SC=SC+NA1
KTR(6)=0
25 Z=SIGN(Z,CL)
IF(Z.LT.0.)GO TO 26
CL1=CL*.02821
SA=SA+CL1
KTR(7)=0
26 Z=SIGN(Z,A)
IF(Z.LT.0.)GO TO 27
C03=12.*A
C031=C03*.03333
SA=SA+C031
KTR(8)=0
27 Z=SIGN(Z,B)
IF(Z.LT.0.)GO TO 28
HC03=12.*(B-2.*A)
HC031=.01639+HC03
SA=SA+HC031
KTR(9)=0
28 Z=SIGN(Z,N03)
IF(Z.LT.0.)GO TO 29
N031=.01613+N03
SA=SA+N031
KTR(10)=0
29 Z=SIGN(Z,P04)
IF(Z.LT.0.)GO TO 30
P041=P04*.03159
SA=SA+P041
KTR(11)=0
30 Z=SIGN(Z,S04)
IF(Z.LT.0.)GO TO 31
S041=S04*.02083
SA=SA+S041
KTR(12)=0
31 DO 35 I=1,6
35 LL(I)=KTR(I)*2+KTR(I+6)*1+1
LL1=LL(1)
GO TO (36,37,38,39),LL1
36 WRITE(6,207) CA, CA1, CL, CL1
207 FORMAT(1H0,3X,2HCA,F11.2,F9.2,12X,2HCL,F12.2,F9.2)
GO TO 152
37 WRITE(6,208)CA, CA1
208 FORMAT(1H0,3X,2HCA,F11.2,F9.2,12X,2HCL,8X,12HMISSING DATA)
GO TO 152
38 WRITE(6,209) CL, CL1
209 FORMAT(1H0,3X,2HCA,8X,12HMISSING DATA,12X,2HCL,F12.2,F9.2)
GO TO 152
39 WRITE(6,210)
210 FORMAT(1H0, 3X, 2HCA, 8X, 12HMISSING DATA, 12X, 2HCL, 8X,
112HMISSING DATA)
152 LL2=LL(2)
GO TO (40,41,42,43),LL2
40 WRITE(6,211)CU,CU1,C03, C031
211 FORMAT(1H ,3X,2HCU,F11.2,F9.2,12X,3HC03,F11.2,F9.2)
GO TO 153
41 WRITE(6,212)CU,CU1
212 FORMAT(1H ,3X,2HCU,F11.2,F9.2,12X,3HC03,7X,12HMISSING DATA)
GO TO 153
42 WRITE(6,213)C03,C031
213 FORMAT(1H ,3X,2HCU,8X,12HMISSING DATA,12X,3HC03,F11.2,F9.2)
GO TO 153
43 WRITE(6,214)
214 FORMAT(1H ,3X,2HCU,8X,12HMISSING DATA,12X,3HC03,7X,
112HMISSING DATA)
153 LL3=LL(3)
GO TO(44,45,46,47),LL3
44 WRITE(6,215)FE,FE1,HCO3,HCO31
215 FORMAT(1H ,3X,2HFE,F11.2,F9.2,12X,4HHC03,F10.2,F9.2)
GO TO 154
45 WRITE(6,216)FE,FE1
216 FORMAT(1H ,3X,2HFE,F11.2,F9.2,12X,4HHC03,6X,12HMISSING DATA)
GO TO 154
46 WRITE(6,217)HCO3,HCO31
217 FORMAT(1H ,3X,2HFE,8X,12HMISSING DATA,12X,4HHC03,F10.2,F9.2)
GO TO 154
47 WRITE(6,218)
218 FORMAT(1H ,3X,2HFE,8X,12HMISSING DATA,12X,4HHC03,6X,
112HMISSING DATA)
154 LL4=LL(4)
GO TO(48,49,50,51),LL4
48 WRITE(6,219)MG,MG1,N03,N031
219 FORMAT(1H ,3X,2HMG,F11.2,F9.2,12X,3HN03,F11.2,F9.2)
GO TO 155
49 WRITE(6,220)MG,MG1
220 FORMAT(1H ,3X,2HMG,F11.2,F9.2,12X,3HN03,7X,12HMISSING DATA)
GO TO 155
50 WRITE(6,221)N03,N031
221 FORMAT(1H ,3X,2HMG,8X,12HMISSING DATA,12X,3HN03,F11.2,F9.2)
GO TO 155
51 WRITE(6,222)
222 FORMAT(1H ,3X,2HMG,8X,12HMISSING DATA,12X,3HN03,7X,
112HMISSING DATA)
155 LL5=LL(5)
GO TO(52,53,54,55),LL5
52 WRITE(6,223)K,K1,P04,P041
223 FORMAT(1H ,3X,1HK,F12.2,F9.2,12X,3HP04,F11.2,F9.2)
GO TO 156
53 WRITE(6,224)K,K1
224 FORMAT(1H ,3X,1HK,F11.2,F9.2,13X,3HP04,7X,12HMISSING DATA)
GO TO 156
54 WRITE(6,225)P04,P041
225 FORMAT(1H ,3X,1HK,9X,12HMISSING DATA,12X,3HP04,F11.2,F9.2)
GO TO 156
55 WRITE(6,226)
226 FORMAT(1H ,3X,1HK,9X,12HMISSING DATA,12X,3HP04,7X,
112HMISSING DATA)
156 LL6=LL(6)
GO TO(56,57,58,59),LL6
56 WRITE(6,227)NA,NA1,S04,S041
227 FORMAT(1H ,3X,2HNA,F11.2,F9.2,12X,3HS04,F11.2,F9.2)
GO TO 157
57 WRITE(6,228)NA,NA1
228 FORMAT(1H ,3X,2HNA,F11.2,F9.2,12X,3HS04,7X,12HMISSING DATA)
GO TO 157
58 WRITE(6,229)S04,S041
229 FORMAT(1H ,3X,2HNA,8X,12HMISSING DATA,12X,3HS04,F11.2,F9.2)
GO TO 157
59 WRITE(6,230)
230 FORMAT(1H ,3X,2HNA,8X,12HMISSING DATA,12X,3HS04,7X,
112HMISSING DATA)
157 WRITE(6,250) SC, SA
250 FORMAT(1H3,13HTOTAL CATIONS,F8.2,1X,4HME/L,9X,12HTOTAL ANIONS,
1F8.2,1X,4HME/L)
DO1=1000.0/(81.3*(2.462+T))
LO1=(DO/DO1)*100.0
Z1=SIGN(Z1,DO)
Z2=SIGN(Z2,NH3)
Z3=SIGN(Z3,C02)
KLK=Z1+Z1+Z2+.5*Z3+4.55
GO TO (490,491,496,492,495,497,494,493),KLK
490 WRITE(6,470)
470 FORMAT(1H3,6HGASES ,2X,12HDO NH3 C02,2X,12HMISSING DATA)
GO TO 503
491 WRITE(6,471)C02
471 FORMAT(1H3,6HGASES ,2X,7HDO NH3,2X,12HMISSING DATA,5X,3HC02,F6.1,
11X,4HMG/L)
GO TO 503
492 WRITE(6,472)NH3,C02
472 FORMAT(1H3,6HGASES ,2X,2HDO,1X,12HMISSING DATA,2X,3HNH3,F6.1,1X,
14HMG/L,5X,3HCC02,F6.1,1X,4HMG/L)
GO TO 503
493 WRITE(6,473)DO,C01,NH3,C02
473 FORMAT(1H3,6HGASES ,2X,2HDO,F5.1,1X,4HMG/L,F9.1,1X,7HPCP SAT,4X,

```

Figure C-7. Program listing of QULPRT—and input data set-up for run.

```

13HNH3,F5.1,1X,4HMG/L,5X,3HC02,F5.1,1X,4HMG/L)
GO TO 503
494 WRITE (6,474)D0,D01,NH3
474 FORMAT(1H3,6HGASLS ,2X,2HD0,F5.1,1X,4HMG/L,F7.2,1X,7HPCT SAT,6X,
13HNH3,F,1,1X,4HMG/L,2X,3HC02,1X,12HMISSING DATA)
GO TO 503
495 WRITE (6,475)D0,D01
475 FORMAT(1H3,6HGASLS ,2X,2HD0,F5.1,1X,4HMG/L,F7.2,1X,7HPCT SAT,6X,
13HNH3 (02,2X,12HMISSING DATA)
GO TO 503
496 WRITE (6,476)D0,D01
476 FORMAT(1H3,6HGASLS ,2X,2HD0,2X,12HMISSING DATA,2X,3HNH3,F5.1,1X,
4HMG/L,2X,3HC02,2X,12HMISSING DATA)
GO TO 503
497 WRITE (6,477)D0,D01,02
477 FORMAT(1H3,6HGASLS ,2X,2HD0,F5.1,1X,4HMG/L,F7.2,1X,7HPCT SAT,2X,
13HNH3,1X,12HMISSING DATA,2X,3HC02,F5.1,1X,4HMG/L)
503 WRITE (6,503)
503 FORMAT(1H3,19HORGANISM( MATTER,19X,9HORGANISMS)
Z1=SIGN(Z1,0)
Z2=SIGN(Z2,0)
KLK=Z1+.5*Z2+2.55
GO TO(504,505,506,507),KLK
504 WRITE (6,504)
504 FORMAT(1H0,5X,3H00,0X,12HMISSING DATA,11X,11HTOTAL COUNT,6X,
112HMISSING DATA)
GO TO 510
505 WRITE (6,505)TOTCNT
505 FORMAT(1H0,7X,3H00,0X,12HMISSING DATA,11X,11HTOTAL COUNT,F17.0,
16H/100ML)
GO TO 510
506 WRITE (6,506)H00
506 FORMAT(1H0,7X,3H00,0X,2,1X,4HMG/L,16X,11HTOTAL COUNT,6X,
112HMISSING DATA)
GO TO 510
507 WRITE (6,507)H00,TOTCNT
507 FORMAT(1H0,7X,3H00,0X,2,1X,4HMG/L,16X,11HTOTAL COUNT,F17.0,
16H/100ML)
GO TO 510
508 WRITE (6,508)H00
508 FORMAT(1H0,7X,3H00,0X,2,1X,4HMG/L,16X,11HTOTAL COUNT,6X,
112HMISSING DATA)
GO TO 510
509 WRITE (6,509)H00,TOTCNT
509 FORMAT(1H0,7X,3H00,0X,2,1X,4HMG/L,16X,11HTOTAL COUNT,F17.0,
16H/100ML)
GO TO 510
510 Z1=SIGN(Z1,COLOR)
Z2=SIGN(Z2,COLOR)
KLK=Z1+.5*Z2+2.55
GO TO(514,515,516,517),KLK
514 WRITE (6,514)
514 FORMAT(1H0,5X,5HCOLOR,4X,12HMISSING DATA,11X,9HCOLORFORMS,8X,
112HMISSING DATA)
GO TO 520
515 WRITE (6,515)COLIFM
515 FORMAT(1H0,7X,5HCOLOR,4X,12HMISSING DATA,11X,9HCOLORFORMS,F19.0,
16H/100ML)
GO TO 520
516 WRITE (6,516)COLOBL,COLOR
516 FORMAT(1H0,5X,5HCOLOR,1X,A1,F4.0,1X,12HCOALT UNITS,8X,
19HCOLORFORMS,8X,12HMISSING DATA)
GO TO 520
517 WRITE (6,517)COLOBL,COLOR,COLIFM
517 FORMAT(1H0,5X,5HCOLOR,1X,A1,F4.0,1X,12HCOALT UNITS,8X,
19HCOLORFORMS,F19.0,6H/100ML)
520 Z1=SIGN(Z1,0)
Z2=SIGN(Z2,PLANKT)
KLK=Z1+.5*Z2+2.55
GO TO(524,525,526,527),KLK
524 WRITE (6,524)
524 FORMAT(1H0,5X,3H 0 ,6X,12HMISSING DATA,11X,9HPLANKTERS,8X,
112HMISSING DATA)
GO TO 530
525 WRITE (6,525)PLANKT
525 FORMAT(1H0,5X,3H 0 ,6X,12HMISSING DATA,11X,9HPLANKTERS,F19.0,
13H/ML)
GO TO 530
526 WRITE (6,526)Q
526 FORMAT(1H0,5X,3H 0 ,F8.1,2X,3HCFS,16X,9HPLANKTERS,8X,
112HMISSING DATA)
GO TO 530
527 WRITE (6,527)Q,PLANKT
527 FORMAT(1H0,5X,3H 0 ,F8.1,2X,3HCFS,16X,9HPLANKTERS,F19.0,3H/ML)
530 Z=SIGN(Z,PH8)
IF(Z.LT.0)GO TO 531
WRITE(6,612)PH8
612 FORMAT(1H0,5X,13PH8 DET IN LAB,F8.2)
GO TO 501
531 WRITE(6,613)
613 FORMAT(1H0,5X,24PH8 NOT DETERMINED IN LAB)
501 WRITE(6,265)
265 FORMAT(1H3,16HOTHER PARAMETERS)
Z1=SIGN(Z1,PHF)
Z2=SIGN(Z2,T)
KLK=Z1+.5*Z2+2.55
GO TO(534,535,536,537),KLK
534 WRITE(6,614)
614 FORMAT(1H0,5X,5PH(F),6X,12HMISSING DATA,6X,14HTEMPERATURE(F),6X,
112HMISSING DATA)
GO TO 540
535 WRITE(6,615)T
615 FORMAT(1H0,5X,5PH(F),6X,12HMISSING DATA,6X,14HTEMPERATURE(F),
1F7.1,1X,15HDEG. CENTIGRAD)
GO TO 540
536 WRITE(6,616)PHF
616 FORMAT(1H0,5X,5PH(F),F16.1,8X,14HTEMPERATURE(F),6X,
112HMISSING DATA)
GO TO 540
537 WRITE(6,617)PHF,T
617 FORMAT(1H0, 5X,5PH(F),F16.1,8X,14HTEMPERATURE(F),F 7.1,1X,
115HDEG. CENTIGRAD)
540 Z1=SIGN(Z1,TURB)
Z2=SIGN(Z2,TDS)
KLK=Z1+.5*Z2+2.55
GO TO(544,545,546,547),KLK
544 WRITE(6,618)
618 FORMAT(1H0,5X,9HTURBIDITY,6X,12HMISSING DATA,2X,5HTDS,6X,
112HMISSING DATA)
GO TO 550
545 WRITE(6,619)TDS
619 FORMAT(1H0,5X,9HTURBIDITY,6X,12HMISSING DATA,2X,5HTDS,F19.1,1X,
14HMG/L)
GO TO 550
546 WRITE(6,620)TURBL,TURB
620 FORMAT(1H0,5X,9HTURBIDITY,6X,A1,F4.0,9X,3HTDS,6X,12HMISSING DATA)
GO TO 550
547 WRITE(6,621)TURBL,TURB,TDS
621 FORMAT(1H0,5X,9HTURBIDITY,6X,A1,F4.0,9X,3HTDS,F19.1,1X,4HMG/L)
550 Z1=SIGN(Z1,COND)
Z2=SIGN(Z2,SIO2)
KLK=Z1+.5*Z2+2.55
GO TO(554,555,556,557),KLK
554 WRITE(6,622)
622 FORMAT(1H0,5X,12HCONDUCTIVITY,3X,12HMISSING DATA,2X,4HSIO2,6X,
112HMISSING DATA)
GO TO 560
555 WRITE(6,623)SIO2
623 FORMAT(1H0,5X,12HCONDUCTIVITY,3X,12HMISSING DATA,2X,4HSIO2,F17.1,
11X,4HMG/L)
GO TO 560
556 WRITE(6,624)COND
624 FORMAT(1H0,5X,12HCONDUCTIVITY,F8.0,1X,5HUMHOS,3X,4HSIO2,6X,
112HMISSING DATA)
GO TO 560
557 WRITE(6,625)COND,SIO2
625 FORMAT(1H0,5X,12HCONDUCTIVITY,F8.0,1X,5HUMHOS,3X,4HSIO2,F17.1,1X,
14HMG/L)
560 Z=SIGN(Z,HARD)
IF(Z.LT.0)GO TO 565
WRITE(6,626)HARD
626 FORMAT(1H0,5X,23HTOTAL HARDNESS AS CAC03,F7.2,1X,4HMG/L)
GO TO 570
565 WRITE(6,627)
627 FORMAT(1H0,5X,23HTOTAL HARDNESS AS CAC03,6X,12HMISSING DATA)
570 GO TO 1
80 WRITE(6,400) L
400 FORMAT(14HIDATA CARD NO., 13, 16H IS OUT OF ORDER)
GO TO 90
90 STOP
END

```

AN X01 QUMPR1

```

5125 250112 LITTLE BEAR RIVER AT WELLSVILLE TELEMETRY SITE
5127 251109 LITTLE BEAR RIVER BELOW WELLSVILLE
5129 252107 LITTLE BEAR RIVER AT WELLSVILLE LOWER BRIDGE
5152 254093 LITTLE BEAR RIVER AT SALT LAKE MERIDIAN
5168 279084 HYRUM RESERVOIR AT STATE PARK BOAT RAMP
5205 287041 LITTLE BEAR RIVER AT PARADISE TELEMETRY SITE
5213 287028 LITTLE BEAR RIVER AT PARADISE LOWER BRIDGE
5224 295012 LITTLE BEAR RIVER AT WHITES TROUT FARM DIVERSION
5246 309984 LITTLE BEAR RIVER AT WEST CANYON BELOW AVON
5270 324457 LITTLE BEAR RIVER BELOW DAVENPORT CREEK NEAR AVON
5274 322950 SOUTH FORK LITTLE BEAR RIVER BELOW DAVENPORT CREEK
5275 320944 SOUTH FORK LITTLE BEAR RIVER ABOVE DAVENPORT CREEK
52804 321977 EAST FORK LITTLE BEAR RIVER AT AVON
52843 376965 EAST FORK LITTLE BEAR RIVER BELOW POKUPINE DAM
52867 405967 EAST FORK LITTLE BEAR RIVER ABOVE POKUPINE RESERVOIR
52887 321945 DAVENPORT CREEK AT SOUTH FORK LITTLE BEAR RIVER
52901 279106 WELLSVILLE STREAM AT LOWER WELLSVILLE ROAD
52902 288028 WHITES TROUT FARM AT PARADISE LOWER BRIDGE
52903 346713 LOGAN RIVER AT HIGHWAY BRIDGE ABOVE STATE DAM
52911 235110 ARTESIAN WELL EAST OF ARCHIBALD ROAD
52911 258108 FIELD DRAIN 1 MILE EAST OF GREENS CORNER
52907 294068 SPRING AT F K ISRAELSEN FARM
52918 312985 SPRING AT FORSBERG ROAD
52510 258107 LADFLA ANDERSON FIELD DRAIN
5125 070168 0940 SLIGHTLY TURBID
5125 070168 0940 TELEMETRY SITE
5125 070168 0940 CLEAR
5125 070168 0940
5125 0701681830940 217 330 63 186 45 207 00 76 06 131 78
5125 070168183 86 03 84- 25 5303950 130 190 114 11- 5176E4320E2
5128 070168 0955 CLEAR
5128 070168 0955 ADJACENT TO BRIDGE
5128 070168 0955 SUNNY
5128 070168 0955
5128 0701681820955 242 352 60 164 90 225 00 22 01 128 77
5128 070168183 89 03 83- 25 5603810 140 205 107 02- 5140E3300F1
** REMOTE STOP

```

Group I - Control Card

Group II - Name Cards

Data for Station 1

Group III - Data Cards in lots of 6

Data for Station 2

Figure C-7. Continued.

Table C-1. Input data cards for Program QULPRT.

Group	Card	Column	Name	Format	Description	
I	1		NSTATS	I5	Number of stations for which sample data are punched	
II	2 to 2 NSTATS	1-6	Name ₁	A6	Mnemonic station designation	
		7-8	blank	2X	blank	
		8-13	Name ₂	A6	UMT grid coordinates of station	
		14-78	Name ₃ -Name ₁₈	16A4	Station name and description	
III	1	1-6	ST1	A6	Six character station mnemonic	
		9-14	DATE	A6	Date of sample collection as MO/DA/YR	
		17-20	TIME	A4	Time sample was taken in military time	
		21-79	APPEAR	14A4,A3	Appearance of the sampled water	
		80	L	I1	1, signifying card one of data group III	
		2	1-20	Same as on Card 1 above		
			21-79	COLL	14A4,A3	Detailed description of the point of collection of the sample
			80	L	I1	2, signifying card two of data group III
		3	1-20	Same as on Card 1 above		
			21-79	WCOND	14A4,A3	Weather condition at time sample taken
	80	L	I1	3, signifying card three of data group III		
		4	1-20	Same as on Card 1 above		
	21-79		CMNTS	14A4,A3	Comments describing any unusual circumstances concerning the sample	
	5	1-6	8-13	DATE	A6	Six character station mnemonic
			14-16	JULDAY	A3	Date of sample in MO/DA/YR
			17-20	TIME	A4	Consecutive day of year
			21-24	CA	F4.1	Time of day of sample in military time
		25-28	CU	F4.1	Calcium in milligrams per liter (mg/l)	
			29-32	FE	F4.1	Copper in mg/l
		33-36	MG	F4.1	Iron in mg/l	
37-40		K	F4.1	Magnesium in mg/l		
41-44		NA	F4.1	Potassium in mg/l		
45-48		CL	F4.1	Sodium in mg/l		
49-52		B	F4.1	Chloride in mg/l		
53-56		A	F4.1	Total ml .02N acid titration to reach methyl range end point ml .02N acid titrant to reach phenolphthalein end point		
57-60		NO3	F4.1	nitrate in mg/l		
61-64	PO4	F4.1	phosphate in mg/l			
65-68	SO4	F4.1	sulfate in mg/l			
69-72	PHF	F4.1	field pH			

Table C-1. Continued.

Group	Card	Column	Name	Format	Description
	6	1-16	Same as card 5 above		
		17-20	DO	F4.1	Dissolved oxygen in mg/l
		21-24	NH3	F4.1	Ammonia in mg/l
		25-28	CO2	F4.1	Carbon dioxide in mg/l
		29-32	Ph	F4.1	pH in the laboratory sample
		33	TURBL	A1	inequality condition for turbidity measurement + for > and - for <
		34-36	TURB	F3.0	Turbidity
		37-40	COND	F4.0	Electrical conductivity in μ mhos/cm
		41-44	TDS	F4.1	Total dissolved solids in mg/l
		45-48	T	F4.1	Field temperature in °C.
		49-52	HARD	F4.0	Total hardness as CaCO ₃ in mg/l
		53-56	SIO2	F4.1	silicon dioxide in mg/l
		57-60	BOD	F4.1	Biological oxygen demand in mg/l
		61	COLORL	A1	inequality condition for color measurement + for >, - for <
		62-64	COLOR	F3.0	Color in cobalt units
		65-69	TOTCNT	E5.0*	Total organism count per 100 ml
		70-74	COLIFM	E5.0	Coliform count per 100 ml
		75-79	FECOL	E5.0	Fecal coliform count per 100 ml
		80	LL	I1	6, signifying card 6 of data group III

*Example: if total count is measured as 5,800,000 per 100 ml, the card would be punched: 580 + 4, with the 5 in column 65.

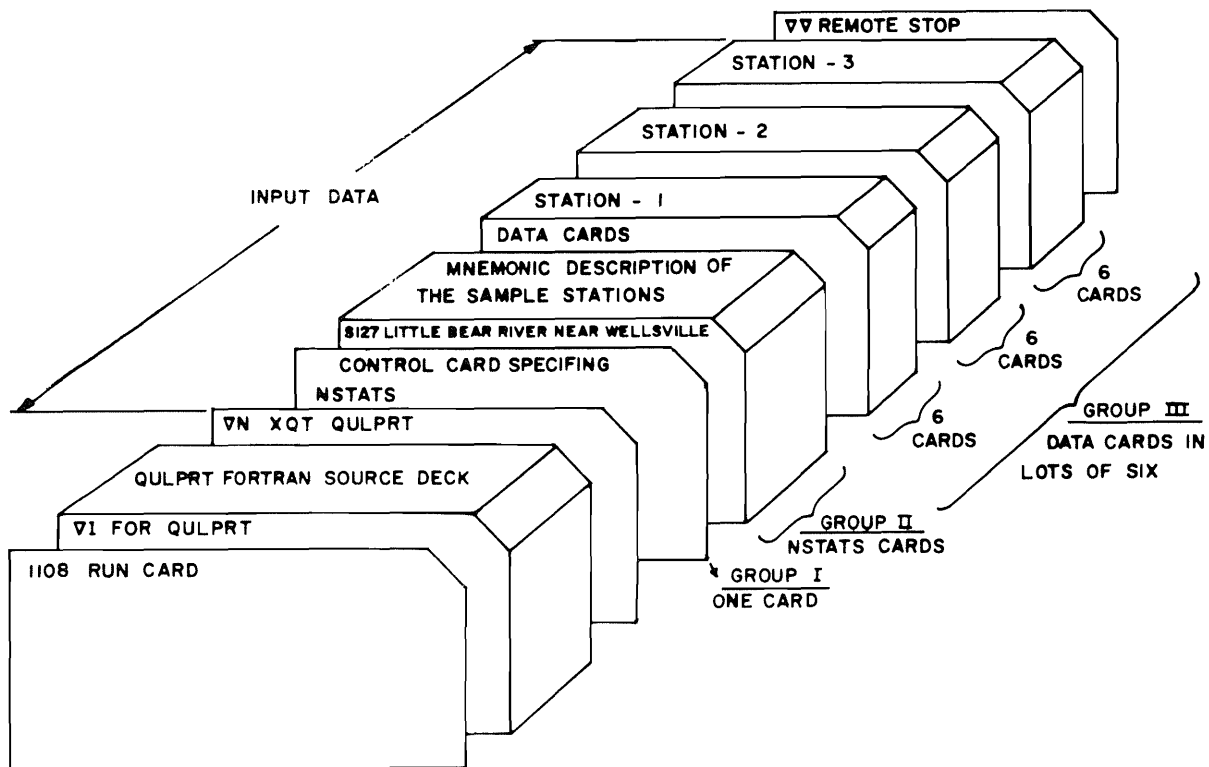


Figure C-8. Deck set-up for QULPRT data input.

```

I FOR SCAN,SCAN
C SCAN OF QUALITY DATA BY DATE AND STATION
C READ STATION NAME CARDS FOR AT LEAST ALL STATIONS SCANNED
C READ DATE CARDS FOR ALL WEEKS DESIRED SCANNED
C DATA INPUT SORTED ACCORDING TO STATION WITH DATES CHRONOLOGICAL
C DATA FOR STATIONS SEPARATED BY 2 CARDS WITH 0'S IN COL 80
C LAST 2 CARDS SHOULD HAVE 0 IN COL 80 AND 9 IN COL 80 RESPECTIVELY
C DATA OUTPUT IS IN SAME SEQUENCE AS READ IN INPUT
REAL MG(25,53),K(25,53),NA(25,53),NO3(25,53),NH3(25,53),O(25,53),
1CA(25,53),CU(25,53),FE(25,53),CL(25,53),B(25,53),A(25,53),
2P04(25,53),PHF(25,53),HARD(25,53),D0(25,53),D01(25,53),C02(25,53),
3PH(25,53),TURBL(25,53),TURB(25,53),COND(25,53),TDS(25,53),T(25,53),
4,SIO2(25,53),BOD(25,53),COLORL(25,53),COLOR(25,53),TOTCNT(25,53),
5COLIFM(25,53),S04(25,53),HC03(25,53),C03(25,53),
INTEGER ST1(25),NAME(25,18),N(25),JULDAY(25,53),IJUL(53),
1IDATE(53),DATE(25,53),TIME(25,53)
DATA BLANK/5H
1 READ(5,201) NSTATS,NWEEKS,IOUT
201 FORMAT(3I5)
DO 51 I=1,NSTATS
51 READ(5,202) (NAME(I,J),J=1,18)
202 FORMAT(A6,2X,A6,16A4)
READ(5,205) (IDATE(J),IJUL(J),J=1,NWEEKS)
205 FORMAT(8(1XA6,A3))
NIMAX=0
NS=0
DO 10 I=1,25
DO 11 J=1,53
READ(5,100) ST1(I),DATE(I,J),JULDAY(I,J),TIME(I,J),CA(I,J),CU(I,J),
1FE(I,J),MG(I,J),K(I,J),NA(I,J),CL(I,J),B(I,J),A(I,J),NO3(I,J),P04(
2I,J),S04(I,J),PHF(I,J),Q(I,J),L,D0(I,J),NH3(I,J),C02(I,J),
3PH(I,J),TURBL(I,J),TURB(I,J),COND(I,J),TDS(I,J),T(I,J),
4HARD(I,J),SIO2(I,J),BOD(I,J),COLORL(I,J),COLOR(I,J),TOTCNT(I,J),
5COLIFM(I,J),LL
100 FORMAT(A6,1X,A6,A3,A4,13F4,1,F6,1,X,I1/16X,4F4,1,A1,F3,0,F4,0,
12F4,1,F4,0,2F4,1,A1,F3,0,2E5,0,5X,I1)
IF(LL.NE.0) GO TO 40
N(I)=J-1
IF(N(I).LT.NIMAX)GO TO 12
NIMAX=N(I)
MAXS=I
GO TO 12
40 IF(LL.NE.5)GO TO 1000
IF(LL.NE.6)GO TO 1000
11 CONTINUE
12 NS=NS+1
IF(LL.EQ.9)GO TO 61
10 CONTINUE
61 DO 20 I=1,NS
M=N(I)
DO 20 J=1,M
Z=SIGN(Z,CA(I,J))
IF(Z.LT.0.)CA(I,J)=100000000.
Z=SIGN(Z,CU(I,J))
IF(Z.LT.0.)CU(I,J)=100000000.
Z=SIGN(Z,FE(I,J))
IF(Z.LT.0.)FE(I,J)=100000000.
Z=SIGN(Z,MG(I,J))
IF(Z.LT.0.)MG(I,J)=100000000.
Z=SIGN(Z,K(I,J))
IF(Z.LT.0.)K(I,J)=100000000.
Z=SIGN(Z,NA(I,J))
IF(Z.LT.0.)NA(I,J)=100000000.
Z=SIGN(Z,CL(I,J))
IF(Z.LT.0.)CL(I,J)=100000000.
HC03(I,J)=12.*2*(B(I,J)-2.*A(I,J))
Z=SIGN(Z,B(I,J))
IF(Z.LT.0.)HC03(I,J)=100000000.
C03(I,J)=12.*A(I,J)
Z=SIGN(Z,A(I,J))
IF(Z.LT.0.)C03(I,J)=100000000.
Z=SIGN(Z,NO3(I,J))
IF(Z.LT.0.)NO3(I,J)=100000000.
Z=SIGN(Z,P04(I,J))
IF(Z.LT.0.)P04(I,J)=100000000.
Z=SIGN(Z,S04(I,J))
IF(Z.LT.0.)S04(I,J)=100000000.
Z=SIGN(Z,PHF(I,J))
IF(Z.LT.0.)PHF(I,J)=100000000.
Z=SIGN(Z,Q(I,J))
IF(Z.LT.0.)Q(I,J)=100000000.
Z=SIGN(Z,HARD(I,J))
IF(Z.LT.0.)HARD(I,J)=100000000.
D01(I,J)=1000./(61.3+(2.462*T(I,J)))
D01(I,J)=(D0(I,J)/D01(I,J))*100.
Z=SIGN(Z,D0(I,J))
IF(Z.LT.0.)D0(I,J)=1000000001.
Z=SIGN(Z,T(I,J))
IF(Z.LT.0.)T(I,J)=100000000.
IF(Z.LT.0.)OR.DC(I,J).GT.100000000.)D01(I,J)=D0(I,J)
Z=SIGN(Z,NH3(I,J))
IF(Z.LT.0.)NH3(I,J)=100000000.
Z=SIGN(Z,C02(I,J))
IF(Z.LT.0.)C02(I,J)=100000000.
Z=SIGN(Z,PH(I,J))
IF(Z.LT.0.)PH(I,J)=100000000.
Z=SIGN(Z,TURB(I,J))
IF(Z.LT.0.)TURB(I,J)=100000000.
Z=SIGN(Z,COND(I,J))
IF(Z.LT.0.)COND(I,J)=100000000.
Z=SIGN(Z,TDS(I,J))
IF(Z.LT.0.)TDS(I,J)=100000000.
Z=SIGN(Z,SIO2(I,J))
IF(Z.LT.0.)SIO2(I,J)=100000000.
Z=SIGN(Z,BOD(I,J))
IF(Z.LT.0.)BOD(I,J)=100000000000.
Z=SIGN(Z,COLOR(I,J))
IF(Z.LT.0.)COLOR(I,J)=100000000000.
Z=SIGN(Z,TOTCNT(I,J))
IF(Z.LT.0.)TOTCNT(I,J)=1000000000000.
Z=SIGN(Z,COLIFM(I,J))
IF(Z.LT.0.)COLIFM(I,J)=1000000000000.
20 CONTINUE
WRITE(6,401)MAXS,NS,(N(I),I=1,NS)
401 FORMAT(1H1,7H MAXS =,I4,5H NS =,I4,7H N(I) =,30I4)
GO TO(130,130,150),IOUT
130 DO 22 I=1,NS
KK=0
DO 135 K1=1,NSTATS
IF(ST1(I).EQ.NAME(K1,1)) GO TO 131
135 CONTINUE
WRITE(6,1002)ST1(I)
1002 FORMAT(1H1,8HSTATION ,A6,15H NAME NOT FOUND)
KK=1
GO TO 136
131 WRITE(6,104) (NAME(K1,J),J=1,18)
104 FORMAT(1H1,8HSTATION ,A6,2X,A6,1X,16A4)
136 WRITE(6,101)
101 FORMAT(1H0,30X,12HGASES (MG/L),19X,16HOTHER PARAMETERS,
17H (MG/L),9X,21HORGANIC MATTER (MG/L),4X,9HORGANISMS)
WRITE(6,110)
WRITE(6,111)
M=N(I)
DO 23 J=1,M
23 WRITE(6,112)ST1(I),DATE(I,J),TIME(I,J),D0(I,J),D01(I,J),NH3(I,J),
1C02(I,J),TURBL(I,J),TURB(I,J),COND(I,J),TDS(I,J),T(I,J),SIO2(I,J),
3BOD(I,J),COLORL(I,J),COLOR(I,J),TOTCNT(I,J),COLIFM(I,J)
IF(KK)137,138,137
137 WRITE(6,1002)ST1(I)
138 IF(KK.EQ.0)WRITE(6,104) (NAME(K1,J),J=1,18)
WRITE(6,301)
301 FORMAT(1H0,34X,14HCATIONS (MG/L),28X,13HANIONS (MG/L),21X,
116HOTHER PARAMETERS)
WRITE(6,106)
DO 22 J=1,M
WRITE(6,303)ST1(I),DATE(I,J),TIME(I,J),CA(I,J),CU(I,J),FE(I,J),
1MG(I,J),K(I,J),NA(I,J),CL(I,J),HC03(I,J),C03(I,J),NO3(I,J),
2P04(I,J),S04(I,J),PHF(I,J),PH(I,J),HARD(I,J),Q(I,J)
303 FORMAT(2XA6,1XA6,1XA4,1XF5,1,11(2XF5,1),3XF3,1,4XF3,1,3XF5,1,3XF5,
1)
22 CONTINUE
GO TO (150,1,150),IOUT
150 DO 24 K1=1,NWEEKS
KK1=1
DO 25 I=1,NS
M=N(I)
DO 125 J=1,M
IF(ABS(JULDAY(I,J)-IJUL(K1))-2)310,310,125
125 CONTINUE
GO TO 25
310 GO TO (311,312),KK1
311 KK1=2
WRITE(6,109)IDATE(K1),IJUL(K1)
109 FORMAT(1H1,18HDATA FOR THE WEEK ,A6,12H DAY OF YEAR,1XA3)
WRITE(6,301)
WRITE(6,106)
106 FORMAT(8H STATION6H DATE2X4HTIME3X2HCA5X2HCU5X2HFE5X2HMG6X1HK5X,
12HNA 5X,2HCL,4X,4HHC03,4X,3HC03,4X,3HP04,4X,3HS04,3X,
23PHF,4X,3PHL,4X4HHARD,6X1H0)
312 WRITE(6,303)ST1(I),DATE(I,J),TIME(I,J),CA(I,J),CU(I,J),FE(I,J),
1MG(I,J),K(I,J),NA(I,J),CL(I,J),HC03(I,J),C03(I,J),NO3(I,J),
2P04(I,J),S04(I,J),PHF(I,J),PH(I,J),HARD(I,J),Q(I,J)
25 CONTINUE
KK1=1
110 FORMAT(8H STATION6H DATE,2X4HTIME6X2HDO3X7HPCT SAT4X3HHN35X3HCO2,
14X4HTURB,4X,4HCOND,5X,3HTDS,4X,4HTEMP,4X,4HSIO2,5X,3HBOD,4X,
15HCOLOR,5X,6HTOTCNT,5X,6HCOLIFM)
111 FORMAT(1H ,62X,8HUMH05/CM,9X,6HDEG. C,29X,6H/100ML,5X,6H/100ML)
DO 26 I=1,NS
M=N(I)
DO 126 J=1,M
IF(ABS(JULDAY(I,J)-IJUL(K1))-2)320,320,126
126 CONTINUE
GO TO 26
320 GO TO (321,322),KK1
321 KK1=2
WRITE(6,101)
WRITE(6,110)
WRITE(6,111)
322 WRITE(6,112)ST1(I),DATE(I,J),TIME(I,J),D0(I,J),D01(I,J),NH3(I,J),
1C02(I,J),TURBL(I,J),TURB(I,J),COND(I,J),TDS(I,J),T(I,J),SIO2(I,J),
3BOD(I,J),COLORL(I,J),COLOR(I,J),TOTCNT(I,J),COLIFM(I,J)
112 FORMAT(2XA6,1XA6,1XA4,2XF6,1,4XF5,1,3XF5,1,3XF5,1,2XA1,F5,0,2XF6,0
1,3X,4(F5,1,3X),1XA1,1XF3,0,2(2XF9,0))
26 CONTINUE
24 CONTINUE
1000 WRITE(6,113)
113 FORMAT(1H1,20HCARD IS OUT OF ORDER)
STOP
END

```

Figure C-9. Program listing of SCAN and input data set-up for a run.

```

BN YOT SCAN
 4 28 1
5125 230112 LITTLE BEAR RIVER AT WELLSVILLE TELEMETRY SITE
5127 231109 LITTLE BEAR RIVER BELOW WELLSVILLE
5124 232107 LITTLE BEAR RIVER AT WELLSVILLE LOWER BRIDGE
5152 232993 LITTLE BEAR RIVER AT SALT LAKE MERIDIAN
5168 279084 HYRUM RESERVOIR AT STATE PARK BOAT RAMP
5205 287091 LITTLE BEAR RIVER AT PARADISE TELEMETRY SITE
5213 287028 LITTLE BEAR RIVER AT PARADISE LOWER BRIDGE
5224 295012 LITTLE BEAR RIVER AT WHITES TROUT FARM DIVERSION
5246 309984 LITTLE BEAR RIVER AT WEST CANYON BELOW AVON
5270 324957 LITTLE BEAR RIVER BELOW DAVENPORT CREEK NEAR AVON
5274 322950 SOUTH FORK LITTLE BEAR RIVER BELOW DAVENPORT CREEK
5275 320944 SOUTH FORK LITTLE BEAR RIVER ABOVE DAVENPORT CREEK
SECON 323977 EAST FORK LITTLE BEAR RIVER AT AVON
SEC43 376965 EAST FORK LITTLE BEAR RIVER BELOW PORKUPINE DAM
SEC62 405963 EAST FORK LITTLE BEAR RIVER ABOVE PORKUPINE RESERVOIR
SD00 323945 DAVENPORT CREEK AT SOUTH FORK LITTLE BEAR RIVER
SW01 229106 WELLSVILLE STREAM AT LOWER WELLSVILLE ROAD
STF00 288028 WHITES TROUT FARM AT PARADISE LOWER BRIDGE
SLR00 346213 LOGAN RIVER AT HIGHWAY BRIDGE ABOVE STATE DAM
U2311 235110 ARTESIAN WELL EAST OF ARCHIBALD ROAD
U2611 258108 FIELD DRAIN 1 MILE EAST OF GREENS CORNER
U2907 294068 SPRING AT E K ISPAELSEN FARM
U3199 312985 SPRING AT FOPSBERG ROAD
U2510 258107 LADELL ANDERSON FIELD DRAIN
060366154 061666167 062366174 063066181 070766188 071466195 072166202 072866209
080466216 081166223 081866230 082566237 090166244 090866251 091566258 092266265
092766270 100466277 101166284 101866291 102566298 110166305 110866312 111566319
112966333 120666340 121466348 121966353
5127 0603661540915 00000000 0073031009090250003014130110215 78 5
5127 060366154008000300000084-0250408397501300325 0025 6
5127 0616661671345 00000000 0061027000500255003010000050188 80 5
5127 061666167004000100000082-0750344368001400347 0013 6
5127 0623661741130 00000000 007902880234023400700000050196 80 5
5127 062366174007000000000081-0250638356531500330 0021 4
5127 06306618111115 00000000 00680297003402870006000040201 80 240 5
5127 0630661810094000300000081-0250515430501700325 0014 6
5127 0707661881100 00000000 0088032500250298006014770130177 80 240 5
5127 0707661880086000400000080-0250613399001500330 0011 6
5127 0714661951100 00000000 006802800040029000800970100164 80 260 5
5127 0714661950085000400000083-0250620379501700310 0010 6
5127 0721662021115 00000000 007403300150287000501040000151 80 250 5
5127 072166202005007400000082-0250580396501700320 0002 6
5127 0728662091105 00000000 008803400035030000401270980150 80 230 5
5127 072866209001000300000079-0250640400041700290 0015 6
5127 1214663481115 875 07 00 232 21 112 420 261 07 04 116 80 220 5
5127 121466348 95 03 00 84- 25 5703680 70 300 168 - 5 6
5127 1219663530915 00 00 248 15 95 375 247 05 58 04 84 78 500 5
5127 121466353 94 05 00 84- 25 5702260 50 310 167 06- 5400E3700E2 6
5127
5127
5127
5000 1219663531155 00 00 364 04 38 140 193 14 01 01 50 82 111 5
5000 121966353 123 08 00 91- 25 3901760 00 250 75 09- 5290E3550E2 6
5000
5000
STF00 1011662841335 00 00 30 115 245 252 00 68 03 130 5
STF00 101166284 59 17 50 81- 25 4603120 110 280 35 240E4780F2 6
STF00 1025662981340 00 00 18 112 270 238 00 64 05 90 76 5
STF00 102566298 60 05 80 85- 25 4502980 140 270 46 115E4120E3 6
STF00 1101663051420 168 51 95 155 237 00 24 05 90 76 5
STF00 110166305 52 07 40 85- 25 4702960 090 260 53 6
STF00 1108663121420 241 35 130 155 217 00 49 05 80 76 6
STF00 110866312 75 15 50 82- 25 3902910 070 250 24 6
STF00 1115663191415 00 00 244 97 300 470 239 00 25 03 75 76 5
STF00 111566319 72 10 50 80- 25 3402700 090 290 30- 5 6
STF00 1129663331400 00 00 220 70 75 140 235 00 31 07 96 76 5
STF00 112966333 69 15 40 91- 25 4501720 08 180 194 00 30 09 106 76 5
STF00 1206663401345 00 00 190 08 38 180 270 130 16- 5 6
STF00 120666340 22 70 97- 25 3903720 50 270 23 03 96 76 5
STF00 1214663481330 850 248 12 50 125 228 00 73 03 96 76 5
STF00 121466348 71 05 30 85- 25 4402720 50 300 115 - 5 6
STF00 1219663531055 00 00 320 08 50 165 230 03 25 03 74 78 5
STF00 121966353 100 14 00 84- 25 4202200 20 250 116 23- 5420E4150E3 6
STF00
SW01 1004662771200 00 00 75 225 610 246 05 112 03 115 78 5
SW01 100466277 87 07 00 86- 25 6104620 140 280 35 240E4780F2 6
SW01 1011662841210 53 280 435 281 04 102 03 160 5
SW01 101166284 09 00 85- 25 5753590 120 265 680E3236F3 6
SW01 1025662981220 00 00 40 260 575 250 04 135 03 105 78 5
SW01 102566298 88 01 00 88- 25 5003860 110 280 19 6
SW01 1101663051245 00 00 108 41 240 500 235 04 94 03 30 78 5
SW01 110166305 90 07 00 85- 25 5703630 170 280 15 6
SW01 1108663121210 00 00 268 63 280 475 235 04 82 03 122 78 5
SW01 110866312 92 06 00 83- 25 5003730 090 305 04 6
SW01 1115663191245 00 00 284 45 30 865 242 04 56 03 96 76 5
SW01 111566319 06 00 83- 25 6602220 100 300 - 5 6
SW01 1129663331230 00 00 168 45 200 460 237 06 97 04 30 78 5
SW01 112966333 93 07 00 88- 25 6002520 090 390 - 5 6
SW01 1206663401225 00 00 268 25 95 465 243 05 104 05 125 78 5
SW01 120666340 12 00 95- 25 5601160 90 340 153 04 40 6
SW01 1214663481150 840 226 21 112 455 254 06 84 04 96 80 5
SW01 121466348 94 09 00 88- 25 5503580 80 290 154 - 5 6
SW01 1219663530920 364 19 112 300 254 03 84 05 90 78 5
SW01 121966353 92 17 00 86- 25 6003140 60 300 142 04- 5740E4320E3 6
SW01
SW01
aa REMOTE STOP

```

Group I - Control Card

Group II - Name Cards

Group III - Date Cards

Subgroup A - Data in Chronological Order for first station

Subgroup B - 2 trailer Cards

Subgroups A & B for other stations

Subgroup B - trailer cards for SD00

Subgroup A

Subgroup B

Subgroup A

Subgroup B - 2 trailer Cards with 9 in col. 80 of second card signifying end of input data

Figure C-9. Continued.

Table C-2. Input data cards for program SCAN.

Group	Card	Column	Name	Format	Description
I	1	1-5	NSTATS	I5	Number of stations for which data is being appended ($1 \leq NSTATS \leq 25$)
		6-10	NWEEKS	I5	Number of weeks for which scan by date is desired ($1 \leq NWEEKS \leq 53$)
		11-15	IOUT	I5	Output option: If 1, scan by station and scan by date. If 2, scan by station only. If 3, scan by date only.
II ¹	2, to 2 NSTATS	1-6	Name ₁	A6	Mnemonic station designation
		7-8	blank	2X	blank
		8-13	Name ₂	A6	UMT grid coordinates of station
		14-78	Name ₃ -Name ₁₈	16A4	Station name and description
III	3, to 3 NWEEKS 8	1-80	IDATE, IJUL	(8(1X, A6,A3))	Date (mo/day/year) and day of year for which scan output is to include, ² punched consecutively 8 per card
IV	[(4 ₁ -4 ₂) 5	1-80	quality data		same as card III-5, Table C-1
		1-80	quality data		same as card III-6, Table C-1
	1-5	Name ₁	A5	Station designation	
	80			0(zero)	
	6] NSTATS	1-5	Name ₁	A5	Station designation
		80			0(zero); except 9 if last trailer card

¹ Same as Group II cards for QULPRT (see Table C-1).

² If sample was obtained on a date different than specified by IDATE, IJUL, and output is desired for this sample, two days latitude is allowed; for example if 1/25/69 25 is specified the sample could be obtained 1/23/69 or 1/27/69 and still be included in the output.

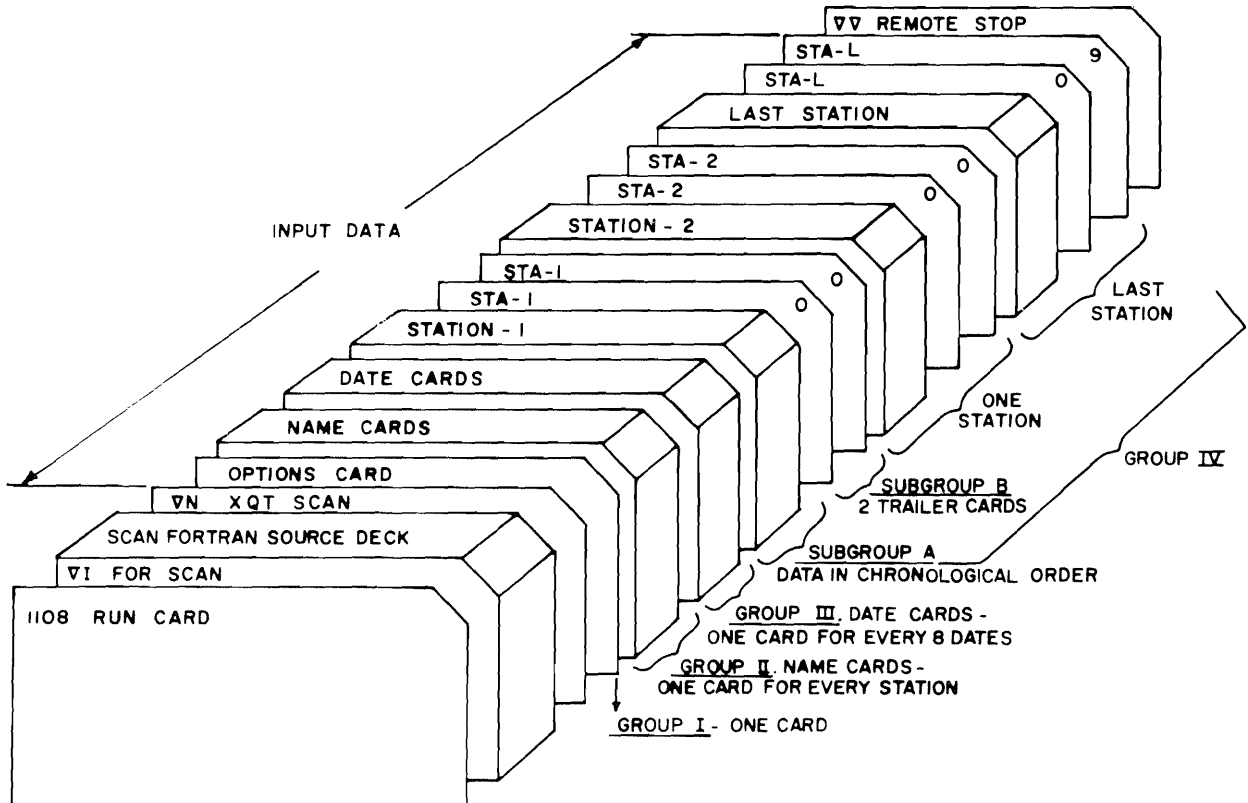


Figure C-10. Deck set-up for SCAN data input.

```

WN FOR PRTPLT
C PRINTPLT
  DIMENSION NX(300),Y(300,10),A(125,60),A0(300,10),FIN(13),ND(12),
  IB(60),IIX(300),IYY(300,10),ITEST(10),VAR(10),PT(10),YMIN(10),
  ZNMIS(10),NYL(10),IS(10),DATE(300),FMT(14)
  DATA BLANK,ZERO,DASH,TICK,ORIG/1H,1H0,1H-,1H1,6HORIGIN/
  Z=1.
  LL=9
  DO 5 I=1,121
  DO 5 J=1,60
  B(J)=BLANK
  5 A(I,J)=BLANK
  DO 35 J=1,55
  35 A(2,J)=TICK
  DO 65 J=1,55,6
  65 A(1,J)=DASH
  DO 31 I=3,121
  A(I,1)=DASH
  31 A(I,55)=DASH
  DO 52 I=2,121,10
  52 A(I,56)=TICK
  1 READ(5,201)STA,YEAR,NMP,LP,SCXX,NMIN
  201 FORMAT(A6,A4,2I5,F10.0,1I10)
  IF(LL.NE.9)GO TO 71
  READ(5,109)NY,FIN
  READ(5,113)FMT
  113 FORMAT(13A6,A2)
  109 FORMAT(I2,13A6)
  READ(5,110)(VAR(I),PT(I),ITEST(I),I=1,NY)
  110 FORMAT(10(A6,A1,I1))
  READ(5,111)(YMIN(J),J=1,NY)
  READ(5,112)(NYL(J),J=1,NY)
  111 FORMAT(10F6,0)
  112 FORMAT(10I5)
  71 I=0
  30 I=I+1
  READ(5,FIN)DATE(I),NX(I),(Y(I,J),J=1,NY),LL
  IF(LL.EQ.0.OR.LL.EQ.9) GO TO 32
  GO TO 30
  32 N=I-1
  IF (N.LE.0) GO TO 1
  SCXX=10./SCXX
  DO 22 I=1,N
  IIX(I)=SCXX*(NX(I)-NMIN)+2.5
  IF(IIX(I).GT.121)IIX(I)=121
  IF(IIX(I).LT.1)IIX(I)=1
  22 CONTINUE
  DO 4 J=1,NY
  4 NMIS(J)=0.
  ND(I)=NMIN
  DO 41 I=2,12
  41 ND(I)=ND(I-1)+SCXX+.5
  DO 70 J=1,NY
  IF(ITEST(J).EQ.0)GO TO 78
  DO 77 I=1,N
  IF(Y(I,J).LE.0.)GO TO 77
  Y(I,J)=ALOG10(Y(I,J))
  77 CONTINUE
  78 YMAX=Y(I,J)
  DO 10 I=2,N
  IF(Y(I,J).GT.YMAX)YMAX=Y(I,J)
  10 CONTINUE
  S=(YMAX-YMIN(J))/9.
  I=1
  IF (S.LE.1)GO TO 75
  ISI=NYL(J)
  DO 66 I=ISI,10000,ISI
  IF (S.LE.I)GO TO 75
  66 CONTINUE
  75 S=I
  SCLY = 6.0/S
  IF(NMP.NE.0)GO TO 21
  B(1)=YMIN(J)
  DO 20 JI=7,55,6
  20 B(JI)=B(JI-6)+S
  21 DO 15 I=1,N
  IYY(I,J)=SCLY*(Y(I,J)-YMIN(J))+1.5
  IF(IYY(I,J).GT.55)IYY(I,J)=55
  IF(IYY(I,J).LT.1)IYY(I,J)=1
  IX=IIX(I)
  IY=IYY(I,J)
  AO(I,J)=A(IX,IY)
  Z=SIGN(Z,Y(I,J))
  IF(Z)13,14,14
  13 NMIS(J)=NMIS(J)+1
  Y(I,J)=I0.E+20
  GO TO 15
  14 A(IX,IY)=PT(J)
  15 CONTINUE
  IF(NMP.NE.0)GO TO 68
  WRITE(6,101) STA,YEAR,VAR(J),IS(J),SCXX,N,NMIS(J)
  101 FORMAT(1H17HDATA FOR STATION ,A6,2H ,A6,2H ,A6,2X10HONE INCH =,
  114,7H UNITS,16H TIME ONE INCH =,F5.1,5H DAYS,5X6HNOBS =,I5,
  22X6HNMIS =I5)
  DO 85 L=1,55
  IF(B(56-L).EQ.BLANK) GO TO 81
  80 WRITE(6,103)B(56-L),(A(I,56-L),I=1,121)
  GO TO 85
  81 WRITE(6,104)(A(I,56-L),I=1,121)
  85 CONTINUE
  103 FORMAT(1X,F4.0,121(A1))
  WRITE(6,104)(A(I,56),I=1,121)
  104 FORMAT(5X,121A1)
  WRITE(6,108)(ND(I),I=1,12)
  108 FORMAT(1H ,3X,12(I4,6X))
  DO 67 I=1,N
  IX=IIX(I)
  IY=IYY(I,J)
  67 A(IX,IY)=AO(I,J)
  IF(LP.EQ.0)GO TO 70
  IF(J.EQ.NY)GO TO 69
  GO TO 70
  68 IF(J.NE.NY)GO TO 70
  69 WRITE(6,115)STA,YEAR,SCXX,N
  115 FORMAT(32HMULTIPLE PLOT DATA FOR STATION ,A6,8H, YEAR ,A4,17H, TIM
  1E ONE INCH =,F5.1,6H DAYS,2X6HNOBS =,I5)
  WRITE(6,116)(VAR(K),K=1,NY)
  116 FORMAT(9HOVARIABLE,10(4XA6))
  WRITE(6,117)(PT(K),K=1,NY)
  117 FORMAT(11H PLOT CHAR 5XA1,9(9XA1))
  WRITE(6,FMT)ORIG,NMIN,(YMIN(K),K=1,NY)
  WRITE(6,120)(IS(K),K=1,NY)
  120 FORMAT(11H UNITS/INCH,6,9I10)
  WRITE(6,121)(NMIS(K),K=1,NY)
  121 FORMAT(11H NO MISSING,I6,9I10)
  DO 86 I=1,N
  86 WRITE(6,FMT)DATE(I),NX(I),(Y(I,K),K=1,NY)
  IF(NMP.EQ.0)GO TO 70
  WRITE(6,119)STA,YEAR,(VAR(I),PT(I),I=1,NY)
  119 FORMAT(8H1STATION,A6,A6,10(1XA6,1XA2))
  DO 90 L=55,1,-1
  90 WRITE(6,104)(A(I,L),I=1,121)
  WRITE(6,104)(A(I,56),I=1,121)
  WRITE(6,108)(ND(I),I=1,12)
  DO 91 I=1,N
  DO 91 K=NY,1,-1
  IX=IIX(I)
  IY=IYY(I,K)
  91 A(IX,IY)=AO(I,K)
  70 CONTINUE
  GO TO 1
  END

```

Input Data for Sample Problem

```

WN XQT PRTPLT
S1271966 0 1 .33333333 0
o(7XA6,I3,4XF5.1,5XF4.0,5XF6.1,F4.1,F6.1,E5.0,19XI1)
(1XA6,I4,F10.2,F10.0,F10.1,F10.0,F10.1,5F10.5)
DO .0 COND*0 TEMPX0 B0000 FLOWGOLG COLC1
  2 5 2 1 5 1
  S127 0603661540915 85 9630408 0325 1300028
  S127 0616661671345 84 10550344 0340 1800013 900E2
  S127 0623661741130 75 8870638 0330 1500021 162E3
  S127 0630661811115 84 10340515 0325 1 00014 240150E3
  S127 0707661881100 86 10170613 0330 1500011 240168E3
  S127 0714661951100 85 10470620 0310 1700010 260140E3
  S127 0721662021115 85 10470580 0320 1700002 250282E3
  S127 0728662091105 81 9980640 0290 1700015 230100E1
  S127 0804662161200 81 998 548 330 170 08 260240E2
  S127 0811662231100 85 1026 559 320 160 11 220157E3
  S127 0818662301145 75 905 275 310 160 23 270780E2
  S127 0825662370905 80 906 305 330 130 20 250160E3
  S127 0901662440900 67 776 245 300 14 05 270120E3
  S127 0908662511015 78 922 310 320 150 08 230980E3
  S127 0915662580930 84 910 325 320 110 23 310140E3
  S127 0922662650925 89 1008 618 320 130 32 280460E3
  S127 0927662701020 88 975 640 310 120 30 2801 5E4
  S127 1004662771155 94 1042 590 300 120 20 290135E3
  S127 1011662841205 99 1073 650 285 110 200420E3
  S1271966 1 1 .33333333 0
  S127 1025662981215 96 1017 580 280 100 13 220890E2
  S127 1101663051230 95 1006 580 320 100 17 200200E2
  S127 1108663121220 103 1040 600 300 80 25 240720E2
  S127 1115663191230 113 1197 610 310 100 21 200178E3
  S127 1129663331220 96 993 610 370 90 200
  S127 1206663401220 590 305 80 16 270850E3
  S127 1214663481115 95 936 570 300 70 220
  S127 1219663530915 94 880 570 310 50 06 500700E2

```

Group I - Control specs for data that follows

Subgroup C - Data for first plot

Subgroup A - Specs for control options - next Batch

Subgroup B - Control specs for data that follows

Subgroup C - Data for next plot

Subgroup A - Same as above

Figure C-11. Program listing of PRTPLT and input data set-up of run.

Table C-3. Input data cards for program PRTPLT.

Group	Card	Column	Name	Format	Description		
I	1	1-6	STA	A6	Six character mnemonic symbol identifying the station (i.e. S12.7)		
		7-10	YEAR	A4	Four character mnemonic symbol identifying the X axis data (or time period) (a) year data was taken (i.e. 1966), or (b) write DIST here if Fig. C-5 is the desired form of output.		
		11-15	NMP	I5	Option specification: If zero plot one Y variable against the X variable If 1 plot all Y variables (the Y array) against the X variable		
		16-20	LP	I5	List option when NMP = 0 If zero suppress listing of data If \neq zero list the input data		
		21-30	SCLX	F10.0	Scale factor for the X variable. The X data are plotted in increments of 10/SCLX units per inch.		
	2	31-40	NMIN	I10	Specification of the origin for the X axis.		
			1-2	NY	I2	Number of separate Y variables to be plotted, $1 \leq NY \leq 10$.	
		3	3-80	FIN	13A6	Format of the input data which must provide for reading DATE (I), NX(I), (Y(I,J), J=1, NY) and LL in that order. LL is a control variable, read on every data card—where I is the sequence of data to be read in for a given variable, NX is (a) the day of year, or (b) distance, depending upon whether Fig. C-5 or Fig. C-6 type of plot is desired.	
			1-80	FMT	(13A6,A2)	Format specification for the output list. It must provide for printing DATE(I),NX(I),(Y(I,K), K=1,NY) in that order.	
			4	1-6	VAR(1)	A6	Label for the first Y variable
				7	PT(1)	A1	Plotting character for VAR(1)
				8	ITEST(1)	I1	Log ₁₀ transformation option for the first Y variable. If zero, no transformation is made. If 1, a log ₁₀ transformation is made.
			5	9-14	VAR(2)	A6	Same as above, but
	15	PT(2)		A1	for the second Y		
	16	ITEST(2)		I7	variable		
17-80	VAR(I)	A6		—and so on as for			
	PT(I)	A1		first and second Y			
	ITEST(I)	I1		variables, until I=NY			
1-8	YMIN(1)	F8.0		Origin for first Y variable.			
9-80			Provide the rest of the YMIN vector in the same format as YMIN(1).				

Table C-3. Continued.

Group	Card	Column	Name	Format	Description
	6	1-5	NYL(1)	I5	Incrementing index for scaling the first Y variable.
		6-10	NYL(2)	I5	Incrementing index for scaling the second Y variable.
		11-50	NYL(I)	I5	—and so on for as for first and second NYL variables, until I=NY
IIA	See Fig. C-12	80			0 or 9 punch; if punch is 0, subgroup IIB consists one card, I-1; if punch is 9, subgroup IIB consists of cards I-1 to I-6 to control the plots for the next data set.
IIB	See Fig. C-12				same as control card I-1
IIC	See Fig. C-12				(a) Data to be plotted by time for a given station, arranged in any date order for a given station; cards III-5 and III-6, Table C-1 may be used if desired if card I-2 above specifies a format to read up to any NY variables on these cards. (b) If data are to be plotted by station for a given date, then group IIIC cards are arranged by station for a given date. The LL control variable must appear on every data card.

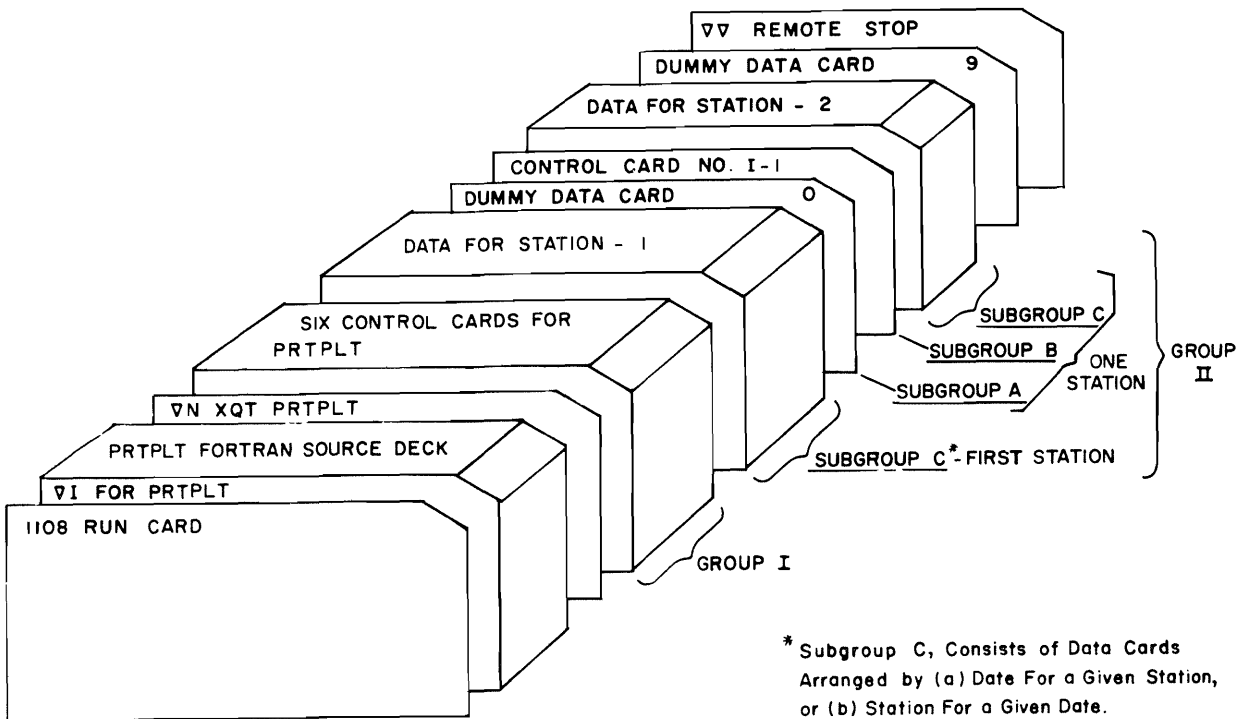


Figure C-12. Deck set-up for PRTPLT data input.

APPENDIX D

FOURIER SERIES CURVE FITTING

Many natural phenomena characteristically display cyclic patterns of variation, primarily in response to seasonal and diurnal influences. Water temperature and dissolved oxygen concentration, are excellent examples of such cyclic variables.

A Fourier series of the general form

$$Y_i = a + \sum_{j=1}^n p_j \cdot \sin\left(\frac{2\pi \cdot j}{L} \cdot X_i\right) + \sum_{j=1}^n q_j \cdot \cos\left(\frac{2\pi \cdot j}{L} \cdot X_i\right) + \epsilon_i \quad (D-1)$$

is well suited to the representation of cyclic phenomena. In this equation,

- Y_i = "i th" observed value of the dependent variable
- X_i = "i th" value of the cyclic independent variable (time)
- L = cyclic period in the independent variable
- n = number of terms in the Fourier series model
- ϵ_i = deviation of the "i th" observed value of the dependent variable from the predicted value
- p_j and q_j = regression coefficients

This equation is linear in form, if each trigonometric term is considered a coded variable. In this form, linear regression techniques may be employed in fitting the equation to data.

Equation D-1 can be shown to be equivalent to

$$Y_i = a + \sum_{j=1}^n C_j \cdot \sin\left(\frac{2\pi \cdot j}{L} \cdot X_i + A_j\right) + \epsilon_i \quad (D-2)$$

in which

$$A_j = \tan^{-1}\left(\frac{p_j}{q_j}\right) = \text{phase shift angle for the "j th" term (radians)}$$

$$C_j = \frac{p_j}{\sin A_j} = \text{coefficient of the "j th" term}$$

Equation D-1 is rearranged in the form of Equation D-2 to allow greater ease of visualization and to reduce the number of terms. Figure D-1 graphically displays the physical significance of the model parameters C_1 , C_2 , A_1 , and A_2 for a two-term Fourier series model.

For the special case where $n = 1$, Equation D-2 reduces to a sine-curve. Both single and multiple term Fourier series have been used extensively in this study to represent time variations in cyclic water quality parameters.

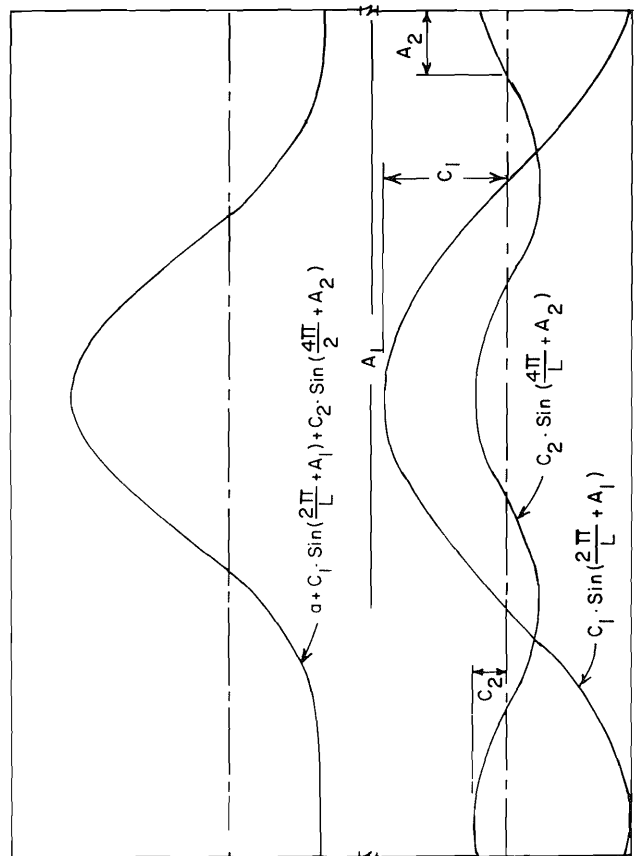


Figure D-1. Graphical representation of a two-term Fourier series.

APPENDIX E

OPERATION OF THE WATER QUALITY SIMULATION MODEL

The water quality simulation model has been developed as a tool, to be used in studying problems of water resources planning and management, as they relate to water quality. The following sections explain procedures involved in using the computer program WAQUAL which is comprised of the individual water quality submodels. Specific instructions for using the program include a discussion of the computational facilities required, directions for specifying simulation options and a description of the data deck requirements.

The Program

Figure E-1 is a listing of the computer program WAQUAL which is the integrated water quality simulation model. This program consists of algorithms for five submodels, listed in Table E-1; the subprogram names, given to each of these submodel algorithms, are also listed. Figure E-1, the WAQUAL program listing, plainly marks each subprogram. The "prior simulation requirements" column lists the subprograms that must be run prior to the one indicated in order to provide the necessary input information to the subprogram in question. The hydrology submodel HYDRO is an independent program described in Appendix G. The output from HYDRO is fed into WAQUAL in the form of punched cards. This independence is not necessary; it is merely the mode of operation found most convenient during development. The "system model" term connotes HYDRO as a subprogram to WAQUAL, even though they are physically separate program decks.

The program WAQUAL will:

- (1) simulate, for the main channel and selected branches, the distance profiles for each month of the year for:
 - (a) mean monthly specific electrical conductance
 - (b) mean monthly stream temperature
 - (c) mean monthly dissolved oxygen

- (2) simulate for the main channel and selected branches, the representative monthly diurnal profiles at selected system node points:
 - (a) hourly temperatures over the 24 hour period
 - (b) hourly values of dissolved oxygen over the 24 hour period

A sample of the computer printout is shown in Figure E-3. The stream profiles displayed graphically in Appendix F were plotted from such printout information. The printout, in addition to providing the simulation information from WAQUAL also provides the D.O. simulation in the "percent saturation" form and also repeats information used as input.

Instructions for using this program and further explanations are given in the following sections. These instructions include: (a) discussion of the computer facility required, (b) directions for specifying WAQUAL program options, and (c) definitions of input variables and format specification for each variable.

Computer Requirements

WAQUAL has been programmed in Fortran V for the Univac 1108 electronic digital computer; Figure E-1 is a listing of the program. WAQUAL is dimensioned to handle four branches adjacent to the main stem, with 15 reaches for each branch, and five reservoirs and five effluent discharges. Table E-2 summarizes this capability, which of course can be changed to suit any situation by merely altering the corresponding dimension statements.

Dimensioned in the manner indicated, the program requires approximately 20,000 thirty-two-bit words of memory storage. Complete running time of the 1108 for a one year simulation of the 11 reach Little Bear River system is 28 seconds (14 seconds compilation and 14

Table E-1. WAQUAL subprograms.

Submodel	Subprogram Name	Prior Simulation Requirements
Conductivity	ELCON	HYDRO
Monthly temperature	WATEMP	HYDRO
Diurnal temperature	DITEMP	HYDRO,WATEMP
Monthly D.O.	MDISOX	HYDRO,WATEMP
Diurnal D.O.	DDISOX	HYDRO,WATEMP,DITEMP

Table E-2. Summary of simulation model dimensions.

System component	Number
branches	5 ^a
reaches per branch	15
reservoirs	5
M & I discharges	5
control points	5

^a Including the main stem.

seconds execution). The program is in punched-card form and utilizes punched-card data. Tape storage has not been used.

Without the program list option, the output for a one year simulation run, calling for all five water quality subprograms may be as little as 55 pages or as much as 130 pages, depending on the number of reaches being simulated.

Program Options

The program user has the option of specifying the incorporation or exclusion of any of the five subprograms listed in Table E-1. The electrical conductance and monthly water temperature subprograms may be included or deleted entirely at the discretion of the program user, except when prerequisite to another specified model, as indicated in Table E-1. The procedure for entering model option specifications on punched cards is detailed in Table E-3.

Data Requirements

Data are supplied to the water quality simulation program in punched-card form. Details concerning card formats, variable names, etc., are in Table E-3. The data required may be divided into eight groups. These groups will be discussed in order of their appearance in the data deck.

System definition

The program user must specify the number of branches in the river system being simulated, number of years to be simulated, number of control points, number of reservoirs, number of municipal and industrial waste discharges, mean altitude of the prototype system, model option indicators and location of tributaries, division points between reaches, control points, reservoirs, and waste discharge points.

A convenient coding system has been derived to specify the location of any point on the river system, in

terms of the branch on which it is situated and river miles from the mouth of that branch. The format of the location designation is b.xxx. Where "b" is the number of the branch on which the point is situated and "xxx" is the distance from the mouth of the branch in tenths of a mile. For example, the designation 2.062 means that the point is located 6.2 miles from the mouth of branch two.

The serial specification of the months of the simulation year are required for labeling purposes. In the current study the water year, beginning with October first, has been used as the simulation year.

Equilibrium temperature

Here, a constant and coefficient are provided for Equation 19, to define monthly variations in equilibrium stream temperature at every node point in the system. If the monthly water temperature submodel is not a specified option these cards may be omitted.

Diurnal temperature and D.O. model parameters

Next, each of the four parameters (C_1 , A_1 , C_2 , and A_2) for the two-term Fourier series diurnal temperature index submodel (Equation 25) is given for each month of the simulation. Twelve monthly values of each DTI model parameter are entered on one card. The four cards are arranged in the order indicated above. This is followed by the parameters for the diurnal dissolved oxygen index model (Equation 53) for each month. If either or both of the diurnal models are excluded from the simulation, the parameter cards pertaining to that model may be omitted.

Hydraulic relationships

Multipliers and exponents for Equation 8 are provided here to define the relationships between flow rate and cross sectional area of flow. Coefficients and exponents must also be provided for the exponential relationship similar to Equation 8 for mean depth of flow.

Monthly water quality submodel parameters

Each of the water quality submodels requires a reach-by-reach definition of input and transport parameters. The data to be read in consists of submodel parameters for conductivity, monthly temperature, monthly BOD, and monthly D.O., in that order, for every reach in the system. The input format calls for reading the cards in sets, beginning with the first set, corresponding to lowest reach on the main stem, proceeding to the highest reach on the main stem, then from the lowest reach on the lowest tributary branch in the system to the most upstream reach on that branch, followed by the lowest reach on the next tributary upstream, etc., finally ending with the highest reach on the most upstream tributary of the hydrologic system. Each set consists of four cards, completely defining the input and in-transit models for that

reach. The data input requirements for a typical river reach are discussed individually below.

Electrical conductance. Because electrical conductance is essentially a conservative quality parameter, it is necessary only to define input model parameters. The natural surface inflow model requires a multiplier, a , and an exponent, b , relating conductivity to rate of flow, in accordance with Equation 11. Groundwater conductance is assumed constant over time for any given reach. This conductance is read in here. A two-term Fourier series representation has been provided for the simulation of conductivity of surface irrigation return flows. The mean annual conductance, multipliers, C , and phase shifts, A , are included at this point in the data deck for each reach. If the conductivity model is not called, the above data are omitted.

Temperature. Natural surface inflow temperatures are related to mean monthly atmospheric temperature by Equation 19. The constant and coefficient for this relationship must be provided via data input.

Monthly groundwater inflow temperatures are simulated by Equation 18, which is a simple sine-curve representation of the annual cycle of groundwater temperature. This equation requires the mean annual temperature ($^{\circ}\text{C}$), a multiplier, C , and a phase angle shift, A (radians).

The temperature of surface irrigation return flow is assumed to be related to mean monthly atmospheric temperature (Equation 19). Again, the constant and multiplier are provided as data input. The heat exchange coefficient has been assumed to be related exponentially to the rate of combined inflow to the reach (Equation 21). A multiplier and an exponent are required for each reach.

None of the temperature information is to be included if the monthly water temperature model is not incorporated in the simulation.

BOD and D.O. In simulating BOD and dissolved oxygen changes in a reach, the first step is to approximate the BOD and D.O. concentration and deoxygenation rate constant for each component of inflow. The BOD of natural surface inflows are represented in Equation 50 as simple sine-curve. Each characteristic element of this relationship (BOD , C , and A) must be defined. The deoxygenation rate constant ($\text{base } 10, \text{ day}^{-1}$), given at this deck location, is assumed to be constant throughout the year. BOD of surface irrigation return flows and groundwater inflows and the deoxygenation rate constant for these components are assumed constant through the year and are simply read in as mean annual values. Provision is made in the program for decreasing the deoxygenation

rate constant of Equation 32 as organic material stabilization proceeds. The amount of decrementation in deoxygenation rate constant within the reach ($\text{base } 10, \text{ day}^{-1}$) must be specified.

Other BOD information required for Equation 32 is: scour rate constant (mg/l/day) deposition rate constant ($\text{base } 10, \text{ day}^{-1}$) for organics, difference between laboratory and river deoxygenation rate constants ($\text{base } 10, \text{ day}^{-1}$), anaerobic decay rate constant for benthic deposits ($\text{base } 10, \text{ day}^{-1}$), and areal BOD of stream bottom deposits (gm/sq. meter). It should be emphasized, here, that Equation 32 has been programmed on the computer using base 10, rather than base e exponents.

Annual cycles in dissolved oxygen concentrations of natural surface inflow and irrigation return are simulated by a two-term Fourier series (Equation 49). Again, mean annual values, multipliers, C , and phase shifts, A , must be provided for each of these models. A sine-curve model, similar to Equation 49, simulates D.O. concentrations in groundwater inflow, requiring mean annual temperature, a coefficient, C , and phase shift, A , as input. All of these data are omitted if the monthly D.O. modeling option is not specified.

Finally, for the case where diurnal variations are to be simulated, an average productivity constant (pf in Equation 55) is entered for each month of the year. These factors are determined by a process of trial and error during model development in which diurnal D.O. model results are altered by changing pf until a satisfactory approximation of the observed annual pattern for diurnal stream D.O. is obtained.

Reservoir data

If reservoirs are included in the hydrologic system to be simulated, the following modeling data must be obtained, beginning with the most downstream reservoir on the main stem and ending with the most upstream reservoir on the highest tributary stream:

1. Conductivity of water in storage at the beginning of the simulation
2. Volume of water in storage at the beginning of the simulation (acre-feet)
3. Reservoir storage capacity (acre-feet)
4. Mean annual temperature ($^{\circ}\text{C}$), coefficients, C , and phase shifts, A , for a four-term Fourier series representation of the annual discharge temperature cycle ($^{\circ}\text{C}$)
5. Mean annual BOD (mg/l), coefficient, C , and phase shift, A , for sine-curve representation (Equation 50) of the annual cycle in BOD of the reservoir discharge stream
6. Mean annual D.O. (mg/l), coefficient, C , and phase shift, A , for sine-curve representation (Equation 51) of the annual cycle in discharge stream dissolved oxygen concentration

If any monthly water quality submodel is not included in the simulation, reservoir data relating to that submodel may be entered on the data card as zeroes.

Atmospheric temperature

If monthly stream temperatures are to be simulated, mean monthly atmospheric temperatures (F) must be provided for each month of the year.

Monthly data

For every month of simulation a quantitative and qualitative description of each municipal-industrial waste discharge must be provided as an input to the simulation program. The water quality simulation model employs the results of a reach-by-reach hydrologic simulation model, in punched card form, to define the hydrologic inputs to the system.

The data input format calls for all municipal and industrial (M & I) waste discharge data for any given month to precede the system hydrologic data for that month. The data required in each of these categories are discussed briefly in the following paragraphs.

Municipal and industrial waste discharges. Monthly definition of M & I waste discharge flow and quality characteristics consists of the following:

1. Mean monthly rate of discharge (cfs)
2. Mean monthly conductivity of the waste stream (micro-mhos/cm)
3. Mean monthly waste stream temperature (°C)
4. Mean monthly waste stream D.O. concentration (mg/l)
5. Mean monthly waste stream BOD (mg/l)
6. Deoxygenation rate constant (base 10, day⁻¹)
7. Hourly diurnal discharge indexes
8. Hourly diurnal temperature indexes
9. Hourly diurnal D.O. indexes
10. Hourly diurnal BOD indexes

If any of the monthly quality submodels are not to be included in the simulation, the parameters relating to this submodel may be punched as zeroes. If any of the diurnal submodels are to be excluded from the simulation, the associated hourly diurnal index card should be omitted. This information must be provided for all effluent discharge points in the system prior to the hydrologic data.

Hydrologic data. Monthly hydrologic data consists of a reach-by-reach tabulation of natural surface inflow (cfs), surface irrigation return flow (cfs), groundwater inflow (cfs) and diversions (cfs). For reaches representing surface impoundments, the above data are supplemented by net direct precipitation (cfs), reservoir storage at the end of the month (acre-feet), and reservoir depth above the discharge inlet (ft.). Net direct precipitation is defined as precipitation falling directly on the water surface less evaporation loss.

As shown in Table E-3, hydrologic data for one reach is presented on a single card. The hydrologic data must be assembled in the order of reach simulation, that is, beginning with the most upstream reach on the main stem and proceeding downstream to the point of confluence with the most upstream tributary, shifting to the upper end of that branch, proceeding to the reach ending at its mouth, then shifting to the main stem reach to which that branch is tributary and proceeding on downstream until the next tributary branch is encountered or until the last reach on the main stem has been simulated.

The hydrologic data input is provided on punched cards generated by the hydrology submodel. The hydrologic data must be integrated into the data deck for the water quality simulation in the manner described above. Figure E-2 is a listing of the data deck, as it was assembled for a one month (October, 1968) simulation of the Little Bear River system.

Table E-3. WAQUAL simulation model data deck set-up.

Card	Col	Format	Variable Name	Definition	Remarks
1	1-5	I5	NBR	No. of branches in the system	not more than 5
	6-10	I5	NYR	No. of years to be simulated	
	11-15	I5	NCPTS	No. of control points designated	not more than 5
	16-20	I5	NRES	No. of reservoirs	not more than 5
	21-25	I5	NEF	No. of M & I effluent discharges	not more than 5
	26-30	I5	ALT	Mean altitude of the hydrologic system	
	31-35	I5	IV	Conductivity model option indicator	0 = No; 1 = Yes
	36-40	I5	IW	Monthly D.O. model option indicator	0 = No; 1 = Yes
	41-45	I5	IX	Diurnal D.O. model option indicator	0 = No; 1 = Yes
	46-50	I5	IY	Monthly water temperature model option indicator	0 = No; 1 = Yes
2	51-55	I5	IZ	Diurnal water temperature model option indicator	0 = No; 1 = Yes
	1-4	I4	NBRCH(J)	No. of beginning reach on branch "J"	repeat for J=1 through NBR on this one card
	5-8	I4	NLRCH(J)	No. of last reach on branch "J"	
	9-12	I4	NTRCH(J)	No. of main stem reach to which branch "J" is tributary (0 for J=1)	
3	1-80	15F5.3	RCLOC(I,J)	Location of downstream end of reach "I" and upstream end of uppermost reach	All reaches on one branch on one card: As many cards as there are branches
4	1-25	5F5.3	CPTLOC(IC)	Location of control points "IC" ^a	IC=1 to NCPTS
5	1-25	5F5.3	RESLOC(IR)	Location of reservoir "IR" ^a	IR=1 to NRES; Omits of NRES=0
6	1-25	5F5.3	EFLOC(IE)	Location of effluent discharge point "E" ^a	IE=1 to NEF
7	1-72	12A6	AMO(K)	Abbreviation of month no. "K"	K=1 to 12
8	1-80	16F5.1	ATEQ(I,J,1)	Equilibrium temperature constant	one pair for both ends of every reach. One set of cards for each branch. Omit if IY=0
9	1-80	16F5.3	ATEQ(I,J,2)	Equilibrium temperature coefficient	
10	1-72	12F6.3	AD(K,1)	Diurnal temperature index model parameter for each month	omit 10-13 if IZ=0
11	1-72	12F6.3	AD(K,2)		
12	1-72	12F6.3	AD(K,3)		
13	1-72	12F6.3	AD(K,4)		

Table E-3. Continued.

Card	Col	Format	Variable Name	Definition	Remarks
14	1-72	12F6.3	ADO(K,1)	Diurnal dissolved oxygen index model parameters for each month	omit 14-16 if IX=0
15	1-72	12F6.3	ADO(K,2)		
16	1-72	12F6.3	ADO(K,3)		
17	1-72	12F6.3	ADO(K,4)		
18	1-5	F5.1	RH(J)	Mean depth multiplier ^b	
	6-10	F5.1	PH(J)	Mean depth exponent	
	11-15	F5.1	RA(J)	Area of flow section multiplier	
	16-20	F5.1	PA(J)	Area of flow section exponent	
19	1-5	F5.0	AECS(I,J,1)	Surface inflow conductivity constant ^b	omit 19 if IV=0
	6-10	F5.3	AECS(I,J,2)	Surface inflow conductivity exponent	
	11-15	F5.0	AECGI(I,J)	Groundwater conductivity (μ mhos/cm)	
	16-20	F5.0	AECIR(I,J,1)	Mean annual irrigation flow conductance	
	21-25	F5.0	AECIR(I,J,2)	First term irrig. return flow conductivity coefficient	
	26-35	F10.8	AECIR(I,J,3)	First term irrig. return flow conductivity phase shift	
	36-40	F5.0	AECIR(I,J,4)	Second term irrig. return flow conductivity coefficient	
41-50	F10.8	AECIR(I,J,5)	Second term irrig. return flow conductivity phase shift		
20	1-5	F5.1	ATS(I,J,1)	Surface inflow temperature constant ^b	omit 20 if IY=0
	6-10	F5.3	ATS(I,J,2)	Surface inflow temperature coefficient	
	11-15	F5.1	ATGI(I,J,1)	Groundwater temperature constant	
	16-20	F5.1	ATGI(I,J,2)	Groundwater temperature coefficient	
	21-30	F10.8	ATGI(I,J,3)	Groundwater temperature phase shift	
	31-35	F5.1	ATIR(I,J,1)	Irrigation return flow temperature constant	
	36-40	F5.3	ATIR(I,J,2)	Irrigation return flow temperature coefficient	
	41-45	F5.1	RK(I,J)	Heat exchange coefficient multiplier	
46-50	F5.1	PK(I,J)	Heat exchange coefficient exponent		
21	1-5	F5.1	ABODS(I,J,1)	Surface inflow mean annual ultimate BOD ^b	omit 21 if IW=0
	6-10	F5.1	ABODS(I,J,2)	Surface inflow ultimate BOD coefficient	
	11-15	F5.3	ABODS(I,J,3)	Surface inflow ultimate BOD phase shift	
	16-20	F5.2	R1S(I,J)	Surface inflow deoxygenation rate constant (base 10)	
	21-25	F5.1	BODIR(I,J)	Irrigation return flow ultimate BOD	
	26-30	F5.2	R1IR(I,J)	Irrigation return flow deoxygenation rate constant (base 10)	
	31-35	F5.1	BODGI(I,J)	Groundwater ultimate BOD	
	36-40	F5.2	R1GI(I,J)	Groundwater deoxygenation rate constant (base 10)	
	41-45	F5.2	R1B(I,J)	Deoxygenation rate decrement (base 10)	
	46-50	F5.2	RP(I,J)	Scour rate constant	
51-55	F5.2	R3(I,J)	Deposition rate constant for organics		
56-60	F5.2	RR(I,J)	Difference between lab and river deoxygenation rate constants (base 10)		

Table E-3. Continued.

Card	Col	Format	Variable Name	Definition	Remarks
	61-65	F5.4	R4(I,J)	Anaerobic decay rate constant for benthic deposits	
	66-70	F5.1	BBOD(I,J)	Areal BOD of stream bottom (mg/sq.m.)	
22	1-5	F5.1	ADOS(I,J,1)	Surface inflow mean annual D.O. (mg/l) ^b	
	6-10	F5.3	ADOS(I,J,2)	Surface inflow first term D.O. coefficient	
	11-15	F5.3	ADOS(I,J,3)	Surface inflow first term D.O. phase shift	
	16-20	F5.3	ADOS(I,J,4)	Surface inflow second term D.O. coefficient	
	21-25	F5.3	ADOS(I,J,5)	Surface inflow second term D.O. phase shift	
	26-30	F5.1	ADOIR(I,J,1)	Irrigation return flow mean annual D.O.	
	31-35	F5.3	ADOIR(I,J,2)	Irrigation return flow first term D.O. coefficient	
	36-40	F5.3	ADOIR(I,J,3)	Irrigation return flow first term D.O. phase shift	
	41-45	F5.3	ADOIR(I,J,4)	Irrigation return flow second term D.O. coefficient	omit 22 if IW=0
	46-50	F5.3	ADOIR(I,J,5)	Irrigation return flow second term D.O. phase shift	
	51-55	F5.1	ADOGI(I,J,1)	Groundwater mean annual D.O. (mg/l)	
	56-60	F5.3	ADOGI(I,J,2)	Groundwater D.O. coefficient	
	61-65	F5.3	ADOGI(I,J,3)	Groundwater D.O. phase shift	
23	1-60	12F5.1	PCON(I,J,K)	Productivity constant for each month ^b	omit 23 if IW=0
24	1-5	F5.0	ECST(IR,1)	Conductivity of water in storage at beginning of simulation	
	6-11	F6.0	VSTI(IR,1)	Volume of water in storage at beginning of simulation (acre-feet)	
	12-17	F6.0	VMAX(IR)	Storage capacity of reservoir (acre-feet)	
	18-22	F5.1	AT(IR,1,1)	Mean annual temperature of reservoir discharge (°C)	
	23-27	F5.1	AT(IR,1,2)	First term coefficient in reservoir discharge temp. model	
	28-32	F5.1	AT(IR,1,3)	Second term coefficient in reservoir discharge temp. model	
	33-37	F5.1	AT(IR,1,4)	Third term coefficient in reservoir discharge temp. model	IR=1 to NRES
	38-42	F5.1	AT(IR,1,5)	Fourth term coefficient in reservoir discharge temp. model	omit if NRES=0
	43-47	F5.3	AT(IR,2,1)	First term phase shift in reservoir discharge temp. model	
	48-52	F5.3	AT(IR,2,2)	Second term phase shift in reservoir discharge temp. model	
	53-57	F5.3	AT(IR,2,3)	Third term phase shift in reservoir discharge temp. model	
	58-62	F5.3	AT(IR,2,4)	Fourth term phase shift in reservoir discharge temp. model	
25	1-5	F5.1	ABDR(IR,1)	Mean annual ultimate BOD of reservoir discharge (mg/l)	
	6-10	F5.1	ABDR(IR,2)	Coefficient in reservoir discharge BOD model	
	11-15	F5.3	ABDR(IR,3)	Phase shift in reservoir discharge BOD model	

Table E-3. Continued.

Card	Col	Format	Variable Name	Definition	Remarks
	16-20	F5.1	ADOR(IR,1)	Mean annual D.O. of reservoir discharge (mg/l)	
	21-25	F5.1	ADOR(IR,2)	Coefficient in reservoir discharge D.O. model	
	26-30	F5.3	ADOR(IR,3)	Phase shift in reservoir discharge D.O. model	
26	1-60	12F5.1	TAIR(K)	Average of mean daily temperatures for each month	omit if IY=0
27	1-5	F5.1	QEF(IE,JF)	Mean monthly discharge rate at effluent point "IEF" (EFS)	
	6-10	F5.1	ECEF(IE,JE)	Mean monthly conductance at effluent point "IEF"	
	11-15	F5.1	TEF(IE,JE)	Mean monthly effluent temp. at effluent point "IEF" (°C)	
	16-20	F5.1	DOEF(IE,JE)	Mean monthly effluent D.O. at effluent point "IEF" (mg/l)	
	21-25	F5.1	BODEF(IE,JE)	Mean monthly effluent BOD at effluent point "IEF" (mg/l)	
	26-30	F5.2	R1EF(IE,JE)	Mean monthly deoxygenation rate constant (day ⁻¹ , base 10)	
28	1-72	24F3.2	QEFI(IEF,MT)	Diurnal discharge index at effluent point "IEF"	IEF=1 to NEF
29	1-72	24F3.2	TEFI(IEF,MT)	Diurnal temperature index at effluent point "IEF"	omit 27-31 if NEF=0 omit 29 if IZ=0
30	1-72	24F3.2	DOEFI(IEF,MT)	Diurnal D.O. index at effluent point "IEF"	omit 30 if IX=0
31	1-72	24F3.2	BODEFI(IEF,MT)	Diurnal BOD index at effluent point "IEF"	omit if IX=0
32	1-5	F5.1	QA(I,J)	Diffuse natural surface inflow (cfs)	
	6-10	F5.1	QIR(I,J)	Irrigation return flows (cfs)	
	11-15	F5.1	QGI(I,J)	Groundwater inflow (cfs)	repeat for all reaches ^c
	16-20	F5.1	QD(I,J)	Diversions (cfs)	
	21-25	F5.1	QEV	Reservoir evaporation (cfs)	cols 21-37
	26-31	F6.0	VST(IR)	Volume of stored water at end of month (acre-feet)	omit cols 21-37 if reach is not a reservoir
	32-37	F6.1	RD(IR)	Depth from reservoir surface to outlet works (feet)	

^aLocation designations are coded so that X.xxx, X is the branch on which the point is located and xx.x is the distance from the mouth of the branch in miles.

^bCard 18 for branch no. 1 (main stem), cards 19 through 23 for every reach on that branch, beginning with the reach nearest the downstream end of the system; card 18 for branch no. 2 cards 19 through 23 for every reach on that branch, starting with the nearest the mouth, etc.

^cStarting with month no. 1 (Oct.) cards 27 through 31 for each effluent discharge point, followed by card no. 32 for each reach in the system, beginning with the highest reach on the main stem, proceeding downstream until a reach with tributary branch is contacted. Next enter card 32 for all reaches on the tributary branch, followed by the card for the reach to which the branch is a tributary, etc. until finally card 32 for the lowest reach on the main stem is the last card for the month.

APPENDIX F

COMPARISON OF OBSERVED AND SIMULATED 1968 WATER QUALITY PROFILES

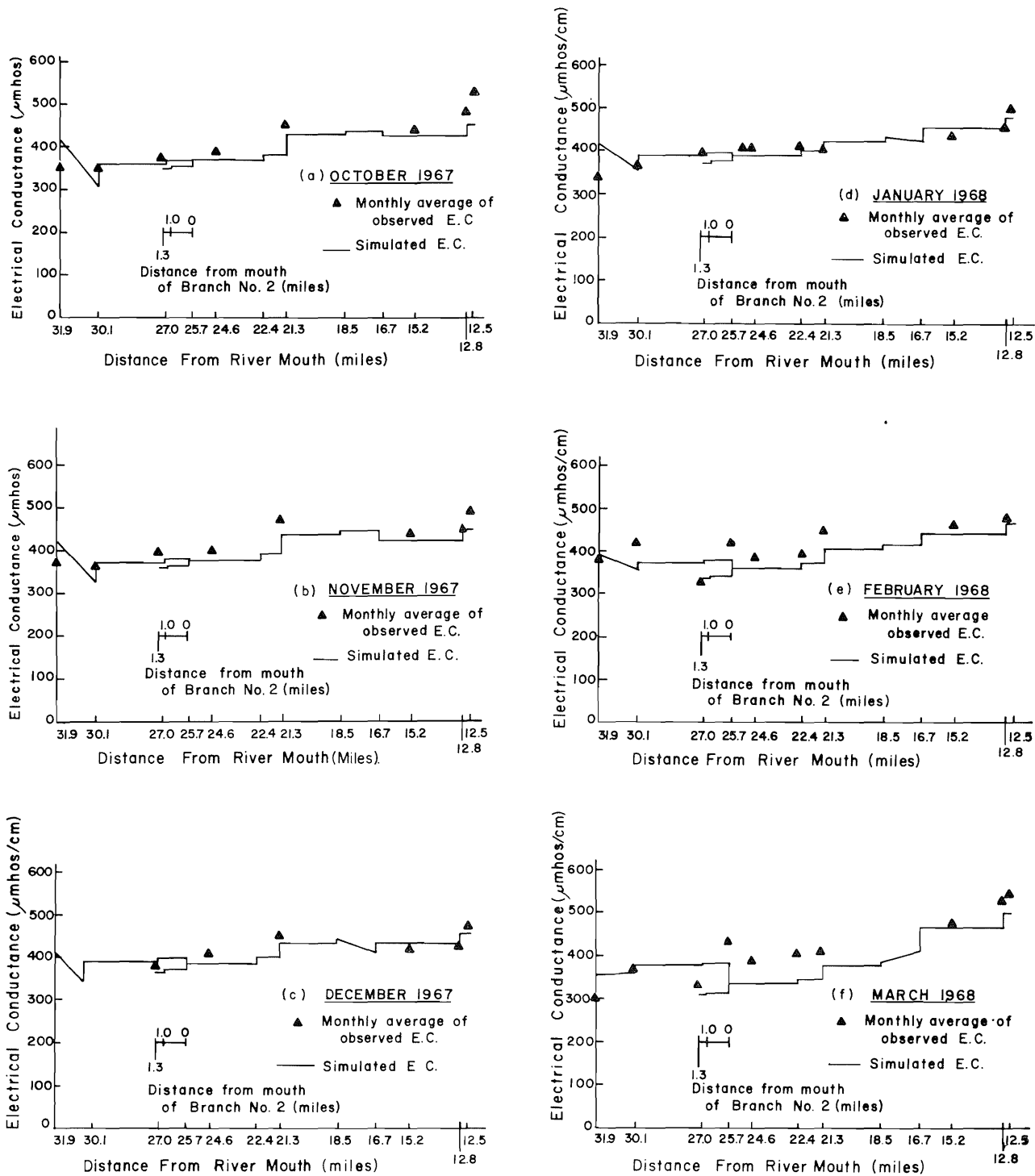


Figure F-1. Comparison of observed and simulated 1968 electrical conductivity profiles.

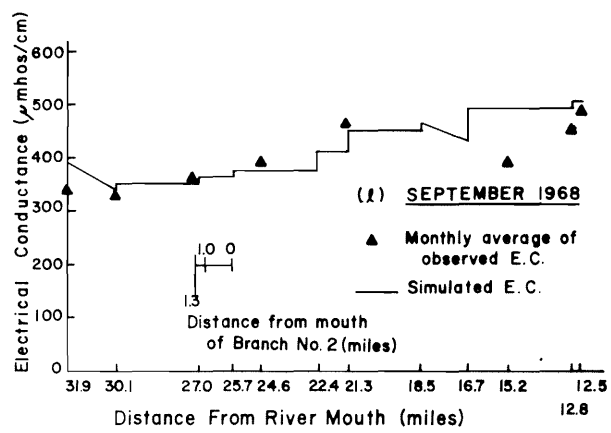
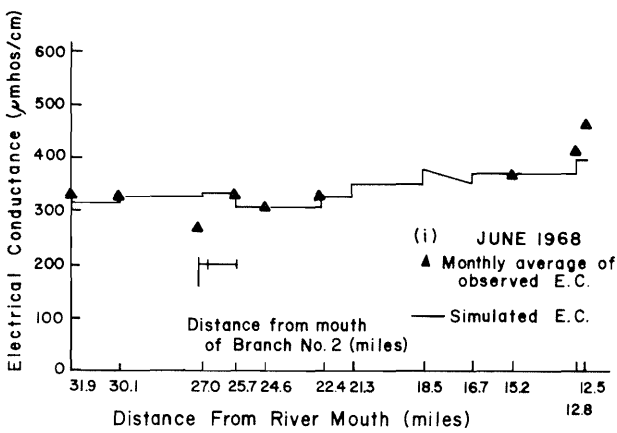
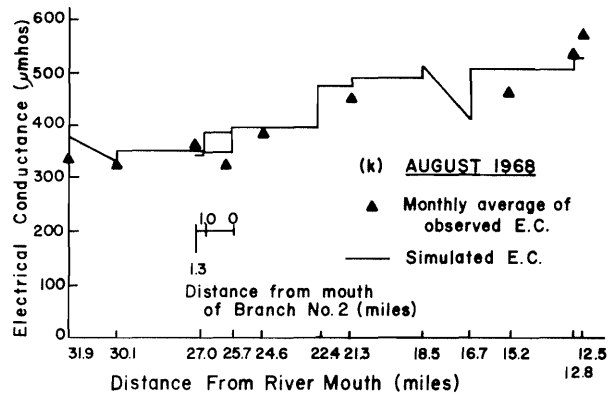
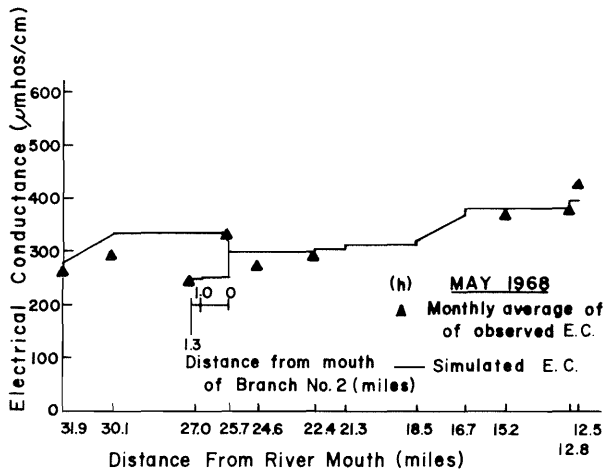
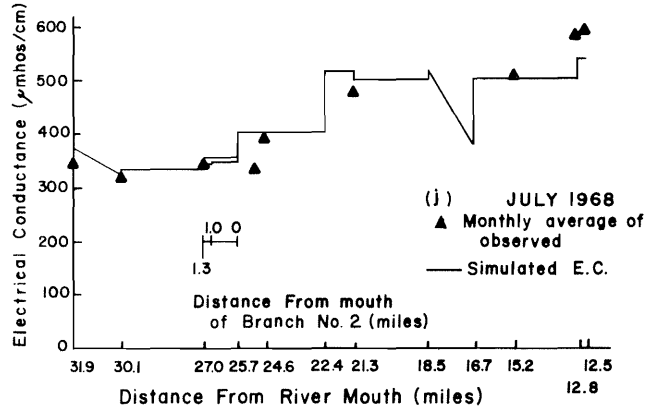
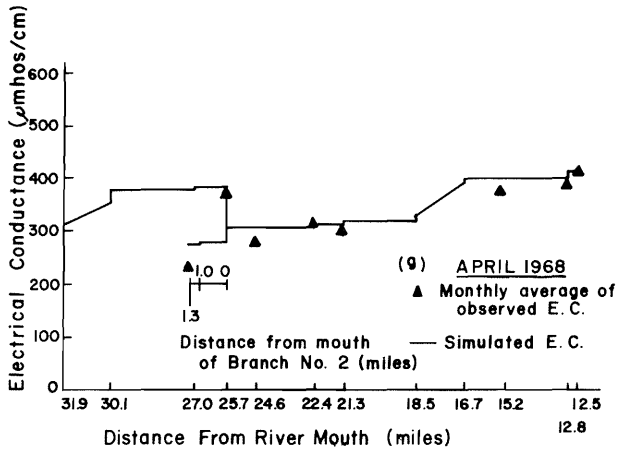


Figure F-1. Continued.

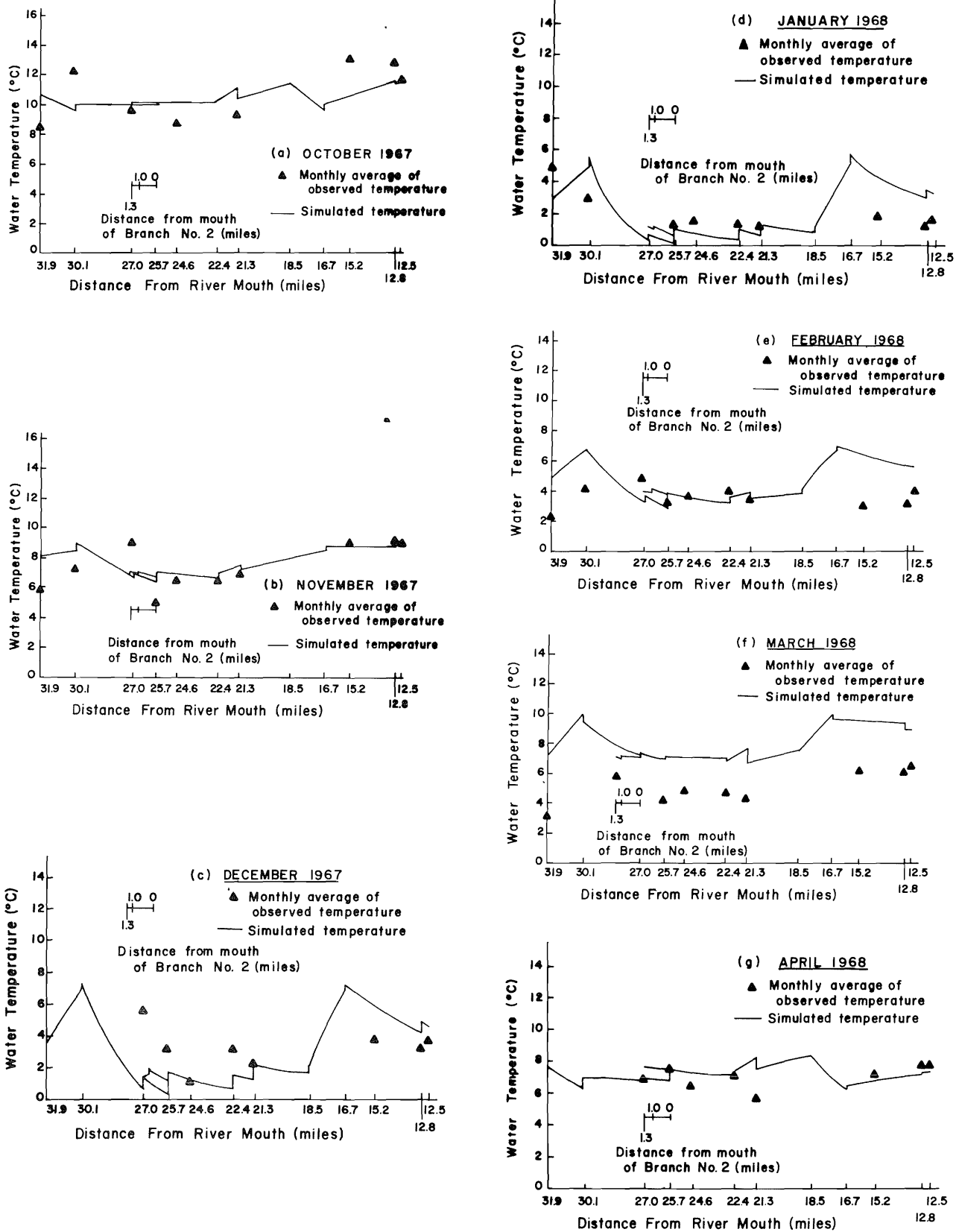


Figure F-2. Comparison of observed and simulated 1968 stream temperature profiles.

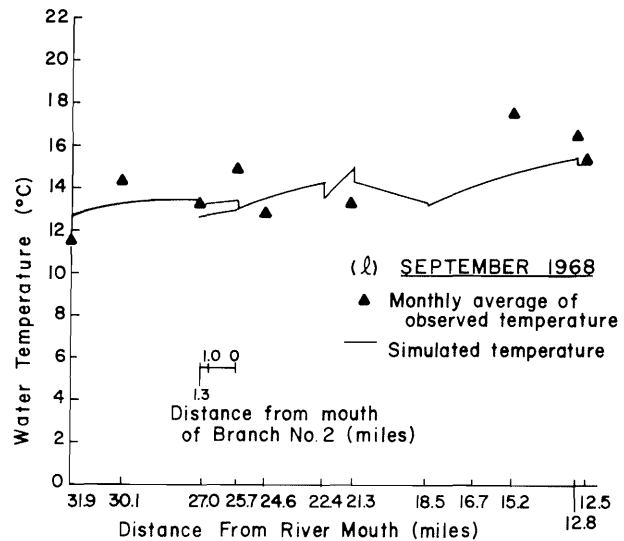
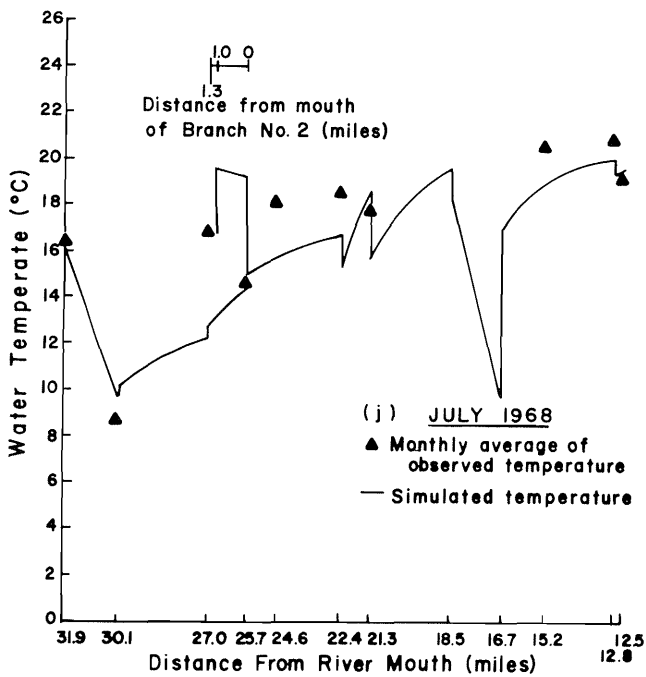
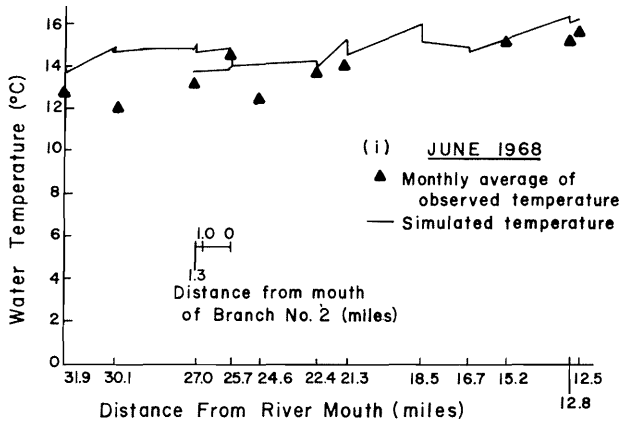
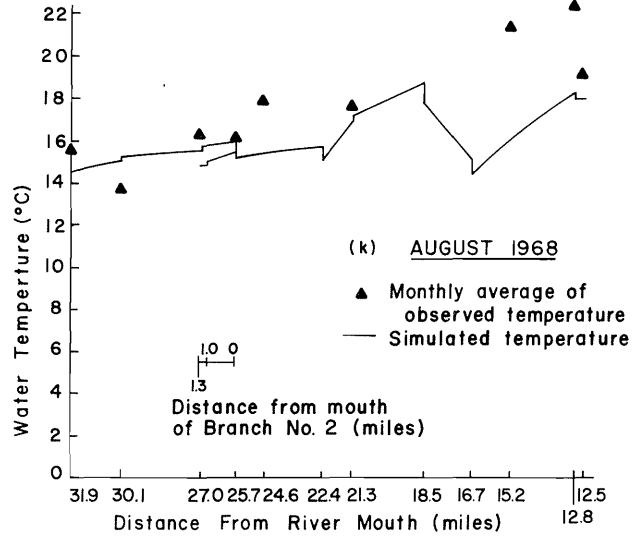
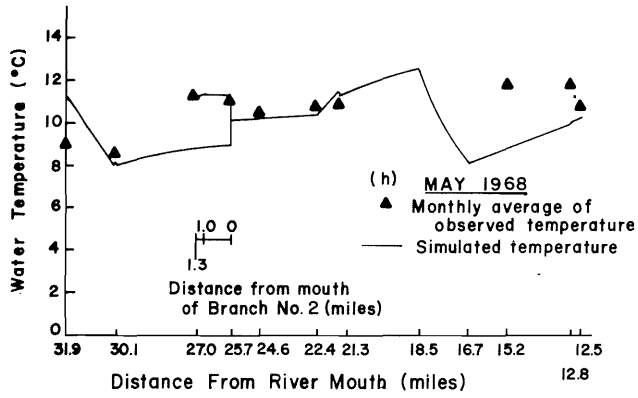


Figure F-2. Continued.

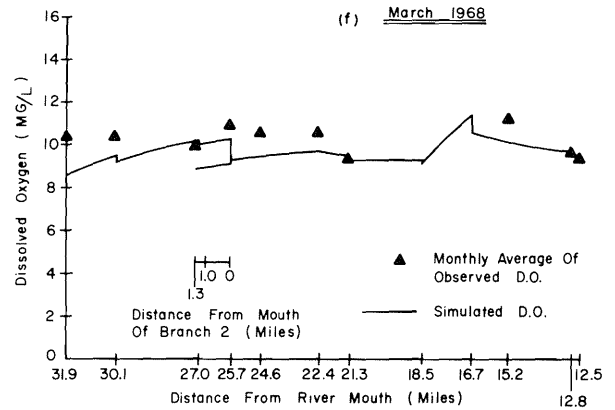
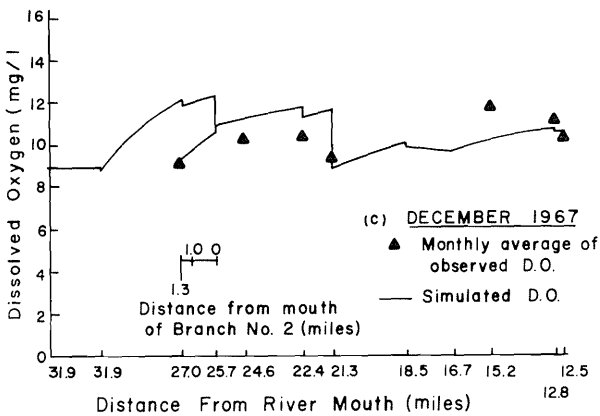
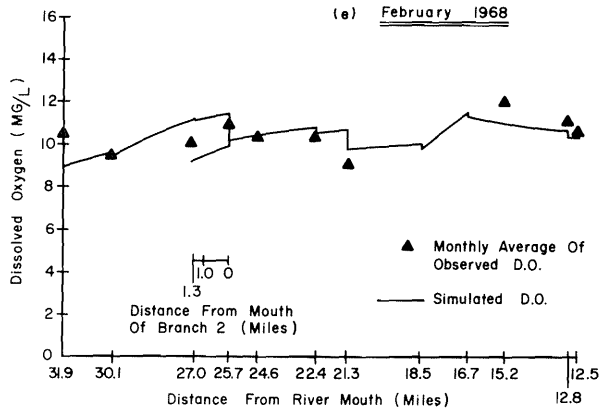
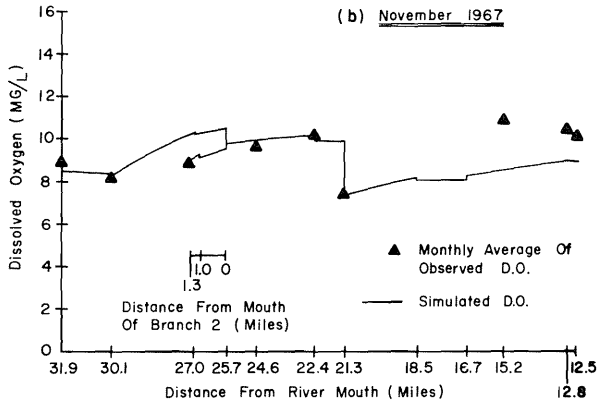
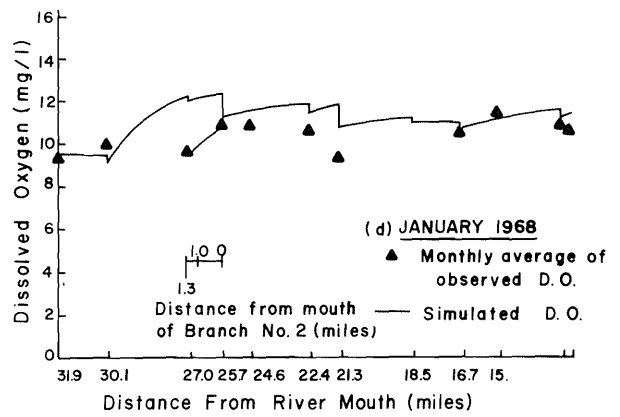
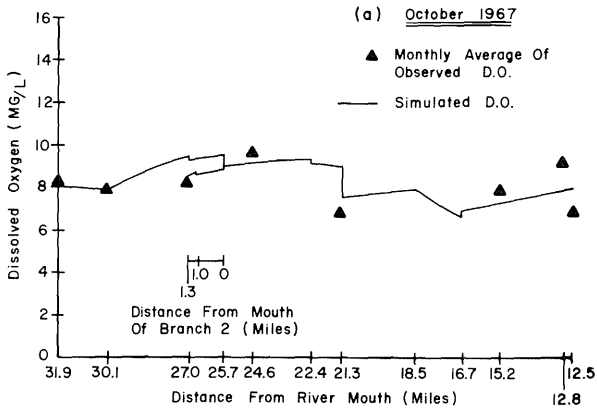


Figure F-3. Comparison of observed and simulated 1968 dissolved oxygen profile.

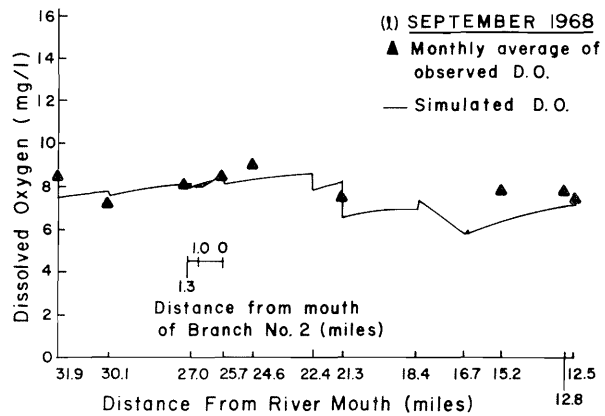
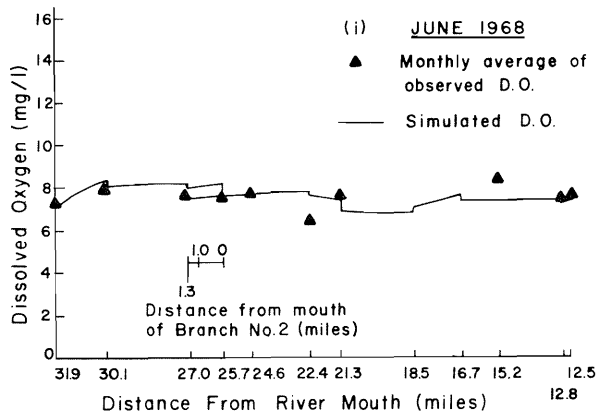
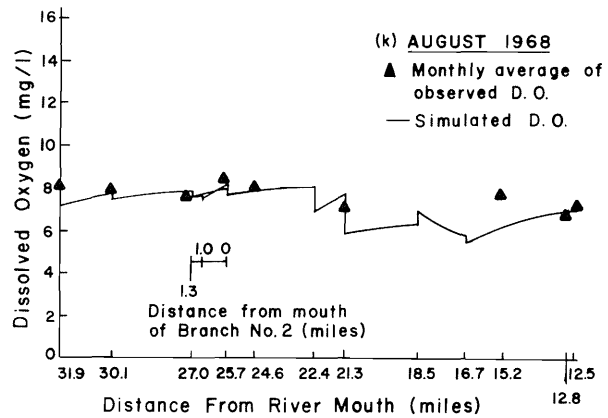
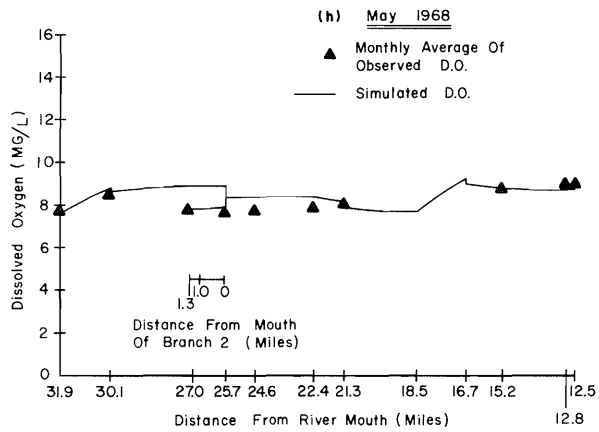
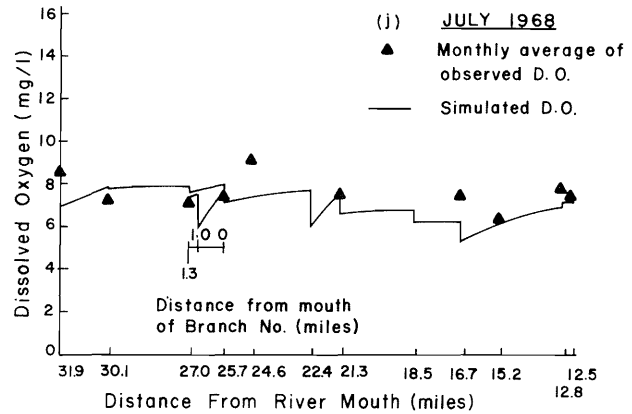
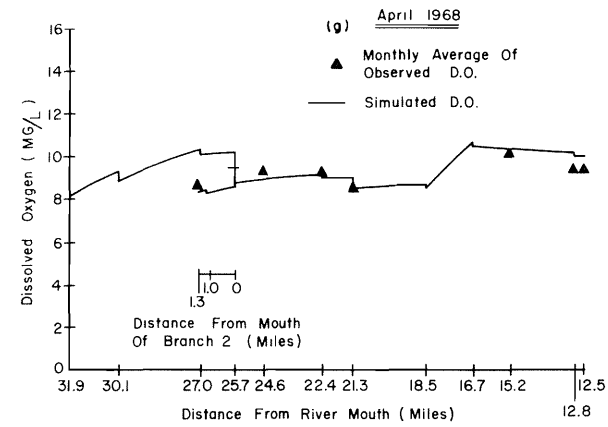


Figure F-3. Continued.

APPENDIX G

HYDROLOGY MODEL COMPUTER PROGRAMS—(1) HYDRO, (2) BUDGET—INSTRUCTIONS FOR USE

The computer programs for the hydrologic model of a river basin were coded in FORTRAN V for use on the UNIVAC 1108 digital computer. Both programs require the same deck set-up and yield the same results except that HYDRO is designed for using only data for one year at a time and can iterate over selected model parameters whereas BUDGET can take input data for up to 30 years and output a mean and standard deviation budget for the data input. The program BUDGET is designed for use primarily after a particular model has been validated and stochastic information about the system is desired.

A schematic diagram of the model is given in Figure G-1 with the flow chart shown in Figure G-2. Table G-1 gives the notation used in the programming of the model.

Both programs are designed to run in a batch mode, that is, after completing one simulation run control is passed to the start of the program to start another run if data are supplied for it. The data are separated into three

groups of cards. The first group, consisting of 20 cards, merely contains labels for the tabular budget which will be output and are read only once during a run. The second group consisting of 8 cards, is the control and parameter initialization cards for the particular river basin being simulated. The last group contains the actual input data for that run.

Detailed instruction for preparing the three groups of data cards needed as input to the program are given in Tables G-2, G-3, and G-4 respectively. Table G-5 gives the valid iteration codes that may be specified when using HYDRO.

A diagram of the correct deck set-up for a run is shown in Figure G-3. A listing of program HYDRO with sample problem input data is shown in Figure G-4. A listing of program BUDGET with a listing of the correct deck set-up for simulating the two study areas is shown in Figure G-5. The computer output for the run set up in Figure G-5 is included in Figure G-6.

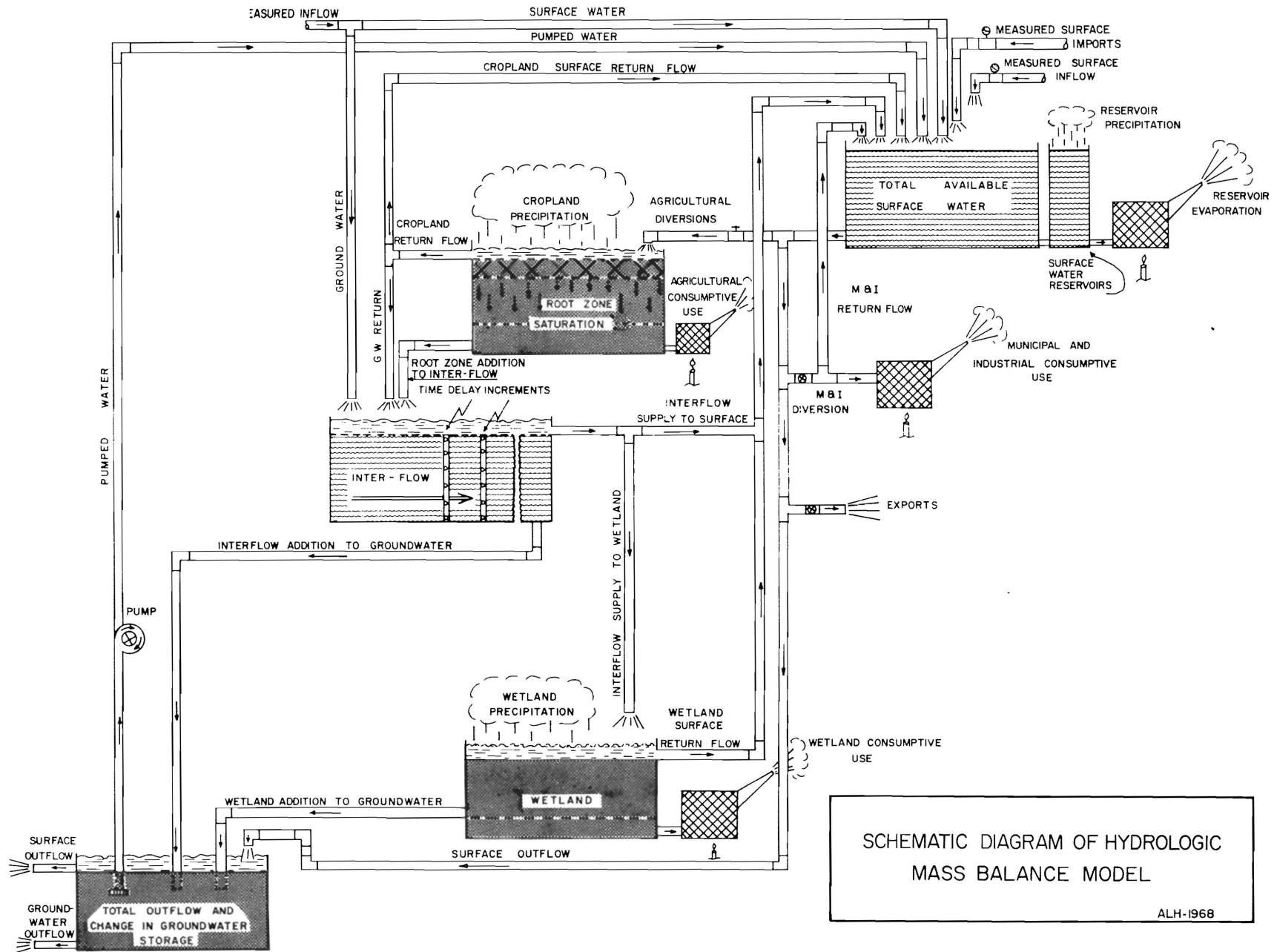


Figure G-1. Schematic diagram of hydrologic mass balance model.

HYDROLOGIC MASS BALANCE MODEL

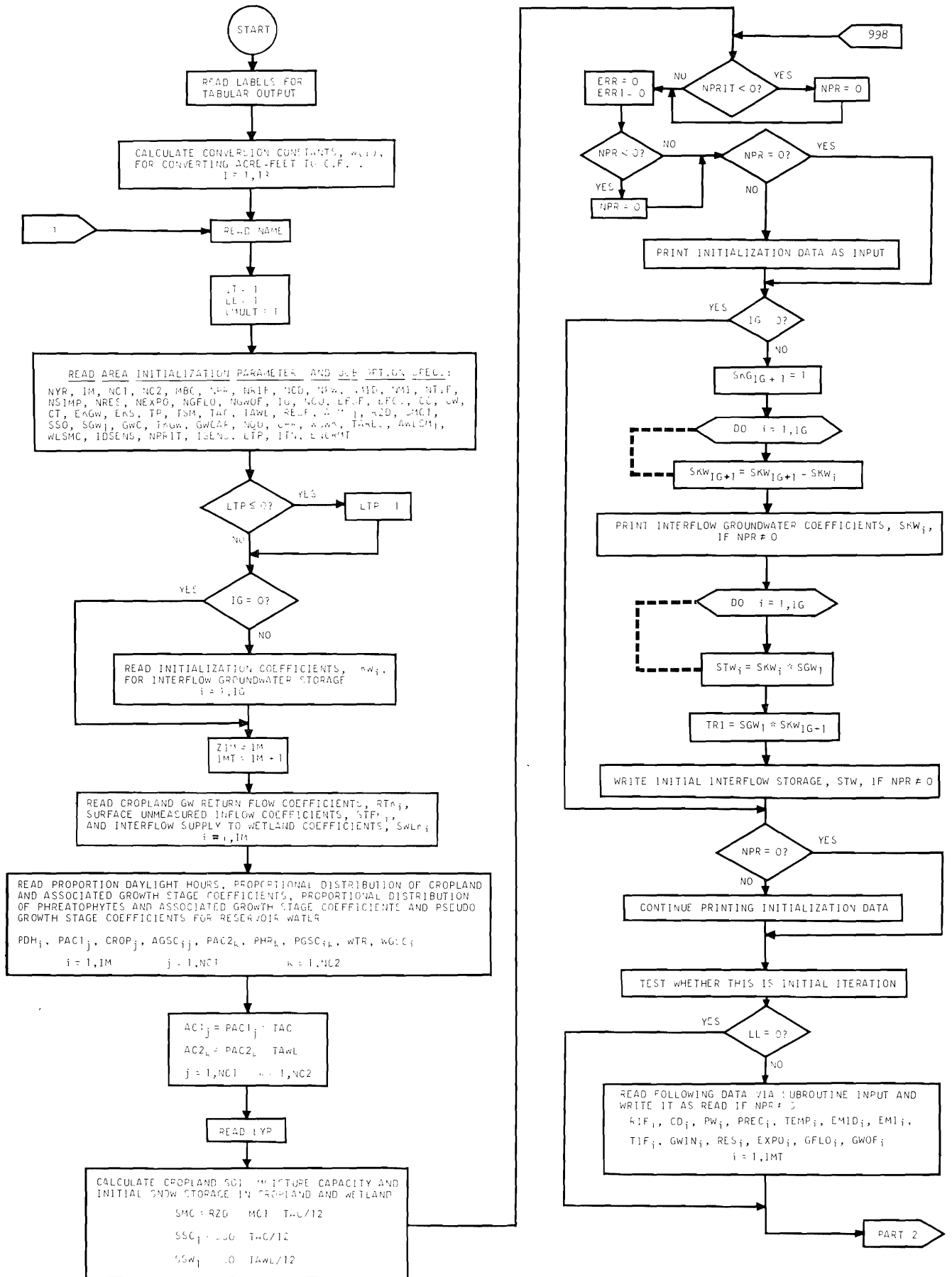


Figure G-2. HYDRO-BUDGET computer program flow chart.

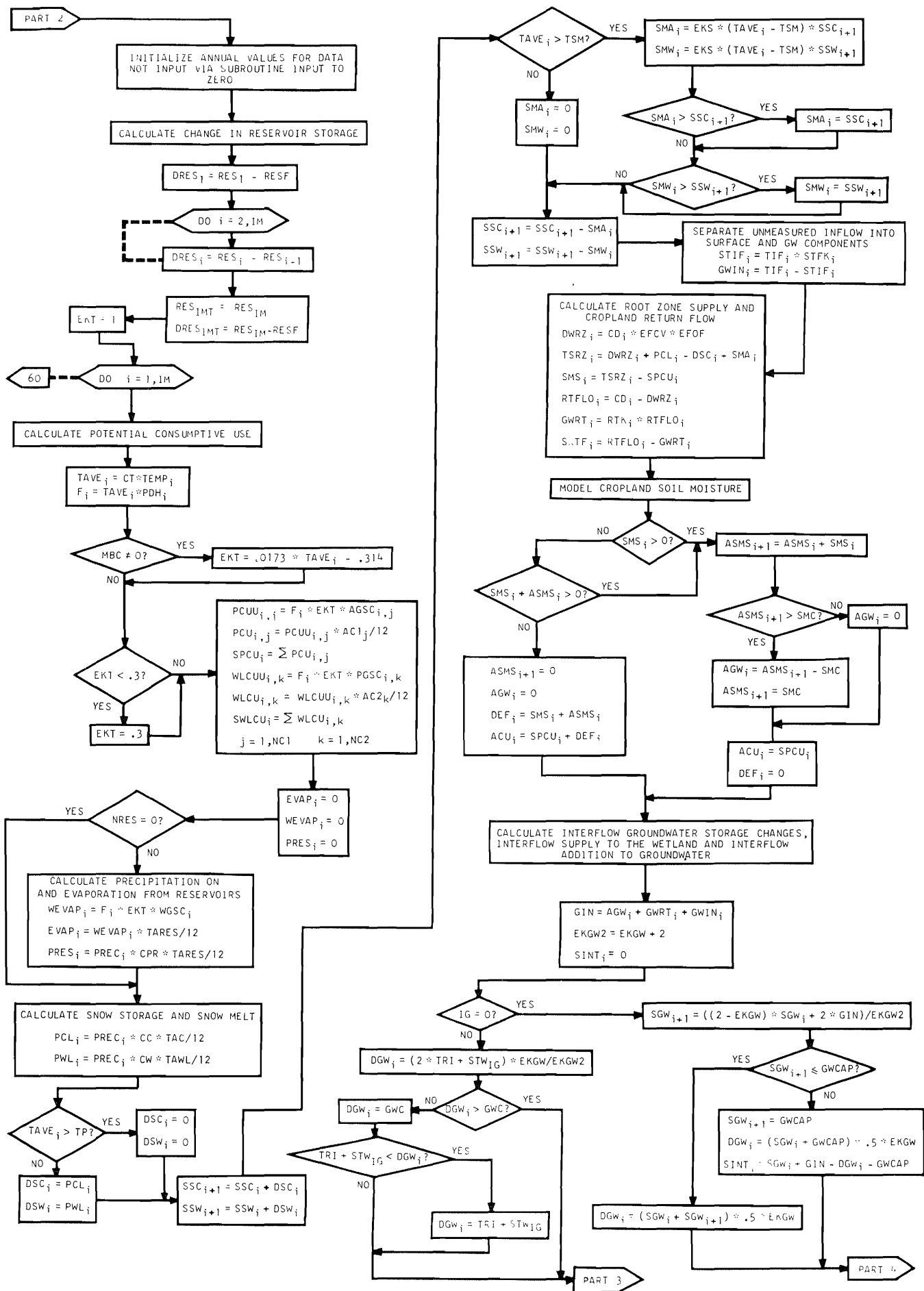


Figure G-2. Continued.

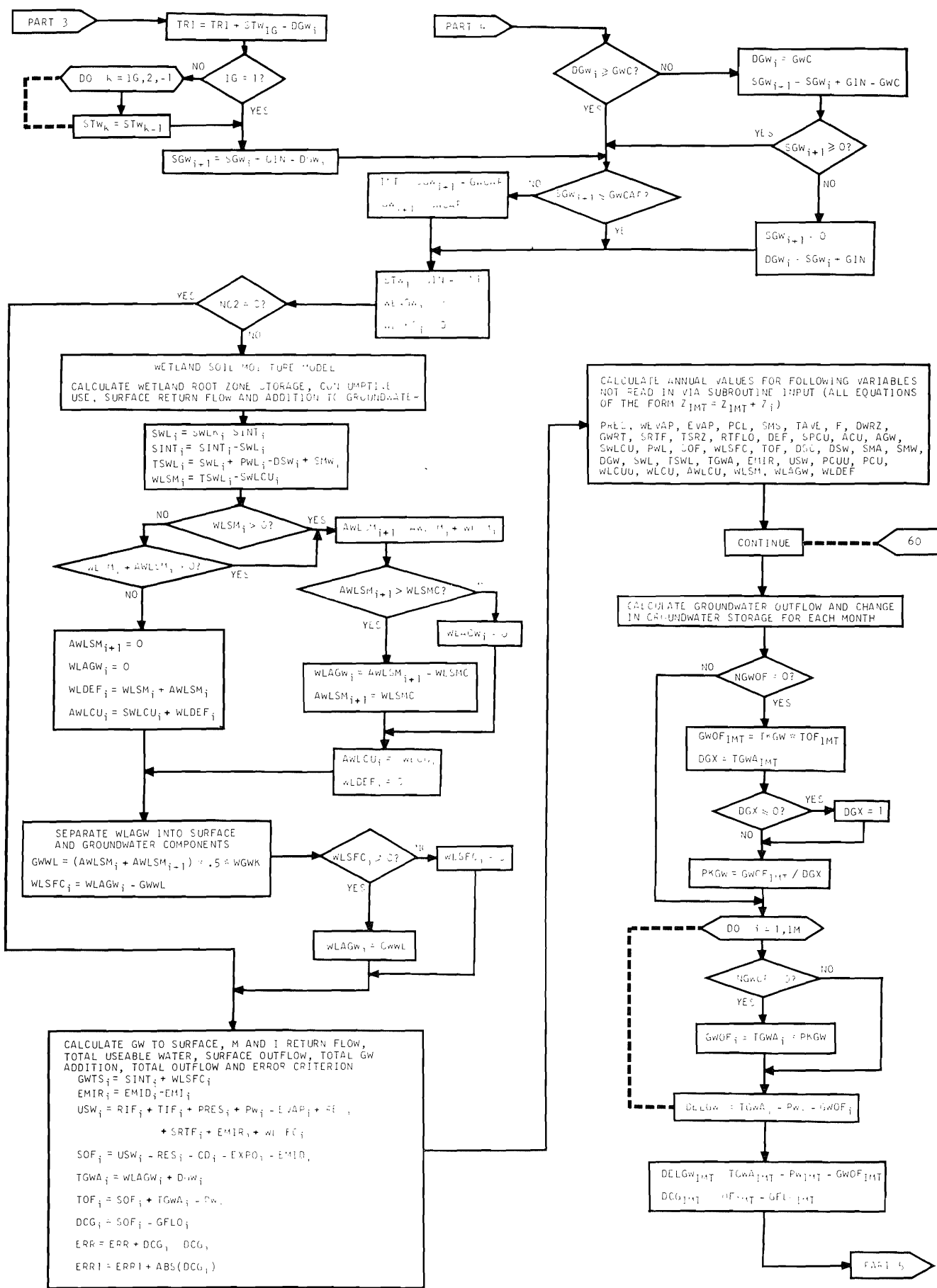


Figure G-2. Continued.

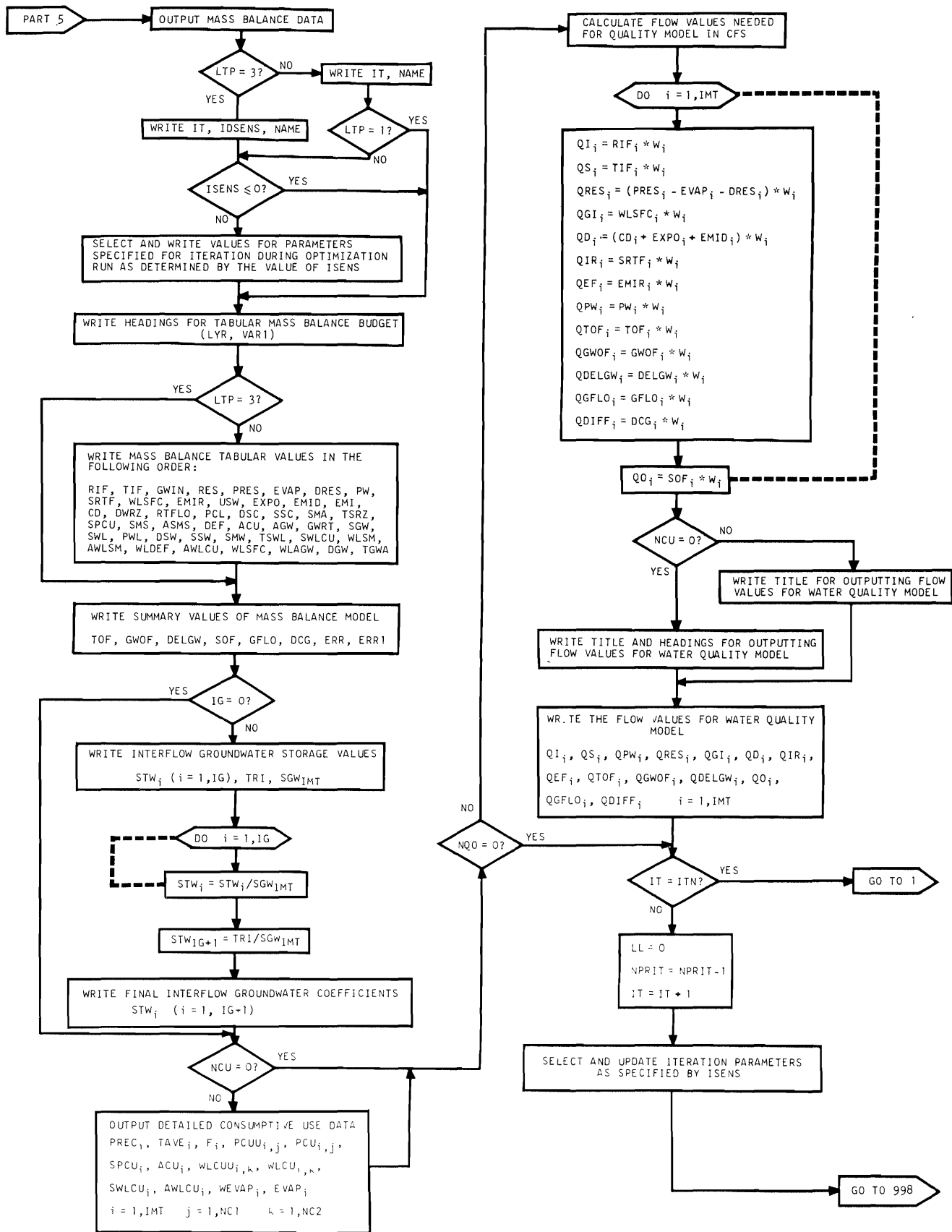


Figure G-2. Continued.

Table G-1. Notation used in the computer program of the hydrologic mass balance model.

Symbol	Description
AC(J)	Area of cropland in crop J (acres)
AC2(J)	Area of wetland in phreatophyte J(acres)
ACU	Actual cropland consumptive use (acre-ft)
ACU1	Label for ACU
AGSC(I,J)	Growth stage coefficient for crop J during month I (dimensionless)
AGW	Root zone storage addition to interflow groundwater storage vector (acre-ft)
AGW1	Label for AGW
ASMS	Accumulated cropland soil moisture storage vector (acre-ft)
ASMS1	Label for ASMS
ASMS(1)	Initial soil moisture storage (acre-ft)
AWLCU	Actual wetland consumptive use vector (acre-ft)
AWLCU1	Label for AWLCU
AWLSM	Accumulated wetland soil moisture storage (acre-ft)
AWLSM1	Label for AWLSM
AWLSM(1)	Initial wetland soil moisture storage (acre-ft)
BCF	Label for Blaney-Criddle "F"
CC	Precipitation adjusting coefficient for cropland (dimensionless)
CD	Agricultural diversions (acre-ft)
CD1	Label for CD
CPR	Reservoir precipitation adjusting coefficient (dimensionless)
CROP(J)	Label for crop J
CT	Temperature adjusting coefficient (dimensionless)
CV	Conversion factor for changing acre-ft/day to cfs (43560/86400)
CW	Precipitation adjusting coefficient for wetland (dimensionless)
DCG	Difference between computed and gaged surface outflow vector (acre-ft)
DCG1	Label for DCG
DEF	Cropland consumptive use deficit (acre-ft)
DEF1	Label for DEF
DELGW	Change in groundwater storage (acre-ft)
DELGW1	Label for DELGW
DGW	Interflow additions to groundwater storage (acre-ft)
DGW1	Label for DGW
DGX	Yearly addition to groundwater (acre-ft)
DRES	Change in reservoir storage (acre-ft)
DRES1	Label for DRES
DSC	Cropland snow storage added (acre-ft)
DSC1	Label for DSC
DSW	Wetland snow storage added (acre-ft)
DSW1	Label for DSW
DWRZ	Diverted water into cropland root zone storage (acre-ft)
DWRZ1	Label for DWRZ
EFCV	Conveyance efficiency of agricultural diversions (dimensionless)
EFOF	Farm irrigation efficiency (dimensionless)
EKGW	Decay constant for interflow groundwater (dimensionless)
EKGW2	EKGW + 2
EKS	Decay constant for snowmelt ($^{\circ}F^{-1}$)
EKT	Blaney-Criddle temperature coefficient
EMI	Municipal and industrial consumptive use (acre-ft)
EMI1	Label for EMI
EMID	Municipal and industrial diversion (acre-ft)
EMID1	Label for EMID
EMIR	Municipal and industrial return flow vector (acre-ft)
EMIR1	Label for EMIR
ENCRMT	Incrementing value or constant associated with the iteration parameter (same dimension as parameter)
ERR	Sum of squared differences between measured and computed surface outflow vector (acre-ft) ²
ERR1	Sum of absolute difference between measured and computed surface outflow vector (acre-ft)
EVAP	Reservoir evaporation (acre-ft)
EVAP1	Label for EVAP
EXPO	Surfaces export (acre-ft)
EXPO1	Label for EXPO
F	Blaney-Criddle 'F' vector
GFLO	Gaged surface outflow (acre-ft)
GFLO1	Label for GFLO
GIN	Total inflow to interflow groundwater storage vector (acre-ft)
GWC	Minimum groundwater discharge from interflow storage (acre-ft)
GWCAP	Interflow storage capacity (acre-ft)
GWIN	Subsurface unmeasured inflow (acre-ft)
GWIN1	Label for GWIN
GWOFF	Measured groundwater outflow (acre-ft)
GWOFF1	Label for GWOFF
GWRT	Cropland groundwater return flow (acre-ft)
GWRT1	Label for GWRT
GWTS	Groundwater to surface (acre-ft)
GWTS1	Label for GWTS
GWWL	Wetland addition to groundwater vector (acre-ft)
IDSENS	Label of parameter selected for iteration
IG	Number of time increments selected for delay of interflow groundwater
IM	Time increments per year (12)
ISENS	Code specification for the iteration parameter
ITN	Number of iteration desired
LTP	Print option selected during iteration
LYR	Label for years being simulated
MBC	Option specification for consumptive use model
NAME	Descriptive name for the area being simulated (label)

Table G-1. Continued.

NCD	Number of agricultural diversions	QEX	Export vector (cfs)
NCU	Print option for detailed consumptive use output	QEX1	Label for QEX
NC1	Number of agricultural crop classifications	QGFLO	Gaged surface outflow vector (cfs)
NC2	Number of phreatophytes classifications	QGFLO1	Label for QGFLO
NEXPO	Number of exports	QGI	Groundwater to surface vector (cfs)
NGFLO	Number of measured surface outflows	QGI1	Label for QGI
NGWOF	Number of measured or estimated groundwater outflows	QGWOF	Groundwater outflow vector (cfs)
NMI	Number of municipal and industrial consumptive uses	QGWOF1	Label for QGWOF
NMID	Number of municipal and industrial diversions	QI	Measured surface inflow in main channel vector (cfs)
NPR	Print option for input data	QI1	Label for QI
NPRIT	Number of initial data printouts desired during iteration	QIR	Cropland surface return flow vector (cfs)
NPW	Number of pumps	QIR1	Label for QIR
NQO	Print option for obtaining values needed for water quality model in cfs	QMID	Municipal and industrial diversion vector (cfs)
NRES	Number of reservoirs in the system	QMID1	Label for QMID
NRIF	Number of measured surface inflows (main stem primarily)	QO	Computed surface outflow vector (cfs)
NSIMP	Number of measured surface imports	QO1	Label for QO
NTIF	Number of unmeasured ground and surface water inflows	QPW	Pumped water vector (cfs)
NYR	Number of years to be simulated	QPW1	Label for QPW
PAC1(J)	Proportion of cropland in crop J	QRES	Change in reservoir storage vector (cfs)
PAC2(J)	Proportion of wetland in phreatophyte J	QRES1	Label for QRES
PCL	Cropland precipitation (inches)	QS	Unmeasured surface inflow to main channel vector (cfs)
PCL1	Label for PCL	QS1	Label for QS
PCU	Cropland potential consumptive unit use array (acre-ft)	QTOF	TOF vector converted (cfs)
PCUU	Cropland potential consumptive unit use array (inches)	QTOF1	Label for QTOF
PDH(I)	Proportion of daylight hours for month I	RES	Reservoir storage (acre-ft)
PGSC(I,J)	Growth stage coefficient for phreatophyte J during month I	RES1	Label for RES
PHR(J)	Label for phreatophyte J	RESF	Initial reservoir storage (acre-ft)
PKGW	Ratio of yearly groundwater outflow to yearly addition to groundwater	RIF	Measured surface inflow in the main stem (acre-ft)
PREC	Unadjusted monthly precipitation (inches)	RIF1	Label for RIF
PREC1	Label for PREC	RTFLO	Cropland return flow (acre-ft)
PRES	Reservoir precipitation (inches)	RTFLO1	Label for RTFLO
PRES1	Label for PRES	RTK(I)	Cropland groundwater return flow coefficient for month I
PW	Pumped water (acre-ft)	RZD	Root zone depth (feet)
PW1	Label for PW	SGW	Accumulated interflow groundwater storage (acre-ft)
PWL	Wetland precipitation (inches)	SGW1	Label for SGW
PWL1	Label for PWL	SGW(1)	Initial interflow groundwater storage (acre-ft)
QCD	Cropland diversions (cfs)	SIMP	Measured surface imports (acre-ft)
QCD1	Label for QCD	SIMP1	Label for SIMP
QD	Total diversions (cfs)	SINT	Interflow groundwater storage transferred to surface (acre-ft)
QD1	Label for QD	SINT1	Label for SINT
QDELGW	Change in groundwater storage (average cfs for time period specified in output)	SKW(I)	Initialization coefficients for interflow groundwater storage for compartment I
QDELGW1	Label for QDELGW	SMA	Cropland snowmelt (acre-ft)
QDIFF	Difference between computed and gaged surface outflow (cfs)	SMA1	Label for SMA
QDIFF1	Label for QDIFF	SMC	Cropland soil moisture capacity (acre-ft)
QEF	Municipal and industrial return flow (cfs)	SMC1	Water holding capacity of the root zone (inches/foot)
QEF1	Label for QEF	SMS	Change in cropland soil moisture storage vector (acre-ft)
		SMS1	Label for SMS
		SMW	Wetland snowmelt (acre-ft)
		SMW1	Label for SMW
		SOF	Computed surface outflow vector (acre-ft)

Table G-1. Continued.

SOF1	Label for SOF	TKGW	Proportion of total outflow passing unaged below the gage control as interflow or groundwater flow (acre-ft)
SPCU	Sum of cropland potential consumptive use (acre-ft)	TOF	Total outflow plus change in groundwater storage vector (acre-ft)
SPCU1	Label for SPCU	TOF1	Label for TOF
SRTF	Cropland surface return flow (acre-ft)	TP	Threshold temperature for snow storage (°F)
SRTF1	Label for SRTF	TRI	Interflow groundwater in last compartment of interflow storage (acre-ft)
SSC	Cropland accumulated snow storage at beginning of month (acre-ft) vector	TSM	Threshold temperature for snowmelt (°F)
SSC1	Label for SSC	TSRZ	Total supply to cropland root zone storage (acre-ft)
SSO	Initial snow storage (inches)	TSRZ1	Label for TSRZ
SSW(I)	Wetland accumulated snow storage at beginning of month I (acre-ft)	TSWL	Total supply to wetland (acre-ft)
STA	Six character code for name for the area being simulated	TSWL1	Label for TSWL
STA1	Six character code for name for the area being simulated	USW	Total available surface water vector (acre-ft)
STA2	Six character code for name for the area being simulated	USW1	Label for USW
STFK(I)	Surface unmeasured inflow coefficient for month I	VAR1	Labels for months and year for column headings of output
STIF	Surface unmeasured inflow (acre-ft)	WEVAP	Reservoir evaporation vector (inches)
STIF1	Label for STIF	WGSC	Pseudo growth stage coefficient vector for reservoir water
STW(I)	Interflow groundwater in compartment I of interflow storage (acre-ft)	WGWK	Decay constant for wetland groundwater outflow
SWL	Interflow surface supply to wetland (acre-ft)	W(I)	Conversion factor for changing acre-ft/month to cfs for month I
SWL1	Label for SWL	WLAGW	Wetland addition to groundwater storage (acre-ft)
SWLCU	Sum of wetland potential consumptive use (acre-ft)	WLAGW1	Label for WLAGW
SWLCU1	Label for SWLCU	WLCU	Wetland potential consumptive unit use array (acre-ft)
SWCK(I)	Interflow supply to wetland coefficient for month I (acre-ft)	WLCUU	Wetland potential consumptive unit use array (inches)
TAC	Cropland area (acres)	WLDEF	Wetland soil moisture storage deficit vector (acre-ft)
TARES	Total area of reservoirs (acres)	WLDEF1	Label for WLDEF
TAVE	Adjusted temperature (°F)	WLSFC	Wetland surface return flow (acre-ft)
TAWC	Wetland area (acres)	WLSFC1	Label for WLSFC
TEMP	Unadjusted monthly temperature (°F)	WLSM	Change in wetland soil moisture storage (acre-ft)
TEMP1	Label for TEMP	WLSM1	Label for WLSM
TGWA	Total addition to groundwater storage vector (acre-ft)	WLSMC	Wetland soil moisture capacity (acre-ft)
TGWA1	Label for TGWA	WTR	Label for reservoir water
TIF	Unmeasured surface and subsurface inflow (acre-ft)		
TIF1	Label for TIF		

Table G-2. Preparation instructions for Group I input cards (20 cards; output label designations).

Card	Col	Format	Name	Definition
1	1-25	5A5	R1F1	Measured inflow
	26-50	5A5	T1F1	Unmeasured inflow
	51-75	5A5	RES1	Reservoir storage
2	1-25	5A5	DRES1	Change in reservoir
	26-50	5A5	USW1	Useable surface water
	51-75	5A5	CD1	Cropland diversions
3	1-25	5A5	DWRZ1	Diverted water to cropland root zone storage
	26-50	5A5	PW1	Pumped water
	51-75	5A5	GW1N1	Groundwater inflow
4	1-25	5A5	PCL1	Cropland precipitation
	26-50	5A5	TSRZ1	Root zone supply
	51-75	5A5	SMS1	Root zone supply-P.C.U.
5	1-25	5A5	ASMS1	Accumulated cropland soil moisture
	26-50	5A5	SPCU1	Cropland potential consumptive use
	51-75	5A5	DEF1	Consumptive use deficit
6	1-25	5A5	ACU1	Actual cropland consumptive use
	26-50	5A5	PREC1	Input precipitation
	51-75	5A5	RTFLO1	Cropland return flow
7	1-25	5A5	EMI1	Municipal and industrial use
	26-50	5A5	SWLI	Interflow supply to wetland
	51-75	5A5	PWL1	Wetland precipitation
8	1-25	5A5	SWLCU1	Wetland consumptive use
	26-50	5A5	EXPO1	Exports
	51-75	5A5	SOF1	Surface outflow
9	1-25	5A5	TEMP1	Input temperature
	26-50	5A5	BCF	Blaney-Criddle "F"
	51-75	5A5	DELGW1	Change in GW storage
10	1-25	5A5	SSC1	Accumulated snow storage
	26-50	5A5	SMA1	Snow melt on cropland
	51-75	5A5	DSC1	Snow storage added to cropland
11	1-25	5A5	AGW1	Cropland addition to interflow
	26-50	5A5	SGW1	Accumulated interflow
	51-75	5A5	DGW1	Interflow added to groundwater
12	1-25	5A5	TOF1	Outflow and change in ground- water storage
	26-50	5A5	GFLO1	Gaged surface outflow
	51-75	5A5	DCG1	Difference between computed and gaged surface outflow

Table G-2. Continued.

13	1-25	5A5	GWOF1	Groundwater outflow
	26-50	5A5	GWRT1	Cropland groundwater return flow
	51-75	5A5	SRTF1	Cropland surface return flow
14	1-25	5A5	DSW1	Snow storage on wetland
	26-50	5A5	SMW1	Snow melt on wetland
	51-75	5A5	TGWA1	Total addition to groundwater storage
15	1-25	5A5	PRES1	Reservoir precipitation
	26-50	5A5	EVAP1	Reservoir evaporation
	51-75	5A5	WLSM1	Wetland supply-potential wetland consumptive use
16	1-25	5A5	AWLCU1	Actual wetland consumptive use
	26-50	5A5	AWLSM1	Accumulated wetland soil moisture
	51-75	5A5	WLDEF1	Wetland consumptive use deficit
17	1-25	5A5	WLAGW1	Wetland addition to groundwater
	26-50	5A5	TSWL1	Total supply to the wetland
	51-75	5A5	SIMP1	Important surface water
18	1-25	5A5	EMID1	Municipal and industrial diversions
	26-50	5A5	EMIR1	Municipal and industrial return flow
	51-75	5A5	WLSFC1	Wetland surface outflow
19	1-25	5A5	STIF1	Unmeasured surface inflow
	26-50	5A5	GWTS1	GW to surface water
	51-75	5A5	SINT1	Interflow to surface water
20	1-75	13A6	VAR1	13 time increment (months) labels heading their respective columns in the budget output

Table G-3. Preparation instructions for Group II input cards (8 cards; control and parameter initialization)^a

Card	Col	Format	Name	Definition
1	1-80	20A4	NAME	Area name and identification designation
2	1-06	A6	STA	Area identification (mnemonic)
	7-08	I2	NYR	No. of years ≤ 30
	9-10	I2	IM	Time increments per year $1 \leq IM \leq 12$
	11-12	I2	NC1	No. of agricultural crops ≤ 13
	13-14	I2	NC2	No. of phreatophytes ≤ 9
	15-16	I2	MBC	0(zero) value for Blaney-Criddle method of CU calculation 1(one) for modified Blaney-Criddle method
	17-18	I2	NPR	1 for printing input data 0 for suppressing printing of input data
	19-20	I2	NRIF	No. of measured inflows
	21-22	I2	NCD	No. of cropland diversions
	23-24	I2	NPW	No. of wells (pumped water measurement)
	25-26	I2	NMID	No. of municipal & industrial use diversions
	27-28	I2	NMI	No. of municipal & industrial uses
	29-30	I2	NTIF	No. of unmeasured surface inflows
	31-32	I2	NIMP	No. of surface imports
	33-34	I2	NRES	No. of reservoirs
	35-36	I2	NEXPO	No. of measured surface exports
	37-38	I2	NGFLO	No. of gaged outflows
	39-40	I2	NGWOF	No. of groundwater outflows
	41-42	I2	IG	No. of time increments for delay in transitional groundwater storage $\leq IM$
	43	I1	NCU	1 for printing consumptive use and interflow storage detail 0 for suppressing above printing
	44-46	F3.2	EFOF	Farm irrigation efficiency
	47-49	F3.2	EFCV	Conveyance efficiency for water diverted to cropland
	50-54	F5.3	CC	Adjusting coefficient for cropland precipitation
55-59	F5.3	CW	Adjusting coefficient for wetland precipitation	
60-64	F5.3	CT	Adjusting coefficient for cropland temperature	
65-68	F4.3	EKGW	Decay constant for interflow added to groundwater	
69-72	F4.3	EKS	Decay constant for snowmelt	
73-76	F4.1	TP	Threshold temperature for snow storage	
77-80	F4.1	TSM	Threshold temperature for snow	

Table G-3. Continued.

Card	Col	Format	Name	Definition
3	1-06	A6	STA1	Area identification
	7-14	F8.0	TAC	Area of cropland in acres
	15-22	F8.0	TAWL	Area of wetland in acres
	23-30	F8.0	RESF	Reservoir storage at beginning of period in acre-feet
	31-36	F6.0	ASMS _{1,1}	Initial value of soil moisture storage in acre-feet
	37-41	F5.2	RZD	Root zone depth in feet
	42-46	F5.2	SMC1	Water holding capacity of root zone in inches/ft.
	47-51	F5.2	SSO	Initial value of snow storage in inches
	52-59	F8.0	SGW _{1,1}	Initial value of interflow storage in acre-feet
	60-67	F8.0	GWC	Minimum discharge from interflow in acre-feet
	68-72	F5.3	TKGW	Proportion of outflow going under the gage as groundwater outflow
	73-80	F8.0	GWCAP	Capacity of interflow storage
	4	1-6	A6	STA2
7-8		I2	NQO	Print option for water quality hydrology output if non zero (If > 1 then only those values used by WAQUAL as output)
11-15		F5.3	CPR	Adjusting coefficient for reservoir precipitation
16-20		F5.3	WGWK	Decay constant for wetland GW outflow
21-30		F10.0	TARES	Total area of reservoirs in acres
31-40		F10.0	AWLSM _{1,1}	Initial value of wetland soil moisture storage in acre-feet
41-50		F10.0	WLSMC	Wetland soil moisture capacity in acre-feet

If selective iteration is desired when using HYDRO, then the following variables must be supplied on card 4. If supplied they are ignored by BUDGET.

4	51-56	A6	IDSENS	Identification label of the parameter selected for iteration
	57-58	I2	NPRIT	Number of input data printouts desired after initial printout if NPR≠0
	59-60	I2	ISENS	Code specification for the parameter selected for iteration. See Table A-5 for valid specification codes.
	61-62	I2	LTP	Prints entire BUDGET without iteration information. Prints entire BUDGET with iteration information. Prints only last with 5 line 7 Budget.

Table G-3. Continued.

Card	Col	Format	Name	Definition
	63-65	I3	ITN	Number of iterations desired Incrementing interval or constants associated with the parameter selected for iteration.
	66-75	F10.0	ENCRMT	
5	Initialization coefficients for the interflow storage (STW) punched in FORMAT(14X,12F5.3). This card is needed only when IG \neq 0.			
6	Cropland groundwater return flow coefficients (RTK) punched in FORMAT(14X,12F5.3).			
7	Unmeasured surface inflow coefficients (STFK) punched in FORMAT(14X,12F5.3).			
8	Supply to wetland coefficients (SWLK) punched in FORMAT(14X,12F5.3).			

^a All unmeasured values are initial estimates, modified by trial as validation proceeds.

Table G-4. Preparation instructions for Group III input cards for data vectors (number of cards is dependent upon amount of data used).

Card ^a		
1	Proportion of daylight hours (PDH) punched in FORMAT (14X,12F5.4).	9 ₁ to 9 _{NPW} Pumped water data in acre-ft.
2	Proportion of crop area (AC1) FORMAT (10X,13F5.3).	10 FORMAT specification for reading PREC vector (must be included).
2 ₁ to 2 _{NC1}	Crop label and growth stage coefficients (CROP; AGSC) punched in FORMAT (8X,A6,12F5.3). Include only if NC1 > 0.	10 ₁ Precipitation data in inches.
3	Proportion of phreatophyte area (AC2) punched in FORMAT (10X,13F5.3).	11 FORMAT specification for reading TEMP vector (must be included).
3 ₁ to 3 _{NC2}	Phreatophyte label and growth stage coefficients (PHR;PGSC) punched in FORMAT (98X,A6,12F5.2). Include only if NC2 > 0.	11 ₁ Temperature data in F.
4	Label and use coefficients for reservoir water (WTR;WGSC) punched in FORMAT (8X,A6,12F5.2). Include only if NRES > 0.	12 FORMAT specification for reading EMID vector (include only if NMID > 0).
5	Label for years, mean, and standard deviation punched in FORMAT (10X,14A5). (Should have NYR+2 labels punched).	12 ₁ to 12 _{NIMD} Municipal & industrial diversion data in acre-ft.
6	FORMAT specification for reading RIF vector (include only if NRIF > 0).	13 FORMAT specification for reading EMI vector (include only if NMI > 0).
6 ₁ to 6 _{NRIF}	Measured inflow data in acre-ft.	13 ₁ to 13 _{NMI} Municipal and industrial use (depletion) data in acre-ft.
7	FORMAT specification for reading SIMP vector (include only if NIMP > 0).	14 FORMAT specification for reading TIF vector (include only if NTIF > 0).
7 ₁ to 7 _{NIMP}	Surface input in acre-ft.	14 ₁ to 14 _{NTIF} Unmeasured inflow data in acre-ft.
8	FORMAT specification for reading CD vector (include only if NCD > 0).	15 FORMAT specification for reading RES vector (include only if NRES > 0).
8 ₁ to 8 _{NCD}	Cropland diversion data in acre-ft.	15 ₁ to 15 _{NRES} Reservoir storage at end of month in acre-ft.
9	FORMAT specification for reading PW vector (include only if NPW > 0).	16 FORMAT specification for reading EXPO vector (include only if NEXPO > 0).
		16 ₁ to 16 _{NEXPO} Measured export data in acre-ft.
		17 FORMAT specification for reading GFLO vector (include only if NGFLO > 0).
		17 ₁ to 17 _{NGFLO} Gaged outflow data in acre-ft.
		18 FORMAT specification for reading GWOF vector (include only if NGWOF > 0).
		18 ₁ to 18 _{NGWOF} Groundwater outflow data in acre-ft.

^aSubscripts refer to number of cards used for a given vector.

Table G-5. Iteration specification codes (ISENS) that may be selected for HYDRO.

Code	Parameter Affected	Description
1	IG&SKW	Change time increment of interflow GW storage delay by ENCRMT each iteration. Specification of this option requires reading ITN-2 cards designing values to the interflow GW coefficient (SKW ₁) following the regular Group III data cards specified hereafter—FORMAT for reading SKW is (14X,12F5.3).
2	EFOF	Change farm irrigation application efficiency by ENCRMT each iteration.
3	SGW(1)&GWCAP	Change interflow GW cap by ENCRMT each iteration and keep initial condition of interflow storage at capacity.
4	CC	Change cropland precipitation adjustment coefficient by ENCRMT each iteration.
5	CW	Change wetland precipitation adjustment coefficient by ENCRMT each iteration.
6	CT	Change temperature adjustment coefficient by ENCRMT each iteration.
7	EKGW	Change exponential decay constant for interflow storage added to GW by ENCRMT each iteration.
8	EKS	Change exponential decay constant for snowmelt by ENCRMT each iteration.
9	TP	Change threshold temperature for snow storage by ENCRMT each iteration.
10	TSM	Change threshold temperature for snowmelt by ENCRMT each iteration.
11	ASMS(1)	Change initial cropland soil moisture storage by ENCRMT each iteration.
12	RZD	Change cropland root zone depth by ENCRMT each iteration.
13	SMC1	Change root zone water holding capacity by ENCRMT each iteration.
14	SSO	Change initial snow storage by ENCRMT each iteration.
15	SGW(1)	Change initial interflow storage by ENCRMT each iteration.
16	GWC	Change minimum GW discharge from interflow storage by ENCRMT each iteration.
17	TKGW	Change proportion of total outflow assumed to be GW outflow by ENCRMT each iteration.
18	GWCAP	Change capacity of interflow storage by ENCRMT each iteration.
19	CPR	Change adjustment coefficient for reservoir precipitation by ENCRMT each iteration.
20	WGWK	Change exponential decay constant for wetland soil moisture added to GW by ENCRMT each iteration.
21	AWLSM(1)	Change initial wetland soil moisture storage by ENCRMT each iteration.
22	WLSMC	Change wetland soil moisture capacity by ENCRMT each iteration.
23	RTK _i	Change cropland groundwater return flow coefficients by reading in a new set each iteration. Require ITN-1 cards trailing the regular Group III data deck. Read FORMAT for RTK is (14X,12F5.3).
24	AWLSM(1)WLSMC	Change wetland soil moisture capacity by ENCRMT each iteration and keep initial condition at WLSMC.
25	STFK _i	Change inflow coefficients by reading a new set of each iteration. Requires ITN-1 cards trailing regular Group III data deck punched in FORMAT (14X,12F5.3).
26	SWLK _i	Change wetland supply coefficients by reading a new set each iteration. Require ITN-1 cards trailing the regular Group III data deck punched in FORMAT (14X,12F5.3).

Table G-5. Continued.

Code	Parameter Affected	Description
27	TIF	Change amount of unmeasured surface inflow by a multiplication factor increased by ENCRMT each iteration.
28	GWOF	Change amount of groundwater outflow by a multiplicative factor increased by ENCRMT each iteration.
29	PREC	Change unadjusted input precipitation by reading a new set of values each iteration punched in FORMAT (14X,13F5.2). This option requires that ITN-1 PREC cards trail the Group III input data.
30	TEMP	Change unadjusted temperature by reading a new set of values each iteration punched in FORMAT (14X,13F5.1). This option requires that ITN-1 TEMP cards trail the regular Group III input data.
31	PAC1	Change percent distribution of cropland areas by reading a new set of values each iteration. Input FORMAT is (10X,14F5.3). This option requires ITN-1 PAC1 cards trail the regular Group III input data.
32	PAC2	Change present distribution of wetland areas by reading a new set of values each iteration. Input FORMAT is (10X,14F5.3). This option requires ITN-1 PAC2 cards trail the regular Group III input data.

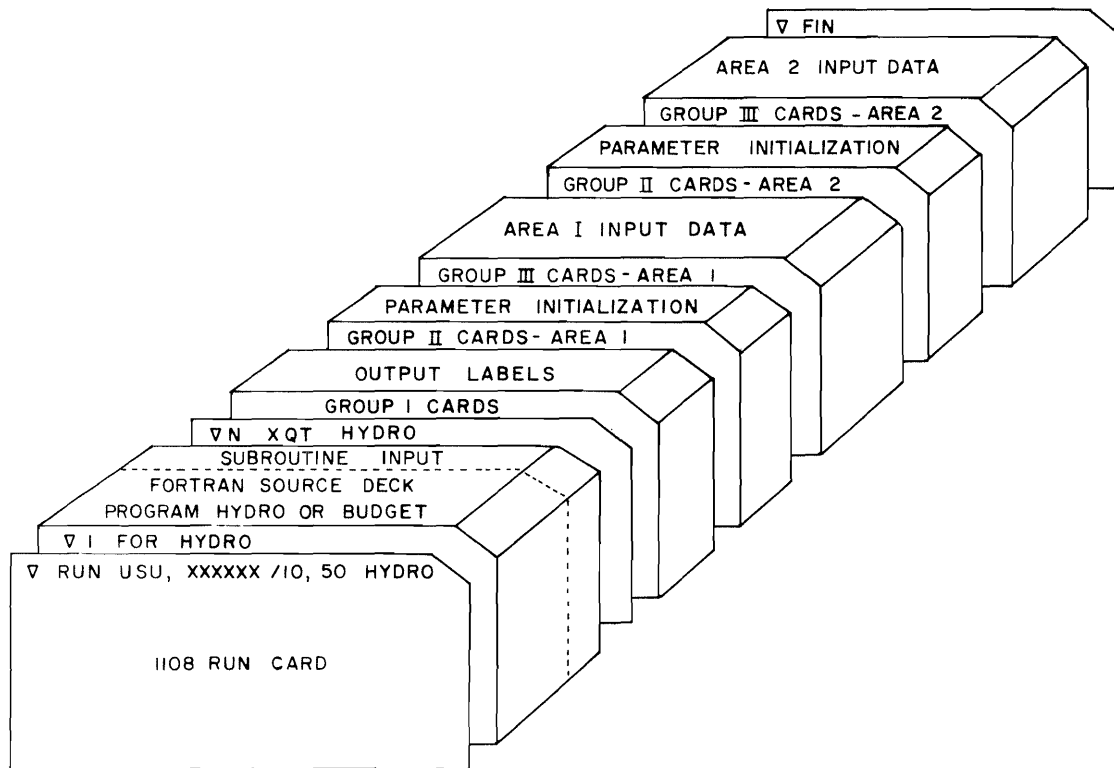


Figure G-3. Deck set-up for running HYDRO or BUDGET.

```

# RUN USU,XXXXX,1,100,12 LEON HUBER
# DPR
#I FOR HYDRO-HYDRO
C C HYDROLOGIC MASS BALANCE MODEL PROGRAM
COMMON LXR
INTEGER NAME(20)
DIMENSION PDH(12),AC1(14),RIF(13),F(13),CD(13),PW(13),PREC(13),
1PCL(13),DWRZ(13),GWOF(13),TSRZ(13),TEMP(13),AGSC(12,14),TAVE(13),
2PCUU(13,14),PCUI(13,14),PGSC(12,13),AC2(13),WLCU(13,13),PWL(13),
3SWLCU(13,13),SPCU(13),SWLCU(13),SMS(13),ASMS(13),DEF(13),ACU(13),
4AGW(13),EMI(13),TIF(13),SWL(13),SOF(13),SGW(13),DGO(13),RTFLO(13),
5SRES(13),EXPO(13),TOF(13),GWRT(13),SRTF(13),STW(12),SKW(13),PHR(13),
6CROP(14),DRES(13),USW(13),GFL0(13),DCG(13),SSC(13),SSW(13),
7SMAI(13),SMW(13),DSC(13),DSW(13),RTK(12),GWIN(13),
8AWLCU(13),PRES(13),EVAP(13),WGSC(12),WLSM(13),AWLSM(13),WLAGW(13),
9WDEF(13),TSM(13),STFK(12),SWLK(12),EMTD(13),EMTR(13),WEVAP(13),
DIMENSIONRIF(15),TIF(15),RES1(5),DRES1(5),USW1(5),CD1(5),PW1(5),
1DWRZ1(5),GWOF1(5),PCL1(5),TSRZ1(5),SMS1(5),ASMS1(5),SPCU1(5),
2DEF1(5),ACU1(5),AGW1(5),RTFLO1(5),EMI1(5),SWL1(5),PWL1(5),SSC1(5),
3SWLCU1(5),EXPO1(5),TEMP1(5),BCF(5),DGO1(5),SOF1(5),
4PREC1(5),GFL01(5),DCG1(5),SMAI1(5),DSC1(5),SGW1(5),TOF1(5),
5GWRT1(5),SRTF1(5),SMW1(5),DSW1(5),VAR1(13),GWIN1(5),
6AWLCU1(5),PRES1(5),EVAP1(5),WLSM1(5),AWLSM1(5),WLAGW1(5),
7WLAGW1(5),TSM1(5),TGWA1(5),EMTD1(5),EMTR1(5),WLSFC1(5),DELGW1(5),
8W(13),Q(13),QF(13),QF1(13),QD(13),QD1(13),QEF(13),QD1(13),
9WLSFC(13),DELGW(13),DRES(13),OPW(13),TGWA(13),PAC1(14),PAC2(13),
10TOF(13),QGWOF(13),DELGW(13),QGFL0(13),QDIFF(13),QCD(13),QEX(13),
20MID(13),SIMP(13),SIMP1(5),STIF(15),STIF1(13),GWTS1(5),GWTS1(13),
3SINT(15),SINT(13)
DATA Q11,QS1,QG1,QD1,QIR1,QEF1,QD1,DRES1,OPW1 QTOF1,QGWOF1,
10DGM1,QGFL01,QDIFF1/2H0I,2H0S,3H0G1,2H0T,3H0E,2H0Q,4H0RES,
23H0P, 4H0T0F,5H0G0F,4H0D0G,5H0G0F0,5H0D0FF/
DATA QCD1,QEX1,QMID1/3H0C0,5H0EX0,4H0MID/
C C
C C READ LABELS FOR BUDGET OUTPUT
C C
READ(5,500) RIF1,TIF1,RES1
READ(5,500) DRES1,USW1,CD1
READ(5,500) DWRZ1,PW1,GWIN1
READ(5,500)PCL1,TSRZ1,SMS1
READ(5,500) ASMS1,SPCU1,DEF1
READ(5,500) ACU1,PREC1,RTFLO1
READ(5,500) EMI1,SWL1,PWL1
READ(5,500) SWLCU1,EXPO1,SOF1
READ(5,500) TEMP1,BCF,DGO1
READ(5,500) SSC1,SMAI,DSC1
READ(5,500) AGW1,SGW1,DGO1
READ(5,500) TOF1,GFL01,DCG1
READ(5,500) GWOF1,GWRT1,SRTF1
READ(5,500) DSW1,SMW1,TGWA1
READ(5,500) PRES1,EVAP1,WLSM1
READ(5,500) AWLCU1,AWLSM1,WLAGW1
READ(5,500) WLAGW1,STW1,SIMP1
READ(5,500)EMTD1,EMTR1,WLSFC1
READ(5,500)STIF1,GWTS1,SINT1
500 FORMAT(15A5)
READ(5,501) VAR1
501 FORMAT(13A6)
CV=43560./3600.*24.)
W(1)=CV/31.
W(2)=CV/30.
W(3)=W(1)
W(4)=W(1)
W(5)=CV/28.
W(6)=W(1)
W(7)=W(2)
W(8)=W(1)
W(9)=W(2)
W(10)=W(1)
W(11)=W(1)
W(12)=W(2)
W(13)=CV/365.
1 READ(5,101) NAME
101 FORMAT(20A4)
IT=1
LL=1
CMULT=1.
C C
C C READ INITIALIZATION PARAMETERS
C C
READ(5,102)STA,NYR,IM,NC1,NC2,MRC,NPR,NRIF,NC0,NPW,NMID,NMI,NTIF,
1NSIMP,NRES,NEXPO,NGFLO,NGWOF,IG,NCU,EFOF,EFCV,CC,CW,CT,EGKW,EKS,
2TP,TSM
102 FORMAT(A6,18I2,I1,2F3.2,3F5.3,2F4.3,2F4.1)
READ(5,103)STA1,TAC,TAWL,RESF,ASMS(1),R2D,SMC1,SSO,SGW(1),GWC,TKGW
1,GWCAP
103 FORMAT(A6,3F8.0,F6.0,3F5.2,2F8.0,F5.3,F8.0)
READ(5,107)STA2,N00,CPR,GGWK,TARFS,AWLSM(1),WLSMC,IDSFNS,NPRIT,
1ISENS,LTP,ITN,ENCRMT
107 FORMAT(A6,I4,2F5.3,3F10.0,A6,3I2,I3,F10.0)
IF(LTP.LE.0)LTP=1
C C
C C READ INITIALIZATION COEFFICIENTS FOR INTERFLOW GW STORAGE
C C
IF(IG.EQ.0)GO TO 2
READ(5,104)(SKW(I),I=1,IG)
104 FORMAT(14X12F5.3)
2 ZIM=IM
INT=IM+1
C C
C C READ CROPLAND GROUNDWATER RETURN FLOW COEFFICIENTS
C C
READ(5,104)(RTK(I),I=1,IM)
C C
C C READ SURFACE UNMEASURED INFLOW COEFFICIENTS
C C
READ(5,104)(STFK(I),I=1,IM)
C C
C C READ INTERFLOW SUPPLY TO WETLAND COEFFICIENTS
C C
READ(5,104)(SWLK(I),I=1,IM)
C C
C C READ PROPORTION OF DAYLIGHT HOURS
C C
READ(5,130)(PDH(I),I=1,IM)
130 FORMAT(14X12F5.4)
C C
C C READ PROPORTION CROP AREAS AND GROWTH STAGE COEFFICIENTS
C C
IF(NC1)DO 10,5
5 READ(5,106)(PAC1(J),J=1,NC1)
106 FORMAT(10X,14F5.3)
DO 6 J=1,NC1
READ(5,105) CROP(J),(AGSC(I,J),I=1,IM)
105 FORMAT(8X46,12F5.2)
6 ACI(J)=TAC*PAC1(J)
C C
C C READ PROPORTION PHREATOPHYTE AREAS AND GROWTH STAGE COEFFICIENTS
C C
10 IF(NC2)15,15,11
11 READ(5,106)(PAC2(J),J=1,NC2)
DO 12 J=1,NC2
READ(5,105)PHR(J),(PGSC(I,J),I=1,IM)
12 AC2(J)=TAWL*PAC2(J)
C C
C C READ RESERVOIR WATER SURFACE GROWTH STAGE COEFFICIENTS
C C
15 IF(NRES.NE.0)READ(5,105)WTR,(WGSC(I),I=1,IM)
C C
C C READ INPUT DATA
C C
READ(5,1000)LYR
1000 FORMAT(10X,14A5)
C C
C C CALCULATE CROPLAND SOIL MOISTURE CAPACITY AND INITIAL SNOW STORAGE
C C THE CROPLAND AND WETLAND
C C
SMC=R2D*SMC1*TAC/12.
SSC(1)=SSO*TAC/12.
SSW(1)=SSO*TAWL/12.
C C
C C PRINT ORIGINAL INPUT DATA IF NPR NE 0
C C
998 IF(NPRIT.LT.0)NPR=0
ERR=0.
ERR1=0.
IF(NPR.EQ.0)GO TO 13
WRITE(6,507)NAME
507 FORMAT(*1INPUT DATA FOR *20A4)
WRITE(6,508)STA,NYR,IM,NC1,NC2,MRC,NPR,NRIF,NC0,NPW,NMID,NMI,NTIF,
1NSIMP,NRES,NEXPO,NGFLO,NGWOF,IG,NCU,EFOF,EFCV,CC,CW,CT,EGKW,EKS,
2TP,TSM
508 FORMAT(1XA6,19I3,2F5.2,3F6.3,2F6.1)
WRITE(6,509)STA1,TAC,TAWL,RESF,ASMS(1),R2D,SMC1,SSO,SGW(1),GWC,
1TKGW,GWCAP,SMC,SSC(1),SSW(1)
509 FORMAT(1XA6,3F10.0,F8.0,3F6.2,2F10.0,F8.3,4F10.0)
WRITE(6,701)STA2,N00,CPR,GGWK,TARFS,AWLSM(1),WLSMC,IDSFNS,NPRIT,
1ISENS,LTP,ITN,ENCRMT
701 FORMAT(1XA6,I4,2F10.0,3F10.0,2XA6,3I3,I5,F15.5)
13 IF(IG.EQ.0)GO TO 14
SKW(IG+1)=1.
DO 7 I=1,IG
7 SKW(IG+1)=SKW(IG+1)*SKW(I)
IF(NPR.NE.0)WRITE(6,511)(SKW(I),I=1,IG),SKW(IG+1)
511 FORMAT(1X*INTERFLOW GW STORAGE COEF*13F8.3)
DO 8 I=1,IG
8 STW(I)=SKW(I)*SGW(I)
TRI=SGW(1)*SKW(IG+1)
IF(NPR.NE.0)WRITE(6,512)(STW(I),I=1,IG),TRI
512 FORMAT(1X*INITIAL INTERFLOW STORAGE*13F8.0)
14 IF(NPR.EQ.0)GO TO 20
WRITE(6,560)LYR,VAR1
WRITE(6,560)(PAC1(J),J=1,NC1)
510 FORMAT(1X25HCROP GW RETURN FLO COEF +12F9.3)
WRITE(6,517)(STFK(I),I=1,IM)
517 FORMAT(1X25HSURFACE TIF COEFFICIENTS +12F8.3)
WRITE(6,518)(SWLK(I),I=1,IM)
518 FORMAT(1X25HINTERFLO SWL COEFFICIENTS+12F8.3)
WRITE(6,502)(PDH(I),I=1,IM)
502 FORMAT(1X25HPROPORTION DAYLIGHT HOURS+12F8.4)
IF(NC1.EQ.0)GO TO 91
WRITE(6,503)(PAC1(J),J=1,NC1)
503 FORMAT(2X*PROP CROPS*14F8.3)
WRITE(6,520)(AC1(J),J=1,NC1),TAC
520 FORMAT(2X*CROP AREAS*15F8.0)
WRITE(6,504)(C,CROP(J),(AGSC(I,J),I=1,IM),J=1,NC1)
504 FORMAT(1X13,1XA6,7H,K COEF,AX,12F8.2)
91 IF(NC2.EQ.0)GO TO 93
WRITE(6,505)(PAC2(J),J=1,NC2)
505 FORMAT(1X15HPROP WLPW AREAS+13F8.3)
WRITE(6,521)(AC2(J),J=1,NC2),TAWL
521 FORMAT(6X*WLPW AREAS*14F8.0)
WRITE(6,504)(J,PHR(J),(PGSC(I,J),I=1,IM),J=1,NC2)
93 IF(NRES.NE.0)WRITE(6,522)WTR,(WGSC(I),I=1,IM)
522 FORMAT(1H0A6,7H,K COEF,11X,12F8.2)
200 IF(LL.EQ.0)GO TO 19
IF(NRIF.NE.0,AND,NPR.NE.0)WRITE(6,506)RIF1
506 FORMAT(25X5A5)
CALL INPUT(NRIF,1,IM,0,IF,NPR)
IF(NCIMP.NE.0,AND,NPW.NE.0)WRITE(6,506)SIMP1
CALL INPUT(NSIMP,1,IM,SIMP,NPR)
IF(NC0.NE.0,AND,NPR.NE.0)WRITE(6,506)CD1
CALL INPUT(NC0,1,IM,CD,NPR)
IF(NPW.NE.0,AND,NPR.NE.0)WRITE(6,506)PW1
CALL INPUT(NPW,1,IM,PW,NPR)
IF(NPR.NE.0)WRITE(6,506)PREC1
CALL INPUT(1,1,IM,PREC,NPR)
IF(NPR.NE.0)WRITE(6,506)TEMP1
CALL INPUT(1,1,IM,TEMP,NPR)
IF(NMID.NE.0,AND,NPR.NE.0)WRITE(6,506)EMTD1
CALL INPUT(NMID,1,IM,EMTD,NPR)
IF(NMI.NE.0,AND,NPR.NE.0)WRITE(6,506)EMI1
CALL INPUT(NMI,1,IM,EMI,NPR)
IF(NTIF.NE.0,AND,NPR.NE.0)WRITE(6,506)TIF1

```

Figure G-4. Listing of program HYDRO with data input and program output.


```

CALL INPUT(TIF,1,IM,TIF,NPR)
IF (NRES,NE,0,AND,NPR,NE,0)WRITE(6,506)RES1
CALL INPUT(NRES,1,IM,RES,NPR)
IF (NEXP0,NE,0,AND,NPR,NE,0)WRITE(6,506)EXP01
CALL INPUT(NEXP0,1,IM,EXP0,NPR)
IF (NGFLO,NE,0,AND,NPR,NE,0)WRITE(6,506)GFLO1
CALL INPUT(NGFLO,1,IM,GFLO,NPR)
IF (NGWOF,NE,0,AND,NPR,NE,0)WRITE(6,506)GWOF1
CALL INPUT(NGWOF,1,IM,GWOF,NPR)
C
C      INITIALIZATION OF ANNUAL COLUMN AND TOTALS FOR ALL ITEMS NOT
C      CALLED BY SURROUTINE INPUT
C
18 SSC(IMT)=0.
STIF(IMT)=0.
GWIN(IMT)=0.
GWTS(IMT)=0.
SINT(IMT)=0.
SSW(IMT)=0.
SMA(IMT)=0.
DSC(IMT)=0.
SMW(IMT)=0.
DSW(IMT)=0.
SGW(IMT)=0.
DGW(IMT)=0.
DCG(IMT)=0.
DRES(IMT)=0.
USW(IMT)=0.
DWRZ(IMT)=0.
PCL(IMT)=0.
TSRZ(IMT)=0.
SPCU(IMT)=0.
EMTR(IMT)=0.
SMS(IMT)=0.
DEF(IMT)=0.
ACU(IMT)=0.
AGW(IMT)=0.
RTFLO(IMT)=0.
SWL(IMT)=0.
PWL(IMT)=0.
AWLCU(IMT)=0.
SWLCU(IMT)=0.
TAVE(IMT)=0.
F(IMT)=0.
SOF(IMT)=0.
TOF(IMT)=0.
GWRT(IMT)=0.
SRTF(IMT)=0.
PRES(IMT)=0.
EVAP(IMT)=0.
WEVAP(IMT)=0.
WLSM(IMT)=0.
WLAGW(IMT)=0.
TGW(IMT)=0.
WLSFC(IMT)=0.
DELGW(IMT)=0.
IF (NC1)21+21,19
19 DO 20 K=1,NC1
PCUU(IMT,K)=0.
20 PCU(IMT,K)=0.
21 IF (NC2)24+24,22
22 DO 23 K=1,NC2
WLCU(IMT,K)=0.
23 WLCU(IMT,K)=0.
24 CONTINUE
C
C      CALCULATE CHANGE IN RESERVOIR STORAGE. RES(I) IS STORAGE AT END
C      OF PERIOD I.
C
DRES(I)=RES(I)-RESF
DO 16 I=2,IM
16 DRES(I)=RES(I)-RES(I-1)
RES(IMT)=RES(IM)
DRES(IMT)=RES(IMT)-RESF
C
C      BUDGET CALCULATIONS BEGIN HERE
C
EKT=1.
DO 60 I=1,IM
C
C      CALCULATE POTENTIAL CONSUMPTIVE USE
C
TAVE(I)=CT*TEMP(I)
F(I)=TAVE(I)*PDH(I)
IF (MRC,NE,0)EKT=.0173*TAVE(I)-.314
IF (EKT,LT,.3)EKT=.3
SPCU(I)=0.
IF (NC1)29+29,27
27 DO 28 K=1,NC1
PCUU(I,K)=F(I)*EKT*AGSC(I,K)
PCU(I,K)=PCUU(I,K)*AC1(K)/12.
28 SPCU(I)=SPCU(I)+PCU(I,K)
29 SWLCU(I)=0.
IF (NC2)32+32,30
30 DO 31 K=1,NC2
WLCU(I,K)=F(I)*EKT*PGSC(I,K)
WLCU(I,K)=WLCU(I,K)*AC2(K)/12.
31 SWLCU(I)=SWLCU(I)+WLCU(I,K)
C
C      CALCULATE PRECIPITATION AND EVAPORATION FROM RESERVOIR
C
32 EVAP(I)=0.
WEVAP(I)=0.
PRES(I)=0.
IF (NRES,EQ,0) GO TO 205
WEVAP(I)=F(I)*EKT*WGSC(I)
EVAP(I)=WEVAP(I)+TARES/12.
PRES(I)=PREC(I)+CPR*TARES/12.
C
C      CALCULATE SNOW STORAGE AND SNOW MELT
C
205 PCL(I)=PREC(I)+CC*TAC/12.
PWL(I)=PREC(I)+CW*TAW/12.
IF (TAVE(I).GT,TP) GO TO 301
DSC(I)=PCL(I)
DSW(I)=PWL(I)
GO TO 302
301 DSC(I)=0.
DSW(I)=0.
302 SSC(I+1)=SSC(I)+DSC(I)
SSW(I+1)=SSW(I)+DSW(I)
IF (TAVE(I).GT,TSM) GO TO 305
SMA(I)=0.
SMW(I)=0.
GO TO 310
305 SMA(I)=EKS+(TAVE(I)-TSM)+SSC(I+1)
SMW(I)=EKS+(TAVE(I)-TSM)+SSW(I+1)
IF (SMA(I).GT,SSC(I+1))SMA(I)=SSC(I+1)
IF (SMW(I).GT,SSW(I+1))SMW(I)=SSW(I+1)
310 SSC(I+1)=SSC(I+1)-SMA(I)
SSW(I+1)=SSW(I+1)-SMW(I)
C
C      CALCULATE SURFACE UNMEASURED INFLOW AND GW INFLOW
C
STIF(I)=TIF(I)*STFK(I)
GWIN(I)=TIF(I)-STIF(I)
C
C      CALCULATE ROOT ZONE SUPPLY AND CROPLAND RETURN FLOW
C
DWRZ(I)=CD(I)*EFCV+EFOF
TSRZ(I)=DWRZ(I)+PCL(I)-DSC(I)+SMA(I)
SMS(I)=TSRZ(I)-SPCU(I)
RTFLO(I)=CD(I)-DWRZ(I)
GWRT(I)=RTK(I)+RTFLO(I)
SRTF(I)=RTFLO(I)-GWRT(I)
IF (SMS(I))33,33,35
33 IF (SMS(I)+ASMS(I))34+34,35
34 ASMS(I+1)=0.
AGW(I)=0.
DEF(I)=SMS(I)+ASMS(I)
ACU(I)=SPCU(I)+DEF(I)
GO TO 45
35 ASMS(I+1)=ASMS(I)+SMS(I)
IF (ASMS(I+1)-SMC)38,38,40
38 AGW(I)=0.
GO TO 43
40 AGW(I)=ASMS(I+1)-SMC
ASMS(I+1)=SMC
43 ACU(I)=SPCU(I)
DEF(I)=0.
C
C      CALCULATE INTERFLOW GW STORAGE CHANGES, INTERFLOW TO SURFACE
C      AND INTERFLOW ADDITION TO GROUNDWATER
C
45 GIN=AGW(I)+GWRT(I)+GWIN(I)
EKGW2=EKGW+2.
SINT(I)=0.
IF (IG,EQ,0) GO TO 66
DGW(I)=(TRI+TRI+STW(IG))*EKGW/EKGW2
IF (DGW(I).GT,GWC) GO TO 62
DGW(I)=GWC
IF (TRI+STW(IG).LT,DGW(I)) DGW(I)=TRI+STW(IG)
62 TRI=TRI+STW(IG)-DGW(I)
IF (IG,EQ,1) GO TO 65
DO 63 K=IG,2,-1
63 STW(K)=STW(K-1)
65 SGW(I+1)=SGW(I)+GIN-DGW(I)
GO TO 67
66 SGW(I+1)=(12.-EKGW)*SGW(I)+GIN+GIN)/EKGW2
IF (SGW(I+1).LE,GWCAP) GO TO 46
SGW(I+1)=GWCAP
DGW(I)=(SGW(I)+GWCAP)*.5*EKGW
SINT(I)=SGW(I)+GIN-DGW(I)-GWCAP
GO TO 64
46 DGW(I)=(SGW(I)+SGW(I+1))*5*EKGW
64 IF (DGW(I).GE,GWC) GO TO 67
DGW(I)=GWC
SGW(I+1)=SGW(I)+GIN-GWC
IF (SGW(I+1).GE,0.) GO TO 67
SGW(I+1)=0.
DGW(I)=SGW(I)+GIN
GO TO 68
67 IF (SGW(I+1).LE,GWCAP) GO TO 68
SINT(I)=SGW(I+1)-GWCAP
SGW(I+1)=GWCAP
68 STW(I)=GIN-SINT(I)
WLAGW(I)=0.
WLSFC(I)=0.
IF (NC2,EQ,0) GO TO 253
C
C      CALCULATE INTERFLOW SUPPLY TO WETLAND AND INTERFLOW TO SURFACE
C      CALCULATE WETLAND ROOT ZONE STORAGE, CONSUMPTIVE USE, WETLAND
C      SURFACE RETURN FLOW AND GROUNDWATER ADDITION
C
SWL(I)=SINT(I)+SWL(K(I))
SINT(I)=SINT(I)-SWL(I)
TSWL(I)=SWL(I)+PWL(I)-DSW(I)+SMW(I)
WLSM(I)=TSWL(I)-SWLCU(I)
IF (WLSM(I))215,215,220
215 IF (WLSM(I)+AWLSM(I))216,216+220
216 AWLSM(I+1)=0.
WLAGW(I)=0.
WDEF(I)=WLSM(I)+AWLSM(I)
AWLCU(I)=SWLCU(I)+WDEF(I)
GO TO 250
220 AWLSM(I+1)=AWLSM(I)+WLSM(I)
IF (AWLSM(I+1)-WLSMC)225,225,230
225 WLAGW(I)=0.
GO TO 235
230 WLAGW(I)=AWLSM(I+1)-WLSMC
AWLSM(I+1)=WLSMC
235 AWLCU(I)=SWLCU(I)
WDEF(I)=0.

```

Figure G-4. Continued.

charge and time of day. This is due, not to large diurnal variations in streamflow, as might be supposed (examination of recorder tapes showed almost no diurnal variations in flow), but rather to changes in the time of sampling which happened to coincide with date.

Total meq. was dropped in further analyses because, as indicated by the high correlation coefficient, most information contributed by this computed variable is already available through directly measured variables, such as hardness, conductivity and TDS. The reduced set of 24 variables was analyzed, using a composite of data from three stations and data from each of the three stations independently. The resulting correlation tables, Table H-3, are generally comparable, with the following differences. The correlation pattern between the logarithm of coliform count and other variables is entirely different for station S-27.5 than those shown for the other two stations. Also, the correlation between dissolved oxygen and the chemical parameters at station S-27.5 differs greatly from those at the two lower stations. Correlations between D.O. and date, time and temperature are consistent from station to station, however. Analysis of the composite data indicates a high correlation between TDS or conductivity and nitrates and phosphates. This correlation disappears in the individual analysis of station S-27.5 and is much lower at station S-15.2. The high correlation is maintained at S-12.5. This indicates that care must be exercised in lumping data from more than one station to determine relationships among the water quality variables.

Specific parameter models

The correlation tables were used in screening the variables which could be included in linear models to describe the important water quality parameters. Parameters for which models are particularly needed include coliform

count, hardness, TDS, pH, phosphate, and nitrate. The correlation tables indicated the futility of trying to express either phosphates or nitrates in terms of variables measured during this study. Therefore, relationships were determined by regression analysis only for the total dissolved solids (TDS), hardness (H), pH, and coliform count. The results of the analysis are summarized in Table H-4. The regression coefficients differed to some extent from station to station due to variations in the water quality regimen from upper to lower reaches of the system.

All of the models shown are statistically significant, especially those of the TDS and hardness models. Although the pH and coliform count models are statistically significant, a large amount of unexplained variation still remains. The high buffering capacity of this system, as illustrated by the high bicarbonate concentration, results in very little variation in pH levels. Some of the reported variation in pH may be caused by the colorimetric method of determination of pH which was used during much of the data gathering phase of the project. In the particular pH range encountered, it was extremely difficult to discern color changes corresponding to a pH change of 0.2 to 0.4 pH units. At a later date an electronic pH meter was obtained which improved the accuracy of pH measurement.

Summary

Complete tables of correlation coefficients have been prepared using data from 3 stations on the Little Bear River. These tables display, in a compact and concise format, information depicting the interdependence among water quality variables. The application of these tables as tools in the development of specific relationships between water quality parameters has been demonstrated.

1. Date																					
2. Time	.18																				
3. Distance	.38	.04																			
4. Calcium	-.30	-.10	.35																		
5. Magnesium	-.55	-.27	.32	.27																	
6. Potassium	-.22	.42	.44	.43	.13																
7. Sodium	.76	.16	.09	.41	.56	.18	.38	.45													
8. Chloride	.73	.48	.72	.32	.57	.03	.42	.23	.22												
9. Bicarbonate	.43	.63	.20	-.24	.81	.21	.12	.33	.44	.36	.22	.08									
10. Carbonate	-.14	-.05	.49	.71	.64	.66	.08	-.18	-.32	-.27	.01	-.17	.38	.15							
11. Nitrate	-.27	-.26	.49	.50	.39	.52	-.48	-.12	.05	-.11	-.05	-.22	-.17	.64	.40	.20	.94	.37	.62	.62	.34
12. Phosphate	.68	.37	-.04	.43	.36	-.17	-.13	-.37	-.45	.14	.34	.29	.53	-.60	.17	.72	.41	.37	.62	.35	.34
13. Sulfate	.45	-.29	-.38	.29	.30	-.27	-.17	.17	.15	.77	.77	.82	.29	-.05	.01	-.62	-.30	.20	.28	.35	.34
14. pH	-.14	-.05	-.06	-.35	.14	-.18	-.14	.85	.82	.59	.11	.11	.67	.72	.11	.12	.26	-.38	.28	.34	.34
15. Discharge	-.19	.38	-.03	.04	.58	.73	-.19	.82	.11	.92	.57	.07	-.06	.49	.47	.20	.20	.38	.28	.34	.34
16. D. O.	.09	.12	.06	.50	.50	.62	.14	.63	-.08	.18	-.07	.37	.53	.39	.39	.39	.39	.39	.39	.39	.39
17. Ammonia	-.11	-.23	-.27	-.27	-.37	-.02	.51	-.10	-.18	-.14	.45	.45	.45	.45	.45	.45	.45	.45	.45	.45	.45
18. Conductivity	.13	.11	.30	.01	-.32	-.33	.18	.08	.45	.46	.46	.46	.46	.46	.46	.46	.46	.46	.46	.46	.46
19. TDS	.90	-.01	.08	.08	.22	.39	.24	-.33	-.31	.49	.49	.49	.49	.49	.49	.49	.49	.49	.49	.49	.49
20. Temperature	.04	.85	.92	-.01	.45	.20	-.40	.04	.04	.04	.04	.04	.04	.04	.04	.04	.04	.04	.04	.04	.04
21. Hardness	0	.53	-.04	.43	.45	.45	.45	.45	.45	.45	.45	.45	.45	.45	.45	.45	.45	.45	.45	.45	.45
22. BOD	-.05	.40	.30	.44	.44	.44	.44	.44	.44	.44	.44	.44	.44	.44	.44	.44	.44	.44	.44	.44	.44
23. Log (T. Count)	-.09	.40	.43	.32	.32	.32	.32	.32	.32	.32	.32	.32	.32	.32	.32	.32	.32	.32	.32	.32	.32
24. Log (Colif.)	-.80	.17	.17	.17	.17	.17	.17	.17	.17	.17	.17	.17	.17	.17	.17	.17	.17	.17	.17	.17	.17

N = 147

Table H-3A. Composite data from the three stations, S-12.5, S-15.2, and S-27.5.

1. Date																					
2. Time	.44																				
3. Distance	.40	.10																			
4. Calcium	-.04	.20	.32	.51	.27																
5. Magnesium	-.68	.07	.04	.31	.21	.21	.49	.59													
6. Potassium	.12	.38	.45	.15	.19	.15	.32	.59	.57	.49											
7. Sodium	.77	.01	-.03	.44	.62	0	.52	.42	.49	.49											
8. Chloride	.54	.40	.66	.11	.62	.11	.07	.10	.26	.15	.32										
9. Bicarbonate	.40	.61	-.15	-.30	.19	.19	.32	.15	.67	.40	.48	.81	.20	.46	.13	.34	.35	.95	.46	.62	.41
10. Carbonate	-.13	.11	.17	.55	.76	.47	-.11	-.28	.04	-.50	.02	.46	.13	0	-.30	.34	.35	.95	.46	.62	.41
11. Nitrate	-.30	.61	.53	.25	.44	.44	-.51	-.48	.04	-.11	.36	.51	-.03	.25	.22	.95	.46	.62	.41	.40	.40
12. Phosphate	.65	.27	-.09	.36	-.41	-.26	-.44	-.40	-.52	-.11	.36	.51	-.03	.25	.22	.95	.46	.62	.41	.40	.40
13. Sulfate	.49	.28	-.43	.33	-.01	-.59	-.42	-.10	.06	.72	.76	.76	.76	.76	.76	.76	.76	.76	.76	.76	.76
14. pH	-.15	-.41	-.34	-.45	-.54	-.54	-.14	.78	.50	.52	.76	.76	.76	.76	.76	.76	.76	.76	.76	.76	.76
15. Discharge	.27	-.24	-.01	-.44	-.03	-.03	.70	-.18	.71	.25	.08	.66	-.28	-.42	.07	.25	.51	.25	.51	.25	.51
16. D. O.	.17	.41	.13	-.08	.66	.68	.72	.41	-.49	.88	.35	.02	.25	.44	.42	.42	.42	.42	.42	.42	.42
17. Ammonia	.03	.11	.70	.49	.44	.44	.45	.53	.60	.33	.59	.34	.50	.34	.50	.34	.50	.34	.50	.34	.50
18. Conductivity	.01	.38	-.42	-.60	.07	.17	.38	-.37	.42	.42	.42	.42	.42	.42	.42	.42	.42	.42	.42	.42	.42
19. TDS	.88	.01	.75	.65	.65	.24	.41	.48	.48	.48	.48	.48	.48	.48	.48	.48	.48	.48	.48	.48	.48
20. Temperature	.24	.18	.08	-.01	.49	.27	-.25	-.25	.48	.48	.48	.48	.48	.48	.48	.48	.48	.48	.48	.48	.48
21. Hardness	.16	.80	.88	.36	0	.40	.40	.40	.40	.40	.40	.40	.40	.40	.40	.40	.40	.40	.40	.40	.40
22. BOD	-.35	-.51	-.38	-.47	.57	.57	.57	.57	.57	.57	.57	.57	.57	.57	.57	.57	.57	.57	.57	.57	.57
23. Log (T. Count)	-.32	.43	.43	.43	.43	.43	.43	.43	.43	.43	.43	.43	.43	.43	.43	.43	.43	.43	.43	.43	.43
24. Log (Colif.)	.73	.29	.29	.29	.29	.29	.29	.29	.29	.29	.29	.29	.29	.29	.29	.29	.29	.29	.29	.29	.29

N = 63

Table H-3B. Data from station S-12.5, 63 observations.

